THE UNIVERSITY OF SOUTHAMPTON

Novel Chiral Cyclopentadienyl Metal Complexes

Stephen Anthony Harrison BSc.

A thesis submitted in partial fulfilment of the requirements for the degree of Doctor of Philosophy.

The Department of Chemistry

September 2002

UNIVERSITY OF SOUTHAMPTON

ABSTRACT

FACULTY OF SCIENCE

CHEMISTRY

Doctor of Philosophy

NOVEL CHIRAL CYCLOPENTADIENYL METAL COMPLEXES

by Stephen Anthony Harrison

The synthesis and applications of rhodium and ruthenium transition metal complexes containing planar-chiral cyclopentadienyl- and indenyl- ligands have been reviewed and the work of other research groups discussed.

The synthesis of the known two-carbon linked chiral indenyl-phosphine ligand (1*S*)-[2-(3*H*-inden-1-yl)-1-phenylethyl]diphenyl-phosphine **59** has been repeated, and the unexpected rearrangement during the final step of its synthesis, involving the spirocyclic intermediate (*R*,*R*)-spiro[(2-phenylcyclopropane)-1,1′-indene] **114**, has been investigated.

The novel two-carbon linked chiral ligand [(2*R*)-2-cyclohexyl-2-(3*H*-inden-1-yl)ethyl]-diphenylphosphine **121**, has been prepared and its synthesis optimised to provide 61 % yield of enantiopure **121** from commercial vinylcyclohexane. The lithium salt of **121** has been complexed with $[Rh(\mu\text{-}Cl)(CO)_2]_2$ to form it's rhodium(I) complex **154**, with 56 % d.e. induction of planar-chirality. Complexation of **121** with $RuCl_2(PPh_3)_3$ has also been achieved, and the resulting ruthenium(II) complex **147** formed with 60 % d.e. induction of planar-chirality and *complete* control of metal-centred chirality. Unfortunately initial catalytic trials of the ruthenium(II) complex have proved disappointing. The ruthenium complex has been hydrogenated to the tetrahydroindenyl complex **148**.

The novel diphenyl-substituted two-carbon linked ligand *rac*-[1,2-diphenyl-2-(3*H*-inden-1-yl)ethyl]diphenyl-phosphine **128** has been prepared and complexed with $RuCl_2(PPh_3)_3$ to form it's ruthenium complex **149**, with 74 % d.e. induction of planar-chirality.

The novel three-carbon linked indene-phosphine ligand *rac*-[3-cyclohexyl-3-(3*H*-inden-1-yl)propyl]-diphenyl-phosphine **129** has been prepared in 36 % overall yield from malonic acid and cyclohexane carboxaldehyde *via* a synthetic route involving the 1,4-addition of indenyl lithium to an α,β-unsaturated ester. The ruthenium(II) and rhodium(I) complexes **150** and **155** have been prepared from **129** and again show good induction of planar-chirality (66 % d.e. and 48 % d.e. respectively).

In collaboration with Rob Baker (University of Sydney, Australia) the axially-chiral three-carbon linked ligand *rac*-[1-(2-methyl-3H-inden-1-yl)-naphthalen-2-ylmethyl]-diphenylphosphine **145** has been prepared from it's precursor chloride, and complexed with $RuCl_2(PPh_3)_3$ to form ruthenium(II) complex **151** with a high degree metal-centred chirality, 66 % d.e.

X-ray structures six of the above organometallic complexes have been obtained, as well as five X-ray structures of intermediates formed during the syntheses of their ligands.

To Mum and Dad

This thesis contains my own original work carried out while registered as a postgraduate at the University of Southampton, except for the first (review) chapter and where explicitly stated otherwise.

Acknowledgements

Firstly I would like to thank my Ph.D. supervisor Prof. Richard Whitby, without whose constant encouragement and support, none of this work would have been possible. Thanks also to my industrial supervisors, Ray Jones and Barrie Crombie at Syngenta for their support over the past years, and John Blacker at Avecia for his help and support during my industrial placement. Friday evenings at the bar would not have been quite the same without the rest of the Whitby group (members past and present), particularly those who shared the same lab as me during my Ph.D.: Gustavo Saluste, Cliff Veighey, Dave Owen, Alexandre Kasatkin, Don McFarlane, Sally Dixon, Rupert Hunter, Dave Dossett, Dave Norton and Peter Wright.

The excellent analytical services at Southampton have been invaluable for this research, and I would particularly like to thank Joan Street, Neil Wells, John Langley and July Hernman for their help with all things NMR and Mass spec. related. Very special thanks are due to Simon Coles at the EPSRC crystallography service at Southampton, for his patience and constant help while I tried to wrap my head around the intricacies of solving crystal structures.

Special mention also to everyone at BioFocus Plc. Sittingbourne, for all their help, support, proof-reading and beer sessions over the past year.

Thanks especially to my family, for their love, encouragement and emergency financial assistance throughout the ups and downs of the past four years.

Abbreviations

Bn	Benzyl
Bu	Butyl
COD	1,5-Cyclooctadiene
Cp	Cyclopentadienyl
Cy	Cyclohexyl
d.e.	Diastereomeric excess
e.e.	Enantiomeric excess
Et	Ethyl
GC	Gas chromatography
HMPA	Hexamethylphosphoramide
HPLC	High performance liquid chromatography
Ind	Indenyl
IR	Infrared
Me	Methyl
Mp	Melting point
Ms	Methanesulphonate
MsCl	Methanesulphonyl chloride
m/z	Mass / charge ratio
NMR	Nuclear magnetic resonance
N.O.e.	Nuclear Overhauser effect
i-Pr	*iso*-Propyl
TBS	*tert*-Butyldimethylsilyl
TBSOTf	*tert*-Butyldimethylsilyltriflate
Tf	Trifluromethanesulphonate
Tf_2O	Triflic anhydride
THF	Tetrahydrofuran
TLC	Thin layer chromatography
TMEDA	Tetramethylethylenediamine
Ts	Toluenesulphonate
TsCl	Toluenesulphonyl chloride
UV	Ultraviolet

Table of Contents

Abstract i

Acknowledgements ii

Abbreviations iii

1. CHAPTER 1: THE SYNTHESIS AND APPLICATION OF RUTHENIUM AND RHODIUM COMPLEXES CONTAINING PLANAR-CHIRAL LIGANDS. 1

1.1 General Introduction 1

1.2 Cyclopentadienyl-Phosphorous bidentate complexes. 4

1.3 Planar-chiral ruthenium/rhodium complexes. 7

1.4 Induction of planar-chirality 13

1.4.1 Induction of planar-chirality on complexation of Cp- and Ind-ligands 13

1.5 Induction of metal-centred chirality in chiral Cp-Rh/Ru complexes. 20

1.5.1 Induction of metal-centred chirality by non-planar-chiral Cp ligands 20

1.5.2 Induction of metal-centred chirality by planar-chiral complexes 23

1.6 Induction of planar-chirality and metal-centred chirality on complexation of ligands. 30

1.7 Catalysis by indene phosphorous containing Rh/Ru complexes 33

1.8 Conclusions 41

2. CHAPTER 2: SYNTHESIS OF NOVEL CHIRAL BIDENTATE INDENYL-PHOSPHINE LIGANDS CONTAINING A TWO-CARBON BRIDGE. 42

2.1 Background 42

2.1.1 Planar-chiral complexes by face-selective metallation 42

2.1.2 Ligand design concepts for late-transition metals 44

2.1.3 Previous research 44

2.1.4 Aims 45

2.2 Studies into the synthesis of the phenyl-substituted ligand. 47

2.3 Design of an *alpha*-substituted indenyl ligand 49

2.3.1 Synthesis of the cyclohexyl-substituted ligand 49

2.3.2 Optimisation of the cyclohexyl ligand synthesis 52

2.4 Protection strategy for phosphine ligands 55

2.4.1 Phosphine oxides as 'protected' alkyl-diarylphosphines 56

2.4.2 Borane protected alkyl-diarylphosphines 56

2.5 Design of an *alpha,beta*-disubstituted indenyl ligand 57

2.5.1 Synthesis of the di-phenyl-substituted ligand 58

2.6 Conclusions 61

3. CHAPTER 3: SYNTHESIS OF NOVEL CHIRAL BIDENTATE INDENYL LIGANDS CONTAINING A THREE-CARBON BRIDGE AND CO-ORDINATING 'ANCHOR' GROUP. 62

3.1 Background 62

3.1.1 Cp/Indenyl ligands with three/four-atom bridged co-ordinating groups 62

3.1.2 Aims 62

3.2 Design of extended carbon-bridged ligands 63

3.2.1 Attempted modification of the two-carbon bridged ligand synthesis to three-carbon bridged ligands 63

3.2.2 Design of a new synthetic route to three-carbon bridged ligands 64

3.2.3 Synthesis of the three-carbon bridged ligand 65

3.2.4 Further optimisations to the 1,4-addition of indene to ester 131 73

3.2.5 Final optimised synthesis of the three-carbon bridged ligand 77

3.3 Modification of co-ordinating 'anchor' group 77

3.3.1 Chemistry towards inclusion of different 'anchor' groups 78

3.3.2 Synthesis of indene-sulphur bridged ligands 78

3.4 Alternative axially-chiral ligand design 79

3.4.1 Modification of *rac*-2-chloromethyl-1-(2-Methyl-1H-inden-3-yl)-naphthalene. 81

3.5 Conclusions 82

4. CHAPTER 4: SYNTHESIS OF NOVEL RHODIUM AND RUTHENIUM COMPLEXES 83

4.1 Introduction 83

4.2 Synthesis of Ruthenium complexes 84

4.2.1 Complexation of cyclohexyl-substituted two-carbon bridged ligand 121 85

4.2.2 Hydrogenation of 147 to give 4,5,6,7-tetrahydroindenyl complex 148 90

4.2.3 Complexation of diphenyl-substituted two-carbon bridged ligand *rac*-128 93

4.2.4 Complexation of cyclohexyl-substituted three-carbon bridged ligand 129 95

4.2.5 Complexation of Rob Baker three-carbon indene-naphthalene ligand 145 101

4.2.6 Complexation of three-carbon thiomethyl-substituted ligand 141 104

4.2.7 Stability of Ruthenium complexes 105

4.3 Synthesis of Rhodium complexes 107

4.3.1 Complexation of cyclohexyl-substituted two-carbon bridged ligand 121 107

4.3.2 Complexation of cyclohexyl-substituted three-carbon bridged ligand 129 113

4.4 Conclusions 114

5. CHAPTER 5: APPLICATION OF RUTHENIUM COMPLEX 147 TO THE CATALYTIC 'RECONSTITUTIVE CONDENSATION' REACTION. 116

5.1 Introduction 116

5.1.1 The 'Reconstitutive condensation' reaction 116

5.2 Catalytic application of ruthenium complex 147 119

5.2.1 'Reconstitutive condensation' literature conditions 119

5.2.2 'Reconstitutive condensation' using complex 147 120

5.3 Conclusions 123

5.3.1 Possible modifications to complex 147 123

6. CHAPTER 6: CONCLUSIONS AND FURTHER WORK **125**

6.1 Conclusions **125**

6.2 Further work **126**

7. CHAPTER 7: EXPERIMENTAL **130**

7.1 General Techniques **130**

7.1.1 Air and moisture sensitive manipulations 130

7.1.2 Spectroscopic techniques 130

7.1.3 Reagent purification 131

7.1.4 Chromatography 132

7.1.5 Miscellaneous 133

7.2 Experimental for Chapter 2 **134**

7.2.1 Synthesis of two-carbon tethered ligands 134

7.2.2 Synthesis of two-carbon disubstituted ligands 149

7.3 Experimental for Chapter 3 **153**

7.3.1 Synthesis of the three-carbon tethered phosphine ligand 153

7.3.2 Synthesis of three-carbon tethered sulphur ligand 162

7.3.3 Synthesis of axially-chiral indenyl-naphthalene phosphine ligand 163

7.4 Experimental for Chapter 4 **166**

7.4.1 Synthesis of Ruthenium complexes 166

7.4.2 Synthesis of Rhodium complexes 174

8. CHAPTER 8: REFERENCES **177**

9. APPENDICES **182**

Appendix 1 **X-ray Structure of Spiro-cyclopropane (114)**

Appendix 2 **X-ray Structure of Bis-mesylate (122)**

Appendix 3 **X-ray Structure of Spiro-cyclopropane (120)**

Appendix 4 **X-ray Structure of Spiro-cyclopropane (127)**

Appendix 5 X-ray Structure of Bis-*tert*-butyl-ester Compound (135)
Appendix 6 X-ray Structure of Ruthenium Complex (147)
Appendix 7 X-ray Structure of Ruthenium Complex (149)
Appendix 8 X-ray Structure of Ruthenium Complex (150a)-major
Appendix 9 X-ray Structure of Ruthenium Complex (150b)-minor
Appendix 10 X-ray Structure of Ruthenium Complex (151)
Appendix 11 X-ray Structure of Rhodium Complex (154)

1. Chapter 1: The Synthesis and Application of Ruthenium and Rhodium Complexes Containing Planar-Chiral Ligands.

1.1 General Introduction

Following the discovery of *bis* cyclopentadienyl iron or ferrocene, just fifty years ago[1] the development of a whole new area of chemistry began, bringing with it not only complex new synthetic challenges, but also raising many new theoretical problems. Stereochemistry is of particular importance to the organic chemist, and the unique bonding and spatial arrangement of cyclopentadiene and other arene ligands around the metal centre in this class of compounds gives rise to a special type of stereoisomerism. Termed 'planar-chirality',[2] the unsymmetrical substitution around a non-chiral cyclopentadiene ligand leads to optical isomerism when the ligand is complexed to a metal as a result of the pro-chiral nature of the faces of the substituted cyclopentadiene (Figure 1.1).

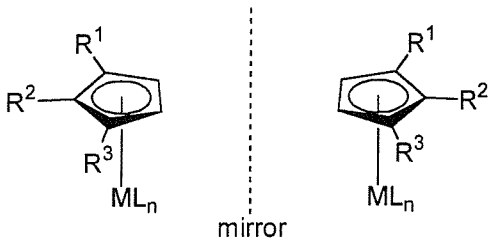

Figure 1.1 Planar-chiral enantiomers.

Over the past two decades, much research has been carried out into the design and use of transition metal complexes as catalytic mediators of organic transformations. In particular complexes of cyclopentadienyl ligands have proven very successful because of their synthetic diversity and the strength of the metal-cyclopentadienyl bond.[3] More recent interest in the scope of transition metal catalysis has involved use of chiral ligands to affect enantioselective transformations, with great success. Buchwald's *ansa*-titanocene catalysed hydrogenation of imines, to produce chiral amines in good yields and high enantiomeric excess, is an example of this success.[4-7]

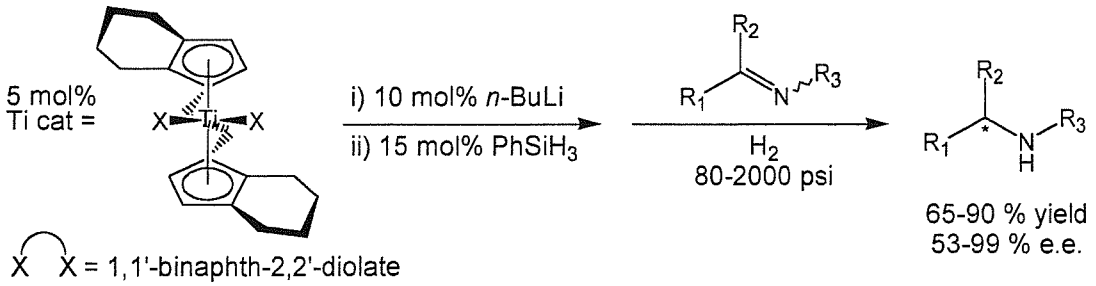

Scheme 1.1

In order to achieve effective asymmetric catalysis, the stereochemical environment around the catalytic site must be controlled. In transition metal catalysis, the catalytic active site is the metal centre, and the surrounding stereochemical environment is controlled by the ligands of the complex. Chirality can arise in transition metal complexes from either a chiral or pro-chiral ligand, 'ligand-derived chirality', or at the metal centre itself, 'metal-centred chirality', although often a combination of both of these is encountered, Figure 1.2. Planar-chirality is a special type of ligand-derived chirality, as this face-dependant chirality can occur in the absence of individual chiral-centred atoms.

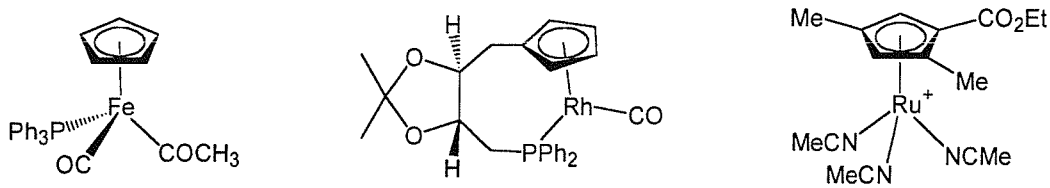

1[8] Metal-centred chirality

2[9] Ligand-derived chirality

3[10] Planar-chirality

Figure 1.2

Planar-chiral transition metal catalysts have been the subject of recent interest, as they enable a source of chirality to be placed very close to the metal centre, and yet, especially in the case of cyclopentadiene ligands, racemisation is unlikely to occur under normal catalytic reaction conditions, owing to the strength of the metal-Cp bond.

The chemistry required to access enantiomerically pure planar-chiral complexes is still somewhat underdeveloped, with current preparations often involving costly resolution procedures of the final complex.[11-13] However planar-chiral complexes of early-transition metals such as zirconium and titanium have found applications as asymmetric catalysts,[3] in particular their planar-chiral *ansa*-metallocenes have found success in a range of organic transformations including hydrogenations,[6] Diels-Alder reactions[14] and carbomagnesiation reactions.[15]

As yet there has been very little research into the use of planar-chiral late-transition metal complexes (such as rhodium/ruthenium/iridium complexes) as asymmetric catalysts of organic transformations. However this area of research holds much promise, as the

number of reactions known to be catalysed by late transition-metal complexes has increased rapidly over the past decade,[16] and continues to do so.

In order to prepare co-ordinatively unsaturated planar-chiral complexes of late-transition metals, a mono-cyclopentadienyl structure is required. Previous research within the Whitby group has led to the development of a C_1-symmetric catalyst model for early transition metals, Figure 1.3,[17] which has achieved good results in asymmetric catalysis (discussed further in Chapter 2).[18] The aim of this Ph.D. research is to continue the current efforts into the application of this successful catalyst model to late-transition metals. This challenging target will require the design of new planar-chiral cyclopentadienyl ligands, complexation of these ligands to suitable late-transition metals and trials of the resulting complexes as asymmetric catalysts.

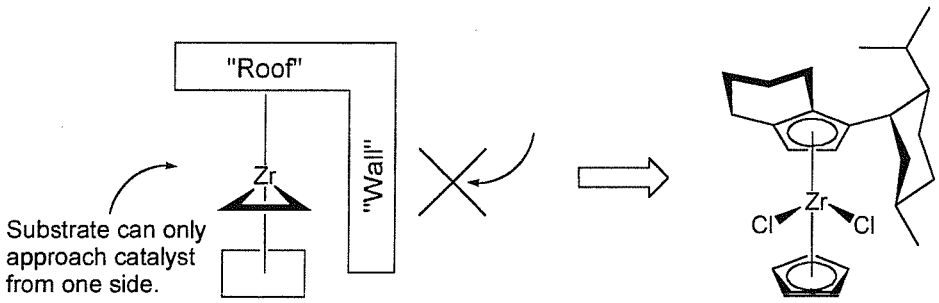

Figure 1.3

The remainder of this introduction shall review the literature concerning planar-chiral ruthenium and rhodium complexes, with particular focus on the induction of planar-chirality upon complexation of unsymmetrically substituted cyclopentadienyl and indenyl ligands. Chiral bidentate cyclopentadienyl-phosphorous ligands of rhodium and ruthenium complexes shall be included in the review and the induction of metal-centred chirality on rhodium and ruthenium Cp complexes shall also be examined. Details of catalytic applications of ruthenium and rhodium Cp- and indenyl-phosphorous complexes shall be covered at the end of the review.

1.2 Cyclopentadienyl-Phosphorous bidentate complexes.

Cp-linked phosphine bidentate ligands are an important class of ligand, especially because their complexes may be expected to gain unique properties, distinct to those of monodentate Cp or phosphine complexes. Complexes of Cp-phosphine bidentate ligands have been recently reviewed,[19] Figure 1.4 shows some example Cp-phosphine linked complexes.

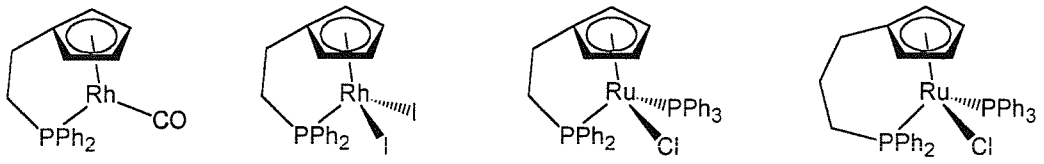

4 **5** ***rac*-6** ***rac*-7**

Figure 1.4

Rhodium (I) complex **4** is the first example of a rhodium Cp-phosphine linked complex and was prepared by reaction of the Cp-anion of the ligand with the rhodium dimer $[RhCl(CO)_2]_2$. Subsequent reaction of **4** with iodine gave the rhodium (III) complex **5**.[20] Complex *rac*-**6** is the first reported ruthenium Cp-phosphine alkyl-linked complex,[21] this was prepared by reaction of the Cp-ligand with $RuCl_2(PPh_3)_3$,[22] and along with complex *rac*-**7**[21] has found use as a catalyst of the reconstitutive condensation reaction between terminal alkynes and allylic alcohols (see Section 1.7).[23]

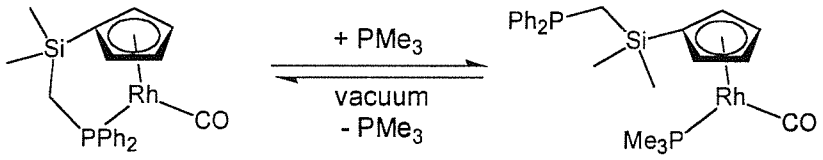

8 **9**

Scheme 1.2

Complexes containing a Cp-phosphine tether may be expected to have similar reactivities and become involved in similar catalytic cycles to their non-tethered analogues. However this will not always be the case, particularly where the length or steric bulk of alkyl tether is sufficient as to enforce a strained geometry around the metal, different to the non-tethered analogue. The strongly bound Cp ligand tethered to a more weakly co-ordinating

phosphine group also allows for the possibility of the phosphine to dissociate/co-ordinate to and from the metal centre during reactions or catalytic cycles. The reversible reaction of complex **8**[24] with trimethylphosphine to displace the linked phosphine group, demonstrates this possibility.

The alkyl link in Cp-phosphine ligands such as those shown in Figure 1.4 is an ideal location to add a source of chirality to the ligand. A chiral group attached along the Cp-phosphine tether should not interfere with the electronic properties of the cyclopentadienyl ring or phosphine group, and will not affect other ligands bound to the metal centre. Tani has used this idea to prepare the first chiral bidentate Cp-phosphorous ligands **10** and **12**, and their rhodium carbonyl complexes (a ruthenium complex of **10** is also reported, with some induction of metal-centred chirality and so is discussed in Section 1.5.1). These optically active ligands contain a 'chiral backbone' derived from L-threitol (**10**) or (S,S)-1,2-trans-dimethylene-cyclopentane (**12**) linking the Cp ring with the phosphorous co-ordinating group. Rhodium Cp-phosphorous complexes **11** and **13** were obtained in moderate yields, 22 % and <20 % respectively, by reaction of the lithium salts of **10** and **12** with the $[Rh(CO)_2Cl]_2$ dimer.[9]

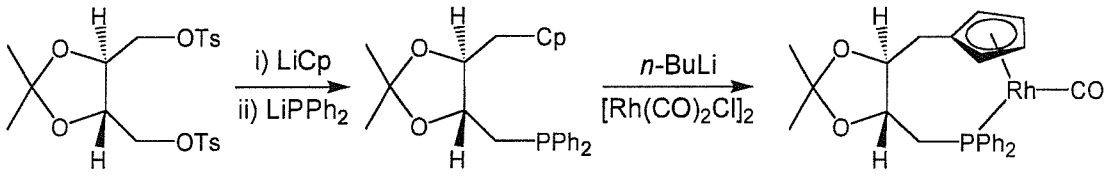

10 **11**

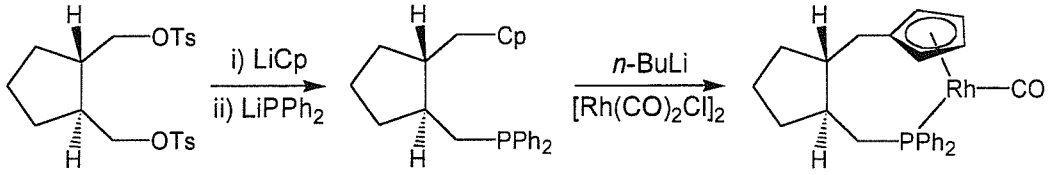

12 **13**

Scheme 1.3

It should be noted that the ruthenium complexes **6** and **7**, see Figure 1.4, are chiral complexes, by virtue of the asymmetric arrangement of ligands around the ruthenium atom. Resolution of the racemate of complex **6** was attempted by replacement of the

chloride ligand with the chiral amine (+)-$NH_2CH(Me)Ph$, and this resulted in the substitution product as a mixture of diastereoisomers. Unfortunately, however, the product was found to be too unstable for the slow fractional crystallisation necessary to separate the diastereoisomers. Metal-centred chirality induced on complexation of chiral ligands is discussed in Section 1.5.

Hidai has reported the planar-chiral ferrocene ligand **15** and its chelate rhodium complex **16** (the ruthenium complex of **15** is also reported, with a high degree of induction of metal-centred chirality, see Section 1.5.1).[25]

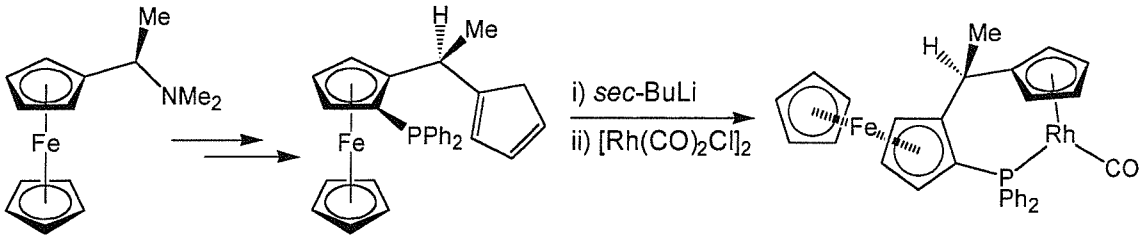

14 **15** **16**

Scheme 1.4

Complex **16** is formed in 66 % yield, by the reaction shown in Scheme 1.4. The ferrocene ligand **15** is an example of a co-ordinatively saturated planar-chiral metallocene, and is therefore inert to reactions at the metal centre. Indeed a common synthesis of planar-chiral ferrocenes such as **15** involves the directed lithiation of the cyclopentadiene ligand while it is complexed to iron, in precursor **14**, followed by a substitution reaction to install the diphenylphosphine group,[26,27] both procedures which would not be possible if the iron metal itself were reactive.

Salzer has reported the chiral Cp-phosphine ligand **17**, and its rhodium ethylene complex **18** by reaction with the $[RhCl(C_2H_4)_2]_2$ dimer, Scheme 1.5.[28] The preparation of enantiopure ligand **17** from styrene was reported shortly after completion of our own work on two-carbon linked chiral indene-phosphine ligands (Chapter 2), and follows a similar synthetic route, this is discussed further in Chapter 2. In previous research within the Whitby group, Brookings has reported the planar-chiral indenyl analogue of **18**,[29] which is formed with some degree of induction of planar-chirality, and discussed further in Section 1.4.1 and Chapter 4.

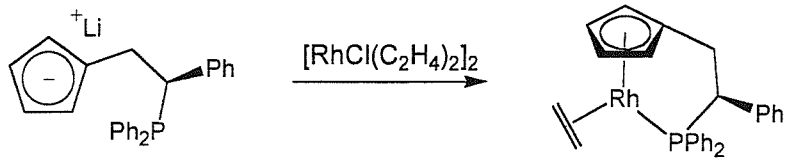

17 **18**

Scheme 1.5

Indenyl-phosphine linked bidentate ligands may also be classified as Cp-phosphine bidentate ligands, however, where the linking chain joins the indenyl-ring at the 1- or 3-position, these ligands fall into the category of unsymmetrically substituted cyclopentadienyl ligands. These ligands contain diastereotopic faces and will therefore form planar-chiral complexes, as such these ligands shall be discussed in Sections 1.3-1.6. No indenyl-phosphine ligands containing a linking chain joining the indenyl-ring at the 2-position or symmetrical 1,3-disubstituted indenyl-phosphine ligands have been reported at the time of writing.

1.3 Planar-chiral ruthenium/rhodium complexes.

The bidentate indene-phosphine ligands **19a-d** have been reported, along with their rhodium carbonyl complexes, Scheme 1.6.[30] Owing to the unsymmetrically substituted Cp-ring of the indenyl ligands, these complexes are formed as a racemic mixture of planar-chiral enantiomers.

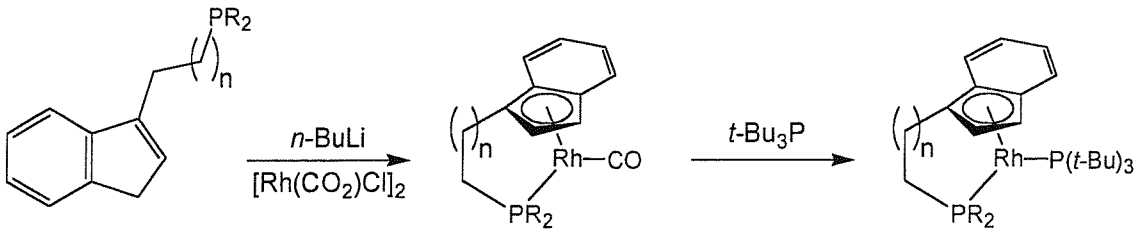

19a-d **20a-d** **21d**

a: R = Cy, **b**,**c**,**d**: R = Ph
a,**b**: n = 2, **c**: n = 3, **d**: n = 4

Scheme 1.6

Tani has investigated the carbonyl substitution reaction of complexes **20b-d** with tri-*tert*-butyl phosphine and found that only the complex of the four-carbon bridged ligand, **20d**, gave a stable substitution product – **21d**. The mechanism for the carbonyl substitution on

the related Ind-$Rh(CO)_2$ complex by a trialkylphosphine, has been studied previously[31] and is thought to occur via an associative pathway, involving an 18-electron η^3-intermediate. However Tani reports, for complex **21d**, good evidence that in this case substitution occurs *via* a dissociative mechanism, whereby the bidentate phosphine dissociates from the metal centre upon co-ordination of the incoming phosphine, then re-coordinates after loss of carbon monoxide. In the case of the complexes containing a two or three-carbon bridged ligand, **20b** and **20c**, although no stable product was isolated, Tani's evidence suggests substitution on these complexes follows the associative pathway, but fails to liberate carbon monoxide, with the unstable product being that of the 18-electron η^3-indenyl species.

These findings show that the presence of, and length of the tether linking the cyclopentadienyl ring and phosphine have a large effect on both the reactivity of the complex, and on the mechanism of its reactions.[30]

Takahashi reported the first isolation of an enantiopure planar-chiral rhodium complex in 1992.[12] In an attempt to prepare enantiopure rhodium and iron complexes containing only planar-chirality, the use of a cyclopentadienyl ligand containing a chiral auxiliary was investigated. The tri-substituted cyclopentadienyl-ester ligand **22** was prepared, and the (–)-menthyl ester introduced as the chiral auxiliary *via* an alcohol exchange reaction. Complexation of the chiral ligand **23** to the rhodium dimer $[RhCl(COD)]_2$ was then performed, resulting in a 1 : 1 mixture of planar-chiral diastereoisomers **24** (i.e. no induction of planar-chirality upon complexation was seen), Scheme 1.7. (Ligand **22** has also been complexed to iron by reaction with $Fe(CO)_5$, followed by iodine, to form chiral mono-Cp-iron complexes).[32]

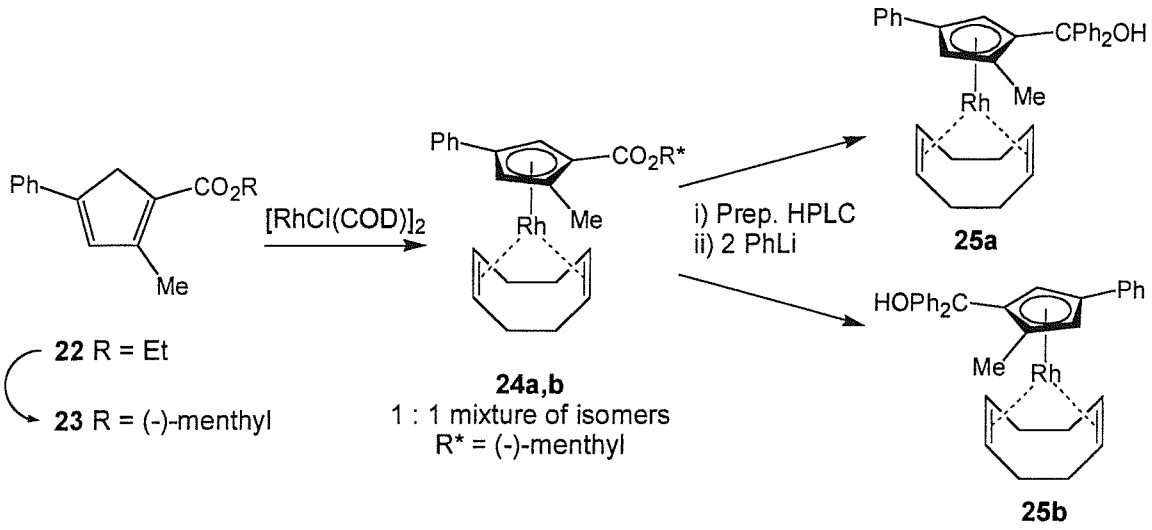

Scheme 1.7

Resolution of the diastereomeric mixture **24** was achieved by preparative HPLC, providing the individual isomers **24a** and **24b** each in at least 95 % d.e. The isomers **24a** and **24b** were then treated individually with an excess of phenyllithium in order to remove the (–)-menthyl chiral auxiliary, and thus form planar-chiral enantiomers **25a** and **25b** each with >95 % e.e.

More recently, Takahashi has reported success in resolving the racemic planar-chiral complex *rac*-**27** into its optically pure enantiomers by the use of liquid chromatography with aqueous β-cyclodextrin as the chiral mobile phase, through a polyamide column, Scheme 1.8.[33]

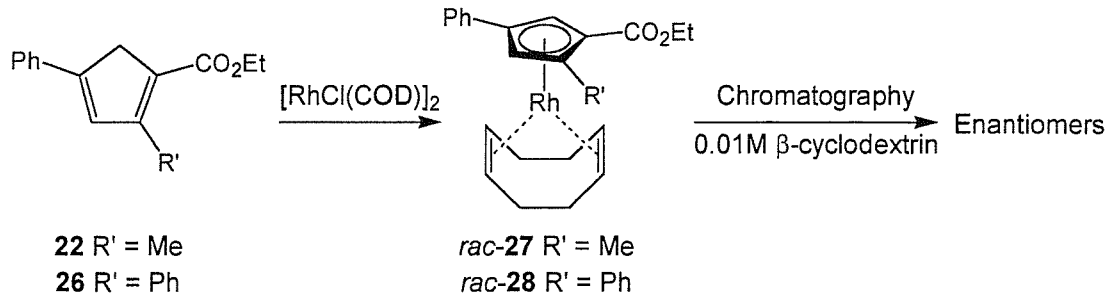

Scheme 1.8

The first non-ruthenocene planar-chiral ruthenium complex has been prepared from a similar ligand to **23**, and reported by Takahashi,[10] Scheme 1.9. Complexation of the (–)-menthyl substituted Cp-ligand **29** to the ruthenium dimer $[(C_6H_6)RuCl_2]_2$ was achieved by reaction with the thallium salt of the ligand. As with the rhodium complexation of

ligand **23**, no induction of planar-chirality was seen during complexation – suggesting that the menthyl group is too remote from the Cp-ring to sufficiently differentiate the energy levels of each Cp-face. Thus the [cyclopentadienyl(η^6-benzene)ruthenium]PF_6 complex **30** was prepared as a 1 : 1 mixture of planar-chiral diastereoisomers.

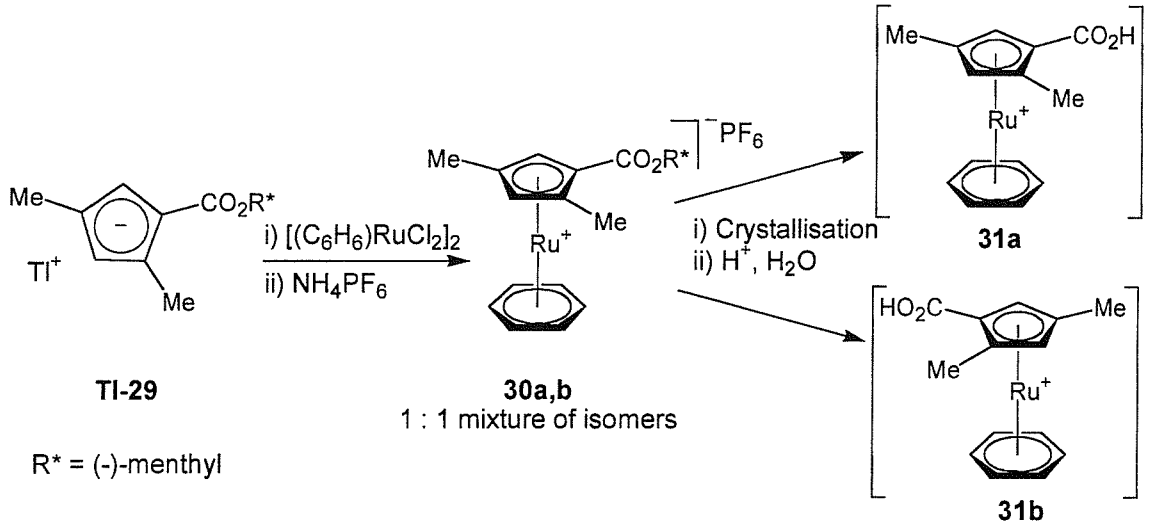

Scheme 1.9

Resolution of the diastereoisomers **30a** and **30b** was achieved in this case by fractional crystallisation. Diastereoisomers **30a** and **30b** were then converted into enantiomers by hydrolysis of the (–)-menthyl chiral auxiliary, to give intermediates **31a,b** which were transformed to acid chlorides and isolated as their amide products **32a,b** following reaction with aniline, Scheme 1.10.

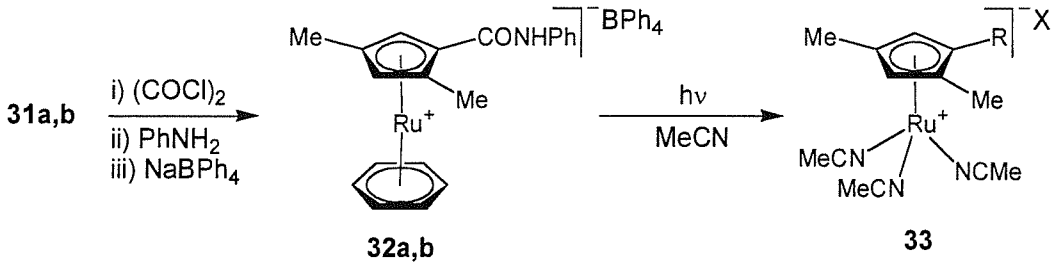

Scheme 1.10

The substitution of the η^6-benzene ligand in optically pure complexes such as **32**, *via* a photo-catalysed ligand exchange reaction with acetonitrile,[34] was also demonstrated.[10] This forms planar-chiral tri-acetonitrile substituted complexes such as **33**, with complete retention of optical purity. It was hoped that the ease of replacement of such acetonitrile

ligands on ruthenium complexes would lead to their planar-chiral Cp-Ru complexes finding applications in asymmetric catalysis.

Following the methodology shown in Schemes 1.8 and 1.9, a variety of analogues of complexes **30**, **31** and **32**, containing different substituents on the Cp ring, have recently been reported.[35] The versatility of Takahashi's tri-substituted cyclopentadienyl ligand series has also been further expanded to include linked Cp-pyridyl and bidentate Cp-phosphorous complexes, Scheme 1.11.[36]

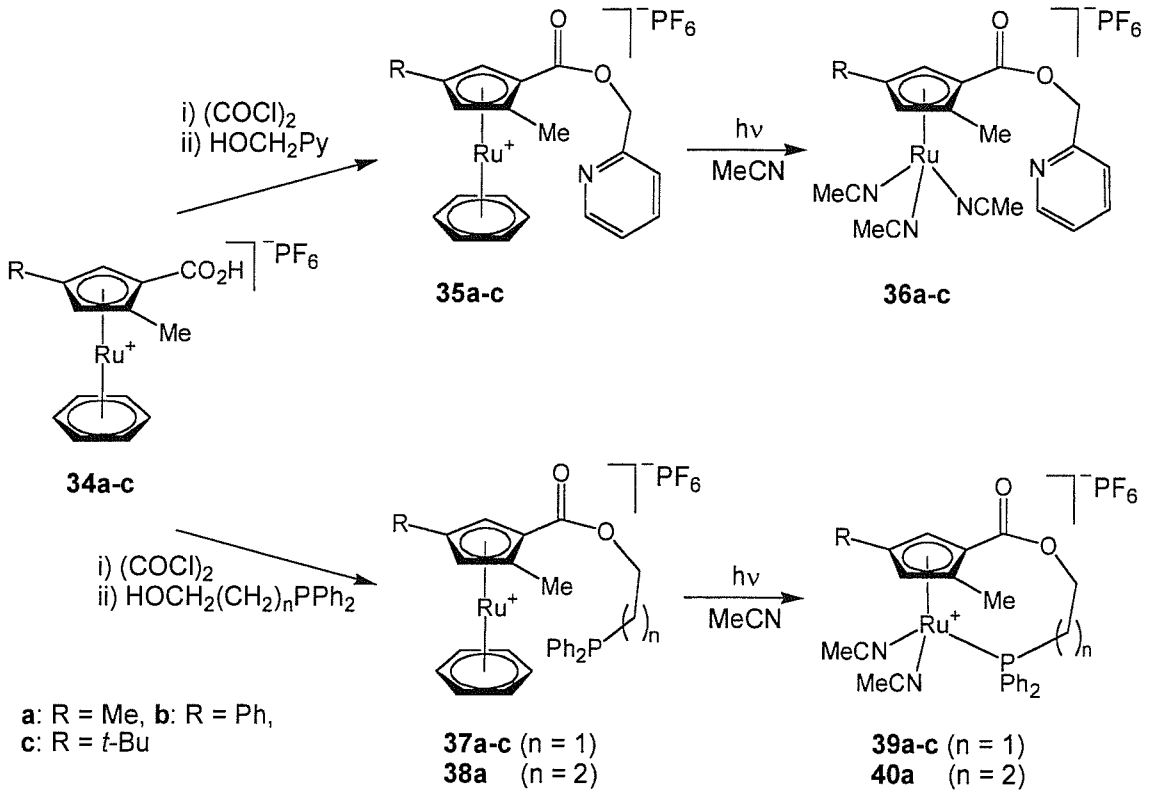

Scheme 1.11

Reaction of complexes *rac*-**34** with oxalyl chloride, followed by esterification with either a pyridyl- or phosphorous-substituted alkyl alcohol, provided Cp-linked complexes **35**, **37** and **38**. Extensive NMR studies of the Cp-pyridyl linked complexes **35**, showed no co-ordination of the pyridyl nitrogen to the ruthenium metal. Displacement of the η^6-benzene ligand with more labile acetonitrile ligands to form complexes **36**, also failed to result in co-ordination of the pyridine nitrogen. Some success in co-ordination of this moiety was seen when two acetonitrile ligands of **36** were substituted by a 2,2'-bipyridine ligand, however the effect was strongly solvent dependent, with co-ordination only seen

in acetone solvent, not in acetonitrile. This suggests that co-ordination of the pyridine nitrogen is very weak under these conditions.

The Cp-phosphorous linked complexes **37** and **38**, also failed to show co-ordination of the anchor group to the ruthenium metal in the presence of the η^6-benzene ligand. However once this was displaced by acetonitrile ligands, to form complexes **39** and **40**, co-ordination of the phosphine to the ruthenium metal occurred, and was confirmed by NMR. The phosphorous-ruthenium co-ordination in complexes **39** and **40**, was found to be independent of solvent, indicating that the phosphorous is tightly bound to the metal, in contrast to the pyridyl group. Both enantiomers of complex **40** were obtained from enantiopure **34**, which was prepared *via* the chiral auxiliary/fractional crystallisation route, shown in Scheme 1.9.

Takahashi has also prepared enantiopure planar-chiral bis-phosphine and vinylidene ruthenium complexes, Scheme 1.12,[37] from precursors prepared *via* his chiral auxiliary/fractional crystallisation route (*cf.* Scheme 1.9). Reaction of the acetonitrile complex **41** (analogue of **33**, Scheme 1.10), with two equivalents of triphenylphosphine, provided the bis-phosphine complex **42**. Reaction with excess triphenylphosphine did not result in the tris-triphenylphosphine complex, but still formed only the bis-triphenylphosphine complex **42** where one acetonitrile ligand remains co-ordinated to the metal.

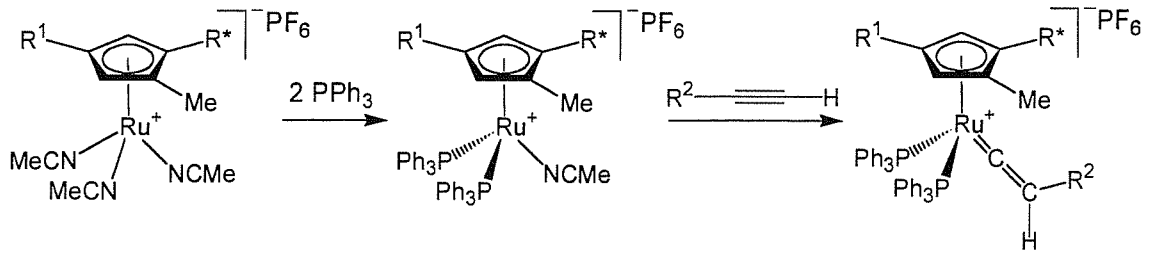

41 **42** **43**

R*=(*l*)- or (*d*)-menthyl
R^1=Me or Ph

Scheme 1.12

Reaction of **42** with a terminal acetylene provided the vinylidene complex **43** directly (note: in neutral ruthenium complexes it is necessary to employ a scavenger reagent, such as NH_4PF_6, for this reaction to proceed – in order to abstract the halogen ligand).

1.4 Induction of planar-chirality

Enantiomerically pure planar-chiral transition metal complexes prepared by induction of planar-chirality on complexation of *pi*-ligands have been recently reviewed.[38] Many types of *pi*-ligands are reviewed, including η^2-alkenes, η^3-allyl ligands, η^4-dienes, η^5-cyclopentadienes and η^6-arenes, and their complexes of many transition metals reported in the literature until mid-2001. Consequently the review only briefly covers rhodium and ruthenium complexes of planar-chiral η^5-cyclopentadienyl ligands. A more detailed and up to date discussion of induction of planar-chirality on complexation of Cp ligands to rhodium and ruthenium is given below (Sections 1.4.1 and 1.6).

1.4.1 Induction of planar-chirality on complexation of Cp- and Ind-ligands

Tani's indene-phosphorous ligand **44** contains a pro-chiral unsymmetrically substituted Cp ring, which will result in planar-chirality upon complexation to a metal, thus upon complexation to rhodium, two diastereoisomers of **45** were formed, in a 69 : 31 ratio (38 % d.e.), Scheme 1.13.[9] This indicated that the chiral backbone of ligand **44** is successful in inducing a degree of planar-chirality, despite the chiral information being somewhat remote (two carbons atoms away) from the indene.

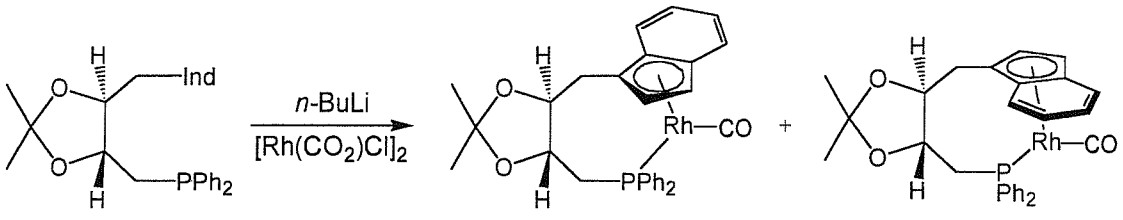

44 **45** 69 : 31

Scheme 1.13

In the search for successful chiral ligands containing diastereotopic faces, the ligand design involving a chiral bicyclic auxiliary fused to a cyclopentadienyl ring has been

studied intensely and found great success in diastereoselective formation of planar-chiral metallocenes of early-transition metals (see Paley,[38] section 2.8). However there has so far only been one reported example of such a fused system successfully applied to a non-metallocene late transition metal. This is the complexation of a series of verbenone-fused indenyl ligands (termed 'verbenindenes') to rhodium, Scheme 1.14.[39]

The 'verbenindene' ligands are synthesised in five steps[40] (including a [1,5]-hydrogen shift isomerisation required to allow deprotonation prior to complexation)[39] from the readily available (1*S*)-(–)-verbenone **46**. Complexation to the rhodium dimer, $[RhCl(COD)]_2$, at a temperature of –78 °C warmed rapidly to 0 °C, provided a single diastereoisomer in 31 % yield of **47**, although much lower selectivities were seen for **48** (23 % d.e., 39 % yield) and **49** (13 % d.e., 38 % yield). Modification of the procedure, involving warming the complexation mixture from –78 °C to 0 °C over 90 minutes, resulted in the same 23 % d.e. for complex **48**, but provided complete selectivity for complex **49** (100 % d.e.), which was now isolated in 62 % yield.

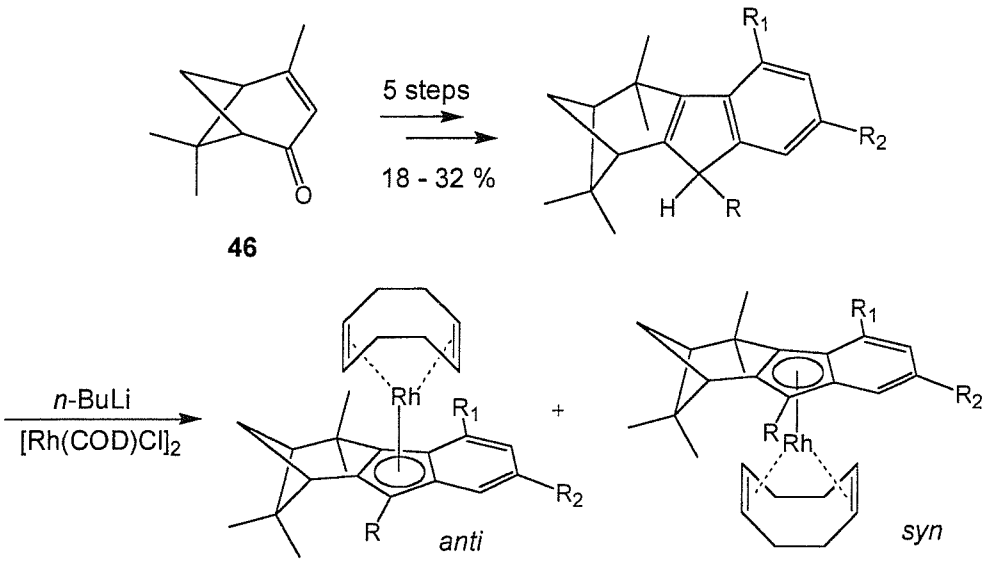

47: R = H, $R_1 = R_2 = OCH_3$, 100% d.e. (*anti*)
48: R = CH_3, $R_1 = R_2$ = H, 23% d.e. (presumed *anti*)
49: R = Ph, $R_1 = R_2$ = H, 13% d.e. or 100% d.e. (*anti*)

Scheme 1.14

In his most recent publication on induction of planar-chirality, Tani has examined the induction of planar-chirality upon complexation of three different chiral Cp-phosphine ligands to rhodium.[41] The three ligands, derived from menthol (**50** and **51**) and isomenthol (**52**), show very different degrees of induction of planar-chirality.

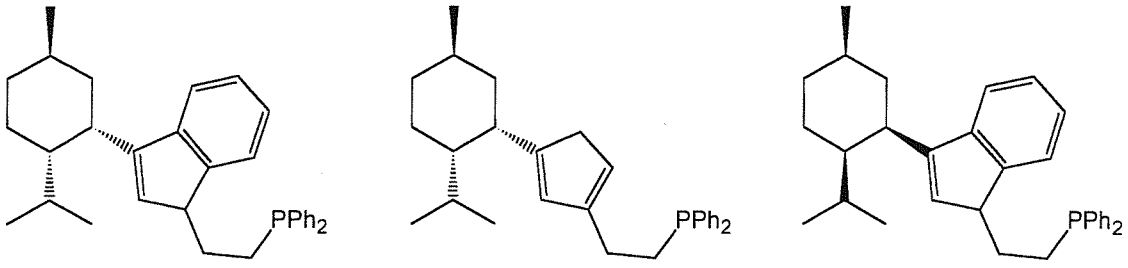

50 **51** **52**

Figure 1.5

The neoisomenthyl ligand **52** was seen to provide the best face-selectivity upon metallation, achieving 74 % d.e for complex **53** (Scheme 1.15). Whereas the indene-neomenthyl ligand **50** showed a low 24 % d.e. face-selectivity upon complexation, and its Cp analogue **51**, showed very poor selectivity, only 8 % d.e. Nevertheless, the three-times greater selectivity seen with indene ligand **50**, compared to Cp ligand **51**, demonstrates the effectiveness of the additional aromatic ring portion of the indene ligand in providing better discrimination between the diastereotopic faces and thus improved induction of planar-chirality. Also noteworthy is the fact that the Cp ligand **51** showed metallation to the opposite Cp-face than with either of the indene ligands, **50** and **52**, again showing that the indene ring system plays an important role in deciding which face is preferential.

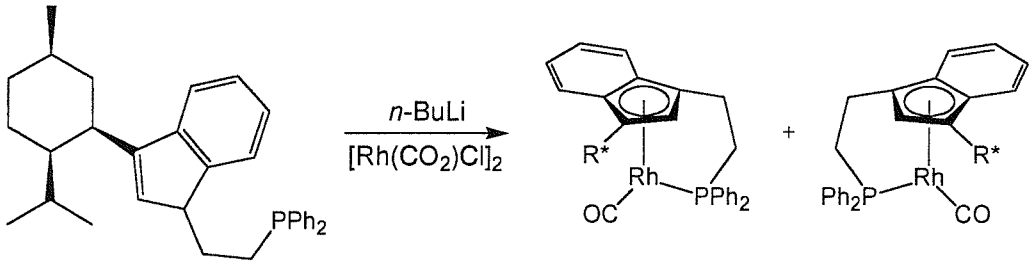

52 **53** 87 : 13

R* = neoisomenthyl

Scheme 1.15

The above result showing low selectivity from complexation of the indene-neomenthyl ligand **50**, is also confirmed by Schumann et al.,[42] in the complexation of neomenthyl-indene, **54**, to the $[RhCl(COD)]_2$ dimer, which achieved only 20 % d.e. Interestingly, in previous research within the Whitby group, Brookings[29] performed preliminary investigations into the complexation of neomenthyl-indene, **54**, to the $[RhCl(CO)]_2$ dimer, and initial results suggested a face-selectivity of 91 % d.e. (10 : 1 ratio) on

complexation. A possible explanation for this apparent difference in selectivity may lie with the differing reaction temperatures and conditions used for these complexations. In the case of Tani,[41] complexations were performed in THF, at 0 °C, whereas Schumann[42] used diethyl ether solutions at –78 °C, Brookings however performed the reaction at room temperature, in THF. Sowa[39] has reported large differences in face-selectivity achieved on complexation of 'verbenindenes' to $[RhCl(COD)]_2$ by simply varying the rate of warming the complexation reaction mixture from –78 °C to 0 °C, therefore the differing face-selectivities seen above may be due to the variation in complexation temperature affecting the thermodynamic ratio of isomers, however further evidence will be required to confirm this.

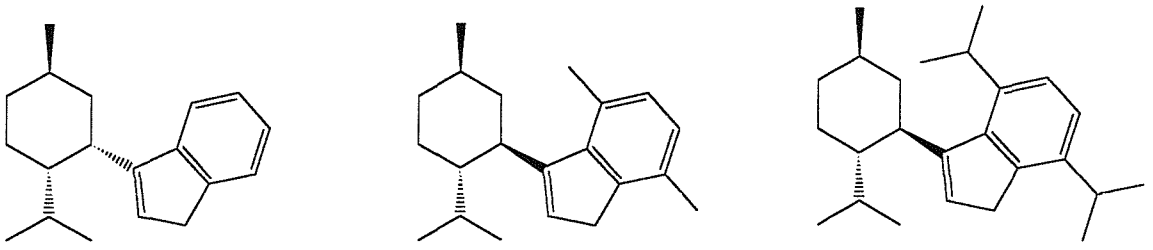

54 **55** **56**

Figure 1.6

Schumann has investigated the indene-menthyl ligands **55** and **56** and examined their complexation to rhodium, to form planar-chiral complexes.[42] Table 1.1 shows the results of diastereoselective complexations of these ligands to different rhodium sources, under varying reaction conditions.

Reaction	Ligand	Conditions	Rhodium source	Yield	$R : S$[†]
1	**55**	Li salt	$[RhCl(COD)]_2$	98 %	2.3 : 1 (39 % d.e.)
2	**55**	Na salt	$[RhCl(COD)]_2$	70 %	1 : 2.0 (–33 % d.e.)
3	**55**	K salt	$[RhCl(COD)]_2$	89 %	1 : 3.0 (–50 % d.e.)
4	**56**	Li salt	$[RhCl(COD)]_2$	75 %	2.2 : 1 (38 % d.e.)
5	**55**	Li salt	$[RhCl(C_2H_4)]_2$	78 %	2.0 : 1[‡] (33 % d.e.)
6	**55**	Na salt	$[RhCl(CO)]_2$	75 %	1 : 1.5[‡] (20 % d.e.)

Table 1.1

[†] The planar-chirality in indenylmetal complexes is assigned *R* or *S*, based on the configuration at the indenyl 1-position, where the metal is treated as being individually bonded to all five Cp-atoms.[2]
[‡] Schumann[42] notes that the major isomer for reactions 5 and 6 is assumed and has not been confirmed.

Complexation of the lithium salt of menthyl-indene ligand **55** to $[RhCl(COD)]_2$ showed a modest face-selectivity of 39 % d.e. When one equivalent of (–)-sparteine was added as an additional chiral auxiliary for the asymmetric complexation of the lithium salt of **55**, little change in diastereoselectivity was seen (38 % d.e.). Substitution of the hard η^5-bound lithium salt by the soft, η^1-bound tri-butyltin derivative also failed to significantly affect the diastereoselectivity upon complexation (35 % d.e.). Addition of 12-crown-4 to the lithium salt **55**, to form the 'naked' anion resulted in a reduction of diastereoselectivity, to 17 % d.e.

Changing from the lithium salt of **55** to using the sodium salt had an interesting effect on the stereochemical outcome of the complexation, with the thermodynamically less favourable *S*-complex formed as the major isomer, in 33 % d.e. This was also seen with the potassium salt of **55**, which resulted in the highest diastereoselectivity seen here, at 50 % d.e., favouring the *S*-isomer. Schumann notes that the reason behind this observation may be the increasing size in ionic radii of the cations (Li = 0.68 Å, Na = 0.97 Å, K = 1.33 Å)[43] and the increasing ability for their anions to form oligomeric structures.[42]

Changing the 4,7-dimethyl-indene group of ligand **55** to the 4,7-diisopropyl substituted ligand **56**, had very little affect on the diastereoselectivity of the complexation, resulting in 38 % d.e. This shows that the steric bulk of the alkyl groups at 4,7 positions have little influence on the different energy levels of each face of the ligand.

Complexation of the lithium salt of **55** to the rhodium ethylene dimer $[RhCl(C_2H_4)]_2$, again give only modest 33 % d.e., and the complexation of sodium salt of **55** to the rhodium carbonyl dimer $[RhCl(CO)]_2$, resulted in even lower selectivity, 20 % d.e.

Schumann also examined complexation of ligand **55** to the iridium dimer $[IrCl(COD)]_2$ and the Molybdenum carbonyl complex $Mo(CO)_6$. However the diastereoselectivities for the iridium (38 % d.e.) and molybdenum (41 % d.e.) complexations were little different to those achieved for rhodium complexes discussed above. Schumann does claim the best result to be a 71 % d.e. on complexation of **55** to the cobalt complex $CoCl_2$(dppe) (although in low 33 % yield). Careful examination of the experimental reported for this work however indicates that in the case of the cobalt complexation, the diastereoselectivity was measured *after* a recrystallisation of the crude material, whereas measurements for the other complexations were taken prior to purification. In which case, in absence of further evidence, this increased diastereoselectivity on complexation to cobalt may be viewed with some scepticism.

Takahashi has examined the 'through space' asymmetric induction by planar-chirality upon complexation of a prochiral tri-substituted arene to planar-chiral ruthenium complexes, Scheme 1.16.[44]

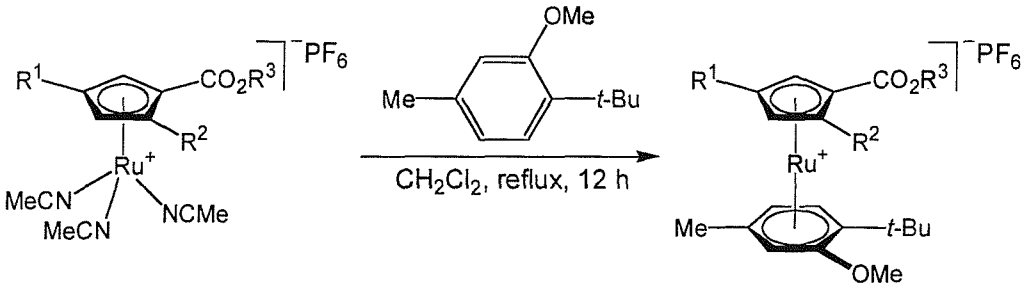

57a-e **58a-e**

a-e: see Table 1.2

Scheme 1.16

Table 1.2 shows selected results from the reaction between 2-*tert*-butyl-5-methylanisole and complex **57**, with varying Cp-substituents. In all cases some degree of induction of planar-chirality has been achieved, with the results of varying the substituents demonstrating that while R^1 seems to play little role in the stereochemical outcome of this reaction, R^2 and R^3 appear influential. This is the first report of effective transfer of planar-chirality from a Cp-ruthenium system to an incoming arene ligand.

Complex	R^1	R^2	R^3	Yield of **58**	d.e. of **58**
57a	Me	Me	Et	98 %	37 %
57b	Ph	Me	Et	98 %	38 %
57c	*t*-Bu	Me	Et	64 %	37 %
57d	Me	OEt	Et	43 %	26 %
57e	Me	Me	Cy	75 %	46 %

Table 1.2

Previous research within the Whitby group has led to the preparation of the chiral indene-phosphine bridged ligand **59**. This has been complexed to the rhodium dimers $[RhCl(CO)_2]_2$[29,45] and $[RhCl(C_2H_4)_2]_2$,[29] with some degree of face-selectivity on complexation, Scheme 1.17.

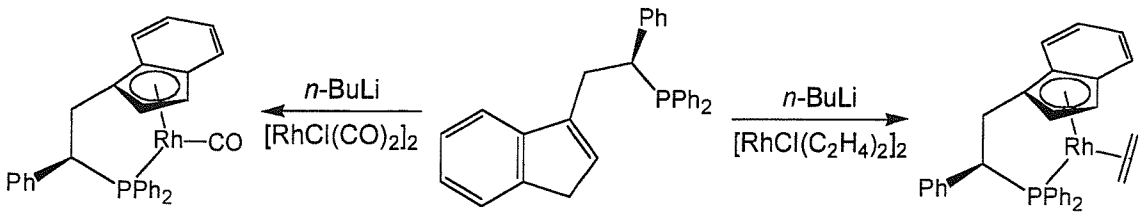

(-)-**60** 50 % d.e.
rac-**60** 43 % d.e.

(*S*)-**59**
rac-**59**

rac-**61** 40 % d.e.

Scheme 1.17

The fact that face-selectivity is seen to such a high degree as 50 % d.e. in complex (–)-**60** is particularly interesting, when considering that the chiral information is two carbon atoms removed from the indene ring whose stereochemistry it is controlling. This may be explained by the suggested mechanism of complexation of the related ligand $[Cp(CH_2)_2PPh_2]^-$ to $[RhCl(CO)_2]_2$, eluded by Poilblanc *et. al.*[20] The proposed mechanism suggests that complexation of the tethered phosphine group to the rhodium dimer occurs prior to chloride displacement by the indenyl anion. Since chloride displacement then takes place *via* a cyclic transition state, such as shown in Figure 1.7, the effect of the remote chiral phenyl substituent becomes reasonable. This mechanism may also explain the consistent small change in face-selectivity when the complexation is performed using the racemate of ligand **59**, since two ligands are suggested to bind to the rhodium dimer prior to displacement of the chloride ligand, and thus form a diastereomeric intermediate.

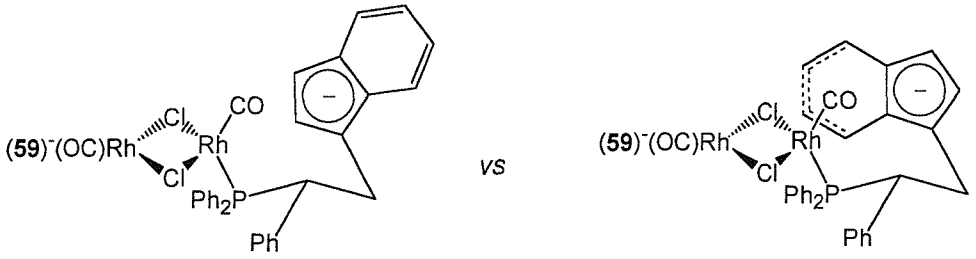

Figure 1.7

Complex **60** has been found to be an active catalyst in hydrosilylation reaction of acetophenone by $PhSiH_3$, with a small enantioinduction seen (up to 10 % e.e.).[29] Complex **61** has been used as hydrogenation catalyst in the hydrogenation of 2-phenyl-1-butene at 20 psi H_2.[29]

1.5 Induction of metal-centred chirality in chiral Cp-Rh/Ru complexes.

1.5.1 Induction of metal-centred chirality by non-planar-chiral Cp ligands

Complexation of the lithium salt of chiral ligand **10** to $RuCl_2(PPh_3)_3$ results in the generation of a new chiral centre at the metal atom, and so some degree of induction of chirality at the new centre may be observed. Upon complexation in 49 % yield, the two metal-centre diastereoisomers were isolated in a 59 : 41 ratio (18 % d.e.). This low selectivity can be attributed to the fact that the chiral information in the ligand is far removed from the new chiral centre.[9]

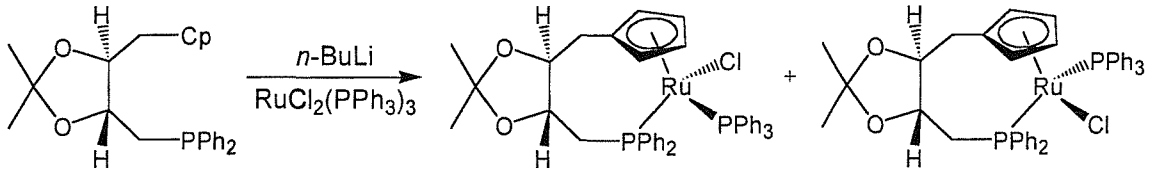

10 **62** 59 : 41

Scheme 1.18

Trost has also performed the reaction shown in Scheme 1.18, producing complex **62** with 20 % d.e.,[23] but then elaborated the complex to determine whether modification of the diol-protecting groups would influence this ratio of diastereoisomers, Scheme 1.19. Hydrolysis of the acetonide with aqueous hydrochloric acid in ethanol provided complex **63**, which retained the 20 % d.e. Subsequent formation of the dibenzyl ether complex **64** again resulted in unchanged 20 % d.e. However derivatisation with *tert*-butyldimethylsilyl triflate gave a 43 % d.e. of the bis-TBS complex **65**. The diastereoisomers of **65** were separated by preparative HPLC, and the individual diastereoisomers of **65** were found to isomerise upon warming to 80 °C, to restore the 43 % d.e. ratio, suggesting that this is the thermodynamic ratio of isomers.

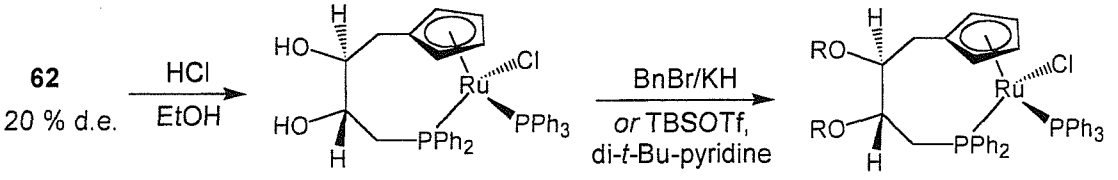

63 20 % d.e.

64: R = Bn, 20 % d.e.
65: R = TBS, 43 % d.e.

Scheme 1.19

Following the discovery of the isomerisation of complex **65**, Trost has investigated alternative ligands **66** and **68** which are specifically designed to achieve high stereoinduction at the metal centre upon complexation to ruthenium, Scheme 1.20.[23] Ligand **66** contains a chiral centre *alpha* to the phosphine group on the Cp-phosphorous linker and by being close to the metal centre, this should provide improved induction of metal-centred chirality upon complexation, whereas ligand **68** contains a very bulky dihydroanthraceno moiety as a steric barrier in order to enhance the stereocontrol upon complexation.

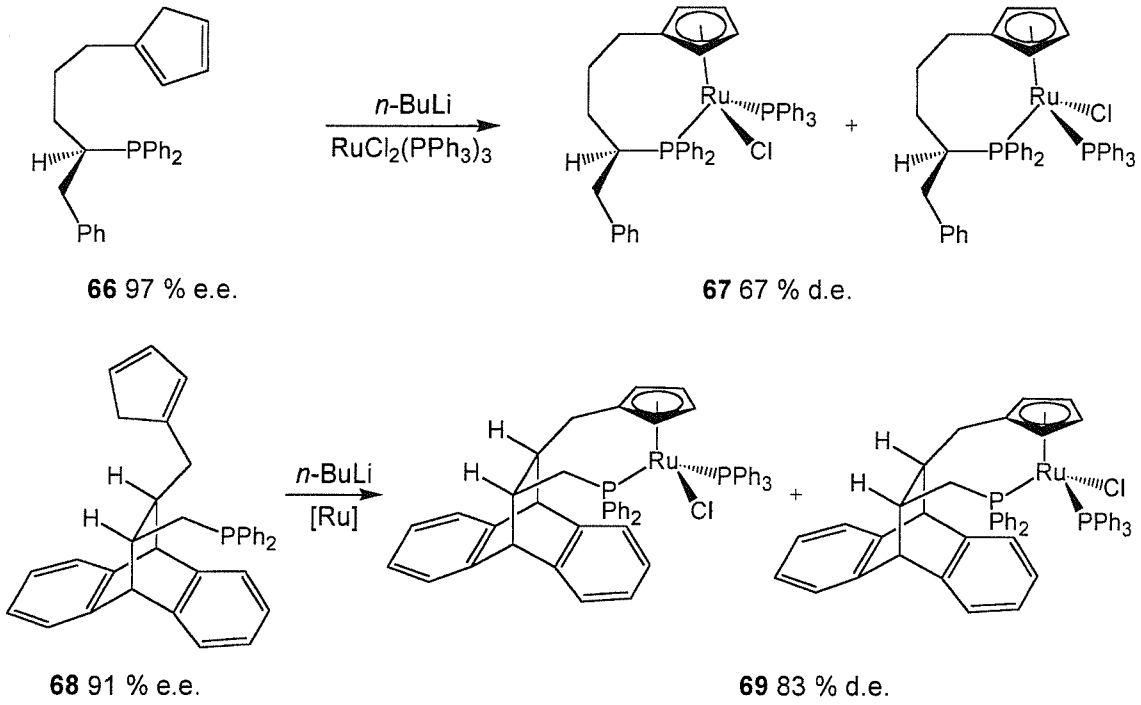

Scheme 1.20

Scheme 1.20 shows both ligands **66** and **68** were successful in achieving good metal-centre diastereocontrol upon complexation, particularly in complex **69**. These complexes were then used by Trost in the catalytic reconstitutive condensation reaction (detailed in Section 1.7).[23,46]

In an attempt to design a ligand which will be able to enforce a controlled stereochemistry at the metal centre of a complex during a catalytic reaction, Brunner has reported a new tridentate Cp-phosphine-pyridine ligand **70** and its ruthenium complex **71**, Scheme 1.21.[47] On complexation to ruthenium he reports a 92 % yield of an 85 : 15 ratio of the product complex and a "by-product with NMR similar to <the product>".[47]

Although he does not confirm that the by-product is the diastereoisomer of **70**, this is likely, and therefore the 85 : 15 ratio shows a 70 % d.e. on complexation.

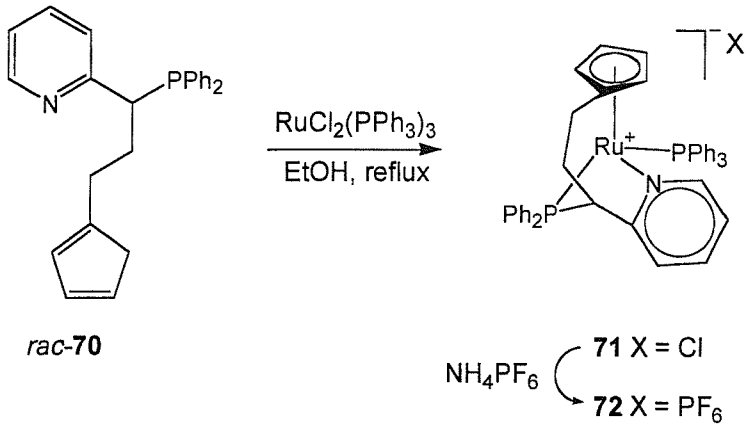

Scheme 1.21

Crystallisation of **72** provided the diastereomerically pure complex. Attempts to resolve the enantiomers, by reaction of **72** with the chiral phosphine ligand (*S*)-$PPh_2N(Me)CHMePh$ in refluxing ethanol, provided none of the expected diastereomeric product, but instead resulted in a new tris-phosphine complex, where the pyridine arm of the tridentate ligand had been displaced by a Ph_2POEt ligand. (The Ph_2POEt ligand is presumed to have formed by cleavage of the P-N bond from (*S*)-$PPh_2N(Me)CHMePh$ during the reaction in ethanol).

The chiral enantioenriched (66 % e.e.) Cp-phosphine ligand **73** has been prepared and complexed to ruthenium, Scheme 1.22.[48] The complex **74** is formed with 54 % d.e. induction of metal-centred chirality.

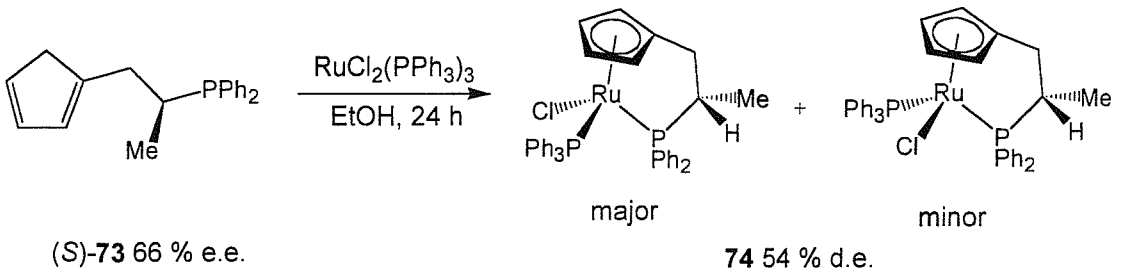

Scheme 1.22

Resolution by reaction of *rac*-**74** with AgOTf and chiral amine (*S*)-$H_2NCH(Me)Ph$ provided the four diastereoisomers in a 38 : 38 : 12 : 12 ratio, the same reaction with the

enantioenriched **74** provided the four diastereoisomers in a 64 : 13 : 19 : 4 ratio. However the configuration at the metal centre was found to be unstable with epimerisation occurring when the complex was stored in solution for several days (no final ratio of diastereoisomers is given, but it is noted that the complex decomposed after longer storage times). Owing to the epimerisation of the metal-centre, no attempt was made to separate the diastereoisomers.

1.5.2 Induction of metal-centred chirality by planar-chiral complexes

Continuing studies into planar-chiral complexes **20a-d** Tani has investigated the induction of metal-centred chirality by these planar-chiral complexes, upon their addition reaction with alkyl halides, Scheme 1.23.[49] The resulting rhodium(III) acetyl complexes **75a-d** were formed with a high degree of diastereo-control, as shown in Table 1.3.

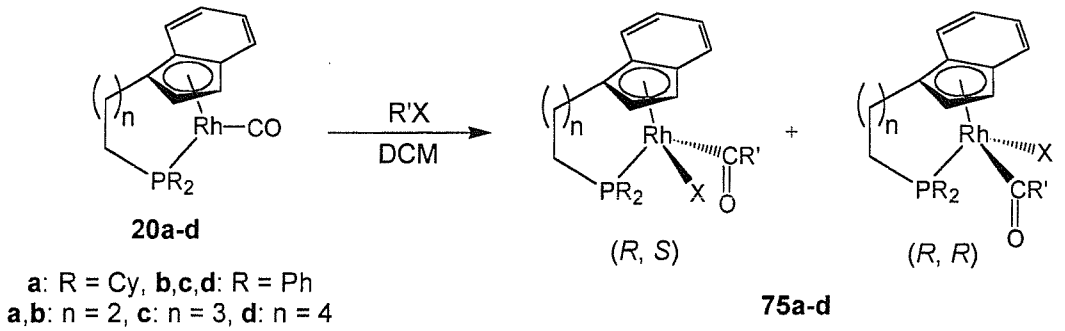

Scheme 1.23

Tani found that both the length of the Cp-phosphorous linker and the bulkiness of the incoming R′ group had a great influence on reactivity and stereochemical outcome. Complex **20b**, with the shorter two-carbon linker, proved more active than that with a four-carbon linker, **20d** (Table 1.3, reactions 2 and 5). This is suggested to be because of the smaller Indene(centroid)-Rh-P angle in complex **20b**, which would allow more reaction space at the metal than with the longer-chain complexes. However diastereoselectivity showed the opposite trend, with the more hindered three and four-carbon linked complexes **20c** and **20d** conferring higher stereochemical control on the resulting complex. Also interestingly, the three and four-carbon linked complexes gave the opposite metal-centred stereochemistry to that of either of the two-carbon linked complexes. Only addition reactions involving R′ = Me or Et successfully formed the acyl

complexes, with the smaller methyl group showing the greater reactivity and the ethyl group showing greater stereocontrol. Larger alkyl groups than ethyl failed to react, whereas more active groups such as allyl or benzyl halides reacted rapidly but produced many side-products.

Reaction	Complex	R′X	Time	Yield	*R, S* : *R, R*
1	**20b**	MeI	1 hour	90 %	33 : 67 (34 % d.e.)
2	**20b**	EtI	1 hour	83 %	4 : 96 (92 % d.e.)
3	**20c**	MeI	1 hour	97 %	89 : 11 (78 % d.e.)
4	**20d**	MeI	1 hour	92 %	85 : 15 (70 % d.e.)
5	**20d**	EtI	13 hours	77 %	98 : 2 (96 % d.e.)
6	**11**	MeI	1 hour	99 %	64 : 36 (28 % d.e.)

Table 1.3

As a comparison between the ability of planar-chirality and ligand-chirality to direct the stereochemical outcome of this reaction, Tani compared the addition reactions of methyl iodide to complex **20d** to the chiral-at-ligand Cp-phosphorous four-carbon bridged complex **11** (see Scheme 1.3).[9] The results showed that whereas both complexes achieved approximately the same conversion in one hour, the planar-chiral complex achieved 70 % d.e. in this reaction and the chiral-at-ligand complex **11** only achieved a 28 % d.e. This shows good evidence that the planar-chiral environment around a transition metal should much better control the stereochemistry of stoichiometric or catalytic reactions, compared to more 'remote' chirality seen in chiral-at-ligand complexes such as **11**.

In further work by Tani, the reactions of chiral neomenthyl and neoisomenthyl complexes **53**, **76** and **77** with alkyl halides were examined, Scheme 1.24.[41]

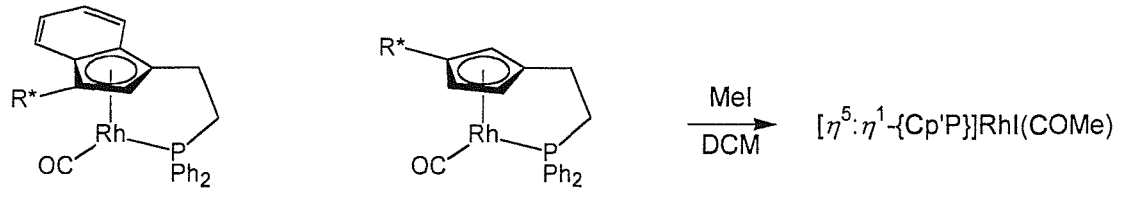

53 R* = neoisomenthyl
76 R* = neomenthyl

77 R* = neoisomenthyl

Scheme 1.24

Table 1.4 shows the results for the addition reaction of methyl iodide to complexes **53**, **76** and **77**. From these results it is clear that the indenyl complexes **53** and **76** provide much greater induction of metal-centred chirality, than the analogous Cp complex **77**. The improved selectivities can be attributed to the tetra-substituted Cp of the indenyl complexes being able to provide a tighter controlled stereochemical environment around the metal centre, than the di-substituted Cp complex.

Reaction	Complex	R′X	Time	Yield	*major* : *minor*	
1	**53**	MeI	2 hours	95 %	96 : 4	(92 % d.e.)
2	**76**	MeI	2 hours	93 %	98 : 2	(96 % d.e.)
3	**77**	MeI	1 hour	79 %	78 : 22	(56 % d.e.)

Table 1.4

An interesting comparison here is to compare the results of complexes **53** or **76** with that of the similar two-carbon linked indenyl complex **20b**, Table 1.3. Whereas complex **76** achieved an induction of metal-centred chirality of 96 % d.e., complex **20b** achieved only 34 % d.e. This demonstrates the benefits of the additional stereocentre-containing ligand substituent on **76**, in the outcome of this reaction.

In a further example of the stereochemical control of complexes of the neoisomenthyl ligand series, reactions of the product of the methyl iodide addition reaction to complex **53** have been investigated. Tani has shown that treatment of the methyl addition product **78** with $AgBF_4$ provides the methyl migration product, **79**,[41] with complete stereocontrol, Scheme 1.25.[50] This reaction has been shown to be reversible, again with complete stereo control, indicating that the stereo-controlled migration of the alkyl group to the carbonyl is likely to form part of the mechanism of addition of alkyl halides to rhodium carbonyl complexes. No evidence was found for carbonyl migration.[50]

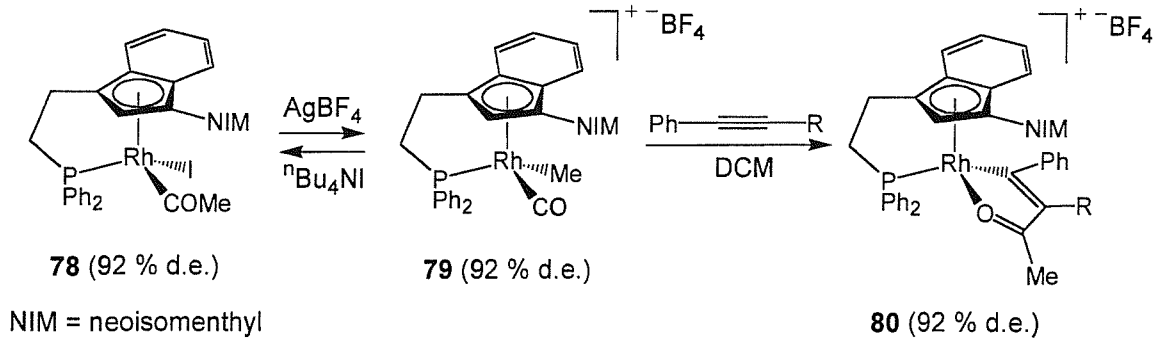

78 (92 % d.e.)

NIM = neoisomenthyl

79 (92 % d.e.)

80 (92 % d.e.)

Scheme 1.25

A reaction of the methyl migration product **79** has also been studied. As evidence to show the metal-centred chirality controlled by the {3-(neoisomenthyl)Ind$CH_2CH_2PPh_2$} ligand **52** is configurationally stable, complex **79** (in 92 % d.e.) has been reacted with 1-phenylpropyne, as shown in Scheme 1.25, to form the alkenyl complex **80**.[51] The stereochemistry of this reaction has been completely conserved, which is impressive considering the three-step mechanism involving methyl migration into the carbonyl, followed by rhodaacylation of the alkyne, then intramolecular co-ordination of the acyl oxygen to rhodium. Since four isomers from each diastereoisomer of **79** are possible, arising from metal-centred chirality and regiochemistry of the olefin, the reaction has the potential to provide eight isomers. However only two isomers are seen, one isomer from each diastereoisomer of **79**, with the same isomer ratio as **79** – thus metal-centred chirality did not racemise or epimerise throughout the reaction, and the regiochemistry of the olefin was completely controlled.

When this reaction was performed with the analogous complex containing no neoisomenthyl group, [[η^5:η^1-(Ind$CH_2CH_2PPh_2$)]Rh(CO)Me]BF_4 **75b** in 46 % d.e., some loss of stereocontrol was seen. Whereas the starting material contained a 73 : 27 ratio of isomers, the product of phenylpropyne addition gave a 69 : 24 : 5 : 1 mixture, indicating that the stereochemical environment about the metal is less effective when the fourth Cp-substituent is not present.

The same reaction was attempted with the related indenyl complex [Rh(Ind)(PPh_3)(CO)Me]BF_4, containing indene and phosphine groups not connected by a linker, and thus containing no planar-chirality or ligand chirality. However this complex did not react with phenyl-propyne at room temperature, which again demonstrates the difference in reactivities seen with the linked bidentate complexes.

Takahashi has investigated the multiple ligand transfer reaction between a Cp-iron complex **81** and planar-chiral Cp-ruthenium complexes **57a-c**, to form the planar-chiral and metal-centred chiral complexes **82a-c**, Scheme 1.26.[52]

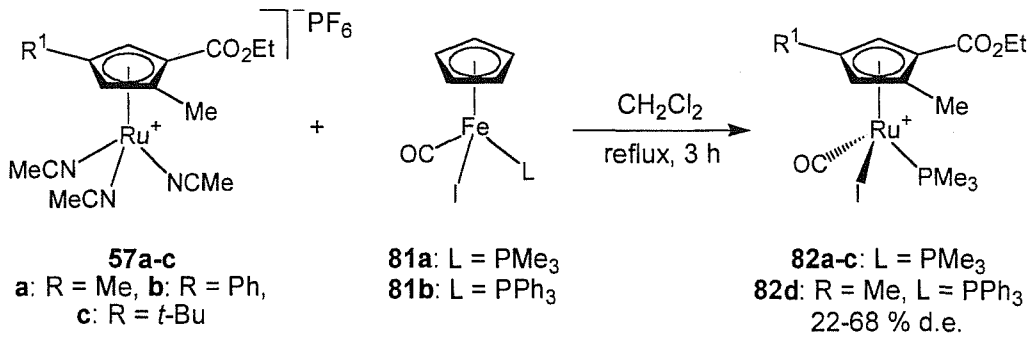

57a-c
a: R = Me, **b**: R = Ph,
c: R = *t*-Bu

81a: L = PMe_3
81b: L = PPh_3

82a-c: L = PMe_3
82d: R = Me, L = PPh_3
22-68 % d.e.

Scheme 1.26

The results from this reaction show that the planar-chiral cyclopentadienyl ligand on ruthenium is effective at inducing metal-centred chirality in the product of the ligand transfer reaction. The yield and extent of induction was found to depend on the incoming phosphorous ligand and Cp-substituents. Interestingly in this example, the highest induction of metal-centred chirality occurs when the Cp-substituent at R^1 is smallest, i.e. methyl, and the incoming phosphine is trimethylphosphine. Use of larger Cp-substituents such as phenyl or *tert*-butyl, led to reduced diastereoselectivity, and a bulkier incoming ligand, triphenylphosphine, showed lower selectivity and reaction yield. No discussion of the mechanism of asymmetric induction was given.

The chiral ruthenium complexes **82a-d** showed no isomerisation at the metal-centre, under the reaction conditions, suggesting the diastereoselectivity in the reaction product is kinetically controlled. This is in contrast to that found for similar mono-Cp-iron complexes containing the same planar-chiral Cp ligands,[53] where metal-centred chirality was induced by a phosphine ligand substitution reaction. In the case of the iron complexes, isomerisation at the metal centre was found to occur readily under the reaction conditions, suggesting thermodynamic control of the selectivity.

Takahashi has examined the induction of metal-centred chirality by the planar-chirality of ruthenium complexes **39a-c** containing Cp-phosphine bidentate ligands, during an acetonitrile/phosphine ligand exchange reaction, Scheme 1.27.[54]

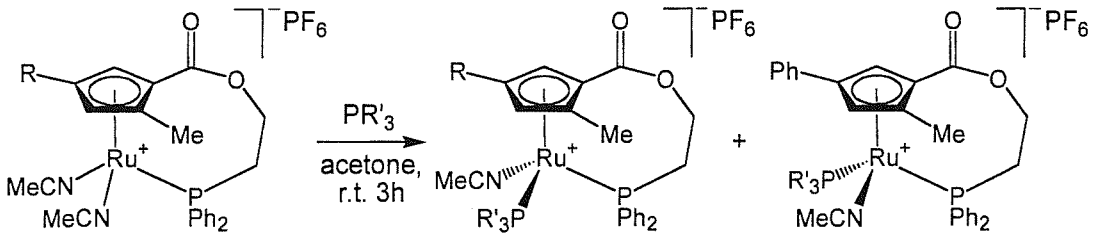

39a-c
a R = Me; **b** R = Ph; **c** R = *t*-Bu

major

minor

83 38-99% d.e.

Scheme 1.27

The reaction was performed using a variety of phosphine and phosphite ligands, and in almost all cases this reaction was seen to proceed with quantitative yield. Clear trends in the stereochemical outcome of the reaction were also evident. In particular, where the R-substituent on the Cp-ligand was bulky (**39c**, R=*t*-Bu), or the incoming phosphine ligand contained bulky groups (such as PPh_3 or PBu_3), the highest diastereoselectivities were observed. Selectivities were reduced where the Cp-substituent R=Me or the phosphine ligand PMe_3 was used, and the phosphite ligands $P(OMe)_3$ and $P(OPh)_3$ only achieved high selectivities where the Cp-substituent R=*t*-Bu was used.

The products of the reaction of triphenylphosphine with **39a** and **39b** were found to slowly isomerise at the metal-centre in solution at room temperature, suggesting that for these products the selectivity was controlled by thermodynamics. None of the other products showed this isomerisation, indicating that they are likely to be the kinetically controlled products.

The induction of metal-centred chirality during the reaction of planar-chiral complexes **39a** and **39b** with bidentate salicylideneaminato ligands **84** has been examined, Scheme 1.28, and found to show very high diastereoselectivities.[55]

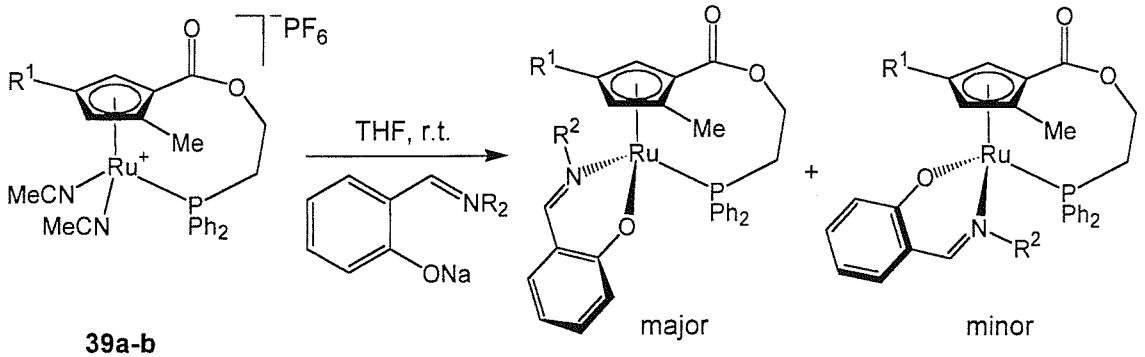

39a-b
a R = Me; **b** R = Ph

84

major

minor

85 44-99% d.e.

Scheme 1.28

The selectivity in the reaction of complexes **39a-b** with ligands of type **84**, was found to depend primarily on the steric interactions between the R^1-Cp substituent and the R^2-N substituent. In the case where either of these substituents are a phenyl ring, the selectivity at the metal centre is very high (>90 % d.e.) and where both R^1 and R^2 are phenyl, only a single diastereoisomer is produced (>99 % d.e.). The reaction yield is also affected by these changes, increasing from 54 % to 67 % when changing from R^2=methyl, R^1=phenyl to R^1=R^2=phenyl. Changing both R^1 and R^2 to methyl groups, results in a large drop in selectivity, to only 48 % d.e. and a small decrease in yield. Substitution of R^2 with an *iso*-propyl group (where R^1=methyl) has little effect on the low selectivity, but further reduces the reaction yield to only 11 %. It is postulated that *pi*-stacking between the two phenyl rings, where R^1=R^2=phenyl, and a phenyl/methyl CH-*pi* interaction where either R^1 or R^2=phenyl, may account for high diastereo-selectivity in these cases.

Single diastereoisomers of the product complexes **85**, were found to slowly epimerise at room temperature in chloroform, and more rapidly in THF or benzene, suggesting that the selectivity of these products is under thermodynamic control.

Further evidence of the importance of the Cp-phosphine tether is also given by this reaction, when the procedure was repeated using a non-tethered analogues of **39a-b** (containing an ethyl ester, in place of the Cp-phosphorous linking ester, and a triphenylphosphine group as the phosphine ligand). In this case, the selectivity on complexation of ligand **84** (R^2=methyl) was reduced to 22 % d.e. for R^1=methyl (**a**) and only 5 % d.e. where R^1=phenyl (**b**).

Hidai has reported the complexation of chiral ferrocene Cp-phosphine bridged ligand **15** to ruthenium, as shown in Scheme 1.29.[25]

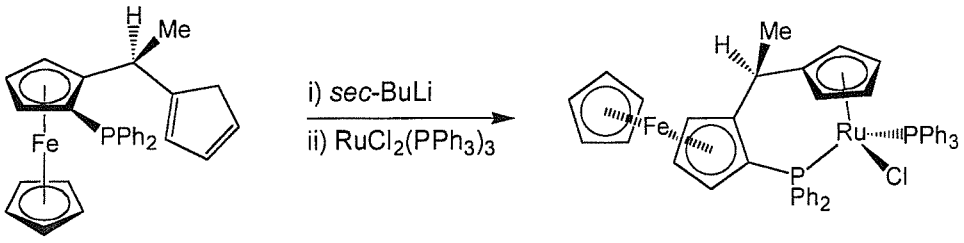

15

86 75 % yield and
100 % d.e. after crystallisation

Scheme 1.29

The complexation of **15** is reported to provide a single diastereoisomer of complex **86**, in 75 % yield, after recrystallisation from ethanol. No mention of the ratio of diastereoisomers prior to recrystallisation is given. Complex **86** has been used as a catalyst and stoichiometric mediator of the Trost's 'reconstitutive condensation reaction',[23] which is discussed in detail in Section 1.7.

Ganter *et al.* have also reported high induction of metal-centred chirality on formation of ferrocene-linked Cp-phosphine complexes **87** and **88**, Figure 1.8.[56] In the case of complex **88**, ^{31}P NMR of the crude material shows that a single diastereoisomer results on complexation of the precursor ligand, which is isolated in 68 % yield.

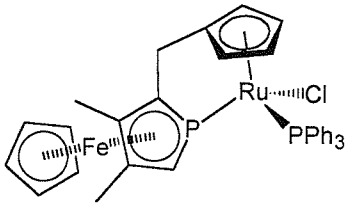

87 63 % yield (90 % d.e.)

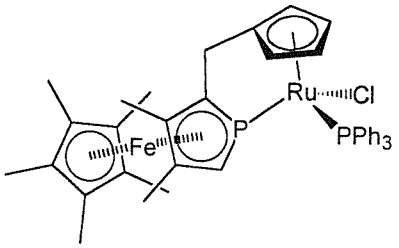

88 68 % yield (>98 % d.e.)

Figure 1.8

Ganter found that conversion of the Cp*-ferrocene substituted complex **88** to its hydride complex, by substitution of the chloride ligand upon reaction with MeOH and NaOMe, gave the Ru-H complex as a single diastereoisomer. Conversion of the hydride complex back to the chloride complex **88** by reaction with chloroform retained the >98 % d.e. of the initial complex. However, the same reactions performed with the sterically less-demanding Cp-ferrocene substituted complex **87** gave a 1 : 1 mixture of metal-centre isomers for the hydride complex, but conversion back to the chloride complex **87** was found to be under thermodynamic control, returning the 90 % d.e. on heating to 90 °C in toluene.

1.6 Induction of planar-chirality and metal-centred chirality on complexation of ligands.

Trost has recently reported two diastereotopic Cp-ligands which show some degree of face-selectivity upon complexation to ruthenium, Scheme 1.30.[23] Ligand **89** reacted with

$RuCl_2(PPh_3)_3$ to form the complex **90** as two diastereoisomers in 23 % d.e. Considering that metal-centred chirality and planar-chirality arise from this complexation, Trost has assigned the 23 % d.e. to the planar-chiral isomers (and thus complete control of metal-centre chirality), by analogy to the high degree of metal-centred control observed with similar complexations not involving planar-chirality in his report.[23]

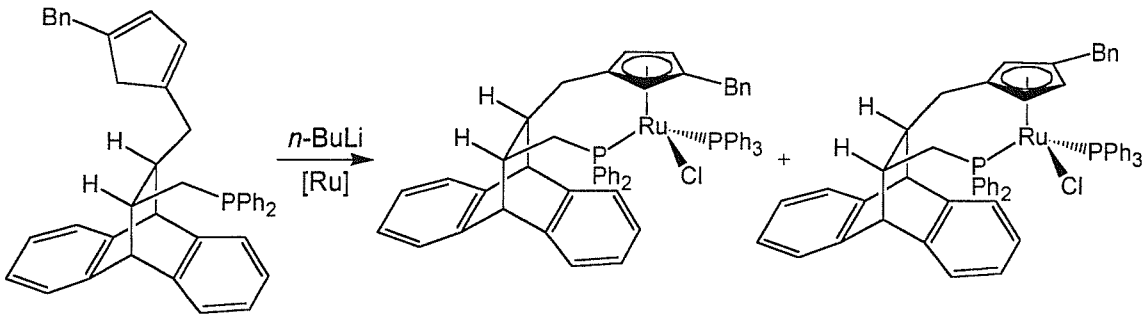

89 91 % e.e. **90** 23 % d.e.

Scheme 1.30

Trost also reports the preparation of planar-chiral complex **92**,[23] however the stereocontrol upon complexation was poor, resulting in a complex mixture of four diastereoisomers (both planar-chiral and metal-centred chiral) and no d.e. could be calculated.

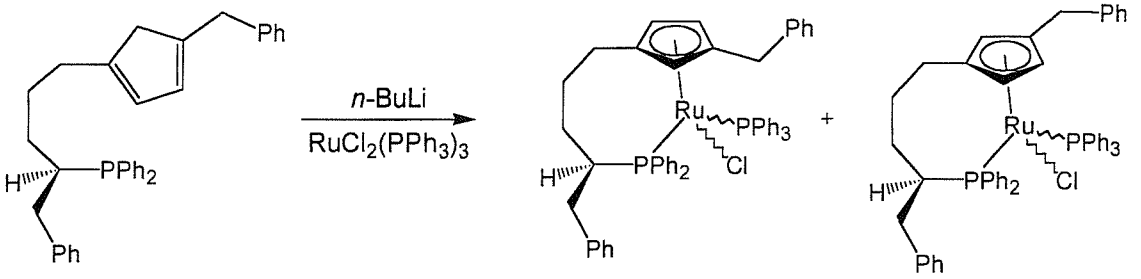

91 97 % e.e. **92** complex mixture

Scheme 1.31

The racemic planar-chiral complex **94**, formed upon complexation of ligand **93** to ruthenium, has also been reported, Scheme 1.32.[23] No stereo-control was seen at the metal centre for this reaction, and thus a 1 : 1 mixture of diastereoisomers resulted. Complexes **90**, **92** and **94** have been found to catalyse the catalytic 'reconstitutive condensation reaction' (detailed in Section 1.7).[23,46]

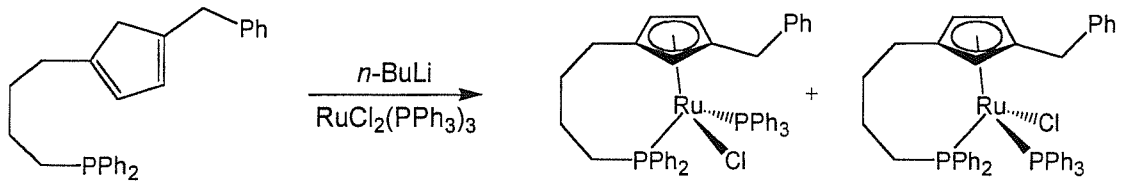

93 **94** 1:1 mixture of diastereoisomers

Scheme 1.32

Takahashi has examined the complexation of pro-chiral dienes to the planar-chiral Cp-phosphine complex **39b**, which involves the induction of metal-centred chirality at ruthenium and planar-chirality of the incoming diene ligand, Scheme 1.33.[57]

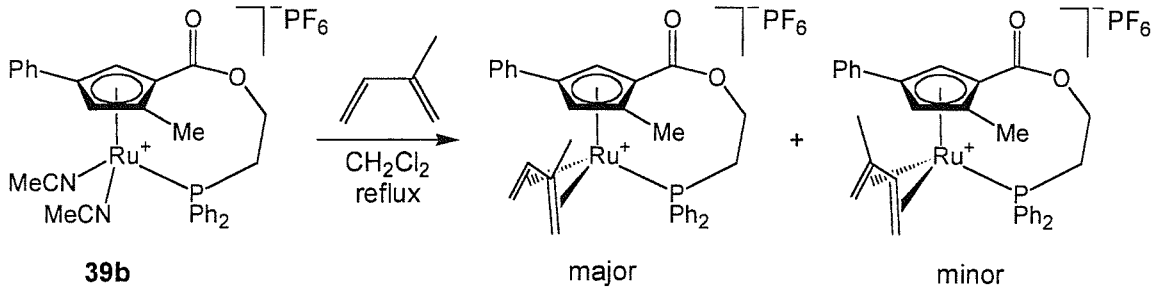

39b major minor

95 86% d.e.

Scheme 1.33

The reaction shown in Scheme 1.33 proceeded to provide **95** as two diastereoisomers (of a possible four), with a d.e. of 86 %. NMR and x-ray structure analysis showed the metal-centred chirality and orientation of the isoprene ligand to be as shown above for the two isomers, neither of the two isomers containing the inverted isoprene ligand, with the methyl group directed away from the Cp, were detected. This shows that the planar-chiral environment created by the tri-substituted Cp-phosphine ligand is effective in inducing metal-centred chirality, and planar-chirality of the incoming diene ligand. It is likely that the face-selectivity of the diene ligand is primarily controlled by the steric interactions between the methyl group of the isoprene ligand, and the bulky phenyl- (minor isomer) or less-demanding hydrogen-substituent (major isomer) of the Cp-ligand. It is also likely that the bulky diphenylphosphine ligand plays some role in assisting the stereochemical outcome of the reaction.

An interesting result was found when this reaction was carried out using the related complex **57b**, which contains a planar-chiral mono-dentate Cp with the same phenyl- and methyl-substituents as **39b**, but with an ethyl ester replacing the linking chain to a

phosphine group. In the case of **57b**, with no Cp-phosphine tether is present, the d.e. of the reaction with isoprene is reduced to on 44 %. This demonstrates the importance of the Cp-phosphine tether in controlling stereo-environment around the metal, without it the Cp ligand is able to rotate around its bonding axis during the course of the reaction, thus lowering the overall selectivity.

The reaction of Cp-phosphine linked complex **39b** with alternative dienes, 1,3-pentadiene, 1,3-hexadiene and 2,4-hexadien-1-ol was also performed, however much lower selectivities resulted (36 %, 36 %, 18 %, respectively). This is not surprising as these dienes do not contain a substituent in the same position as the methyl group of isoprene, therefore the same influential interaction with the phenyl-substituent of the Cp-ligand is not possible.

1.7 Catalysis by indene phosphorous containing Rh/Ru complexes

Ruthenium catalysed reactions have been recently reviewed.[16] The remainder of this introductory chapter shall review the catalytic applications of indene phosphorous containing rhodium and ruthenium complexes, with some relevant asymmetric catalysis by chiral cyclopentadienyl phosphorous complexes included owing to the limited number of chiral indene phosphorous catalysed reactions.

Ruthenium-indene complex $RuCl(Ind)(PPh_3)_2$ has been found to be an active catalyst for the olefin cyclopropanation of styrene by ethyl diazoacetate, Scheme 1.34,[58] although the analogous Cp complex $RuCl(Cp)(PPh_3)_2$ proved more active in this transformation.

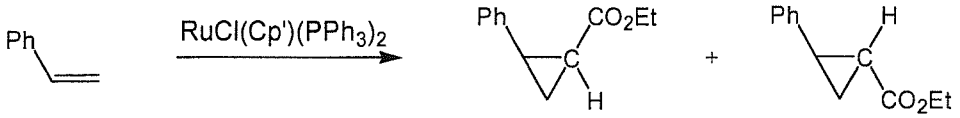

Cp' = Ind 60% (2.1 : 1)
Cp' = Cp 85% (1 : 1.9)

Scheme 1.34

Planar-chiral rhodium menthyl-indene complex **96** has been applied to catalytic asymmetric hydrogenation of itaconic acid, Scheme 1.35.[59] Although a quantitative yield of the hydrogenated methylsuccinic acid resulted, it was obtained in only 18 % e.e., which can be considered very poor induction of chirality considering the presence of both

planar-chirality and ligand chirality in the catalyst. The related complex, (–)-[(COD)(η^5-2-menthyl-4,7-dimethylindenyl)Rh][60] which contains the same menthyl group as **96**, however linked to the indene at the 2-position rather than the 1-position and thus not planar-chiral, was also active in this hydrogenation, achieving a similar 16 % e.e. in the product. From these two results we can see the presence of planar-chirality in this case has not significantly contributed to enantioinduction during the reaction. This may be due to ability of the indenyl ligand in **96** to freely rotate about the Cp-Rh bonding axis during the catalytic cycle. This rotation would effectively scramble any metal-centred stereochemistry that may be achieved by an intermediate in the catalytic cycle (this is known to occur during induction of metal-centred chirality by related planar-chiral complexes).[55,57]

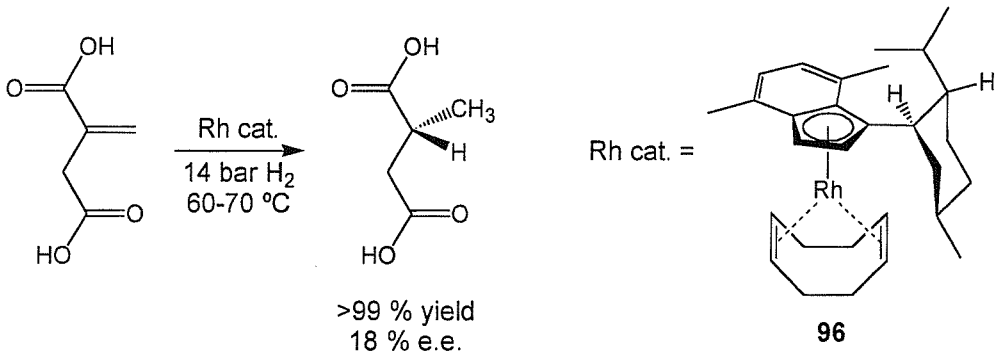

Scheme 1.35

Trost has found the indenyl-ruthenium catalyst [IndRu(PPh_3)$_2$Cl] to be very effective in the ruthenium catalysed redox isomerisation of allyl alcohols, Scheme 1.36.[61] The catalyst and it's Cp-analogue were effective for a variety of isomerisations, with the indenyl catalyst showing greater reactivity than the Cp catalyst in most cases, although somewhat reduced chemoselectivity where secondary mono-substituted olefins or proximal diols are a feature of the substrate.

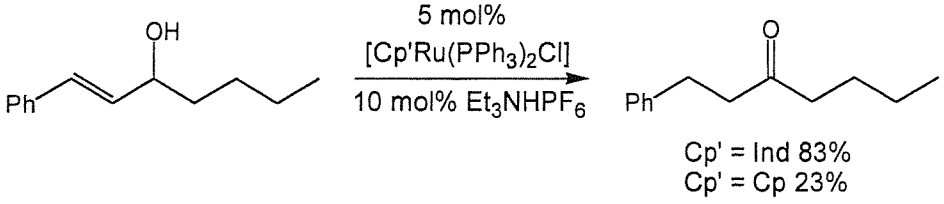

Scheme 1.36

The enhanced reactivity of indenyl complexes compared to their cyclopentadienyl analogues is well known, and has been termed the 'indenyl ligand effect'.[62] The reason behind this increase in reactivity is the ability for an η^5-bound indenyl ligand to 'ring-slip' to form an η^3-bound species during catalysis, owing to the stabilisation by the indene-aromatic ring, Scheme 1.37.[31] This effectively opens up a new co-ordination site on the metal centre, and thus lowers the energy barrier to become involved in catalysis. Numerous studies of this effect have taken place for different transition metals, for example ruthenium[63], iridium,[64] rhodium[65] and iron[66] with many indenyl catalysts having been reported as being vastly superior to their cyclopentadienyl analogues, including several rhodium-indenyl catalysts.[67-69]

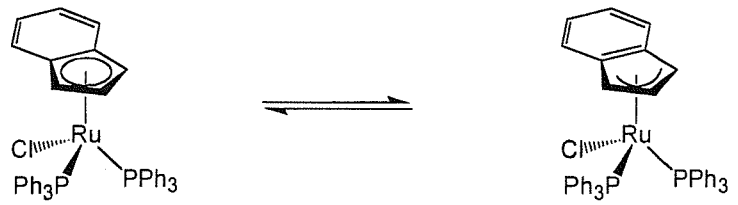

Scheme 1.37

Trost has developed the ruthenium-Cp catalysed addition of a terminal alkyne to an allyl alcohol to generate an α-alkylated-β,γ-unsaturated ketone, termed 'reconstitutive condensation', Scheme 1.38.[23,46,70]

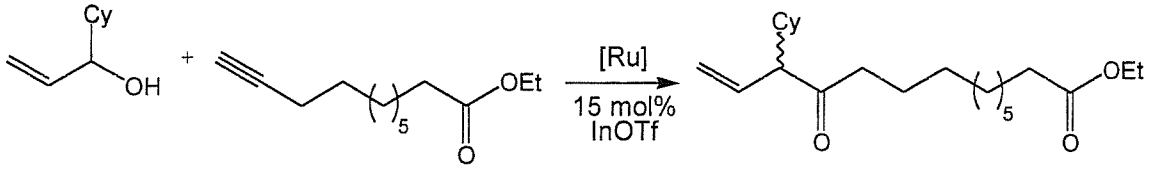

97 **98** **99**

Scheme 1.38

The initial reports of this reaction used the cyclopentadienyl catalyst, $[CpRu(PPh_3)_2Cl]$ along with co-catalyst ammonium hexaflurophosphate to effect the transformation of 1-tridecyne and 3-buten-2-ol to give 3-methyl-1-decen-4-one in 63 % yield.[46] Chapter 5 contains a further discussion of this reaction catalysed by non-chiral complexes.

Table 1.6 shows the results of the reconstitutive condensation reaction performed using several chiral Cp complexes.[23] The results show disappointing enantioinduction by these complexes and although some of the chiral complexes used in the study were mixtures of

diastereoisomers (either planar-chiral of metal-centred) there appeared to be little correlation between degree of diastereo-purity of the catalyst and enantioinduction in the product (for example reactions 2 and 5). The diastereomerically pure complex **65** was also tested, but proved to be unreactive.

Reaction	Complex	Stereochemistry of complex	% Yield	% e.e.
1	**90**	23 % d.e. (planar), 100 % d.e. (metal)	45	30
2	**62**	20 % d.e. (metal), 100 % e.e. (ligand)	72	11
3	**64**	20 % d.e. (metal), 100 % e.e. (ligand)	56	14
4	**67**	67 % d.e. (metal), 97 % e.e. (ligand)	45	25
5	**69**	83 % d.e. (metal), 91 % e.e. (ligand)	61	11

Table 1.6

An interesting result for the reconstitutive condensation reaction has been reported by Hidai,[25] whereby a 10 % yield and 25 % e.e. of product **102** resulted from the reconstitutive condensation reaction shown in Scheme 1.39, catalysed by complex **86.** However when the reaction was performed stoichiometrically, by isolating the initial vinylidene intermediate complex and treating it with the allyl alcohol, a yield of 40 % resulted, with an enantioinduction of 65 % e.e. in the product. This demonstrates the difficulty of designing a suitable asymmetric catalyst for complex catalytic reactions such as the reconstitutive condensation reaction which can involve many stereogenic intermediates in the catalytic cycle.

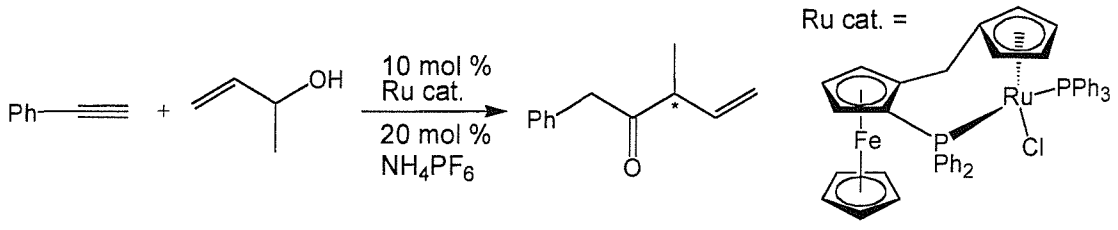

100 **101** **102** **86**

10 % yield, 25 % e.e.

Scheme 1.39

In his previous work, Takahashi has shown complexes **39a-c** provide a well controlled stereochemical environment, able to induce both metal-centred chirality[54] and planar-chirality[57] during ligand exchange reactions. The success of the stereochemical control of

these complexes in stoichiometric reactions make them ideal for trials in asymmetric catalytic reactions. Unsurprisingly therefore, Takahashi has recently reported their use in the first successful asymmetric ruthenium-catalysed allylic amination/alkylation reaction, which is the first example of asymmetric catalysis by a late-transition metal complex that uses planar-chirality as its only source of chirality, Scheme 1.40.[71]

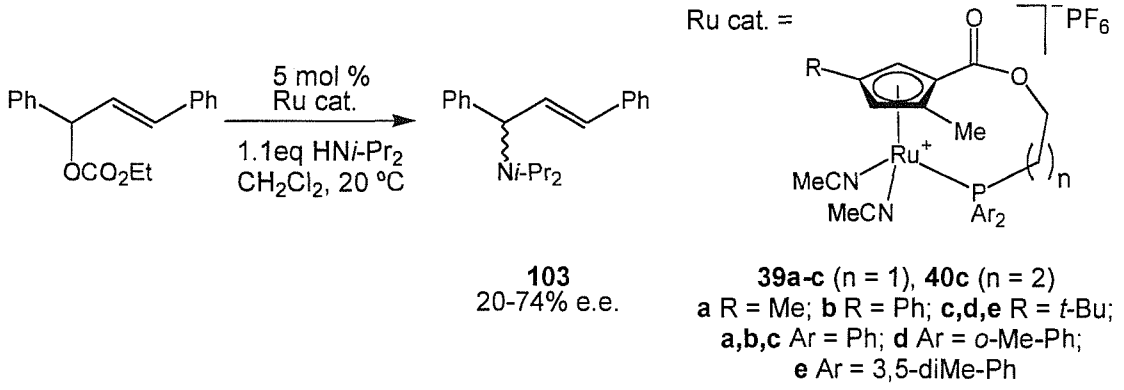

103
20-74% e.e.

39a-c (n = 1), **40c** (n = 2)
a R = Me; **b** R = Ph; **c,d,e** R = *t*-Bu;
a,b,c Ar = Ph; **d** Ar = *o*-Me-Ph;
e Ar = 3,5-diMe-Ph

Scheme 1.40

In the case of all the complexes used, the yield of this reaction was generally high (>90 %), Table 1.7 shows some representative results. From these results, it can be seen that the R group on the Cp-ring plays an important role in the stereochemical control of the reaction. Increasing the steric bulk of the R group results in an increased enantioinduction in the product, favouring the (+)-enantiomer. The change from R=Me to R=Ph brings with it a reversal in the sign of the favoured enantiomer, which suggests there are opposing areas of stereochemical control within the complex, and that by increasing the bulk of the R group, this becomes the dominating factor.

Switching from n=1 to n=2 (i.e. from a 4-atom linker between Cp and phosphorous to a 5-atom linker), results in a slight decrease in the enantioinduction, showing that the linker also plays an important part in the stereochemical environment of the catalyst.

Reaction	Complex	R	n	% Yield	% e.e.
1	**39a**	Me	1	97	35 (–)
2	**39b**	Ph	1	90	20 (+)
3	**39c**	*t*-Bu	1	99	64 (+)
4	**40c**	*t*-Bu	2	94	56 (+)

Table 1.7

When the reaction was performed using the related Cp complex **57c**, which contains no Cp-phosphorous tether substituent – but has an ethyl ester in its place and retains the R=*t*-Bu and methyl-substituents of **39c**, high enantioselectivity (65 % e.e.) was retained. This was surprising, considering the results of a previous study of the stereochemical control induced by bidentate complexes **39** compared to non-tethered complexes **57**,[57] showed that removal of the tether markedly reduced the stereochemical control (*cf.* see Section 1.6, Scheme 1.33 and discussion). This again re-enforces the fact that many different factors govern the stereochemical control in these different reactions, and the results from one reaction may well differ from those of another reaction.

The best results for the allylic amination reaction were found to be with complex **39e** as the catalyst. This complex combines the best R-substituent (R=*t*-Bu), optimum linker chain length (n=2) and adds a more bulky aryl group to the phosphine moiety (Ar=3,5-dimethylphenyl). In this case an e.e. of 74 % (+) was induced on the product of the amination reaction, and demonstrates a further influential factor on the selectivity of the catalyst.

No racemisation of the product of the amination reaction was seen in the reaction mixture, suggesting the enantioselectivity seen here was controlled kinetically.

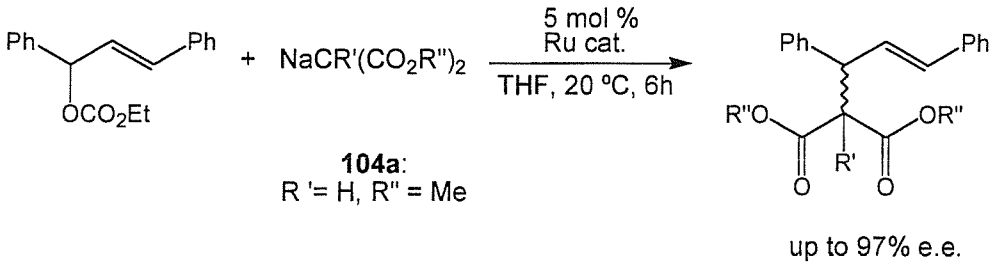

Scheme 1.41

The allylic alkylation reaction shown in Scheme 1.41 was also examined using the same catalysts as for the amination reaction (see Scheme 1.40).[71] This reaction again showed very high yields for the catalysts **39a-e**, however variations to the Cp-phosphorous tether proved to have a large effect on this reaction. When the tether length was extended to n=2, the yield of the catalytic reaction dropped from approaching quantitative yield (97 %) for complex **39c**, to only 14 % for complex **40c**. The effect was even greater when the tether was removed completely (complex **57c**), which resulted in almost complete shutdown of the reaction (3 % yield). The enantioselectivities suffered in the same way when the tether was altered.

For the complexes **39a-e**, the enantioinduction on the products of reaction with nucleophile **104a** were all very good, ranging from 80-97 % e.e. These were seen to decrease slightly when the nucleophile was altered to R′=R′′=Me (as did the reaction yield), but still remained very reasonable (63-83 % e.e.). In contrast to the amination reaction, use of the more bulky aryl groups on the phosphorous atom, failed to impact significantly on the e.e.'s seen here. However the highest selectivity, 97 % e.e., was seen with complex **39d**, which contains *o*-methylphenyl groups on the phosphine.

Park has found the indenyl ruthenium complex **105a** to be a very effective catalyst in the racemisation of chiral secondary alcohols, Scheme 1.42.[72]

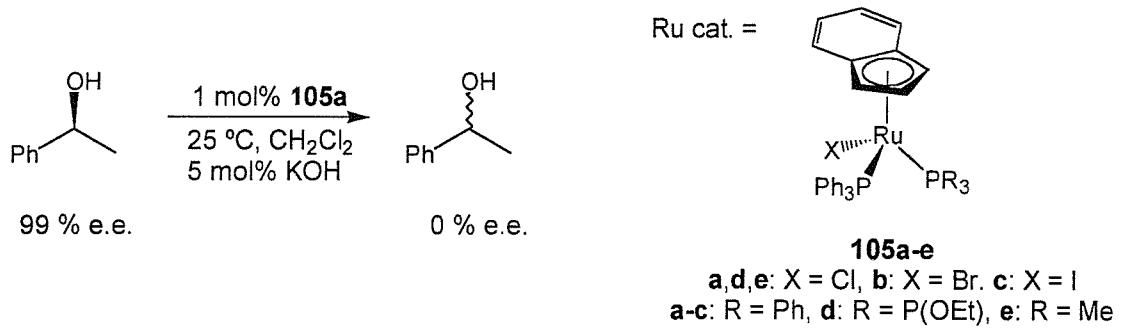

Scheme 1.42

Various indenyl-ruthenium complexes were tested in this reaction, **105a** was found to be the most active catalyst, completely racemising an enantiopure solution of (*S*)-1-phenylethan-1-ol in 20 minutes. The racemisation rate was reduced slightly by exchanging the bound chloride ligand on **105a** with bromide **105b** or iodide **105c**. Exchanging one of the triphenylphosphine ligands for a triethylphosphite ligand, **105d**, significantly slowed the reaction rate and changing to the more electron donating trimethylphosphine **105e** resulted in almost complete shutdown of the catalytic cycle. Use of the cyclopentadienyl analogue [CpRuCl(PPh_3)$_2$] as the catalyst gave a slightly slower reaction rate compared to **105a**, with the enantiopure alcohol (*S*)-1-phenylethan-1-ol converted to 16 % e.e. after 20 minutes.

Several alcohols were tested in the reaction, with success also seen for non-benzylic alcohols, although at a reduced rate. A mechanism for the racemisation has been proposed whereby the Ru-H species formed upon displacement of the chloride ligand of **105a**, is the reactive intermediate.

Combination of this racemisation reaction with enzymatic acylation has achieved success as a method of generating chiral acetates in high yields and e.e.'s, Scheme 1.43.[73]

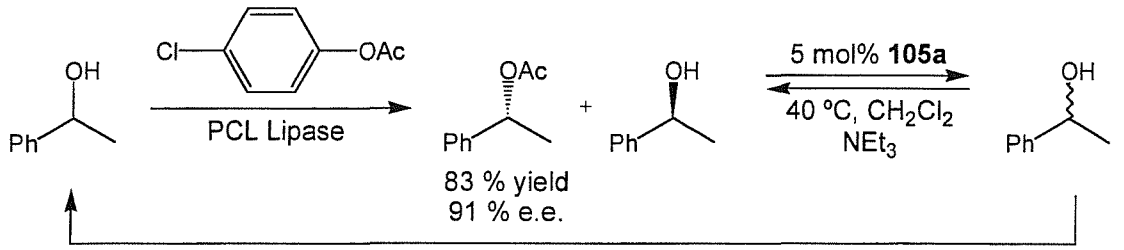

Scheme 1.43

The chiral indene biphop-F (biphop = 1,2-bis[bis(pentafluorophenyl)phosphanyloxy]-1,2-diphenylethane) ruthenium complex **106**, has been used as an effective asymmetric catalyst of the Diels-Alder reaction of methacrolein and cyclopentadiene, Scheme 1.44.[74]

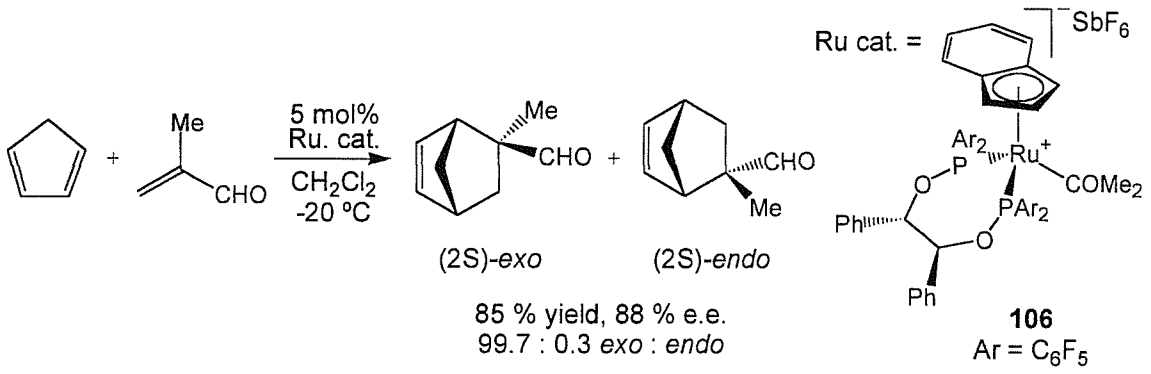

Scheme 1.44

Several indenyl complexes containing varying counter ions and chiral bis-phosphorous ligands were examined for this reaction. Compared to analogous Cp-bis-phosphorous complexes, the exo : endo selectivity was an order of magnitude greater. The reaction rate with these indenyl complexes was generally increased compared to analogous Cp complexes and the variations in rate with different counter ions was less than seen with the Cp analogues. The complexes were also demonstrated to be recovered in high yield from the reaction mixture.

1.8 Conclusions

At the outset of this Ph.D. research, there had been no published examples of the use of non-metallocene planar-chiral complexes of late transition metals as catalysts of organic transformations. The primary reason for this being the lack of convenient syntheses of such enantiopure planar-chiral complexes, with the few published synthetic routes involving long procedures and requiring resolution of enantiomers of the final complexes.[10,12,13] However, this area of chemistry looked very promising, with several new reactions catalysed by later-transition metal complexes being reported.[16]

The aim of the research detailed herein has been to extend the successful ligand design concepts and complexation model (see Chapter 2), developed within our group for preparation of planar-chiral zirconocene catalysts,[17] and apply this model to the design of planar-chiral late-transition metal complexes, with the intention of preparing novel planar-chiral catalysts. Chapters 2 and 3 of this thesis describe the design, optimisation and synthesis of a series of new ligands following our extended design concepts. Chapter 4 details the results of complexation of these ligands to rhodium and ruthenium, to form planar-chiral and metal-centred chiral complexes. Chapter 5 reports our initial attempts at the use of the new complexes as catalysts of organic transformations.

As can be seen from the literature review section, over the course of this Ph.D., the design of planar-chiral late-transition metal catalysts has proved a popular area of research, with several recent publications detailing new syntheses of enantiopure planar-chiral complexes[36,41] and applications of planar-chiral complexes in asymmetric catalysis of organic reactions.[23,71] It is hoped that the research carried out during this Ph.D. shall add to this important area of chemistry.

2. Chapter 2: Synthesis of novel chiral bidentate indenyl-phosphine ligands containing a two-carbon bridge.

2.1 Background

2.1.1 Planar-chiral complexes by face-selective metallation

The literature review in Chapter 1 includes descriptions of the few preparations of enantiomerically and diastereomerically pure planar-chiral Cp-rhodium and Cp-ruthenium transition metal complexes which have been reported to date. These preparations involve either the resolution of planar-chiral enantiomers by chiral chromatography,[33] the resolution of planar-chiral diastereoisomers by fractional crystallisation[10] or chromatography,[12] and the controlled induction of planar-chirality by face-selective metallation of the chiral ligand.[41]

The last of these techniques has the benefit of avoiding costly and often wasteful resolution and chromatography methods, by incorporating a chiral design into the ligand that enables preferential complexation of the metal to only one face of the pro-chiral cyclopentadiene. Such a design is shown in Figure 2.1, here the presence of three different-sized substituents (R^L, R^S, H) form a chiral centre next to the Cp-ring. The differing steric demand of these substituents will result in one face of the cyclopentadiene being effectively blocked by the large R^L group in its lowest energy rotamer about the Cp-chiral-centre bond. This should lead to metallation occurring preferentially on the more accessible Cp face, with the ideal outcome being formation of only a single diastereoisomer of the resulting planar-chiral complex. This 'favoured rotamer' complexation model has found success as the basis for the design of several chiral ligands.[38]

Figure 2.1

Erker's neomenthylindene ligand **107** is a prime example of a chiral ligand which exploits the 'favoured rotamer' complexation model in order to achieve a high induction of planar-chirality on complexation to a transition metal.[75] The C2-symmetric complex **108** was prepared from Li-**107**, in a 93 : 2 : 5 ratio of diastereoisomers, demonstrating the effectiveness of the 'favoured rotamer' about the indene-neomenthyl bond in controlling face-selective metallation.

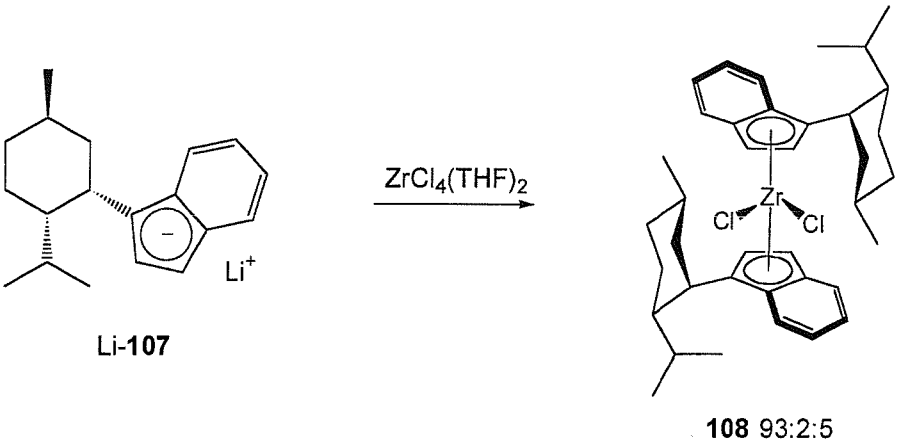

Li-**107** **108** 93:2:5

Scheme 2.1

Whitby and Bell have used ligand **107** to demonstrate the effectiveness of their C1-symmetric catalyst 'Roof' and 'Wall' design, Figure 2.2.[17,18] Again the high induction of planar-chirality is achieved on complexation of **107** to $ZrCpCl_3DME$, and now the less sterically demanding C1-symmetric complex **109** is highly active in catalytic reactions, achieving effective asymmetric catalysis.

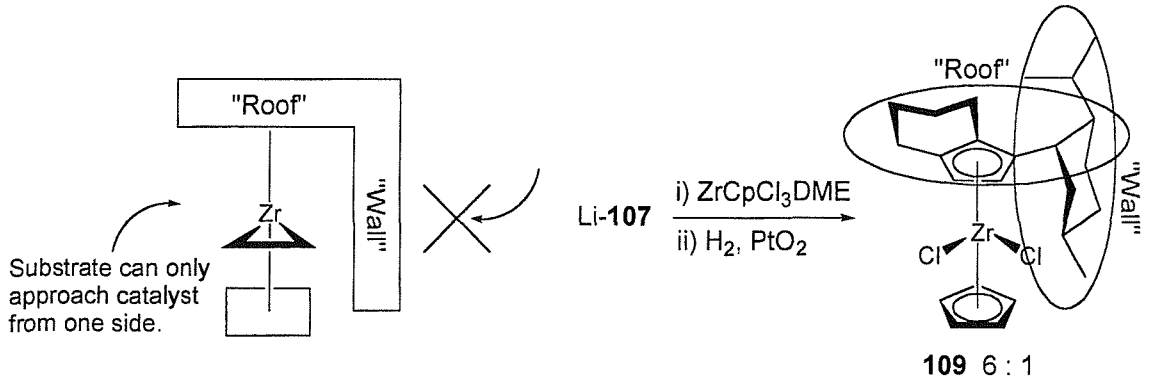

109 6 : 1

Figure 2.2

2.1.2 Ligand design concepts for late-transition metals

Research within the Whitby group has now moved to extend the successful 'favoured rotamer' complexation model and the 'Roof' and 'Wall' catalyst design to later transition metals. As late-transition metallocene complexes are co-ordinatively saturated (and thus inert to catalysis), the metallocene design of catalyst **109** is not suitable for these metals. A new design of chiral bidentate ligand, able to induce face-selective complexation to late-transition metals, has therefore been proposed, Scheme 2.2.[29]

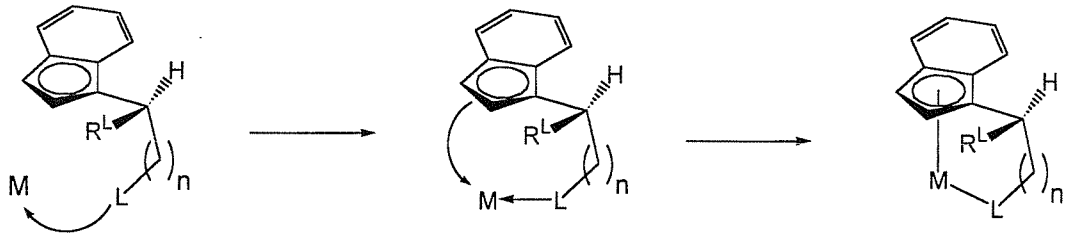

Scheme 2.2

The ligand design shown in Scheme 2.2 incorporates both the key 'favoured rotamer' design concept of chiral ligand **107** and the successful 'roof' and 'wall' design of catalyst **109**, as well as a new 'anchor' co-ordinating group connected to the Cp-ring *via* a short carbon chain, which should help maintain the chiral integrity of the complex during catalytic cycles.

2.1.3 Previous research

In order to develop synthetic routes to ligands of the type shown in Scheme 2.2, previous research within our group[29] has led to the investigation of a reaction originally reported by Reiger,[76,77] in which the ring-opening of styrene oxide by indenyl lithium provides a 3 : 2 mixture of readily separable alcohols **110** and **111**, Scheme 2.3.

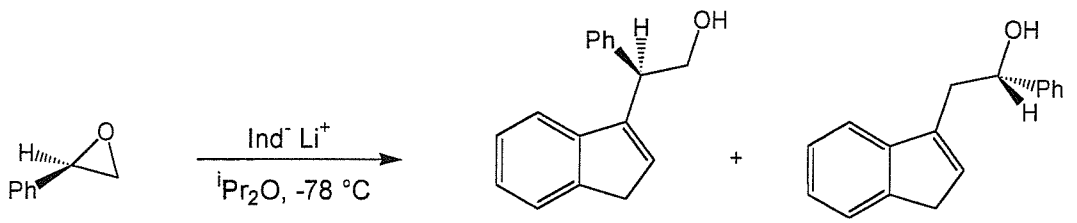

110 (38%) **111** (24%)

Scheme 2.3

Alcohol **110** appeared to be an ideal candidate for activation and displacement of the alcohol by diphenylphosphide, to provide the chiral indene-phosphine ligand **113**, containing a chiral centre *alpha* to indene, as required to achieve the 'favoured rotamer' complexation model. However when this synthesis was initially attempted, the intended ligand **113** was not formed and surprisingly its regioisomer **59**, containing the chiral centre *beta* to indene was isolated, Scheme 2.4.[29]

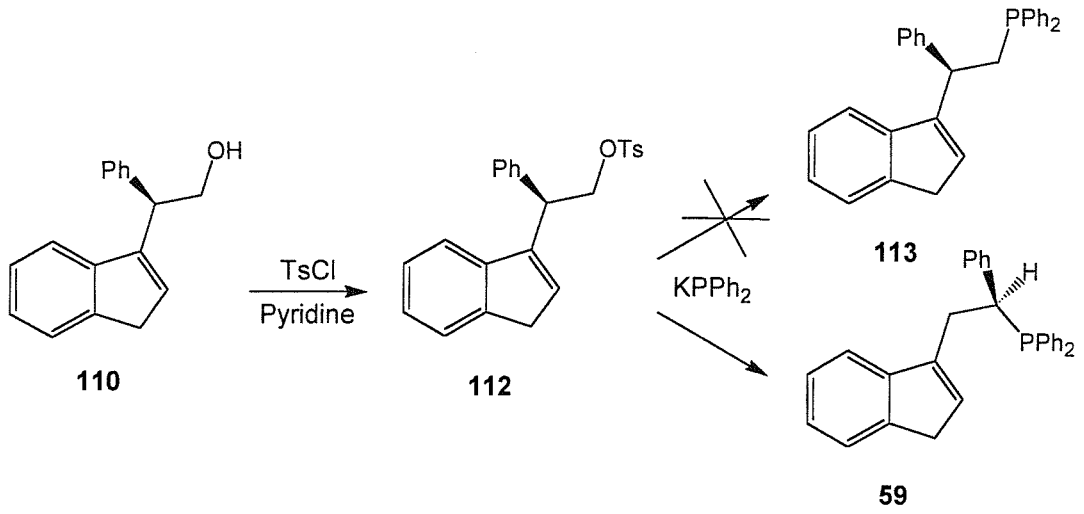

Scheme 2.4

It was proposed that this unexpected rearrangement may have occurred by the formation and subsequent opening of a cyclic intermediate during the final step of the synthesis (this has been investigated below, Section 2.2). Although still a chiral indene-phosphine ligand, the regioisomer **59** does not fulfil the requirements for our 'favoured rotamer' complexation model and so would not be expected to show significant face-selectivity upon complexation to a transition metal[29] (however in a special case, a high degree of face-selectivity was observed, see Scheme 1.17, Section 1.4.1). Therefore a new synthetic route leading to the intended chiral *alpha*-substituted indene-bridged ligand was now required.

2.1.4 Aims

The chiral indenyl-phosphine ligand **59** prepared previously,[29] does not contain the desired *alpha*-chiral centre required by the 'favoured rotamer' design concept in order to

achieve a high degree of face-selectivity upon complexation to transition metals. Therefore this research should initially:

- Investigate the reason for the unexpected rearrangement during the final step of the intended synthesis of ligand **113**.

- Either modify the intended synthetic route to ligand **113**, in order to avoid the rearrangement; or design a new ligand/synthesis to provide an alternative *alpha*-substituted indene bridged ligand.

- Exploit any new or modified ligand syntheses in order to prepare related ligands, containing chiral *alpha*-substituents, which fulfil the design concepts given in Section 2.1.2.

2.2 Studies into the synthesis of the phenyl-substituted ligand.

The unexpected rearrangement during the final step of the intended synthesis of *alpha*-substituted ligand **113** resulted in its *beta*-substituted regioisomer **59** (see Section 2.1.3).[29] This step involves use of potassium diphenylphosphide intended to displace the tosylate group on **112**, however if the diphenylphosphide initially acts as a base, rather than a nucleophile, deprotonation of the indene moiety could lead to intramolecular displacement of the tosylate group to form a spirocyclic intermediate **114**, as proposed in Scheme 2.5. Further diphenylphosphide can then attack spirocycle **114**, opening the strained cyclopropane ring from the more activated (benzylic) site, to form the rearranged ligand **59**.

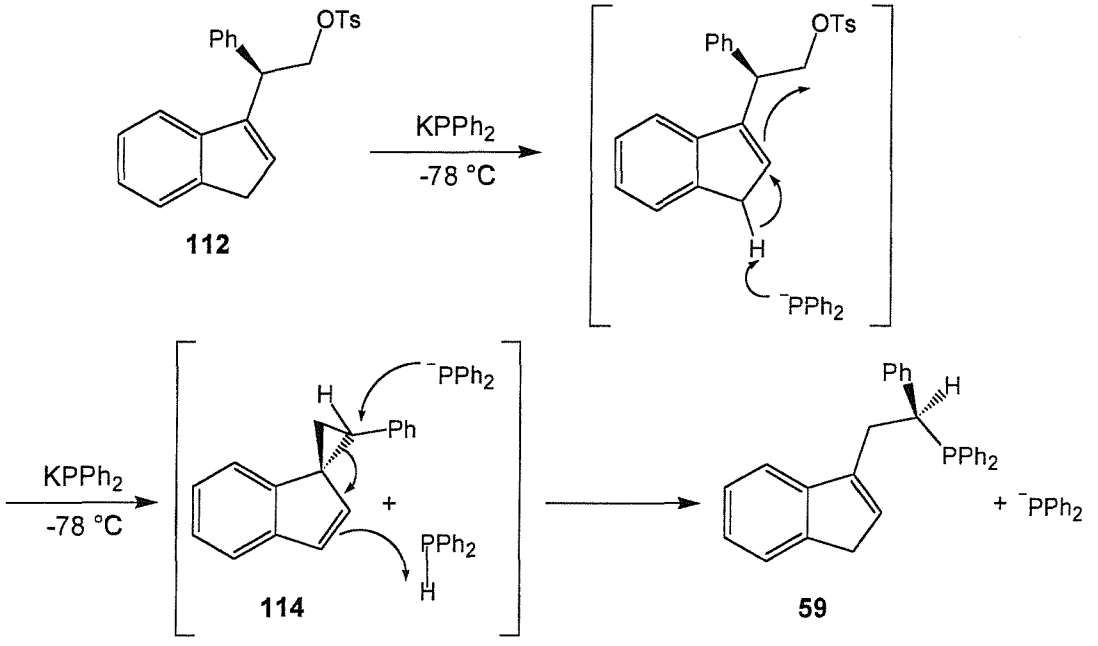

Scheme 2.5

In order to gain evidence for this theory, the spiro-cyclopropane intermediate **114** was prepared as a single diastereoisomer, in 69 % yield, by reaction of tosylate **112** with *n*-butyl lithium in THF at –78 °C, Scheme 2.6. The structure of **114** was confirmed to be as shown by X-ray crystallography, Figure 2.3. Cyclopropane **114** was then treated with potassium diphenylphosphide, under identical conditions to those used during the rearrangement step (*cf.* Scheme 2.4), resulting in an almost quantitative yield of the rearranged ligand **59**. This demonstrates that ring-opening of **114** does occur from the

hindered, but more activated, benzylic site – as would be required for the proposed rearrangement in Scheme 2.5.

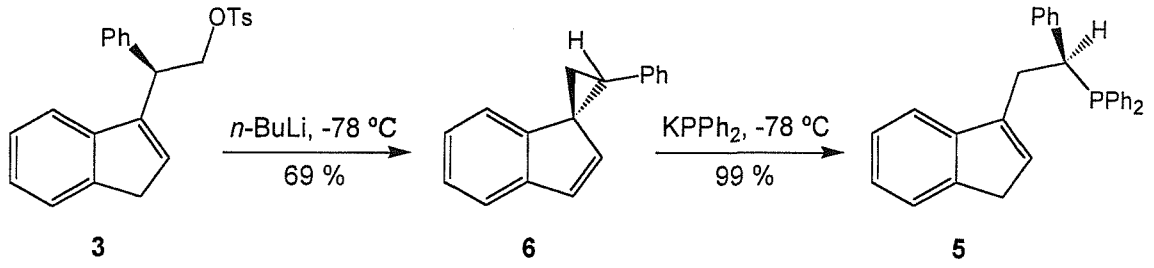

3 **6** **5**

Scheme 2.6

Although the rearrangement may have occurred by the procedure shown in Scheme 2.5, an important experimental observation from the original synthesis remains unexplained. Brookings reported that use of only *one* equivalent of potassium diphenylphosphide effected a 62 % conversion from tosylate **112** to rearranged ligand **59**.[29] However, if the diphenylphosphide first acts as a base, in deprotonating tosylate **112**, then *remaining* diphenylphosphide effects the ring opening of the spirocycle, a maximum yield of only 50 % conversion can be achieved. In order to provide greater than 50 % conversion, a catalytic cycle must be in place to recycle the diphenylphosphine resulting from the cyclopropane ring formation. A suitable catalytic cycle has been included in the proposed rearrangement mechanism in Scheme 2.5 – whereby the diphenylphosphine produced is subsequently deprotonated by the indene moiety, to provide the diphenylphosphide nucleophile which can then effect the required ring opening.

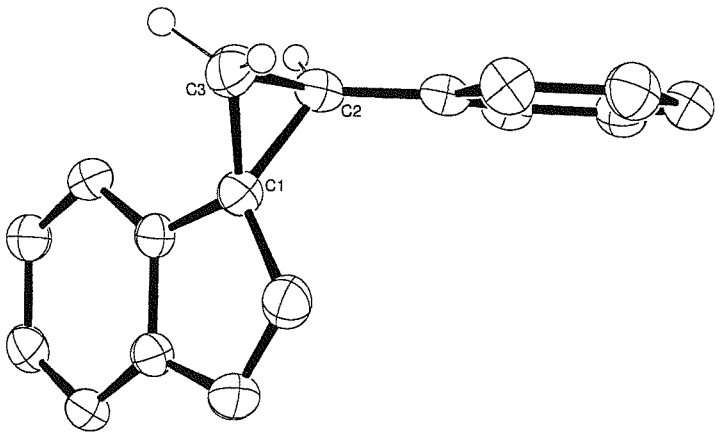

Figure 2.3

ORTEP view of *rac*-114, thermal ellipsoids shown at 50 % probability, H-atoms shown only for C2 and C3. See Appendix 1 for full details.

With knowledge of how this rearrangement is likely to have occurred, we can now begin to examine new ligand syntheses from precursors which can completely avoid the rearrangement mechanism.

2.3 Design of an *alpha*-substituted indenyl ligand

The *beta*-substituted ligand **59**, discussed in Section 2.2, is formed solely because of the presence of an aromatic substituent on the precursor cyclopropane, activating the benzylic position to attack by the diphenylphosphide anion. Therefore, if the aromatic substituent of the spiro-cyclopropane was replaced by a non-aromatic group of sufficient steric bulk, ring-opening would thus be controlled by sterics, as benzylic activation would no longer be a factor, Scheme 2.7. This should lead exclusively to *alpha*-substitution, as required for our 'favoured rotamer' model.

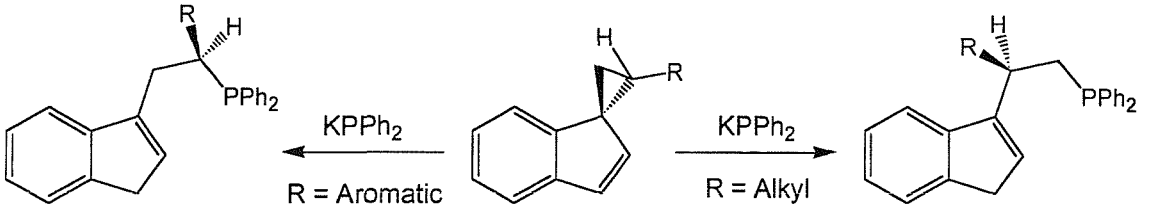

Scheme 2.7

A suitably bulky non-aromatic replacement for the phenyl ring, could therefore be a cyclohexyl ring. The same synthetic route as shown in Schemes 2.3 and 2.4 would still remain viable, as cyclohexyl oxirane **116** is prepared easily by epoxidation of vinyl cyclohexane, and reliable preparations of the enantiopure epoxide are available using either Sharpless's dihydroxylation[78] and epoxide transformation[79] chemistry or Jacobsen's hydrolytic kinetic resolution[80,81] chemistry.

2.3.1 Synthesis of the cyclohexyl-substituted ligand

Scheme 2.8 shows the synthetic route to the enantiopure cyclohexyl-substituted ligand **121**. In the racemic series, cyclohexyl oxirane (+/-)**116** was prepared by epoxidation of vinylcyclohexane with *m*-chloroperbenzoic acid. Enantiopure (97 % e.e.) (*R*)-cyclohexyl oxirane **116** was synthesised in 77 % yield by the method of Sharpless,[79] from the (*R*)-diol **115** which was prepared in 85 % yield and 97 % e.e. by Sharpless asymmetric

dihydroxylation of vinyl cyclohexane.[78] The synthesis of the ligand was then performed in a similar way to the phenyl ligand **59** (*cf.* Scheme 2.3), by opening of the epoxide **116** with indenyl lithium, to give the highly crystalline secondary alcohol **117** in 72 % yield. Recrystallisation from hexane provided **117** as a single enantiomer, >99 % e.e. At this point it was not necessary to optimise conditions of the epoxide opening to favour the *alpha*-substituted primary alcohol (*cf.* **110** *vs.* **111** in Scheme 2.3), as the synthesis of the cyclohexyl ligand shall intentionally pass through the spiro-cyclopropane **120**, and it is the ring-opening of **120** which shall determine the final ligand substitution pattern.

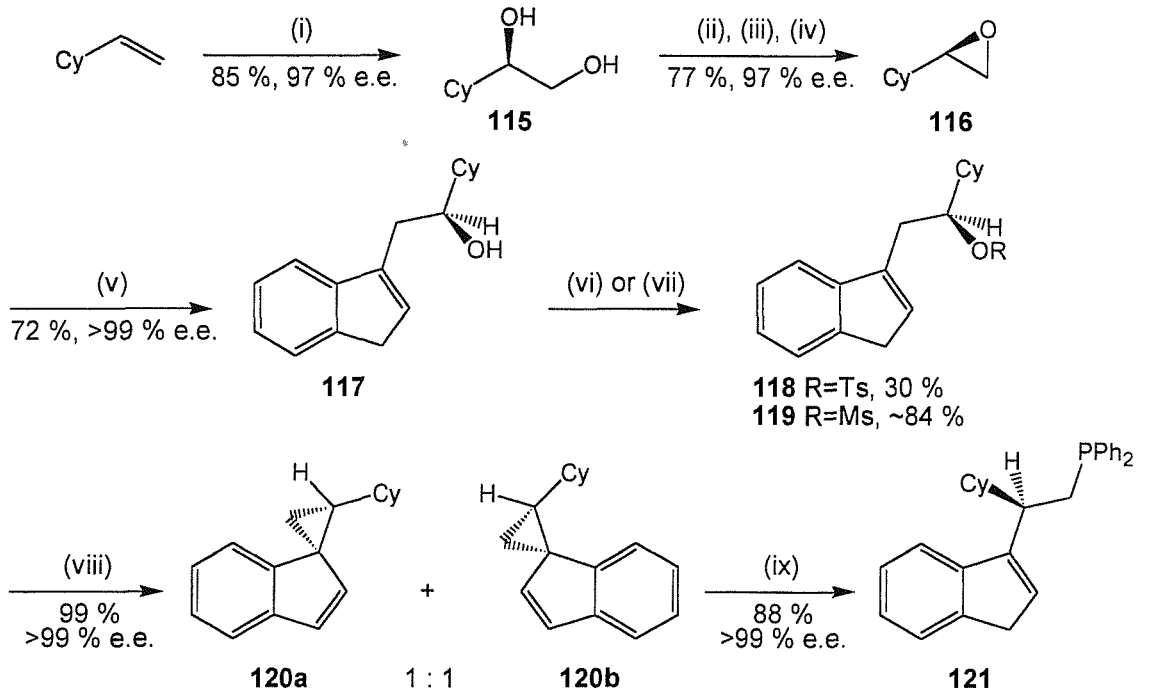

Scheme 2.8

Reagents and conditions: (i) A.D. using (DHQD)$_2$-PYR ligand;[78] (ii) MeC(OMe)$_3$, cat. TsOH, CH_2Cl_2; (iii) Me_3SiCl, CH_2Cl_2, 0 °C; (iv) K_2CO_3, MeOH, 2 h;[79] (v) Indenyl lithium, THF, –78 °C; (vi) MsCl, NEt_3; (vii) TsCl, pyridine, CH_2Cl_2; (viii) n-BuLi, THF, –78 °C; (ix) Ph_2PK, 2 mol% 18-crown-6, THF, 0 °C.

Activation of the secondary alcohol **117**, was attempted as previously by tosylation of the alcohol using tosyl chloride and pyridine in dichloromethane. This reaction proceeded much more slowly than with the primary alcohol **110** of the phenyl ligand series – failing to achieve completion after 48 hours, with only a 30 % yield of the tosylated product **118** after column chromatography and 55 % recovery of unreacted alcohol **117**. Steric hindrance by the cyclohexyl group and proximal indene moiety is the most likely cause of the poor reactivity of this secondary alcohol. Addition of DMAP to this reaction had

little effect on the rate or overall yield. The white-crystalline tosylate **118** also proved to be unstable to storage in air/light at room temperature, with the crystals darkening to black after only one hours' storage. Although the subsequent step to form the spirocycle intermediate **120** was successful by reaction of tosylate **118** with *n*-butyl lithium, an alternative activation method was sought in order to increase the ease and overall yield of the sequence.

To this end, mesylation of the alcohol was employed to form the activated less-sterically demanding mesylate compound **119**. Reaction of the alcohol with mesyl chloride in triethylamine, at –40 °C for two hours achieved clean conversion to the secondary mesylate. The mesylate **119** was then treated with *n*-butyl lithium at –78 °C, to form the desired spiro-cyclopropane intermediate **120** as a 1 : 1 mixture of diastereoisomers, in excellent yield (83 % over two steps).

The final step of the ligand synthesis, opening of the spiro-cyclopropane **120** with diphenylphosphide, initially proved problematic. Using the conditions required to open the phenyl-substituted cyclopropane **114** (Scheme 2.5), of potassium diphenylphosphide in THF at –78 °C, no ring-opening was detected with the cyclohexyl-substituted cyclopropane **120**. Heating the reaction mixture to reflux for 4 hours did however give a small conversion of the cyclopropane to the target ligand **121**. This reduced reactivity compared with the phenyl substituted cyclopropane **114**, can be attributed to the lack of activated benzylic site in cyclopropane **120**. In an attempt to increase the nucleophilicity of the diphenylphosphide anion, and hence increase the rate of reaction, the ring-opening was attempted at room temperature, in the presence of a stoichiometric quantity of 18-crown-6. This led to complete conversion of the cyclopropane **120** (as a 1 : 1 mixture of diastereoisomers) to ligand **121** within 4 hours. Optimisation of this final step led to the preferred conditions whereby a catalytic amount of 18-crown-6 (2 mol%) is employed in the reaction mixture with potassium diphenylphosphide at 0 °C for 16 hours, to provide 88 % isolated yield of **121** as a cloudy air-sensitive oil after column chromatography under argon.

The *alpha*-cyclohexyl-substituted ligand **121** is therefore synthesised in 34 % overall yield and >99 % e.e. from commercial vinylcyclohexane. Chiral HPLC was used at each stage of the synthesis to ensure no loss in chirality occurred.

2.3.2 Optimisation of the cyclohexyl ligand synthesis

The synthetic route to ligand **121**, shown in Scheme 2.8, while sufficient for small scale preparations of the enantiopure ligand, provides only a moderate overall yield of **121** and involves six steps – all but the first and last of which require column chromatography to purify the product. In order to prepare large quantities of the chiral ligand, as would be required when the catalytic testing of transition metal complexes of **121** begins, an efficient synthesis, more applicable to large scale chemistry would be desirable. Optimisation of the individual reaction steps in Scheme 2.8 offers little scope to improve the overall yield of the synthesis, as each step proceeds in relatively high yield already, therefore a re-design of the first five steps of the synthesis of ligand **121** was undertaken.

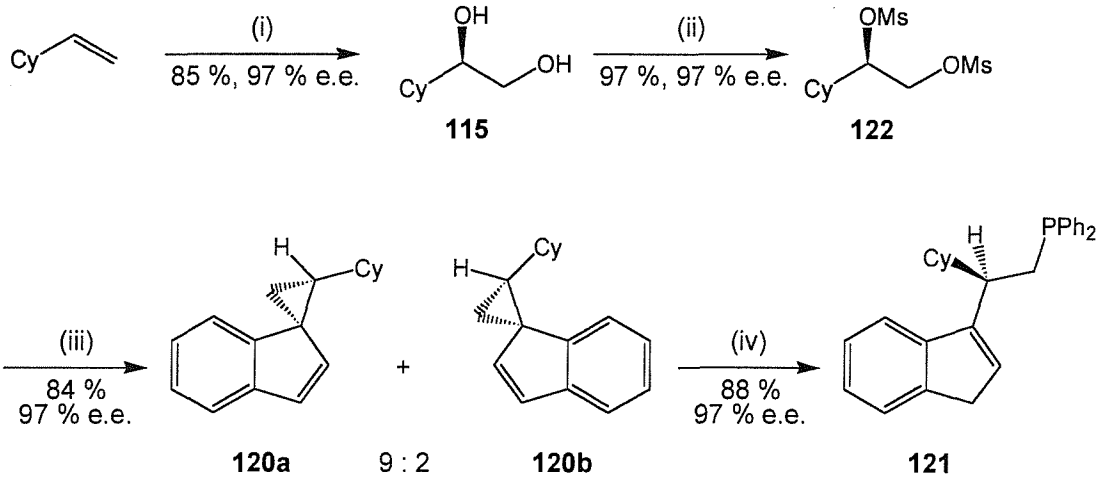

Scheme 2.9

Reagents and conditions: (i) A.D. using $(DHQD)_2$-PYR ligand;[78] (ii) 2 MsCl, NEt_3, CH_2Cl_2, –20 °C (iii) 2 Indenyl lithium, THF, –78 °C; (iv) Ph_2PK, 2 mol% 18-crown-6, THF, 0 °C.

Scheme 2.9 shows the improved synthetic route to **121**. Sharpless asymmetric dihydroxylation[78] again provides the enantioenriched diol **115**, in 97 % e.e. Treatment of **115** with two equivalents of mesyl chloride in triethylamine, then provided bis-mesylate **122** in 97 % yield, after purification by a simple crystallisation from dichloromethane/hexane at 5 °C. Unfortunately this recrystallisation did not enhance the enantiomeric excess, which remains at 97 % e.e. X-ray crystallography confirmed the stereochemistry of **122** was (*R*), as expected,[78] Figure 2.4.

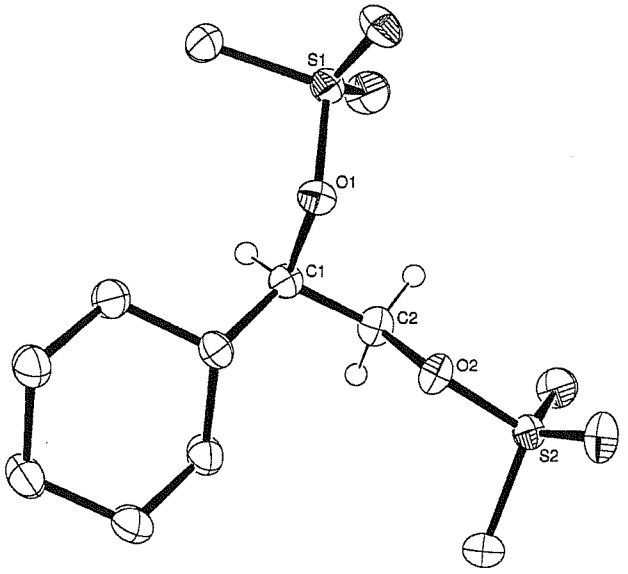

Figure 2.4

ORTEP view of (*R*)-122, thermal ellipsoids shown at 50 % probability, H-atoms shown only for C1 and C2. See Appendix 2 for full details.

Formation of the spirocycle **120** was then performed by addition of one equivalent of indenyl lithium to a suspension of bis-mesylate **122** in THF, at 0 °C, followed by addition of further *n*-butyl lithium – with the intention of passing through mesylate **119** (although in its 1*H*-indenyl tautomer), Scheme 2.10.

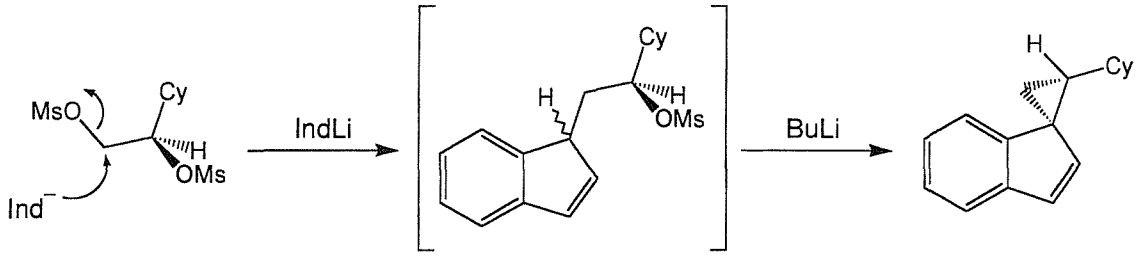

122 (1*H*-indenyl)-**119** (not isolated) **120**

Scheme 2.10

This provided **120** in 52 % yield, surprisingly as a 9 : 2 mixture of diastereoisomers. The different ratio of **120a** : **120b** obtained from this synthetic route compared to that in Scheme 2.8 (*cf.* 1 : 1 ratio from tosylate **118** or mesylate **119**) is surprising, since the reaction of **122** presumably occurs *via* a similar mechanism involving mesylate **119** in its 1*H*-indenyl tautomer. Various reaction conditions (see Table 2.1) all provided the same 9

: 2 mixture of isomers and reaction temperature used (0 °C in this case *vs.* –78 °C previously) was also found not to be responsible for the difference. In the absence of further evidence, the most likely explanation for this 9 : 2 ratio of **120a** : **120b**, is that the formation of the intermediate mesylate (1*H*-indenyl)-**119** occurs with control of stereochemistry at the 1*H*-indenyl position, induced by the chiral mesylate **122**. The resulting diastereoisomers of (1*H*-indenyl)-**119** may then cyclise to the spirocycle with retention of stereochemistry at the 1-indenyl position, resulting in the two isomers of **120a** and **120b**.

Various reaction conditions and optimisations were investigated in order to improve the yield of spirocycle **120**, see Table 2.1.

Reaction	Conditions[§]	Concentration[**]	Yield[††]
1	i) 1.0 eq. indenyl lithium, ii) 1.0 eq. *n*-BuLi	0.080 M	52 %
2	i) 1.2 eq. indene, ii) 2 × 1.2 eq. *n*-BuLi	0.080 M	62 %
3	i) 1.2 eq. indene, ii) 3.0 eq. KH	0.080 M	55 %
4	i) 1.2 eq. indene, ii) 3.0 eq. KH	0.133 M	56 %
5	i) 2.4 eq. indenyl lithium	0.080 M	55 %
6	i) 2.4 eq. indenyl lithium, reverse addition	0.133 M	84 %

Table 2.1

Other conditions: Reactions 1-5: reagents added sequentially to solution (1-3,5) or suspension (4) of dimesylate in THF at 0 °C; Reaction 6: solid dimesylate added to solution of reagents in THF, at 0 °C.

The optimum conditions for this step were found to be addition of the solid bis-mesylate **122** to a 0.13 M solution containing 2.4 equivalents of indenyl lithium (acting as a nucleophile and base) in THF, at 0 °C. These conditions gave the spirocycle **120** (9 : 2 ratio **a** : **b**) as a white crystalline solid, in 84 % yield after simple chromatography (flushing through silica) and removal of excess indene under vacuum.

The major isomer **120a** was recrystallised from ethanol and its structure confirmed by X-ray crystallography, Figure 2.5.

[§] Reactions were monitored by GC, and allowed to proceed until no further increase in product was seen.
[**] Concentration relative to dimesylate in reaction solution, all reactions performed on 2 mmol scale.
[††] Isolated product yield, after purification by chromatography (SiO_2, 100 % petrol).

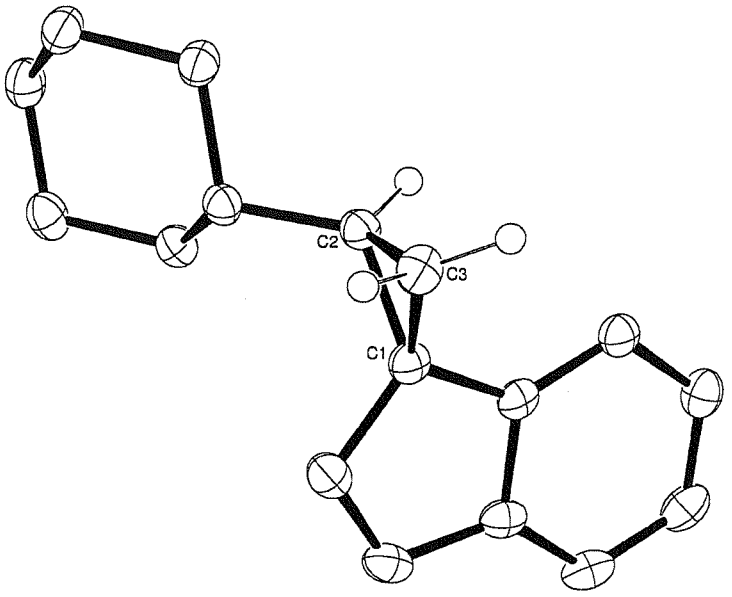

Figure 2.5

ORTEP view of (+)-120a, thermal ellipsoids shown at 50 % probability, H-atoms shown only for C2 and C3. See Appendix 3 for full details.

The final step of the new synthesis of **121** remains unchanged, involving the treatment of spirocycle **120** (although now a 9 : 2 mixture of isomers) with potassium diphenylphosphide in THF and catalytic 18-crown-6, to provide the chiral air sensitive ligand **121** in a much improved overall yield of 61 % and 97 % e.e. from vinylcyclohexane. This improved synthesis involves only four high-yielding steps and purification is much simplified over the previous route, with only the final compound requiring full column chromatography. The versatility of this optimised route is demonstrated by the now routine preparation of ligand **121** on a 50 mmol scale by this method.

2.4 Protection strategy for phosphine ligands

Cyclohexyl-substituted ligand **121** and phenyl-substituted ligand **59** are alkyl-diphenylphosphines and were found, as expected, to oxidise rapidly in air to their phosphine oxides. In order to gain analysis of these sensitive compounds, and enable their convenient handling and long-term storage, some phosphine-protection strategies were investigated.

2.4.1 Phosphine oxides as 'protected' alkyl-diarylphosphines

Phosphine oxides themselves have been used as ideal 'protected' forms of phosphine ligands, [9,25,82] since the 'protection' is achieved by simply standing in air(!) and can be ensured by stirring the phosphine ligand in *m*-chloroperbenzoic acid for only a few seconds. It would be beneficial if our chosen strategy would allow the final purification of the ligands to be performed on the 'protected' ligand, and so avoid the cumbersome column chromatography under argon, currently required in the final stage of synthesis. Unfortunately the phosphine oxides of ligands **121** and **59** were found to be highly polar and virtually insoluble in organic solvents, making chromatography challenging. Deprotection of the phosphine oxides also proved to be inelegant. The most common method uses lithium aluminium hydride to reduce the phosphine oxide,[25,82] trichlorosilane reduction of phosphine oxides is also successful,[9,83] however these techniques require an aqueous workup after the deprotection, which often results in some of the reduced ligand re-oxidising. In light of these problems we chose to examine a different protection method.

2.4.2 Borane protected alkyl-diarylphosphines

Other phosphine protection strategies involve forming sulphur[30,84] or borane[85,86] adducts of the alkyl-diphenylphosphine. The most promising strategy for our ligands appeared to be forming the borane adduct of the alkyl-diphenylphosphine. This is achieved simply by treating the phosphine with borane-methyl sulphide[87] complex or borane-THF[23] complex, Scheme 2.11. Importantly for this work, the lithium diphenylphosphide-borane complex is also known[85] and by using this as the phosphide source in the final step of our ligand synthesis we hope to prepare the borane protected ligand directly from its precursor spirocycle.

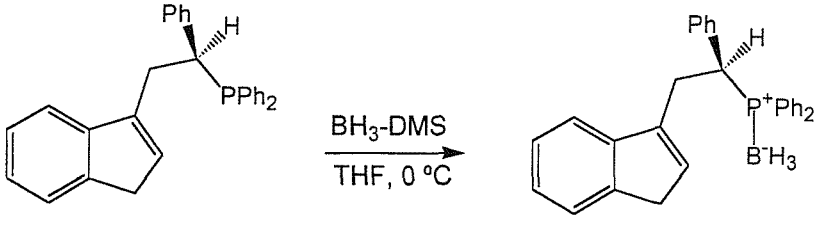

59 **123**

Scheme 2.11

The protected borane adducts of ligands **59** and **121** were prepared quantitatively by treating the ligands with borane-methyl sulphide complex in THF, at 0 °C, for 15 minutes. It was important to control the time and temperature of the reaction, as increased temperature or reaction time led to the formation of by-products in the mixture (most likely caused as a result of hydroboration at the indene double-bond). The borane protected ligands were purified by crystallisation from hexane, to give fine white needles suitable for analysis (unfortunately these were not suitable for X-ray crystallography).

The borane protected cyclohexyl-substituted ligand **124** was also prepared directly from spirocycle **120**, completely avoiding the air-sensitive phosphine, by reaction of the borane adduct of lithium diphenylphosphide with **120** in the presence of HMPA, Scheme 2.12. However the 61 % yield of **124** from **120** was lower than when prepared *via* the uncomplexed diphenylphosphide.

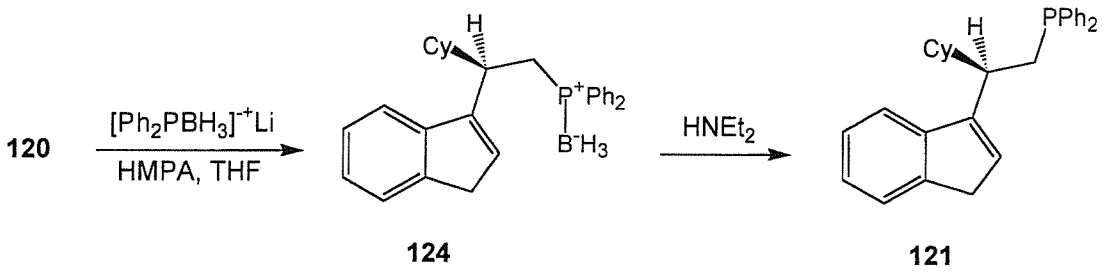

124 **121**

Scheme 2.12

Deprotection of borane protected phosphines can be achieved cleanly by reaction with an amine base.[86-88] The most attractive deprotection system for protected ligands **123** and **124** proved to be by heating the borane adducts in diethylamine, under an inert atmosphere.[87] In the case of **124**, quantitative yield of the decomplexed phosphine ligand **121** was then obtained simply by removal of the diethylamine-borane complex along with remaining diethylamine under high vacuum.

2.5 Design of an *alpha,beta*-disubstituted indenyl ligand

The rearrangement leading to the incorrect *beta*-phenyl-substituted ligand **59**, described in Section 2.2, could also be avoided if the substitution pattern on the spiro-cyclopropane intermediate (*cf.* **114**) was symmetrical. If this were the case, ring-opening by attack of diphenylphosphide would lead to an *alpha,beta*-disubstituted ligand. Since many chiral *alpha,beta*-disubstituted epoxides are available or can be easily prepared in enantiopure

form, we should be able to prepare a chiral *alpha,beta*-disubstituted ligand, to complement the mono-substituted ligands prepared thus far, Scheme 2.13.

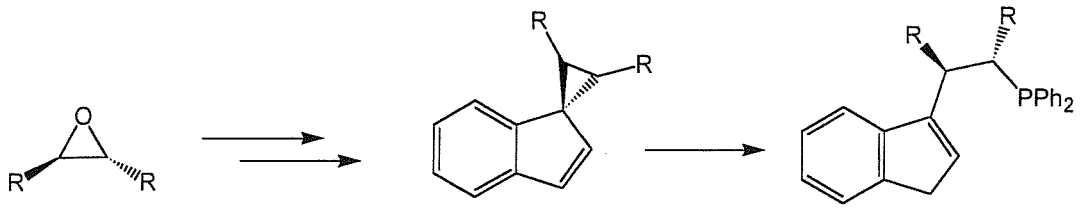

Scheme 2.13

An interesting disubstituted ligand to investigate would be the *alpha,beta*-diphenyl-substituted ligand, containing a phenyl ring *alpha* to the Cp, so that upon complexation we should achieve the same 'favoured rotamer' effect that had been designed into the proposed *alpha*-phenyl-substituted ligand **113**. This would enable an interesting comparison with the *alpha*-cyclohexyl-substituted ligand **121**. The *beta*-phenyl-ring in the disubstituted ligand will increase the bulk of the ligand side-chain, and so the steric-'Wall' effect of the transition metal complex (Figure 2.2) – hopefully to provide greater substrate-selectivity as a catalyst.

2.5.1 Synthesis of the di-phenyl-substituted ligand

Scheme 2.14 shows the synthetic route to the racemic di-phenyl-substituted ligand **128**. The synthesis begins with the reaction of indenyl lithium and commercially available *trans*-stilbene oxide, in THF at 0 °C, to form the secondary alcohol **125** in 60 % yield, as a viscous yellow oil. Tosylation of **125** under standard conditions of tosyl chloride in pyridine, failed completely with no reaction seen after 48 hours, which was not surprising as this substrate is very sterically hindered (*cf.* slow reaction of **117** in Section 2.3).

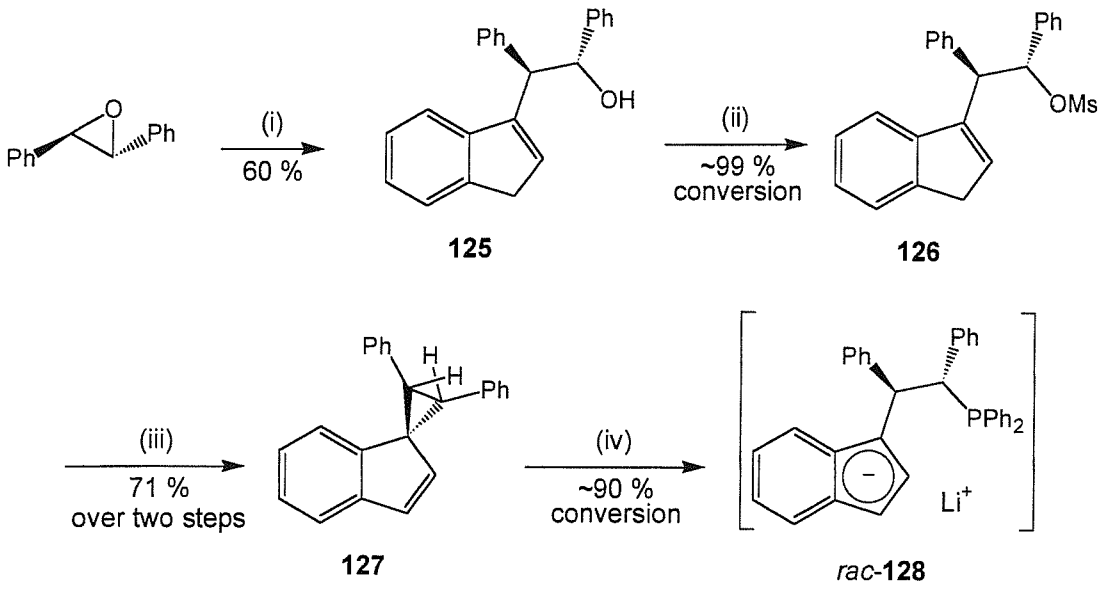

Scheme 2.14

Reagents and conditions: (i) Indenyl lithium, THF, 0 °C; (ii) MsCl, NEt_3, CH_2Cl_2, 0 °C; (iii) n-BuLi, THF, –78 °C; (iv) Ph_2PLi, THF, 20 °C, 64 h.

Preparation of the mesylate of **126** was successful, although required slightly more forcing conditions than had been used previously, by reaction of alcohol **125** with mesyl chloride in triethylamine and dichloromethane, at 0 °C for three hours. Conversion of the mesylate **126** to the di-substituted spirocycle **127** was achieved cleanly by reaction with *n*-butyl lithium at –78 °C, providing **127** as a crystalline solid in 71 % yield over the last *two* steps. Purification of **127** was achieved by recrystallisation from hot ethanol and X-ray crystal analysis confirmed the structure was as shown, Figure 2.6.

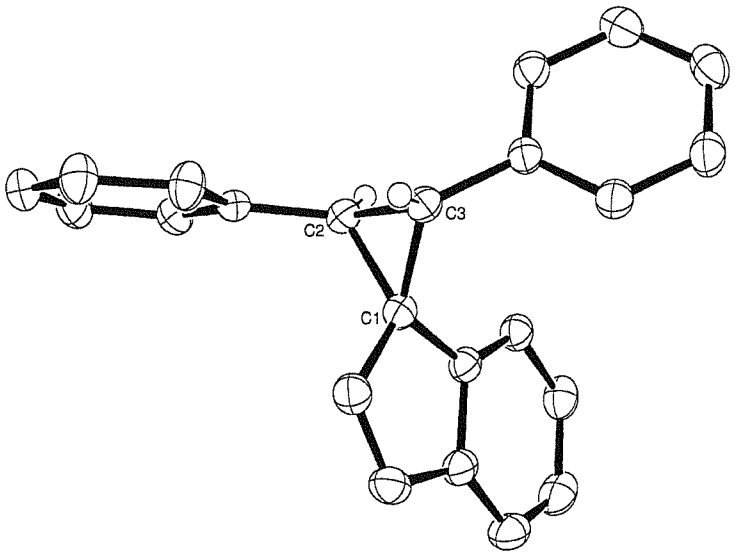

Figure 2.6

ORTEP view of *rac*-127, thermal ellipsoids shown at 50 % probability, H-atoms shown only for C2 and C3. See Appendix 4 for full details.

The final step in the preparation of the *alpha,beta*-disubstituted ligand **128** proved very problematic. Initial attempts to achieve ring-opening of sterically encumbered spirocycle **127** by reaction with potassium diphenylphosphide in the presence of catalytic 18-crown-6 at room temperature (*cf.* Scheme 2.8), were unsuccessful. Increased reaction times (to 64 hours), elevated reaction temperatures and use of stoichiometric 18-crown-6 all showed some indication of reaction when monitored by ^{1}H NMR – with the characteristic indenyl CH and CH_2 resonances observed at δ 6.34 and 2.74 ppm. However integration of these peaks in each case showed less than 10 % conversion had occurred and no material was isolated upon workup of the reaction mixture.

In an attempt to increase the reactivity of the diphenylphosphide anion, the more forcing conditions of lithium diphenylphosphide with HMPA co-solvent were then examined. Reaction of diphenylphosphine and *n*-butyl lithium in THF at –78 °C provided lithium diphenylphosphide, this was treated with spirocycle **127** and HMPA at 20 °C, with solvent concentration 0.4 M relative to spirocycle. Under these vigorous conditions ring-opening did occur, reaching complete consumption of **127** after 16 hours. Mass spectrometry and crude ^{1}H NMR confirmed the presence of the desired ligand **128**. Purification by column chromatography, using degassed solvents, however gave only a 30 % yield of a white solid – which precipitated rapidly from the collected column fractions upon exposure to air. Mass spectrometry showed the precipitated solid to be the phosphine oxide form of the ligand, no non-oxidised ligand was detected.

These results demonstrated ligand **128** to be much more air-sensitive than the previous ligands **59** and **121**, both of which could be handled briefly in air without significant oxidation occurring. Therefore in order to completely avoid exposure of ligand **128** to air before complexation, it was decided not to isolate this ligand, but instead use the crude lithium salt of **128**, formed upon ring-opening of **127**, directly in complexation reactions. To achieve this HMPA could not be used in the final step of the reaction, as HMPA can serve as a ligand on the transition metals we intend to complex **128** with. So a concentrated solution of spirocycle **127** in THF (0.4 M), was treated with lithium diphenylphosphide at room temperature, and stirred for 72 hours, after which time crude ^{1}H NMR showed less than 10 % spirocycle **127** remained in the reaction mixture. The crude lithium salt of **128** was concentrated to dryness under vacuum and used in complexation reactions directly – see Chapter 4.

This route has yet to be optimised, however spirocycle **127** is prepared here in 43 % overall yield from *trans*-stilbene oxide, and the final step in the synthesis of ligand **128** proceeds to greater than 90 % conversion by ^{1}H NMR, ready for direct use in complexation reactions. Owing to time restrictions, only the racemic form of ligand **128** could be prepared, however enantiopure stilbene oxide is readily available, making the enantiopure ligand **128** a good target for future researchers.

2.6 Conclusions

- The unexpected rearrangement seen during the intended synthesis of ligand **113** has been investigated, and evidence that it could have occurred *via* formation of the spiro-cyclopropane intermediate **114** has been gathered.

- The novel chiral *alpha*-substituted indene-bridged ligand **121** has been prepared via an optimised synthetic route in 61 % yield and 97 % e.e. from commercial vinylcyclohexane.

- The protection and deprotection of the alkyl-diaryl ligands **59** and **121** as their borane adducts has been investigated, and found to be a useful strategy to avoid air oxidation of these ligands.

- An *alpha,beta*-diphenyl-substituted indene-bridged ligand **128** has been prepared in four steps from racemic *trans*-stilbene oxide, as its lithium salt, ready for direct complexation to transition metals.

The novel two-carbon indene bridged ligands **121** and **128** prepared here contain a bulky substituent *alpha* to the indene ring, fulfilling the 'favoured rotamer' design requirements (Section 2.1.2) which aims to achieve face-selectivity upon complexation to transition metal complexes. The results of the complexation of these ligands to rhodium and ruthenium are described in Chapter 4.

3. Chapter 3: Synthesis of novel chiral bidentate indenyl ligands containing a three-carbon bridge and co-ordinating 'anchor' group.

3.1 Background

3.1.1 Cp/Indenyl ligands with three/four-atom bridged co-ordinating groups

Trost,[23] Tani[49] and Takahashi[71] have reported wide variations in the catalytic activity and asymmetric induction of various ruthenium Cp-phosphine bidentate complexes, depending on the length of the Cp-phosphine tether chain. This strong effect of tether length on activity makes it important that we expand the diversity of our ligand design to include ligands with longer Cp-phosphine tethers, for comparison of their catalytic activities.

3.1.2 Aims

Following success in preparing the two-carbon bridged indene-phosphine ligands **121** and **128** (Chapter 2), we should now attempt the synthesis of ligands containing a three or four-carbon Cp-phosphine tether. Other important points of diversity which should be investigated include the nature of the Cp-phosphine tether and the type of co-ordinating 'anchor' group used. So this research shall continue with the aims to:

- Preferably modify our existing synthetic route to the two-carbon bridged ligands **121** and **128** in order to increase the Cp-phosphine tether length to three or four atoms or, failing this, design a new synthetic route following the design concepts in Section 2.1.2, to prepare new ligands with three or four-carbon tethers.

- Investigate alternative anchor groups to the diphenylphosphine group currently used in the two-carbon bridged ligands **121** and **128**.

- Examine other substituents or design-frameworks along the indene-phosphine bridge, which continue to follow the ligand design concepts of Section 2.1.2.

3.2 Design of extended carbon-bridged ligands

3.2.1 Attempted modification of the two-carbon bridged ligand synthesis to three-carbon bridged ligands

The optimised synthesis of the two-carbon bridged ligand **121** contains a very efficient route to the enantiopure spiro-cyclopropane **120**, therefore in our search for a synthesis of extended carbon bridged ligands it would be advantageous if we could achieve this simply by opening the spirocycle **120** with a suitable carbon nucleophile.

Methyldiphenylphosphine oxide is commercially available and the methyldiphenylphosphine-borane adduct is easily prepared; both their lithium salts are available on treatment with *n*-butyl lithium and have been reported to act as a nucleophiles in several substitution reactions.[89,90] Methyldiphenylphosphine is also available, however the preparation of its lithium salt requires the somewhat more vigorous conditions of addition of 1.5 M *n*-butyl lithium directly to methyldiphenylphosphine and TMEDA, without reaction solvent.[91] If any of these nucleophiles could achieve effective ring-opening of the spiro-cyclopropane **120**, we would obtain the three-carbon phosphine ligand **129** (possibly requiring a straight forward reduction **129b** or deprotection **129c**), as shown in Scheme 3.1.

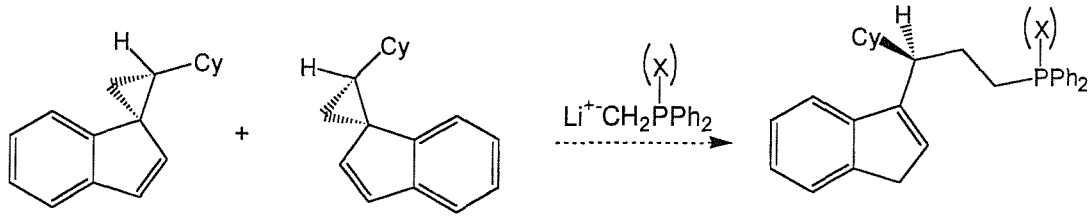

120a **120b**

129a: X = -
129b: X = O
129c: X = BH_3

Scheme 3.1

To investigate this route, the lithium salts of methyldiphenylphosphine,[91] methyldiphenylphosphine-borane,[90] and methyldiphenylphosphine oxide[89] were prepared by the literature methods and treated with the spiro-cyclopropane **120**, under various conditions detailed in Table 3.1.

Unfortunately the results from these reactions were very disappointing, with only *ca.* 10 % conversion of the spiro-cyclopropane **120** to the three-carbon ligand **129**, achieved using the lithium salt of methyldiphenylphosphine, in HMPA, for four days (reaction 8).

Reaction	Nucleophile	Co-solvent	Temp	Conc.[‡‡]	%Conv.[§§]
1	1.2 eq. $LiCH_2P(O)Ph_2$	HMPA	0-20 °C	0.36 M	0
2	1.2 eq. $LiCH_2P(O)Ph_2$	HMPA	–78-20 °C	0.20 M	0
3	2.0 eq. $LiCH_2P(O)Ph_2$	HMPA	–78-20 °C	0.13 M	0
4	1.2 eq. $LiCH_2P(O)Ph_2$	HMPA	–78-90 °C	0.20 M/Tol	0
5	1.2 eq. $KCH_2P(O)Ph_2$	18-crown-6	0-20 °C	0.20 M	0
6	1.2 eq. $LiCH_2P(BH_3)Ph_2$	-	0-20 °C	0.20 M	0
7	1.2 eq. $LiCH_2P(BH_3)Ph_2$	HMPA	0-20 °C	0.20 M	0
8	1.2 eq. $LiCH_2PPh_2$	HMPA	0-20 °C	0.20 M	10

Table 3.1

Other conditions: Reactions 1-8: reagents added sequentially to solution of spiro-cyclopropane 12 in THF (1-3,5-8) or toluene (4) and stirred with ^1H NMR monitoring for 4 days.

Following these results, which indicated little to suggest that optimisation of this reaction would prove fruitful, an alternative method for the preparation of the three-carbon ligand **129** was sought.

3.2.2 Design of a new synthetic route to three-carbon bridged ligands

Without the ability to elaborate the two-carbon bridged ligand synthesis to prepare the three-carbon bridged ligand, a new synthetic route is required. Figure 3.1 shows a possible retro-synthetic analysis of the desired three-carbon bridged ligand **129**. The first two retro-synthetic steps resemble the final steps in the synthesis of the two-carbon bridged phenyl-substituted ligand **59** (Section 2.1.3). In the case of the two-carbon bridged ligand these steps resulted in the ring-closure to spiro-cyclopropane **114**, however in the case of the three-carbon bridged ligand, ring closure is less likely to occur as it would result in the formation of a unfavourable strained cyclobutane ring. Importantly, even if the cyclobutane ring were to form, subsequent ring-opening at the

[‡‡] Concentration relative to spirocycle **120** in reaction solution, all reactions performed on a 1 mmol scale.
[§§] Conversion as determined by integration of crude ^1H NMR.

least hindered site of the spiro-cyclobutane should be favourable, resulting in the desired three-carbon bridged ligand (*cf.* ring-opening of **120** to form ligand **121**, Section 2.3.1).

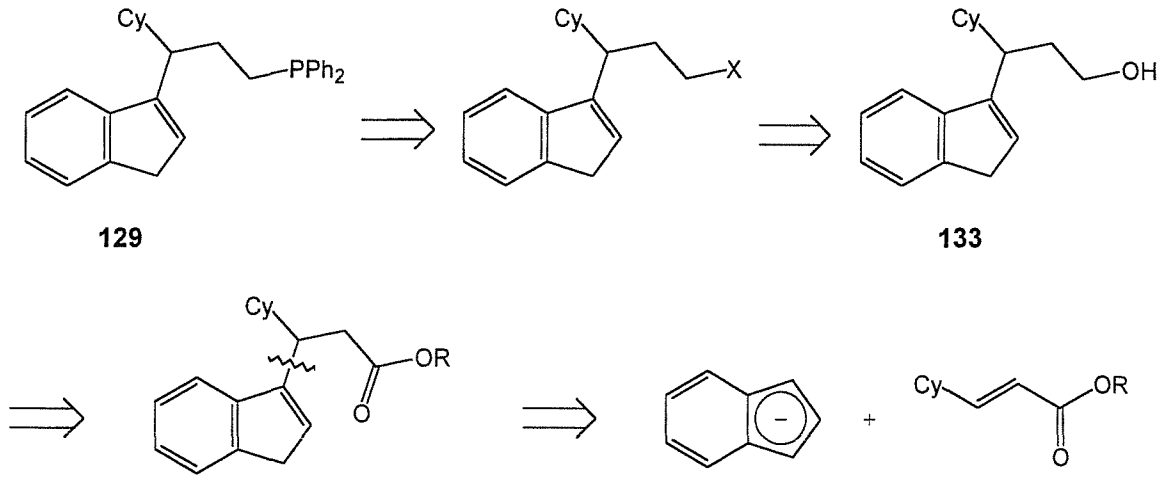

Figure 3.1

Continuing the retro-synthetic analysis, alcohol **133** should be prepared easily by lithium aluminiumhydride reduction of a suitable ester. This leads to the key step in the retro-synthesis, the final disconnection, leading to the precursors of a proposed 1,4-addition of an indenyl anion to a cyclohexyl substituted α,β-unsaturated ester. There is currently no literature precedent for this Michael-type 1,4-addition using an indenyl or cyclopentadienyl anion, however the reaction appears promising and should 1,2 and 1,4-selectivity be a problem, use of bulky ester groups or formation of the indenyl-copper lithium anion may be employed to favour the desired 1,4-addition. Importantly this step also provides an ideal opportunity for control of stereochemistry at the *alpha*-position of the indene-phosphine tether, for example by use of a chiral ester auxiliary or use of a chiral catalysed Michael addition.[92] The results of the forward synthesis of *rac*-**129** *via* this route are discussed below.

3.2.3 Synthesis of the three-carbon bridged ligand

The forward synthesis of ligand **129** begins with the preparation of the *tert*-butyl ester **131**. This ester is readily available by the acid catalysed esterification (78 % yield) of the carboxylic acid product **130** from the Knoevenagel condensation of malonic acid and cyclohexane carboxaldehyde (71 % yield), Scheme 3.2.

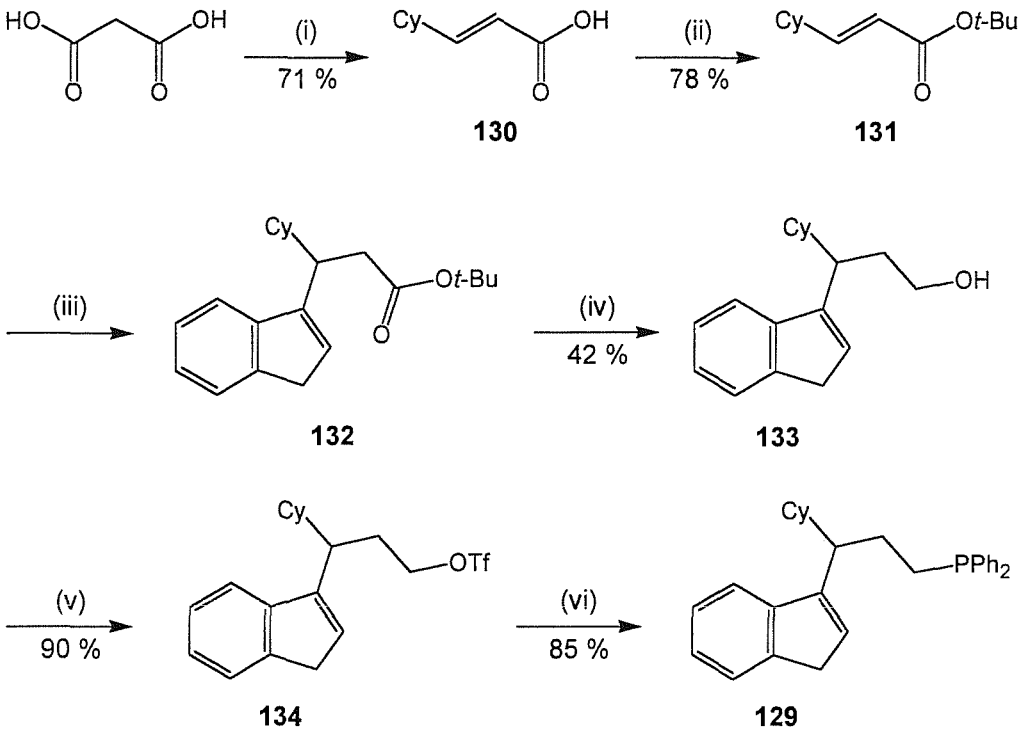

Reagents and conditions: (i) Cyclohexanecarboxaldehyde, pyridine, cat. piperidine; (ii) isobutylene, CH_2Cl_2, cat. H_2SO_4; (iii) IndLi, 0.05 M/THF; (iv) $LiAlH_4$, Et_2O, 0 °C; (v) Tf_2O, pyridine, dichloromethane, 0 °C; (vi) $LiPPh_2$, Et_2O, 0 °C.

Scheme 3.2

The choice of the preparing the bulky *tert*-butyl ester was made with the aim of increasing steric hindrance at the ester carbonyl, in order to minimise possible 1,2-addition of the indenyl anion, in the following key reaction, Scheme 3.3.

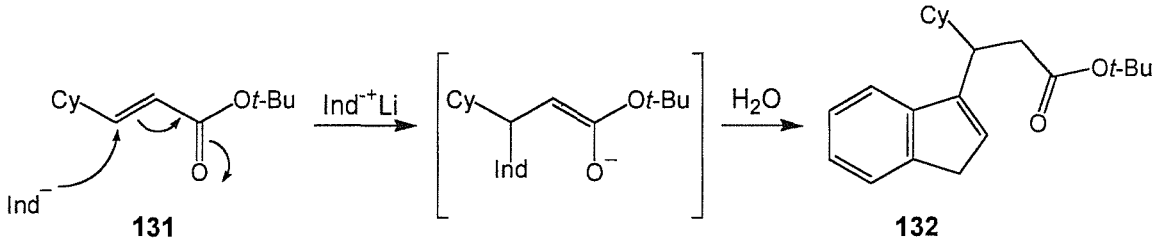

Scheme 3.3

The proposed 1,4-addition reaction of an indenyl anion to the α,β-unsaturated ester **131**, was attempted by the addition of a THF solution of ester **131** to a cold solution of indenyl lithium in THF, at –78 °C. This reaction was monitored carefully by TLC, which indicated the apparent conversion of the starting materials to two close-running new components, initially expected to be the 1,4-addition and 1,2-addition products. Crude ^1H

NMR showed a 5 : 3 mixture of products, however no *trans*-alkene proton resonances were present, which would be expected if the 1,2-addition product had formed. Repeated flash chromatography of the resulting material was required to separate the two products, and once isolated, the *minor* product was confirmed by ^{1}H NMR to be the desired 1,4-addition product **132**.

^{1}H NMR analysis of the major product indicated two sets of *tert*-butyl resonances and double the expected integration for the cyclohexyl protons – but showed only one set of indene resonances. Following further 2D NMR analysis the major product was assigned as the product of a second 1,4-addition reaction, of the enolate of the desired 1,4-addition-product to a further ester molecule, resulting in a di-ester by-product **135**, Scheme 3.4. No mixture of diastereoisomers of **135** were detected, which is not surprising given that the transition state adopted during it's formation is likely to be governed by the steric interactions between the cyclohexyl rings of the two reactants, as shown in Scheme 3.4.

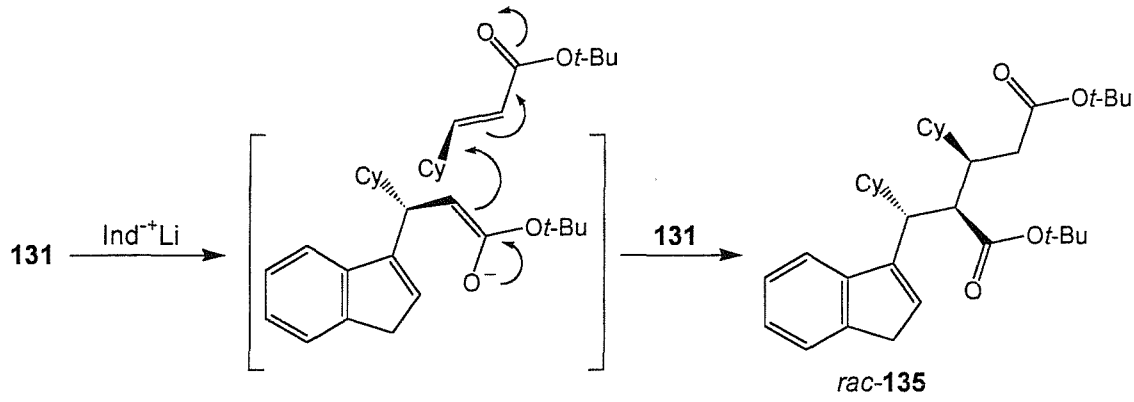

Scheme 3.4

No products of further addition to the di-ester **135** were detected either, which again is not surprising given that **135** is now very sterically hindered, with two cyclohexyl groups and two *tert*-butyl groups in close proximity to each other. The structure of **135** was later confirmed to be as shown by X-ray crystallography, Figure 3.2.

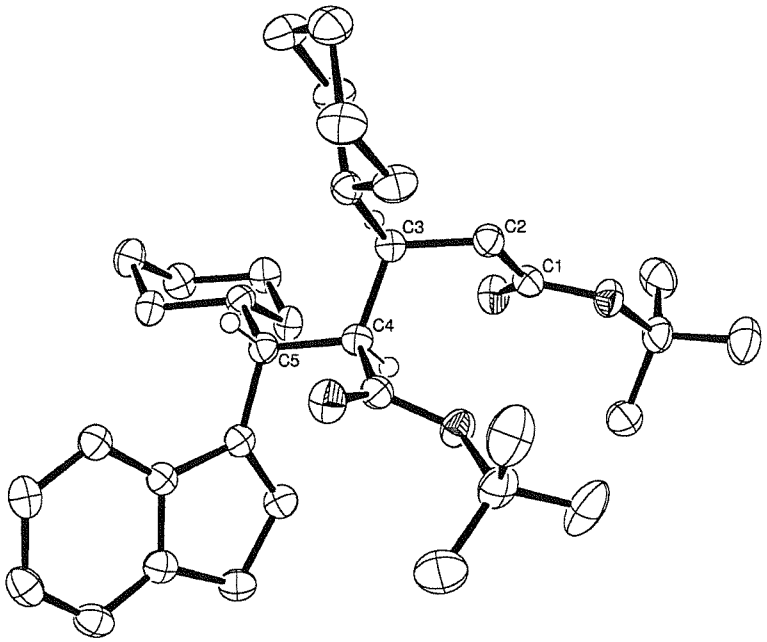

Figure 3.2

ORTEP view of *rac*-135, thermal ellipsoids shown at 50 % probability, H-atoms shown only for C3, C4 and C5. See Appendix 5 for full details.

Having proven that the 1,4-addition of the indenyl anion to the α,β-unsaturated ester was moderately successful, it was now important to optimise the reaction conditions to favour the mono-addition product **132** and minimise production of the double-addition by-product **135**. One would expect less double-addition product to form if the concentration of ester **131** in the reaction was reduced. Another good variation to the conditions would be to increase the quantity of indene present in the reaction, as this may allow the enolate of **132** to reprotonate from excess indene (to give further indenyl lithium) – thus avoiding the possibility of double addition. A summary of the key results from the exploration of different reaction conditions for this transformation is given in Table 3.2.

Reaction	[Ester **26**] / M	Temp. / °C	Ratio Indene:Base	Ratio Product:By-product
1	0.05	0	1.5 : 1	5.6 : 1
2	0.40	0	1.5 : 1	4.9 : 1
3	0.20	20	1.0 : 1	1.9 : 1
4	0.20	20	2.7 : 1	3.8 : 1
5	0.20	–78	2.0 : 1	2.1 : 1
6	0.20	20	2.0 : 1	3.5 : 1

Table 3.2

Other conditions: Reactions 1-6: 1.2 mmol Indenyl lithium prepared from 1.2 mmol n-BuLi and the given ratio of indene, at –78 °C, then 1.0 mmol ester 131 added as THF solution (to achieve total concentration shown), at the given temperature.

A trial reaction combining all the optimum conditions from Table 3.2 was performed to test the overall improvement. The reaction involved addition of ester **131** to a room-temperature solution of indenyl lithium, prepared from a 2.7 : 1 ratio of indene to *n*-butyl lithium, with overall reaction concentration of 0.05 M relative to ester **131**. ^{1}H NMR indicated this reaction achieved a 7 : 1 ratio of product **132** to by-product **135**, a very good improvement over the initial reaction. However the presence of 13 % by-product was still concerning, partly because the double-addition product contains two molecules of **131** (and therefore 26 % of the starting material) but mainly because of the difficulty in separating the product **132** from the double-addition product **135**. Repeated flash column chromatography was required to achieve clean separation of the two compounds – which was time consuming and by no means ideal for large scale synthesis of our ligand. In order to improve the conversion to the mono-addition product **132** and enable large scale preparations of the ligand, further optimisations were required, see Section 3.2.4.

A good temporary solution to the presence of the double-addition product **135**, avoiding the need for repeated chromatography, was to simply proceed directly to the next step in the ligand synthesis without attempting to separate the mixture. The subsequent lithium aluminium hydride reduction of the mixture of **132** and **135**, provides an easily separable mixture of alcohol **133** and the presumed (but not isolated) highly-polar diol **136** from the double-reduction of **135**, Scheme 3.5. Column chromatography (40 % diethyl ether/petrol) of the mixture of alcohols provided **133** as a pale yellow solid, in a moderate 42 % yield over the last two steps.

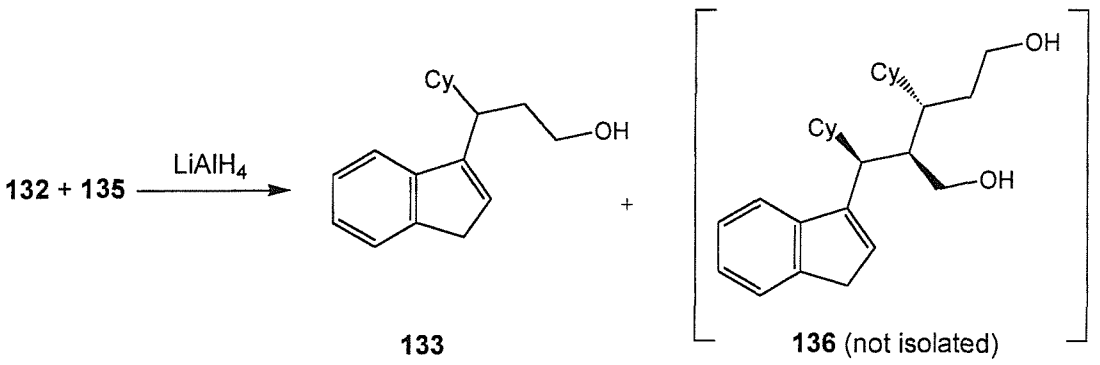

Scheme 3.5

Having prepared alcohol **133**, the next stage involves activation of the alcohol and displacement by the diphenylphosphide anion. As in the synthesis of the two-carbon bridged ligand **121**, the mesylate **137** was prepared by reaction of alcohol **133** with mesyl chloride and triethylamine at –20 °C, over two hours. After aqueous workup, the crude mesylate was isolated as a white oily solid, in 98 % yield, Scheme 3.6.

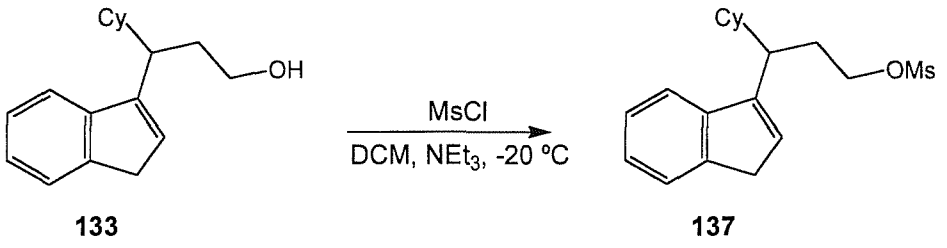

Scheme 3.6

It had been hoped that reaction of mesylate **137** with potassium diphenylphosphide would result in direct displacement of the mesylate to form the three-carbon bridged ligand **129** rather than forming the strained 4-membered spirocycle **138**, would be disfavoured. Mesylate **137** was therefore treated with potassium diphenylphosphide in THF, and stirred for 24 hours. The crude material isolated from the reaction was then treated with borane-methyl sulphide at 0 °C, to form the protected ligand **139**, Scheme 3.7. TLC identified two components present in the crude material and ^{1}H NMR identified the major product to be the spiro-cyclobutane **138**, formed as a 7 : 3 mixture of diastereoisomers, and the minor product as the desired protected ligand **139**. Column chromatography provided the protected ligand **139** in 14 % yield as a white solid, along with the spiro-cyclobutane **138** in 46 % yield, as a clear oil which solidified on standing.

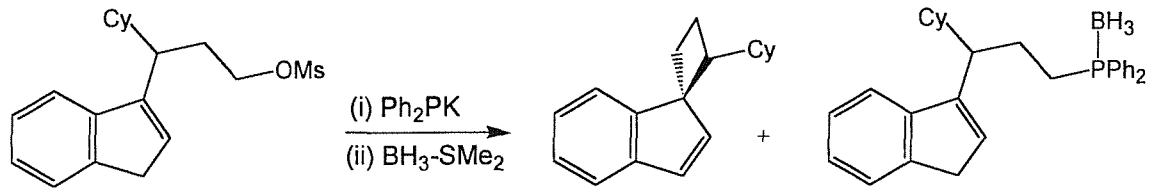

137 **138** 46% **139** 14%

Scheme 3.7

Although slightly disappointing, the presence of both the spiro-cyclobutane **138** and the desired ligand as products of this reaction was an interesting result, especially when considering that an excess of diphenylphosphide had been used in the reaction and thus should have resulted in ring-opening of the spirocycle **138**. This suggests that the spiro-cyclobutane ring is in fact stable to attack by diphenylphosphide, and as such, the 14 % conversion to the desired ligand must have resulted from direct displacement of the mesylate group – i.e. the two products result from competing reaction pathways. To confirm this observation, a sample of spiro-cyclobutane **138** was treated with potassium diphenylphosphide and 18-crown-6, under the conditions successful in achieving ring-opening of the spiro-cyclopropane **120** (Figure 2.8). As had been expected, no reaction was detected by ^1H NMR after 48 hours, proving that **138** is stable to attack from diphenylphosphide.

With the knowledge that there are probably two competing reaction pathways leading to the production of these two products, we should be able to favour production of our desired product by 'tuning' the reaction substrate and conditions – selecting an appropriate leaving group, reaction solvent, and source of diphenylphosphide. To favour the ligand product, we need to avoid the deprotonation of the indene group by our source of diphenylphosphide. This should be possible by simply using a more active leaving group, or a less 'basic' source of diphenylphosphide.

The trifluromethanesulphonate group is a suitably more active leaving group than mesylate, therefore triflate **134** was chosen as an alternative to mesylate **137**. Reaction of alcohol **133** with triflic anhydride and pyridine in dichloromethane, gave a 90 % yield of triflate **134** as a pale green oil, after aqueous workup, Scheme 3.8.

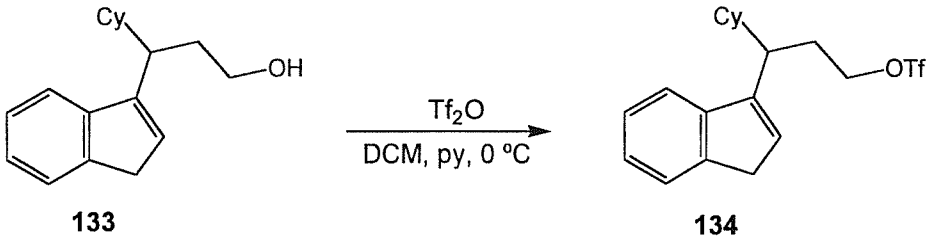

133 **134**

Scheme 3.8

Triflate **134** was found to be unstable to storage for more than 24 hours at –30 °C, and also proved difficult to handle in THF solution – rapidly darkening from pale green to deep purple/black and completely hardening to a glass-like solid in less than one hour at room temperature, presumably owing to trace triflic acid causing polymerisation of the THF.

Reaction of triflate **134** with two equivalents of Ph_2PMgBr (a less basic source of the diphenylphosphide nucleophile, prepared from magnesium bromide and lithium diphenylphosphide) showed encouraging results. ^1H NMR indicated complete consumption of triflate **134**, with no spirocycle **138** present, however only 50 % conversion to the desired ligand was seen, with 50 % conversion to a new by-product. The new by-product was not fully characterised, however a test bromination reaction of triflate **134** with phosphorous tribromide gave an identical crude ^1H NMR to this by-product, so it has been tentatively assigned as the product of bromide having displaced the triflate group, Scheme 3.9.

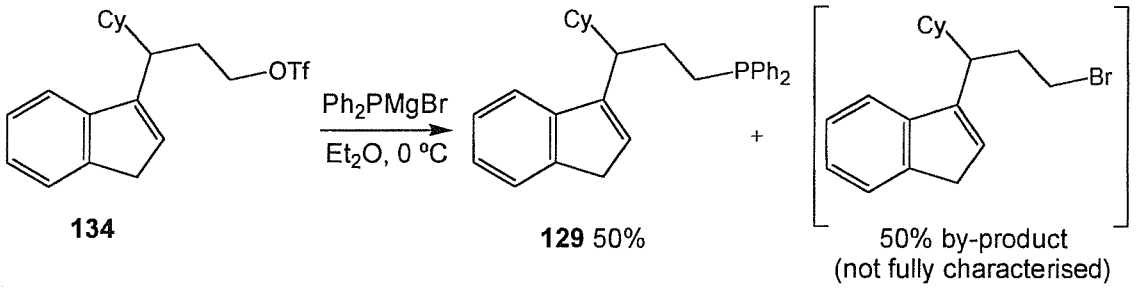

134 **129** 50%

Scheme 3.9

Having successfully displaced the triflate group on **134** without forming any spirocycle, it was important to determine if the phosphide source was crucial for the success of the transformation. If required, the assumed bromide by-product may be avoided by use of $(Ph_2P)_2Mg$ as an alternative source of diphenylphosphide. So triflate **134** was treated with lithium diphenylphosphide (as the phosphide source) and HMPA, with the same solvent,

concentration and temperature as the successful reaction shown in Scheme 3.9. Analysis of the crude material resulting from this reaction showed greater than 90 % conversion to the desired ligand by NMR, demonstrating the Ph_2PMgBr phosphide source was not essential to the success of this reaction.

Further optimisation of the lithium diphenylphosphide reaction avoided the need to use HMPA, with the preferred conditions being triflate in 0.25 M diethyl ether solution at 0 °C, treated with lithium diphenylphosphide and stirred for 18 hours at 20 °C, Scheme 3.10. Column chromatography under argon gave the desired three-carbon bridged ligand **129** in 85 % yield, as a pale yellow air-sensitive oil.

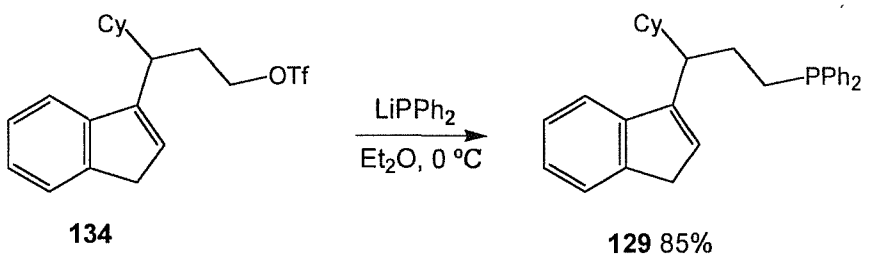

134 **129** 85%

Scheme 3.10

Overall the ligand **129** has been synthesised in 18 % yield over six steps, from malonic acid and cyclohexane carboxaldehyde. However the 1,4-addition of indenyl lithium to the ester **131** remains the lowest yielding step of this synthesis, so before larger quantities of ligand **129** were prepared, some further optimisations of this step were required, and are described below.

3.2.4 Further optimisations to the 1,4-addition of indene to ester 131

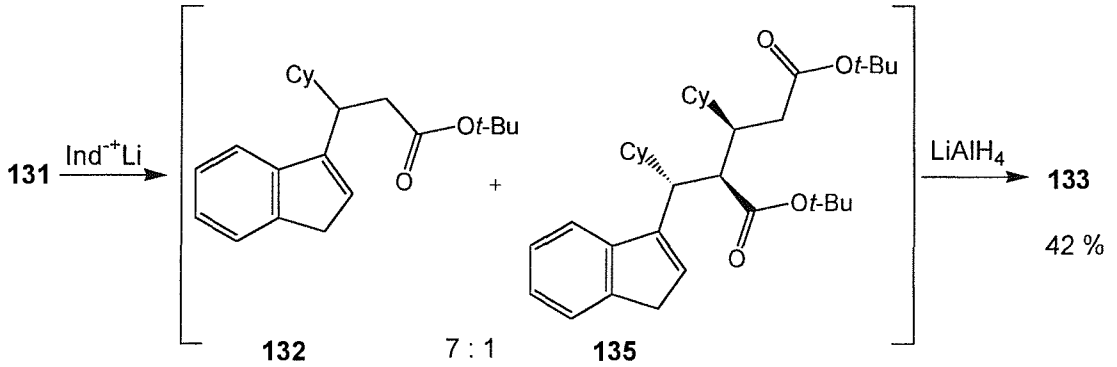

132 7 : 1 **135**

Scheme 3.11

Obtaining only a 42 % yield over the two steps from ester **131** to alcohol **133**, Scheme 3.11, demonstrates that the 1,4-addition reaction requires further optimisation. The maximum yield of **132**, under the current conditions is only 74 %, as a 7 : 1 ratio of products **132** : **135** result from the reaction, and product **135** contains two molecules of the starting material (i.e. 26 % consumed).

The best procedure so far for this conversion involved addition of ester **131** to a room-temperature solution of indenyl lithium, prepared from a 2.7 : 1 ratio of indene to *n*-butyl lithium, with overall reaction concentration of 0.05 M relative to ester **131** (see Table 3.2). Several variations to this procedure were performed, including reversing the order in which the reagents were added. Surprisingly it was found that this reversal of conditions; by simply adding 1.2 eq. of *n*-butyl lithium dropwise to a well stirred mixture of indene and ester **131** at room temperature, resulted in a 89 % conversion to the desired mono-addition product after only 10 minutes, with *no* double-addition product present.
This was a welcome (if a little fortuitous) improvement in the reaction, however conversion to the mono-addition product was not complete by ^{1}H NMR, owing to an 11 % conversion to a new by-product. The new by-product showed alkenyl proton resonances in its ^{1}H NMR at δ 5.53 and 5.37 ppm, along with a large cluster of new aliphatic resonances, integrating to approximately 18 protons. It was therefore assigned as the product of a double 1,2-addition of *n*-butyl lithium to ester **131**, Scheme 3.12.

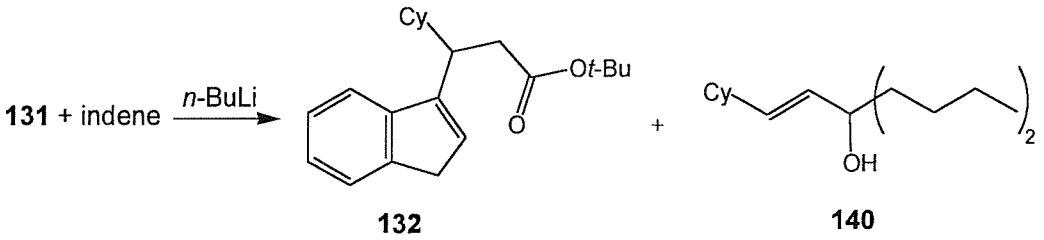

132 **140**

Scheme 3.12

Thankfully the new reaction procedure proved very convenient for rapid testing of conditions in order to minimise the production of the new di-butyl addition product. The results of the variations in concentration, temperature and ratio of indene to *n*-butyl lithium are best summarised in graphical form, see Graphs 3.1, 3.2 and 3.3.

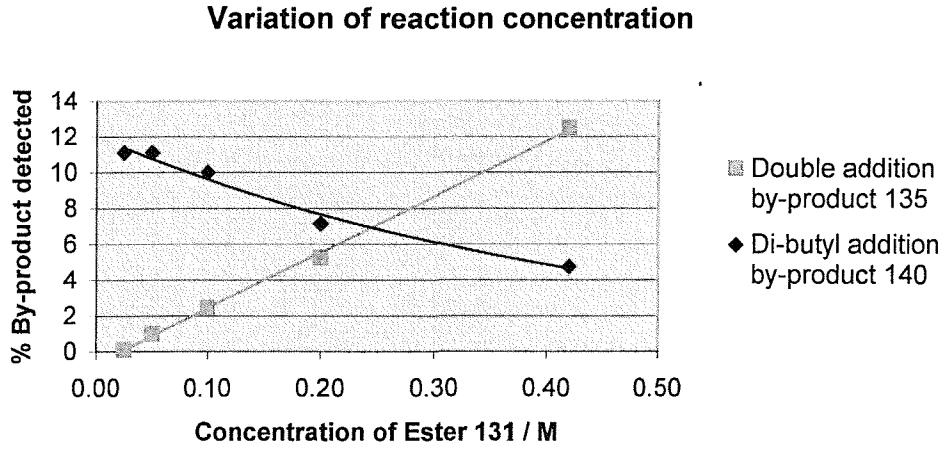

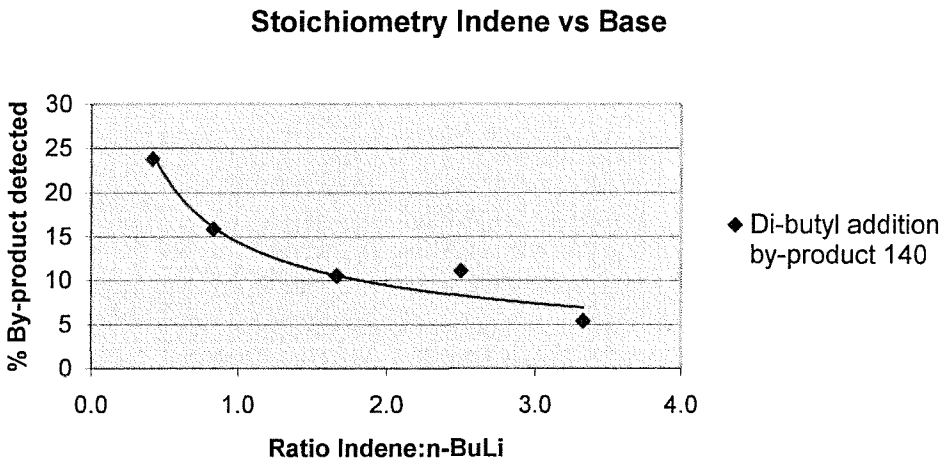

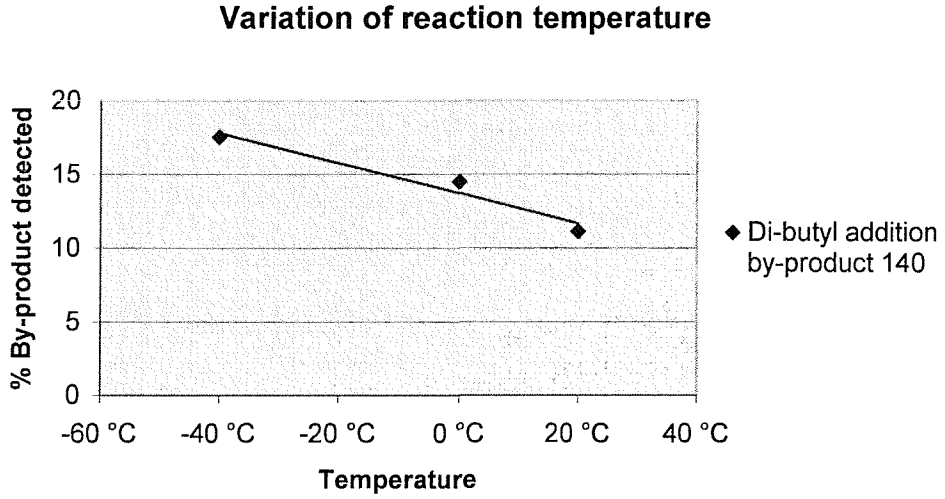

Graphs 3.1 (top), 3.2 (centre), 3.3 (bottom)

General conditions: 1.2 eq. n-BuLi was added dropwise to a 0.05M solution of ester 131 (1 mmol) and 3.0 eq. indene in THF, at room temperature and monitored after 15-20 minutes.

The best reaction conditions after these optimisations were found to be treatment of a 0.05 M THF solution of ester **131** and 4 equivalents of indene, at room temperature, with 1.2 equivalents of *n*-butyl lithium. This resulted in almost clean conversion of **131** to the 1,4-addition product **132**, with less than 5 % of the di-butyl addition by-product **140** detected.

A final optimisation was to vary the base used in the reaction. Use of more sterically hindered bases such as *tert*-butyl lithium or *sec*-butyl lithium should reduce further the di-butyl addition by-product **140**. Also use of a non-nucleophilic base, such as lithium di-isopropylamide, or an inorganic base such as sodium hydride should completely avoid this by-product. The results from these optimisations are detailed in Table 3.3.

Reaction	Base	% Double-addn **135**	% di-Bu addn **140**	% Other	% Product **132**
1	NaH	-	-	-	10 % after 48 h
2	KH	-	-	-	no reaction
3	LDA	16	-	-	84
4	MeLi	-	-	20	80
5	*t*-BuLi	-	4	5	91
6	*s*-BuLi	-	-	-	>99

Table 3.3

Other conditions: Reactions 1-6: base added directly to a 0.05 M THF solution of ester 131 and 3.0 eq. indene at room temperature, reactions 3-6 quenched after 30 minutes, reactions 1 and 2 after 48 hr.

Reaction 6 in Table 3.3 shows *sec*-butyl lithium to be the optimum base for the 1,4-addition reaction of indene to ester **131**, with >99 % conversion (by ^{1}H NMR) to the desired product. With *sec*-butyl lithium as the base, it was found that increasing solvent concentration to 0.20 M had very little affect on the ratio of products – ideal for large scale synthesis of ligand **129**.

This final optimised reaction is now performed routinely on a 40 mmol scale, by addition of *sec*-butyl lithium to a 0.20 M THF solution of ester **131** and three equivalents of indene. After 15 minutes the reaction is quenched and an aqueous workup performed, then the crude 1,4-addition product reduced to the alcohol by $LiAlH_4$ in diethyl ether. This simple procedure provides an 84 % yield of alcohol **133** over the two steps, double the previous yield.

3.2.5 Final optimised synthesis of the three-carbon bridged ligand

Following the final optimisations described above, the synthesis of ligand **129** has now been carried out on a 40 mmol scale, with an overall yield of 36 %, after six steps, Scheme 3.13. Purification by chromatography is only required on three occasions, to obtain ester **131**, alcohol **133** and the final ligand **129**. The borane protected ligand **139** has also been prepared, by reaction of ligand **129** with borane-methyl sulphide complex, to provide an 81 % yield of the air-stable white solid. Complexation of this ligand to rhodium and ruthenium is discussed in Chapter 4.

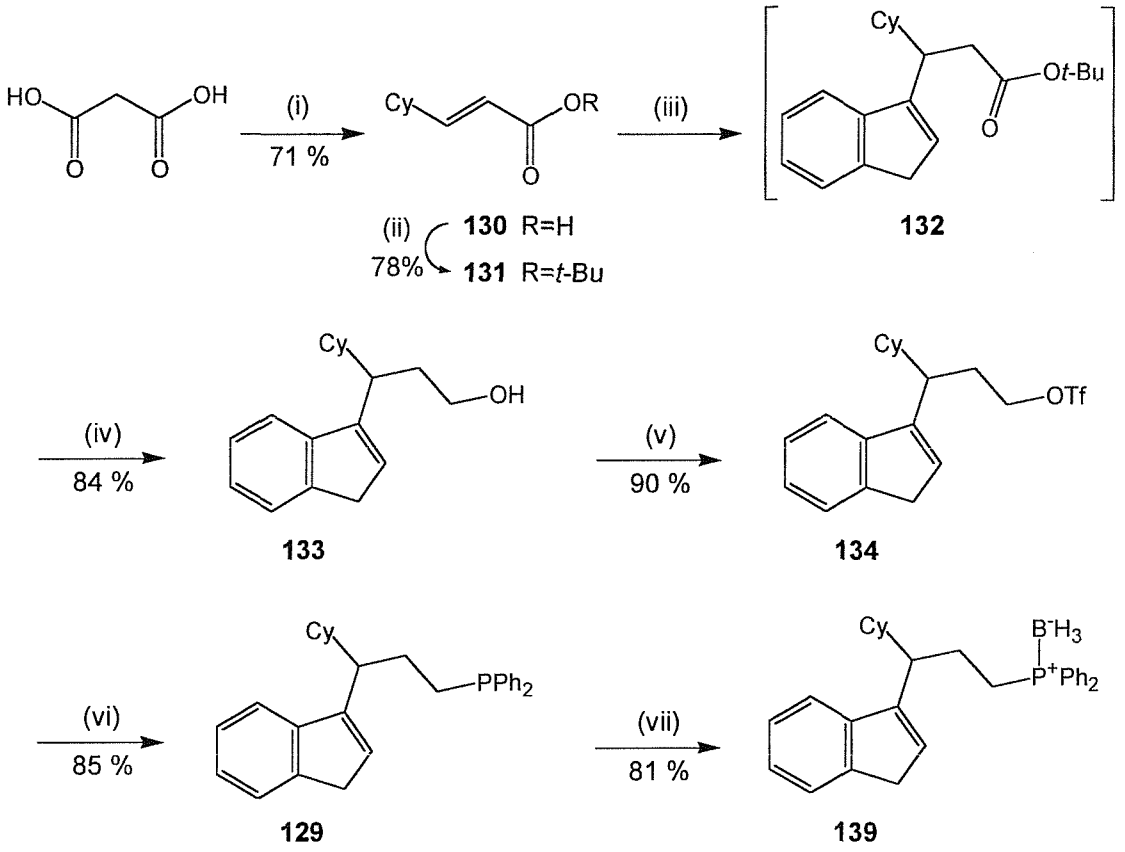

Scheme 3.13

Reagents and conditions: *(i) Cyclohexanecarboxaldehyde, pyridine, cat. piperidine; (ii) isobutylene, CH_2Cl_2, cat. H_2SO_4; (iii) indene, s-BuLi, 0.2 M/THF; (iv) $LiAlH_4$, Et_2O, 0 °C; (v) Tf_2O, pyridine, dichloromethane, 0 °C; (vi) $LiPPh_2$, Et_2O, 0 °C; (vii) BH_3-SMe_2, THF, 0 °C.*

3.3 Modification of co-ordinating 'anchor' group

The nature of the co-ordinating 'anchor' heteroatom on the Cp-tether of bidentate Cp-X ligands can play a very important role in catalytic reactions of the resulting complexes. A

strongly-binding heteroatom may stabilise the binding of the ligand to the metal during vigorous catalytic reaction conditions which could otherwise result in dissociation of the cyclopentadienyl ring from the metal centre. Whereas a 'semi-labile' heteroatom may reversibly dissociate from the metal, serving only as a temporary block to an active co-ordination site. The electronic characteristics of the heteroatom can also have a large affect on the reactivity of metal centre – for example an electron rich co-ordinating group may significantly increase the Lewis basicity of the metal by donation of electron density, affecting it's ability to become involved in some catalytic cycles.

The diphenylphosphine 'anchor' group of ligands **121**, **128** and **129**, described above, is incorporated into the ligand structure only at the final step of its synthesis. Therefore modification of the 'anchor' group should be achieved relatively easily, by simply adjusting the final step of the ligand's preparation – with no need for any major alterations to the ligand synthesis.

3.3.1 Chemistry towards inclusion of different 'anchor' groups

Having available optimised routes to alcohol **133** and triflate **134** (Section 3.2.4), provides two ideal points from which to prepare ligands with an alternative co-ordinating groups to the diphenylphosphine 'anchor' used previously. Elaboration of triflate **134** with various amines, sulphides or alkoxides should lead directly to the corresponding alternative 'anchor' groups. Alcohol **133** may also be functionalised, for example with silicon groups, coupled with alkyl or aryl groups, or even with chloro-diarylphosphines to form phosphinite-type ligands.

3.3.2 Synthesis of indene-sulphur bridged ligands

Transition metal complexes of Cp-bridged ligands containing thio-alkyl and thio-aryl co-ordinating groups are known in the literature,[19] however there have been no reports of indene-bridged ligands containing these 'anchor' groups. The chemistry towards the thio-alkyl and thio-aryl ligands should remain similar to that of the diphenylphosphine ligand **129**, as the anionic lithium salts of the sulphide nucleophiles are available by reaction of the dialkyl- or diaryl-disulphide with *n*-butyl lithium. So this was chosen as an interesting new class of ligands to prepare.

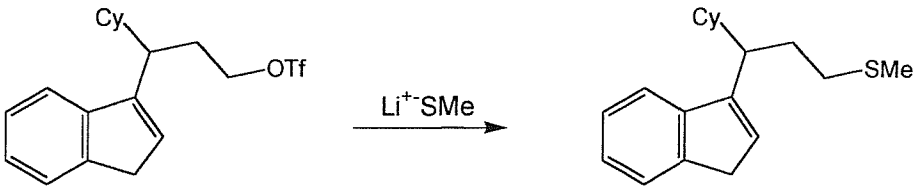

134 141

Scheme 3.14

Thiomethyl-containing ligand **141** was the initial target of this series, Scheme 3.14. Reaction of dimethyl disulphide with *n*-butyl lithium in THF provided a suspension of LiSMe, this was treated with a solution of triflate **134** at –78 °C. ^{1}H NMR confirmed the loss of the triflate, and the presence of a new compound which corresponded with the intended thioether. Column chromatography provided the thiomethyl ligand **141** in 79 % yield, as a pale orange oil. The complexation of this ligand to ruthenium is discussed in Chapter 4.

Plans to prepare further ligands in this series, such as the thiophenyl analogue of **141**, and explore other ligand series such as nitrogen-substituted ligands, were cut short owing to restrictions on time, however this chemistry continues to be developed within the group.

3.4 Alternative axially-chiral ligand design

An alternative planar-chiral complexation model was developed by Baker,[93] intended to resolve the issue of face-selectivity *prior* to complexation, by use of restricted rotation of an axially-chiral ligand. Inclusion of a co-ordinating group constrained to one face of an axially-chiral Cp, and the placement of a bulky substituent 'above' the other face, should force complexation to proceed with complete enantiocontrol to the accessible Cp face, through direct translation of the *axial* to *planar*-chirality upon metallation, Scheme 3.15.

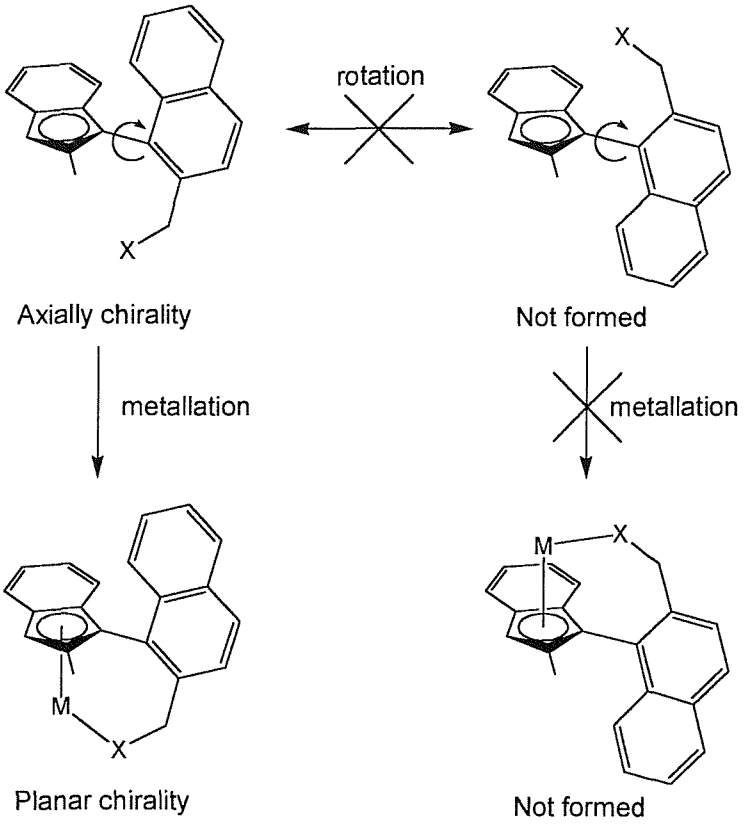

Scheme 3.15

This model has been proved by forming the zirconium complex **143** as a single enantiomer, on complexation of **142** with $Zr(NEt_2)_4$, Scheme 3.16.[94] In collaboration with Rob Baker (University of Sydney) we intend to elaborate this ligand design by inclusion of a diphenylphosphine group, and complex the resultant Cp-phosphine ligand to ruthenium, discussed below.

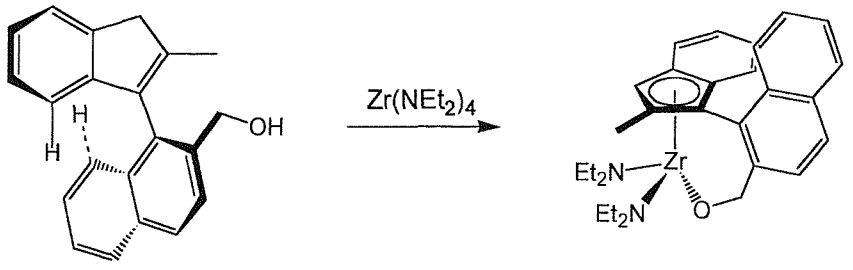

142 >99 % e.e. **143** >99 % e.e.

Scheme 3.16

3.4.1 Modification of *rac*-2-chloromethyl-1-(2-Methyl-1H-inden-3-yl)-naphthalene.

Racemic chloride *rac*-**144** has been provided by Rob Baker (the synthesis of it's precursor alcohol **142** has been reported),[94] for elaboration to the phosphine ligand **145**. The structure of chloride **144** is similar to mesylate **137** and triflate **134**, by having a three-carbon link from the indene to the leaving group, so that upon treatment of **144** with diphenylphosphide, some cyclisation to the spiro-cyclobutane may result. However with chloride **144**, the presence of the aromatic ring in the linking bridge will add rigidity to the carbon chain disfavouring formation of a spirocycle. Also the halide itself is at an activated benzylic position, so we should expect substitution to occur readily here, and hopefully not observe any cyclisation to the spiro-cyclobutane.

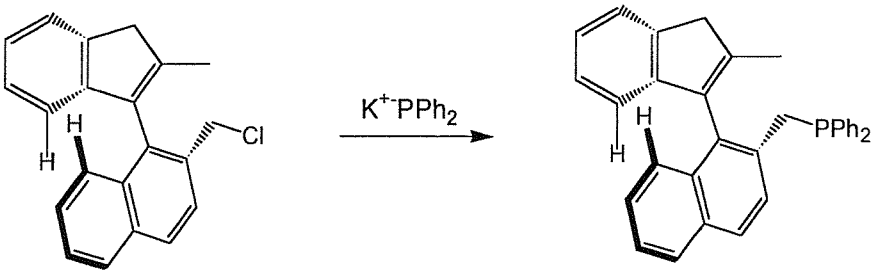

rac-**144** *rac*-**145**

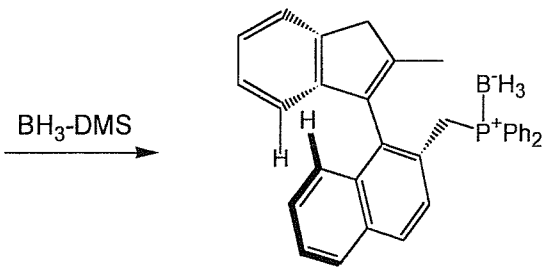

rac-**146**

Scheme 3.15

The reaction shown in Scheme 3.15 was attempted using potassium diphenylphosphide in THF at –78 °C, (no 18-crown-6 was added, as the benzylic chloride should be suitably activated to nucleophilic substitution). After 16 hours, the reaction was complete, and only one non-baseline component was present by TLC. ^{1}H NMR confirmed conversion to a single new compound, with no detected spiro-cyclobutane formed. Column chromatography, under argon, isolated the desired ligand *rac*-**145** as a white air-sensitive

solid, in a moderate 41 % yield. Reaction of *rac*-**145** with borane-methyl sulphide, followed by chromatography gave the protected air-stable ligand *rac*-**146** as white crystals in 72 % yield.
The complexation of ligand **145** to ruthenium is described in Chapter 4.

3.5 Conclusions

- The novel racemic three-carbon bridged phosphine ligand **129** has been prepared, and its synthesis, including a novel 1,4-addition of indenyl lithium to an α,β-unsaturated ester, optimised for large scale (40 mmol) use to provide a 36 % yield of **129** over six steps.

- The novel racemic three-carbon bridged thiomethyl-substituted ligand **141** has been prepared as the first example of a new indene-bridged sulphur ligand series.

- In collaboration with Rob Baker (University of Sydney) the phosphine-substituted axially-chiral indene-naphthalene ligand *rac*-**145** has been prepared from its precursor chloride *rac*-**144**, in 41 % yield.

The three novel ligands prepared here all contain a three-carbon bridge between the indene moiety and co-ordinating group. In the case of ligands **129** and **141**, the cyclohexyl ring substituent *alpha* to the indene ring fulfils the 'favoured rotamer' design requirements (Section 2.1.2) intended to achieve face-selectivity upon complexation to transition metals. The axially-chiral ligand *rac*-**145** gains its chirality from a restrained conformation around the indene-naphthalene bond, and therefore face-selectivity on complexation should be completely controlled. However, metal-centred chirality will still arise from this and other ligands, upon complexation to a suitable metal source, and shall be discussed in Chapter 4.

4. Chapter 4: Synthesis of novel Rhodium and Ruthenium complexes

4.1 Introduction

The syntheses of five novel indene-phosphorous linked ligands have been detailed in Chapters 2 and 3. These ligands contain a bidentate Cp-'anchor' structure, specifically designed for complexation to late-transition metals, Figure 4.1.

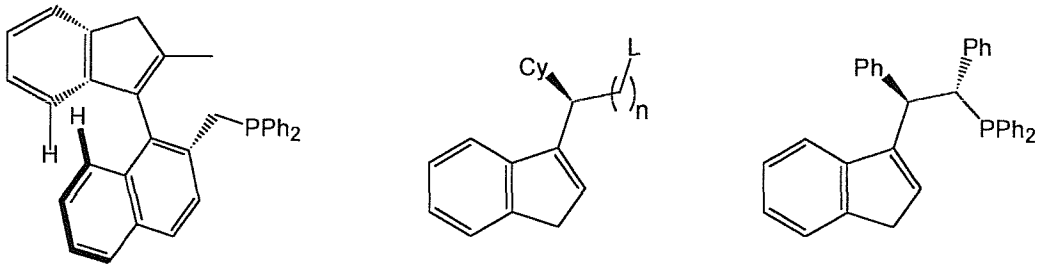

rac-**145**

(*R*)-**121**: n = 1, L = PPh_2
rac-**129**: n = 2, L = PPh_2
rac-**141**: n = 2, L = SMe

rac-**128**

Figure 4.1

Ligands **121**, **129**, **141** and **128** contain a chiral centre on the Cp-'anchor' chain, positioned *alpha* to the indene group, in order to fulfil the requirements of the 'favoured rotamer' complexation model (see Section 2.1.2). This should allow complexation to occur preferentially to one face of the indenyl ligand, thus inducing planar-chirality in the resultant complex, as shown in Scheme 4.1.

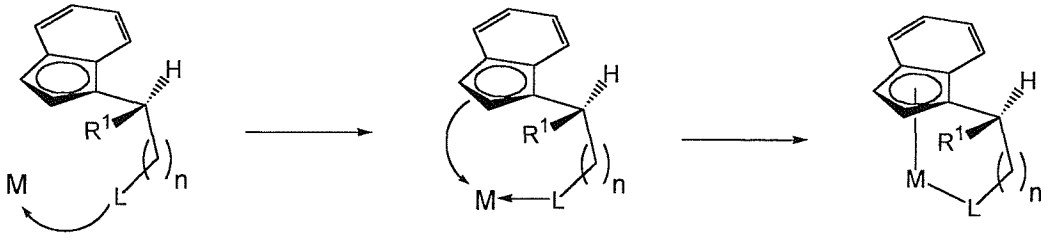

Scheme 4.1

Ligand **145** has been prepared in collaboration with Rob Baker (University of Sydney, Australia), and contains an axially-chiral indene-naphthalene framework, with the diphenylphosphine 'anchor' group confined to one face of the indenyl ring, and the

naphthalene moiety directed above the other face. Induction of planar-chirality is therefore not an issue with this ligand, as metallation can only occur to the face of the indenyl ring containing the diphenylphosphine 'anchor' group. However, complexation to a suitable metal centre could still result in the formation of diastereoisomers owing to incomplete control of the stereochemistry around the metal centre.

Section 4.2 describes the results of complexation of ligands **121**, **128**, **129**, **141** and **145** to ruthenium and the hydrogenation of the ruthenium complex of ligand **121** to its tetrahydroindene analogue. Section 4.3 describes the results of the complexation of ligands **121** and **129** to rhodium.

4.2 Synthesis of Ruthenium complexes

Non-chiral Cp-phosphine tethered ligands are well known,[19] and there are many reports of their ruthenium complexes in the literature, along with recently reported asymmetric catalytic applications of such complexes by Trost[23] and Takahashi.[71] As of yet, however, there have been no reports of the complexation of indenyl-phosphine tethered ligands to ruthenium.

A common preparation of Cp-phosphine tethered complexes of ruthenium involves the reaction of a cyclopentadienyl ligand (often as its lithium anion) the with the commercially available dichloro(tristriphenylphosphine)ruthenium(II) complex $RuCl_2(PPh_3)_3$,[22,23] Scheme 4.2. Where the ligand contains an unsymmetrically-substituted cyclopentadiene linked to a co-ordinating 'anchor' group (such as is the case with our ligands), both planar-chirality *and* metal-centred chirality result on complexation to this ruthenium source. Previous work has shown that the indenyl ligand **59** readily deprotonates with *n*-butyl lithium (see Scheme 1.17, Section 1.4.1),[29] therefore this complexation route should be an appropriate reaction to perform with the indenyl ligands prepared in Chapters 2 and 3.

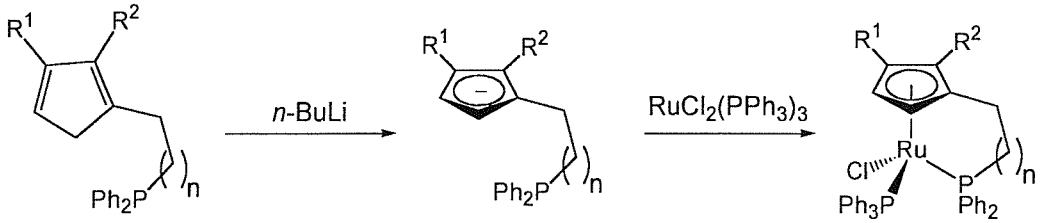

Scheme 4.2

4.2.1 Complexation of cyclohexyl-substituted two-carbon bridged ligand 121

In order to effect complexation to the ruthenium source $RuCl_2(PPh_3)_3$, enantiopure ligand (2*R*)-**121** (Section 2.3) was deprotonated using *n*-butyl lithium at –78 °C in toluene, then treated with a solution of $RuCl_2(PPh_3)_3$ and warmed to reflux for 16 hours, Scheme 4.3. ^{1}H NMR of the crude material showed a mixture of two diastereoisomers had formed, in an 80 : 20 ratio (60 % d.e.). Two close-running components were also visible by TLC, and chromatography through neutral Al_2O_3 provided complex (–)-**147** in 71 % yield, with an increase in the ratio of the major : minor isomers, to 87 : 13 (74 % d.e.).

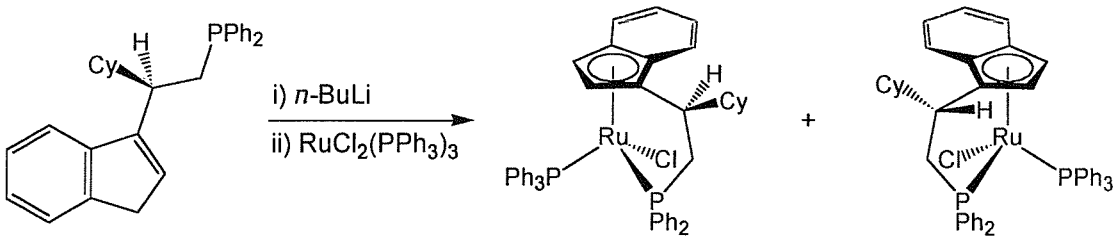

major 80:20 (60 % d.e.) minor

121 **147a** **147b**

Scheme 4.3

Complexation of a bidentate indene-phosphine ligand such as **121** to $RuCl_2(PPh_3)_3$ can result in the formation of up to four diastereoisomers of the product complex, owing to planar-chirality of the pro-chiral indene group, and generation of a chiral centre at the metal atom. In the case of ligand **121**, formation of complex **147** gave only *two* diastereoisomers, indicating complete control of either the metal-centred or planar-chirality. Thus it was vital for this research to determine which diastereomeric pair had been formed.

If the diastereomeric pair is formed as a result of complexation to alternate faces of the indene group, this will result in one diastereoisomer with the indene-aromatic and cyclohexyl groups being on the same side of the CH(Cy)-Ind bond (*syn*) and one isomer with the indene-aromatic and cyclohexyl groups on alternate sides of the CH(Cy)-Ind bond (*anti*). The *anti*-conformation is the intended isomer by our 'favoured rotamer' complexation model, Section 2.1.2. The Cp-protons and tether-chain protons are clearly identifiable in the ^{1}H NMR of **147**, therefore an ideal method of determining if the diastereoisomers are formed a result of planar-chirality, is the use of n.O.e. NMR

experiments to examine through-space interactions between Cp-proton H^a and tether-chain proton H^b, Figure 4.2 shows the expected interactions.

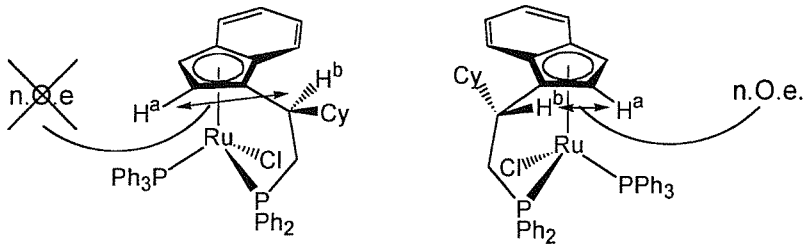

147a (major) **147b** (minor)

Figure 4.2

Proton H^b (major) was confirmed to be at ^1H δ 2.46 ppm (by HMQC correlation with the major isomer's CH(Cy) carbon at ^{13}C δ 37.35 ppm). H^b (minor) was similarly confirmed to be at ^1H δ 2.01 ppm (by HMQC correlation to minor isomer's CH(Cy) carbon at ^{13}C δ 47.45 ppm). The two Cp(major) proton resonances were seen at δ 5.04 and δ 2.28 ppm, and the two Cp(minor) proton resonances were present at δ 5.11 and δ 2.80 ppm. The unusually high-field shift of one Cp-proton in both isomers has been reported to occur with the related Cp-phosphine tethered complex **6**, Figure 4.3.[22] White *et. al.* found evidence that this effect was as a result of shielding of the Cp-proton from a proximal phenyl ring of a triphenylphosphine ligand.

N.O.e experiments were therefore carried out, irradiating H^b and both Cp protons of each diastereoisomer. Irradiation of the Cp(major) protons showed no interactions with H^b(major), whereas irradiation of the Cp(minor) proton at δ 2.80 ppm showed a strong interaction with H^b(minor) at δ 2.01 ppm. The reverse experiment, irradiation of H^b(minor) confirmed the interaction with the Cp(minor) proton at δ 2.80 ppm. These results confirm the diastereoisomers to be planar-chiral diastereoisomers, as shown in Scheme 4.3 and Figure 4.2. A further n.O.e. experiment showed a strong interaction between one of the tether CH_2 protons and the Cp(major) proton at δ 2.28 ppm, this, along with the Cp(minor) evidence above, confirms that the high-field shifted Cp-proton resonances for both isomers occur from the Cp-proton adjacent to the Cp-phosphine tether, as was found by White *et. al.* for the related Cp-phosphine complex **6**, Figure 4.3.[22]

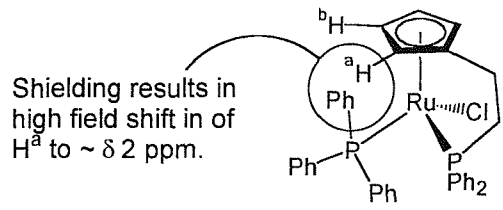

6

Figure 4.3

The fact that only two diastereoisomers have been formed thus indicates that the configuration about the new chiral metal centre is completely controlled by the planar-chirality of the complexed indenyl moiety. The configuration of the metal centre in the major isomer has been proven by X-ray crystallography (see below), but that of the minor isomer has not. However we expect the minor isomer to be as shown in Figure 4.2, based partly on the knowledge that the triphenylphosphine ligand must be proximal to the Cp(minor) proton H^a (see above) in order to effectively shield this proton and cause the high-field shift of its ^{1}H NMR resonance,[22] and also based on precedent from the analogous complexes with 3-carbon tethered ligands, where both the major and minor isomers were characterised by crystallography (see Section 4.2.4).

The results of the complexation of **121** to form ruthenium complex **147** were therefore very encouraging for the success of our 'favoured rotamer' complexation model (see Sections 2.1.2 and 4.1), showing a 60 % d.e. induction of planar-chirality, with only a single metal-centred configuration resulting on complexation to each diastereotopic face. Slow diffusion of pentane into a benzene solution of *rac*-**147** at 5 °C, provided crystals of the major isomer *rac*-**147a**, suitable for X-ray structure analysis, see Figure 4.4.

A comparison table of selected bond lengths and angles for complex **147a**, complex **6** and complex **149a** (described in Section 4.2.3, below) is given in Table 4.1.

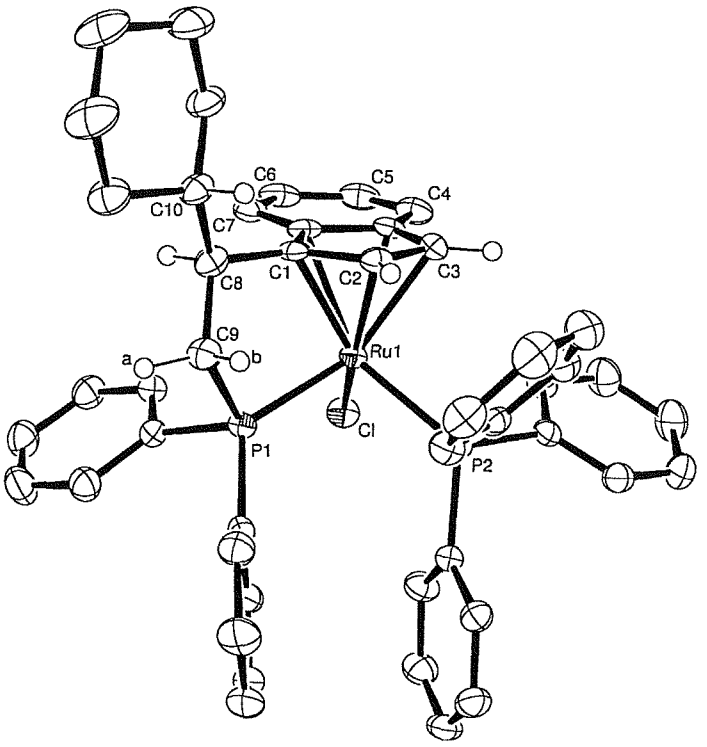

Figure 4.4

ORTEP view of *rac*-147a, thermal ellipsoids shown at 50 % probability, H-atoms shown only for C2, C3, C8, C9 and C10. See Appendix 6 for full details.

Key features of this X-ray structure include: The planar-chiral stereochemistry demonstrated by the forward-facing cyclohexyl group at C8; Alignment, by pi-stacking, of the 'south'-facing phenyl rings of the triphenylphosphine and diphenylphosphine groups; Also the ability of the chloride ligand to fit directly underneath the indene group is a likely reason as to why a defined configuration at the metal centre results on complexation to each face of the ligand – as this positioning minimises steric interactions between the indene aromatic group and the large triphenylphosphine ligand.

An important observation from this X-ray structure is the proximity of the Cp-proton H2 and the 'northern'-facing phenyl ring of triphenylphosphine ligand. The distances from H2 to the *ipso*-C is only 2.8 Å; to *ortho*-C's is *ca.* 3.0 Å; to *meta*-C's is *ca.* 3.3 Å; and to *para*-C is 3.5 Å. This shows that H2 is placed very close to the electron cloud of this phenyl ring, which is almost certainly the reason as to the very high-field shift of this proton in the ^{1}H NMR. Similar distances of *ca.* 3 Å, for the high-field shifted Cp-proton in complex **6** (Figure 4.3) to its proximal phenyl ring have been reported.[22]

	Complex **147a**	Complex **149a**	Cp complex **6**[22]
Ru-C1	2.163(3)	2.159(5)	2.201(5)
Ru-C2	2.166(2)	2.168(5)	2.158(5)
Ru-C3	2.231(2)	2.227(5)	2.208(5)
Ru-C3a	2.304(2)	2.313(5)	2.198(6)
Ru-C7a	2.272(3)	2.261(5)	2.207(6)
Ru-P1	2.272(1)	2.298(1)	2.311(1)
Ru-P2	2.299(1)	2.320(1)	2.307(2)
$Cp_{centroid}$-Ru-P1	115.95	115.47	n/a
$Cp_{centroid}$-Ru-P2	121.44	122.61	n/a
$Cp_{centroid}$-Ru-Cl	124.82	123.89	n/a
Ru-P1-C9-H9a	162.05	161.69 (to Cl1)	n/a
P1-C9-C8-C10	169.62	168.32	n/a
P1-C9-C8-H8	74.46	71.70	n/a

Table 4.1

Selected bond lengths (Å) (with esds) and torsion angles (degrees) for complexes 147a, 149a and 6.

Indenyl-transition metal complexes are known to display some degree of η^5 to η^3 distortion.[62] This can be seen in Table 4.1, for complexes **147** and **149**, by the slightly longer bond lengths between ruthenium and the Cp-bridgehead carbons C3a and C7a compared to the bond lengths of the ruthenium-Cp-carbons C1, C2 and C3 (note this is not seen with the cyclopentadienyl complex **6**). The degree of η^3 distortion can be expressed by the 'slip parameter' Δ, which is calculated as the difference between the average bond lengths of the metal/bridgehead (C3a, C7a) carbons, and the average bond lengths of the metal/cyclopentadienyl carbons C1-C3.

For complex **147**: Δ = (2.288 – 2.187) = 0.10 Å

Values of the slip parameter Δ vary from <=0.03 Å for true η^5 complexes (Cp-complex **6** gives Δ = 0.01 Å) to >=0.42 Å for true η^3 complexes.[95] In the case of complex **147**, this indicates a slight distortion towards η^3 co-ordination of the indenyl ligand.

Trials of complex **147** in catalytic reactions have been performed, see Chapter 5 for a full discussion of the results.

4.2.2 Hydrogenation of 147 to give 4,5,6,7-tetrahydroindenyl complex 148

Indenyl complexes such as **147** will undoubtedly have greatly different electronic characteristics to analogous cyclopentadienyl complexes (such as Cp-complex **6**, Figure 4.3). Whereas the ease of η^5 to η^3 ring-slippage in some indenyl complexes is known to allow greater catalytic activity when compared to their analogous Cp-complexes[62] (see Section 1.7), the "electronic reservoir"[63] of the aromatic indenyl ligand may also preclude indenyl complexes from taking part in some reactions which are catalysed by their analogous Cp-complexes.

Following our initial catalytic trials of complex **147** (see Chapter 5), it seemed prudent to find a method of preparing a cyclopentadienyl analogue of complex **147** in order to directly compare their catalytic activities. Hydrogenation of indenyl ligands complexed to transition metals is common-place with early transition metals such as zirconium and titanium,[3] and formation of the tetrahydroindenyl analogue of complex **147** would provide us with an ideal Cp-analogue of this complex. However few examples have been reported of this hydrogenation with later transition metals, such as ruthenium. The only report of hydrogenation of an indenyl ligand on ruthenium comes from Gansow *et. al.* in 1976.[96] Here the successful hydrogenation of an dinuclear indenyl-ruthenium carbonyl complex with Adams' catalyst, is mentioned very briefly although no experimental details are given.

Therefore hydrogenation of complex **147** was attempted using 10 mol % PtO_2 under a hydrogen atmosphere. Despite having no success after several attempts and various conditions, the literature evidence[96] for the successful hydrogenation of an indenyl-ruthenium complex still gave encouragement and our efforts were rewarded when, under the conditions of 10 % PtO_2 and 1800 psi hydrogen, at 65 °C for three days, successful hydrogenation of complex **147** was achieved. Tetrahydroindenyl complex **148** was therefore prepared in 99 % crude yield, after filtration of the hydrogenation mixture through celite, Scheme 4.4. Final purification of **148** was achieved by column

chromatography through Al_2O_3, to provide complex **148** in 40 % isolated yield, as a bright yellow powder (*cf.* complex **147**, a dark brown solid).

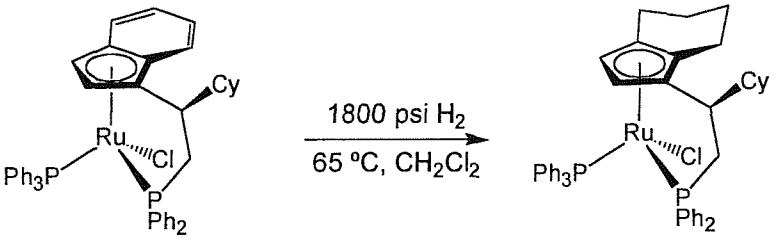

147 (74% d.e.) **148** (74% d.e.)

Scheme 4.4

Integration of the ^{1}H NMR of **148** confirmed the loss of four aromatic protons, and the gain of eight alkyl protons, as well as confirming the retention of the 74 % d.e. of the precursor indenyl complex. The hydrogenation of the aromatic carbons C4-C7 of complex **147** to the alkyl carbons of **148** was also confirmed by the ^{13}C NMR spectrum.

Unfortunately crystallisation and X-ray structure analysis of **148** has not yet been achieved. However an interesting comparison of the major isomers of the indenyl and tetrahydroindenyl complexes **147a** and **148a** can be made from their ^{13}C NMR spectra, which have been assigned and tabulated in Table 4.2. The spectra are remarkably similar, with the resonances and coupling constants almost identical for all but the indene and Cp carbons. This suggests, in the absence of an X-ray structure, that these two complexes exist in very similar conformations, for example Figure 4.5.

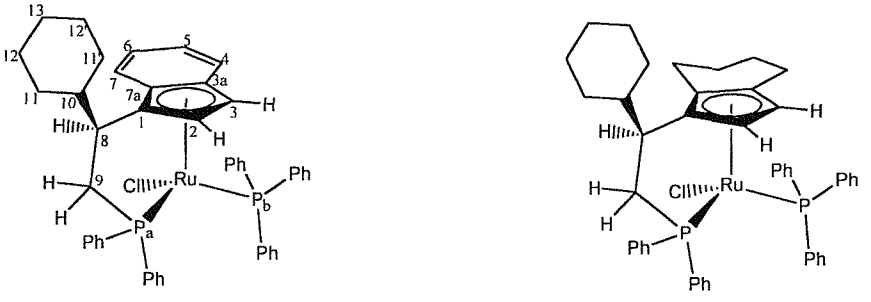

147a **148a**

Figure 4.5 Numbering scheme for ^{13}C NMR data in Table 4.2

Indenyl Complex **147a** (major)				Tetrahydroindenyl Complex **148a** (major)			
Assignment***	δ_C	J_{CP}[a]	J_{CP}[b]	Assignment	δ_C	J_{CP}[a]	J_{CP}[b]
i-Ph	139.76	26.4	-	*i*-Ph (PPh_3)	139.30	-	28.4
i-Ph	139.74	26.5	-	*i*-Ph	139.15	26.4	-
i-Ph (PPh_3)	138.51	-	29.9	*i*-Ph	139.12	26.2	-
o-Ph	135.60	10.6	-	*o*-Ph	135.24	10.9	-
o-Ph (PPh_3)	134.23	-	broad	*o*-Ph (PPh_3)	134.09	-	broad
o-Ph	131.53	9.2	-	*o*-Ph	131.54	9.2	-
7/4	129.94	1.9	1.9				
p-Ph	129.87	1.9	-	*p*-Ph	129.81	2.2	-
p-Ph (PPh_3)	128.91	-	1.4	*p*-Ph (PPh_3)	128.75	-	-
p-Ph	128.09	-	-	*p*-Ph	128.30	-	-
m-Ph	127.97	9.2	-	*m*-Ph	128.12	9.2	-
m-Ph	127.82	8.7	-	*m*-Ph	127.73	8.9	-
m-Ph (PPh_3)	127.77	-	9.4	*m*-Ph (PPh_3)	127.70	-	9.2
5/6	127.65	2.9	-				
5/6	123.80	2.9	-				
7/4	121.93	-	-				
3a	106.96	4.4	1.0	3a	110.92	3.9	1.2
7a	106.42	6.0	1.9	7a	100.67	8.0	1.9
1	94.26	11.6	2.4	1	89.39	14.0	2.2
2	74.59	6.8	2.4	2	80.39	6.5	-
3	66.65	-	-	3	59.08	-	-
9	51.21	32.9	-	9	50.55	33.3	-
8	42.53	19.8	-	8	42.88	19.1	-
10	37.35	4.8	-	10	37.28	5.1	-
11/11'	33.45	-	-	11/11'	33.44	-	-
11/11'	31.14	-	-	11/11'	31.33	-	-
12/12'/13	26.43	-	-	12/12'/13	26.53	-	-
12/12'/13	26.18	-	-	12/12'/13	26.41	-	-
12/12'/13	26.07	-	-	12/12'/13	26.18	-	-
				4/5/6/7	24.09	-	-
				4/5/6/7	23.45	1.7	-
				4/5/6/7	22.70	-	-
				4/5/6/7	21.55	-	-

Table 4.2 100 MHz ^{13}C NMR data (in C_6D_6) for complexes 147a and 148a.

*** Assignments are based on results from ^1H, ^{13}C, DEPT and 2D COSY H-H and C-H correlation experiments. Where the signals could not be unambiguously assigned, all possible assignments are given.

4.2.3 Complexation of diphenyl-substituted two-carbon bridged ligand *rac*-128

Ligand *rac*-**128** (Section 2.5.1) has been complexed to ruthenium in a similar manner to ligand **121** (Section 4.2.1), although in the case of the more air-sensitive ligand **128**, the lithium salt of *rac*-**128** was prepared by the ring-opening of precursor spirocycle **127** with lithium diphenylphosphide, and the ligand was not purified prior to complexation. The crude lithium salt of *rac*-**128** was therefore treated with $RuCl_2(PPh_3)_3$ at –78 °C, in toluene, then warmed to 95 °C for 24 hours, Scheme 4.5. Crude ^1H NMR of the complexation mixture showed the presence of the desired complex **149**, as an 87 : 13 mixture of diastereoisomers (74 % d.e.). ^{31}P NMR confirmed this ratio, but here a second pair of trace resonances were also visible, integration showed the ratio of the minor pair of resonances to the major pair as *ca.* 14 : 1 (87 % d.e.).

Purification of the complex was achieved by chromatography through neutral Al_2O_3, to provide **149** as green/brown solid, and improved 91 : 9 mixture of isomers by ^1H NMR (the second 'trace' pair of isomers was not clearly visible by ^1H NMR, however ^{31}P NMR showed a *ca.* 23 : 1 ratio of the major pair to the minor pair, i.e. 92 % d.e.).

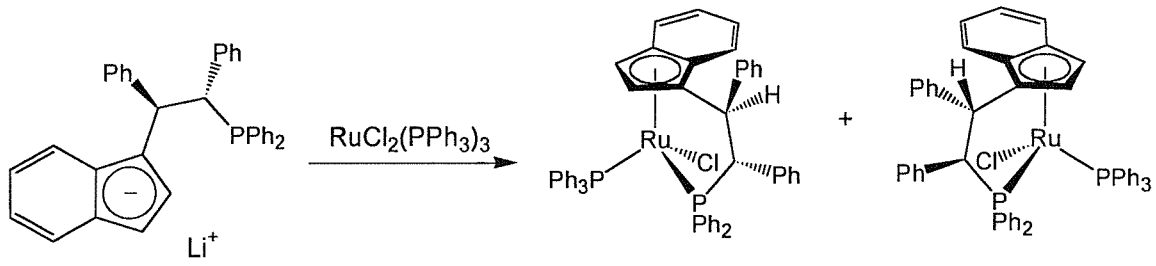

major 87:13 (74 % d.e.) minor

rac-**128** **149a** **149b**

Scheme 4.5

Only two diastereoisomers were clearly visible by ^1H NMR of **149**, with the major Cp-proton resonances at δ 4.88 and 3.47 ppm, and the minor resonances at δ 5.11 and 3.76 ppm. As with complex **147**, n.O.e. experiments were used to determine the origin of these diastereoisomers. The results showed that irradiation of either Cp(major) proton signal gave no interaction with the major tether protons at δ 5.25 and 4.82 ppm, whereas irradiation of the Cp(minor) proton at δ 3.76 ppm gave a strong interaction with the minor tether proton at δ 4.09 ppm. This suggests that the pair of diastereoisomers visible by ^1H NMR are those formed as a result of induction of planar-chirality and therefore the

'trace' pair of diastereoisomers, seen only in the ^{31}P spectrum (major : minor ratio of *ca.* 23 : 1), must be formed due to incomplete control of stereochemistry at the metal centre. Again the high-field shift of one Cp-proton is seen for the major and minor isomer of **149**, although not to the same degree as seen for complex **147**. The benzylic tether-chain protons are seen as double-doublets (owing to ^{31}P coupling) at δ 5.25 and 4.82 ppm for the major isomer, and at δ = 6.15 and 4.09 ppm for the minor isomer.

Again the 'favoured rotamer' design of this ligand has shown great success on complexation. The diastereocontrol at the metal centre, although not complete, was very high (14 : 1) and improved with chromatography. Control of planar-chirality with ligand **128** was improved over the cyclohexyl-ligand **121**, with a 74 % d.e. induction of planar-chirality seen on complexation to ruthenium.

Slow diffusion of pentane into a benzene solution of *rac*-**149**, provided crystals of the major isomer, **149a**, suitable for X-ray crystallography. The structure solution is shown in Figure 4.6.

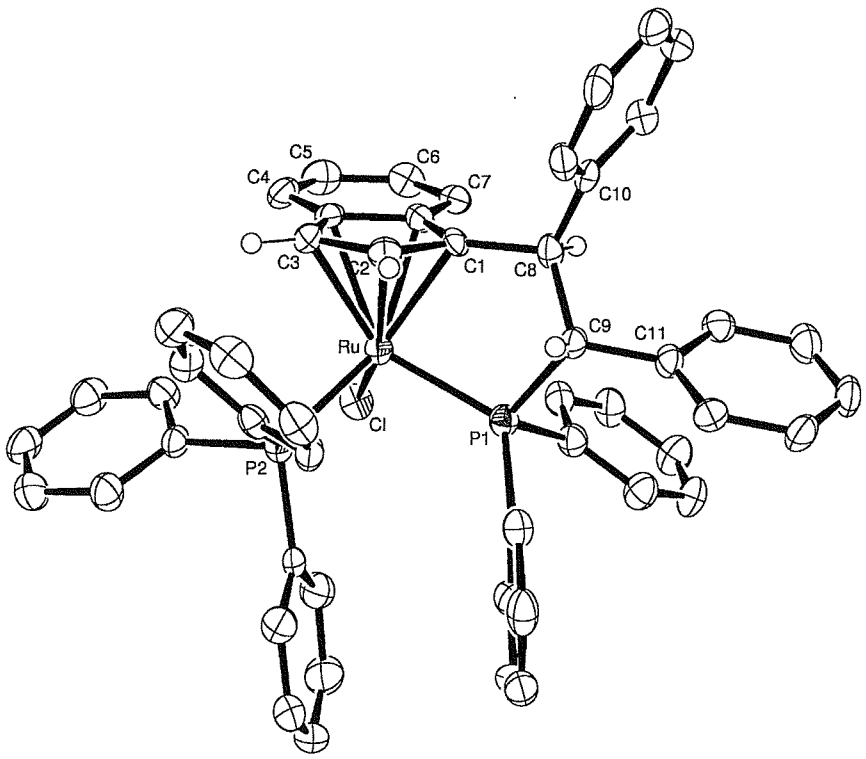

Figure 4.6

ORTEP view of *rac*-149a, thermal ellipsoids shown at 50 % probability, H-atoms shown only for C2, C3, C8 and C9. See Appendix 7 for full details.

A comparison table of selected bond lengths and angles for complex **149a**, and the related complexes **147a** and **6**, have been given in Section 4.2.1 above, in Table 4.1.

From the X-ray data, the degree of η^3 distortion of the indene ligand can be calculated and expressed by the 'slip parameter' Δ^{95} (see Section 4.2.1).

For complex **149a**: $\Delta = (2.287 - 2.185) = 0.10$ Å

Note that the crystal structure of **149a** contains two inequivalent molecules of **149a** in the unit cell. These two molecules retain the same structural conformation as each other, and differ only slightly as a result of similar, but non-identical bond-lengths – therefore Figure 4.6 shows only one of the two molecules, for clarity. (Full tabulated data for both molecules is included in Appendix 7).

For the second molecule of **149a** in the unit cell: $\Delta = (2.312 - 2.188) = 0.12$ Å

These values of the slip parameter Δ show that, as with complex **147a**, a slight distortion towards η^3 co-ordination occurs with complex **149a** (with the second molecule in the unit cell having crystallised with a very slight increase in η^3 distortion than the first molecule).

4.2.4 Complexation of cyclohexyl-substituted three-carbon bridged ligand 129

Following the same complexation procedure as for ligand **121**, the three-carbon tethered indene-phosphine ligand *rac*-**129** (Section 3.2.2) has been complexed with $RuCl_2(PPh_3)_3$ to form complex **150**, Scheme 4.6. ^{1}H NMR of the crude mixture showed an 83 : 17 ratio of two diastereoisomers (66 % d.e.). Two separate components were also visible by TLC, and careful chromatography through neutral Al_2O_3 provided both isomers of complex **150**; the major isomer **150a** eluted first, as a dark red solid, in 55 % yield; the minor isomer **150b** eluted second, as a red/brown solid in 9 % yield.

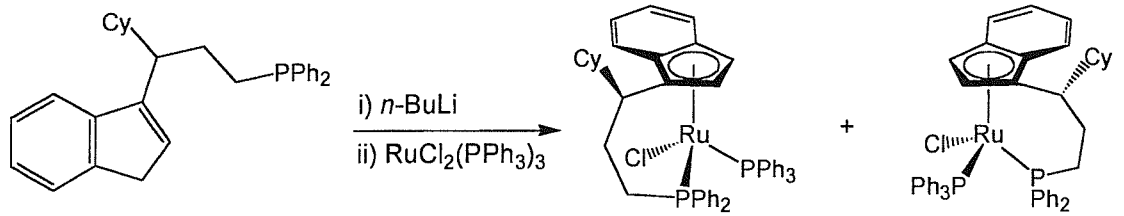

major 83:17 (66 % d.e.) minor

rac-**129** **150a** **150b**

Scheme 4.6

Upon complexation to ruthenium with ligand **129**, as with the analogous two-carbon tethered ligand **121**, the configuration of the new chiral metal centre in complex **150** has been completely controlled by the planar-chirality of the complexed indenyl group. The high degree of induction of planar-chirality (66 % d.e.) achieved with ligand **129**, demonstrates once again the success of the 'favoured rotamer' complexation model and design of these *alpha*-substituted Cp-phosphine ligands.

The ^{1}H NMR of the planar-chiral diastereoisomers **150a** and **150b** shows some striking differences, in particular the positions of the Cp-protons. For the major isomer, **150a**, the Cp-protons are present at δ 4.65 and 3.36 ppm, again showing the high-field shift of one Cp-proton as the result of its proximity to a phenyl ring of the triphenylphosphine ligand.[22] However, for the minor isomer **150b**, both the Cp-protons appear further downfield, at δ = 4.90 and 4.38 ppm, therefore not showing a large high-field shift, which suggests a very different conformation of the ligand in this minor isomer.

Crystallisation of the major isomer **150a** was achieved by slow diffusion of pentane into a benzene solution of the complex, at 5 °C. The minor isomer crystallised fortuitously upon standing of an ethereal solution of **150b** at room temperature for five minutes. The X-ray structures have been solved for both diastereoisomers of complex **150**, see Figures 4.7 and 4.8.

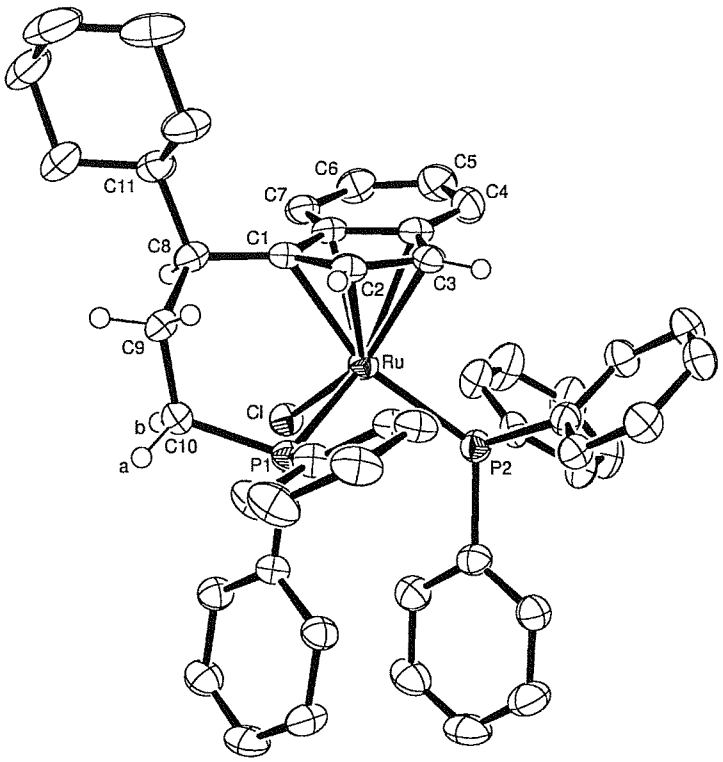

Figure 4.7

ORTEP view of *rac*-150a, thermal ellipsoids shown at 50 % probability, H-atoms shown only for C2, C3, C8, C9 and C10. See Appendix 8 for full details.

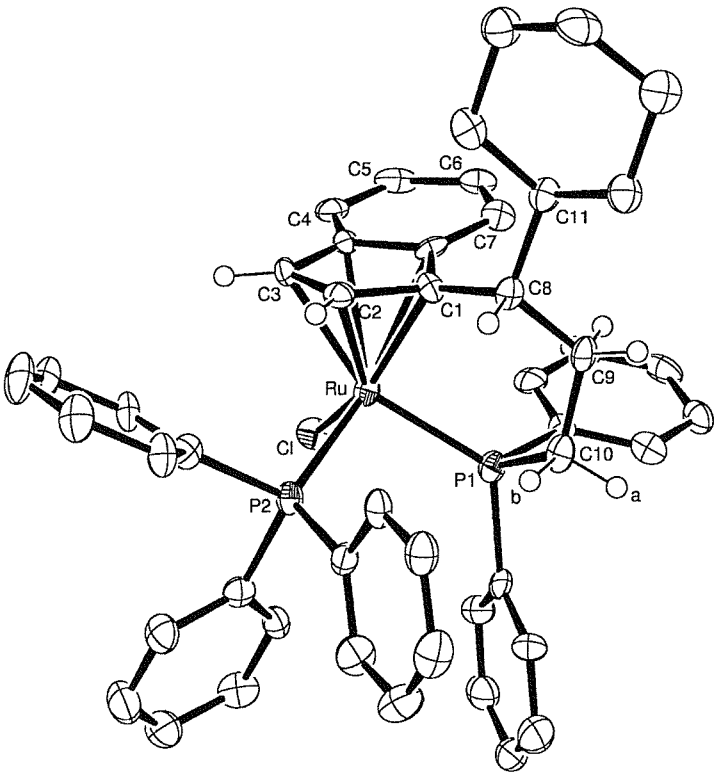

Figure 4.8

ORTEP view of *rac*-150b, thermal ellipsoids shown at 50 % probability, H-atoms shown only for C2, C3, C8, C9 and C10. See Appendix 9 for full details.

It is interesting to compare the X-ray structures of complex **150a** and complex **147**, containing the two-carbon tethered ligand. The additional carbon in the tether-chain of complex **150a** has resulted in a change in orientation of the tethered diphenylphosphine group in this complex. As such, the phenyl rings of the diphenylphosphine group and the triphenylphosphine ligand are now forced together, which gives rise to the very clear pi-stacking arrangement of the 'south'-facing and 'north'-facing phenyl rings of the two groups. The third phenyl ring of the triphenylphosphine ligand is now forced backwards towards, and almost underneath, the indene ring. This has caused a shift in the position of the chloride ligand from sitting directly underneath the indene moiety, in complex **147**, to sitting to the 'west' of the indene group in complex **150a**. The ORTEP view of complex **150a** also shows clearly the proximity of Cp-proton H3 to the 'northern' phenyl ring of the triphenylphosphine group, the probable cause of the high-field shifted Cp resonance in the proton NMR.

The structures of the major and minor isomers of complex **150** are very different, as expected owing to the inversion of planar-chirality. The structure of the minor isomer, **150b**, clearly shows the opposite planar-chiral stereochemistry at C1 to that of **150a**. As a result, the configuration around the metal centre has also inverted, with the triphenylphosphine ligand of the minor isomer now occupying the site taken by the tethered-diphenylphosphine group in the major isomer. Pi-stacking of the phenyl rings is less obvious in the X-ray structure of **150b**, however a clear parallel arrangement of the indene aromatic ring and the backwards-pointing phenyl ring from the diphenylphosphine group can be seen. Alignment of the 'south'-facing phenyl ring of the diphenylphosphine and the 'east'-facing ring of the triphenylphosphine ligand is also evident. The ^{1}H NMR of **150b** failed to show the characteristic high-field Cp-proton shift that was present for the major isomer **150a** and previous complexes **149a** and **147a**. The X-ray structure of **150b** shows the reason for this very clearly – neither Cp-proton H2 or H3 is directed towards the centre of a proximal phenyl ring. The closest phenyl ring to H2 and H3 is the 'north'-facing phenyl ring from the triphenylphosphine ligand, however this is positioned directly between protons H2 and H3, therefore any shielding interaction by the phenyl ring's electron cloud on either proton is much reduced with this isomer.

Table 4.3 shows a comparison of selected bond lengths and torsion angles for diastereoisomers **150a** and **150b**, and complex **151a** (discussed below, Section 4.2.5).

	Complex **150a**	Complex **150b**	Complex **151a**
Ru-C1	2.198(4)	2.191(4)	2.212(4)
Ru-C2	2.156(3)	2.150(4)	2.221(4)
Ru-C3	2.184(3)	2.225(4)	2.210(4)
Ru-C3a	2.345(4)	2.374(4)	2.283(4)
Ru-C7a	2.335(4)	2.387(4)	2.282(4)
Ru-P1	2.260(1)	2.290(1)	2.300(1)
Ru-P2	2.318(1)	2.276(1)	2.327(1)
$Cp_{centroid}$-Ru-P1	118.05	120.70	118.43
$Cp_{centroid}$-Ru-P2	127.24	121.92	127.59
$Cp_{centroid}$-Ru-Cl	121.06	121.36	119.26
Ru-P1-C10-H10a	179.74	179.38	170.44
C10-C9-C8-C11	166.89	173.21	176.81
C10-C9-C8-H8	49.90	56.28	-
P1-C10-C9-C12	-	-	137.46

Table 4.3

Selected bond lengths (Å) (with esds) and torsion angles (degrees) for complexes 150a, 150b and 151a.

The 'slip parameter' Δ^{95} (see Section 4.2.1) showing the degree of η^3 distortion of the indene ligand in complexes **150a** and **150b** has been calculated below:

For complex **150a** (major): $\Delta = (2.340 - 2.179) = 0.16$ Å

For complex **150b** (minor): $\Delta = (2.381 - 2.189) = 0.19$ Å

Interestingly the minor isomer, **150b**, shows a slightly greater distortion towards η^3 co-ordination than the major isomer. Both diastereoisomers of complex **150** show a significantly greater degree of η^3 co-ordination than with the two-carbon tethered ligands of complexes **147a** and **149a**, which may therefore lead to increased catalytic activity with this three-carbon tethered Cp-phosphine complex.[63] Table 4.4 (below) tabulates the ^{13}C NMR assignments for the major and minor isomers of complex **150**.

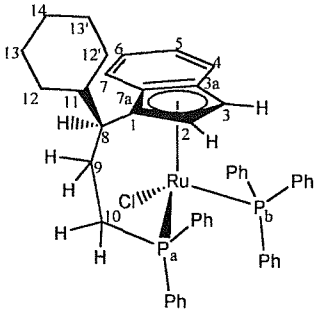

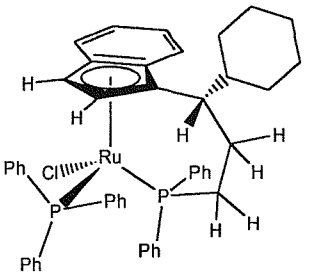

Complex **150a** (major)				Complex **150b** (minor)			
Assignment	δ_C	$J_{CP}{}^a$	$J_{CP}{}^b$	Assignment	δ_C	$J_{CP}{}^a$	$J_{CP}{}^b$
i-Ph	139.32	39.1	-	*i*-Ph	141.90	29.6	-
i-Ph (PPh_3)	138.88	-	35.2	*i*-Ph (PPh_3)	138.89	-	35.2
i-Ph	137.47	43.2	-	*i*-Ph	137.50	43.2	-
o-Ph	135.28	9.7	-	*o*-Ph (PPh_3)	134.71	-	9.7
o-Ph (PPh_3)	133.69	-	10.9	*o*-Ph	132.40	9.7	-
o-Ph	133.28	7.5	-	*o*-Ph	131.96	8.3	-
p-Ph	129.98	2.2	-	*p*-Ph	131.55	2.7	-
p-Ph	128.38	2.4	-	*p*-Ph (PPh_3)	129.15	-	0.7
5/6	128.30	-	-	*p*-Ph	128.87	5.6	-
p-Ph (PPh_3)	128.17	-	1.9	*m*-Ph	128.11	10.0	-
m-Ph	127.89	9.7	-	*m*-Ph	127.80	8.3	-
m-Ph (PPh_3)	127.61	-	9.0	*m*-Ph (PPh_3)	127.46	-	9.5
m-Ph	127.19	9.0	-	5/6	125.82	-	-
5/6	125.81	-	-	5/6	125.65	-	-
4/7	125.73	-	-	4/7	125.18	-	-
4/7	123.93	-	-	4/7	124.61	-	-
3a	110.67	1.5	3.6	3a	119.24	1.6	3.0
7a	105.53	7.3	-	7a	101.13	8.5	1.0
2	84.18	-	-	2	83.22	-	-
1	75.06	13.5	1.1	3	72.64	-	3.4
3	64.38	-	1.2	1	70.78	13.9	-
11	45.68	4.9	-	11	44.31	-	-
8	40.06	2.2	-	8	42.64	-	-
12/12'	30.59	-	-	12/12'	32.13	-	-
12/12'	30.46	-	-	12/12'	31.75	-	-
10	30.37	35.4	1.1	10	29.76	37.2	-
13/13'/14	27.07	-	-	13/13'/14	26.68	-	-
13/13'/14	27.01	-	-	13/13'/14	26.62	-	-
13/13'/14	26.71	-	-	13/13'/14	26.56	-	-
9	26.22	-	-	9	25.55	-	-

Table 4.4 100 MHz ^{13}C NMR data (in C_6D_6) for major and minor diastereoisomers of 150.

The positions and coupling constants for the ^{13}C resonances listed in Table 4.4, appear relatively similar for both isomers, however key differences are the positions of the Cp-carbons C1, C3, 3a and C7a which find themselves in very different environments for the two planar-chiral isomers.

4.2.5 Complexation of Rob Baker three-carbon indene-naphthalene ligand 145

The axially-chiral ligand **145**, developed in collaboration with Rob Baker (University of Sydney, Australia), differs significantly from the previously discussed ligands **121**, **128** and **129**, in that one face of the indene moiety is effectively shielded by the naphthalene group, whereas the other face remains accessible to metallation. Interchange between the two faces cannot occur during complexation, as a result of restricted rotation about the indene-naphthalene bond. This design should therefore allow direct translation of the axial-chirality to planar-chirality, thus enantiopure ligand **145** will lead to a single planar-chiral enantiomer of the resultant complex, and the prepared racemic ligand *rac*-**145**, will lead to a racemic 50/50 mixture of planar-chiral enantiomers. A pair of diastereoisomers may still result from the complexation of *rac*-**145** to the ruthenium source $RuCl_2(PPh_3)_3$ owing to incomplete stereocontrol at the newly formed chiral-metal centre.

Complexation of the lithium anion of *rac*-**145** with $RuCl_2(PPh_3)_3$ was performed under the conditions used for complexation of ligand **121** (Section 4.2.1) and resulted in an 86 : 14 mixture of diastereoisomers (72 % d.e. by ^{31}P NMR). Scheme 4.7 shows these metal-centred diastereoisomers **151a** and **151b**, along with their planar-chiral enantiomers.

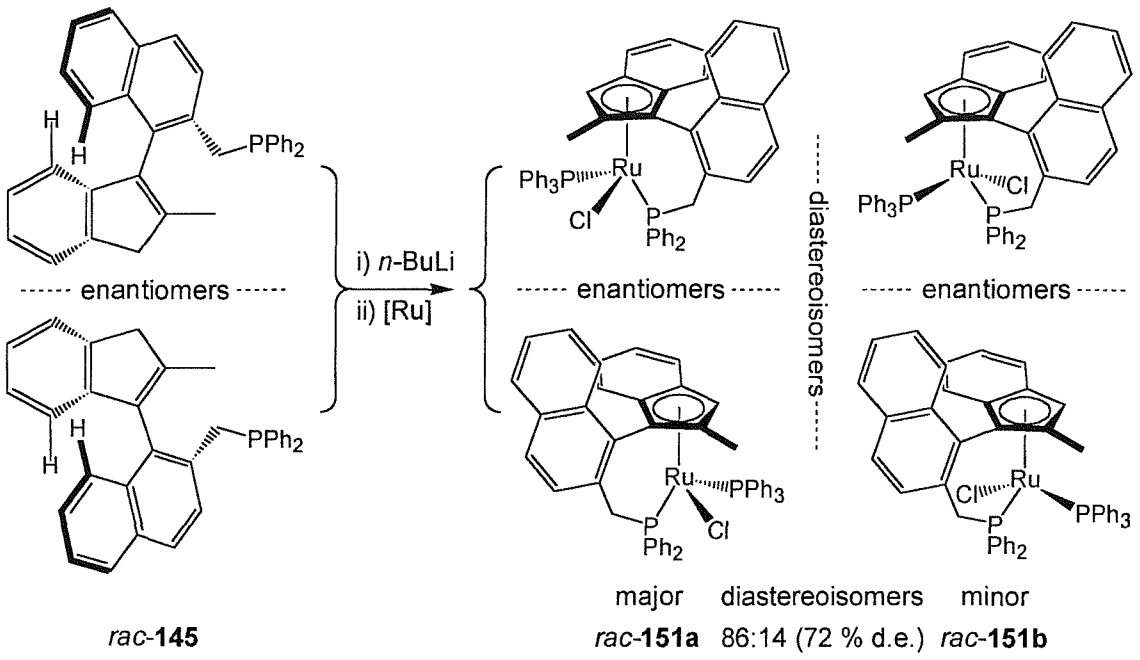

Scheme 4.7

The complex *rac*-**151** was purified by column chromatography through neutral Al_2O_3, and the collected 38 % yield of a brick red solid was now determined to have a slightly reduced diastereomeric excess of 66 % d.e. (83 : 17 ratio of diastereoisomers), by ^{31}P NMR.

The control of stereochemistry at the metal-centre of **151** (72 % d.e.) arising on complexation of ligand **145** is markedly lower than that seen for the analogous complexes of ligands **121**, **129** (complete control) and **128** (>10 : 1 selectivity). Whereas none of the above ligands have been specifically designed to achieve these high levels of diastereocontrol at the metal centre, it is most likely that the high stereocontrol has arisen from the steric repulsion of the triphenylphosphine ligand with the diphenylphosphine 'anchor' group and the indene aromatic ring. The X-ray structures of complexes **147**, **149** and **150** (both planar-chiral isomers) all show the chloride ligand occupies the co-ordination site directly below, or closest to, the indene aromatic ring – allowing the bulky triphenylphosphine group to occupy a less hindered position to side of the Cp-ring. The structure of ligand **145** differs from the previous three-carbon bridged ligand **129** by the presence of the naphthalene group on its Cp-phosphine tether and the methyl group at the C2 position of the Cp-ring. Although sterically bulky, the naphthalene group of ligand **145** is too far removed from the metal centre to afflict the large decrease in control of the

metal-centre stereochemistry on complexation. This decrease is therefore likely to be as a result of the presence of the C2-methyl group in ligand **145**. The methyl group at C2 will have at least one of its protons facing downwards, below the plane of the indene ring and towards the previously less hindered co-ordination site of the metal. The effect of this will be that the co-ordination site 'in front' of the Cp-ring will be now become sterically hindered, possibly even less favourable to the triphenylphosphine group than the site below the indene ring. With both of these sites sterically hindered, they will be of similar steric energy levels, in which case there will be less discrimination by the triphenylphosphine group on formation of the complex, and hence a lower selectivity at the metal-centre will result.

Successful re-crystallisation of **151** by diffusion of pentane into a benzene solution of *rac*-**151** at 5 °C, gave crystals suitable for X-ray analysis. Figure 4.9 shows the ORTEP drawing of **151a**.

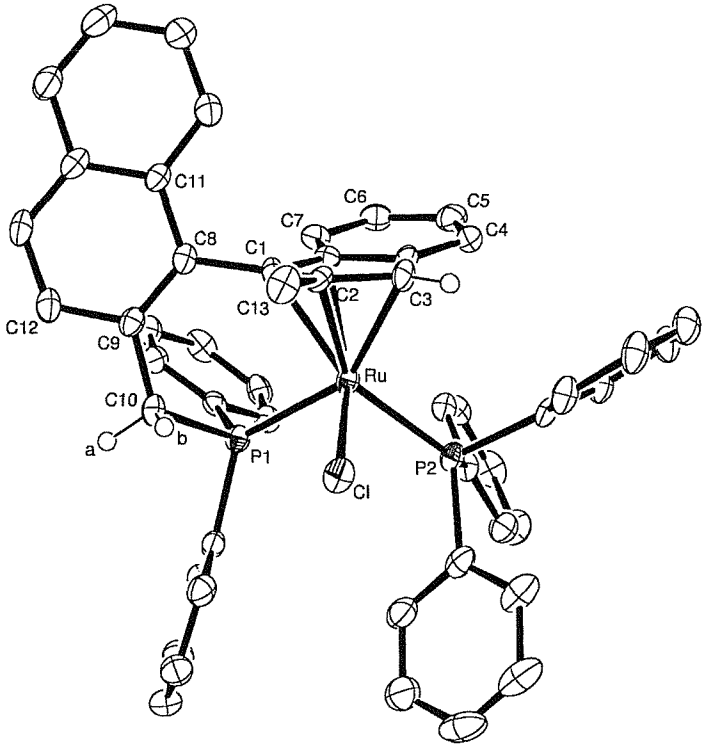

Figure 4.9

ORTEP view of *rac*-151a, thermal ellipsoids shown at 50 % probability, H-atoms shown only for C3 and C10. See Appendix 10 for full details.

The X-ray structure view of complex 151a, Figure 4.9, shows that the C2-methyl group has had a large effect on the structure of this complex. Unlike the previous complexes, for complex 151a we see the chloride ligand pointing forwards, 'in front' of the Cp-ring and directly below the C2-methyl group. The triphenylphosphine ligand and the diphenylphosphine 'anchor' group have therefore both been forced 'backwards' towards the indene ring.

Table 4.3 (Section 4.2.4) contains a list of selected bond lengths and torsion angles for complex **151a**, as well as complexes **150a** and **150b**. From these data, we can calculate Δ, the 'slip parameter' which shows the degree of η^3-distortion for these indenyl complexes.[95] (see Section 4.2.1).

For complex **151a**: Δ = (2.283 – 2.214) = 0.07 Å

As with the X-ray structure of complex **149a**, a second inequivalent molecule of complex **151a** is present in its unit cell, again of the same structural conformation and differing only as a result of similar, but non-identical bond lengths – therefore Figure 4.9 shows only one of the two molecules, for clarity. (Full tabulated data for both molecules is included in Appendix 10).

For the second molecule of **151a** in the unit cell: Δ = (2.283 – 2.214) = 0.07 Å

These low values of Δ suggest this complex is much less distorted towards η^3 co-ordination than the previous complexes. (*cf.* analogous three-carbon bridged complex **150a**, Δ = 0.16 Å).

4.2.6 Complexation of three-carbon thiomethyl-substituted ligand 141

Complexation of the thiomethyl ligand **141** was attempted using the conditions of the complexation of ligand **121** (Section 4.2.1). Thus ligand **141** was deprotonated with *n*-butyl lithium in toluene, then treated with a solution of $RuCl_2(PPh_3)_3$ and warmed to reflux for 16 hours, Scheme 4.8. After this time, crude ^{1}H NMR showed that complexation had clearly occurred, by the presence of the two sharp Cp-H signals at δ

4.89 and 2.98 ppm, with no starting material remaining. Interestingly, no minor Cp-H signals were seen at all, suggesting very good induction of planar-chirality and metal-centred stereocontrol.

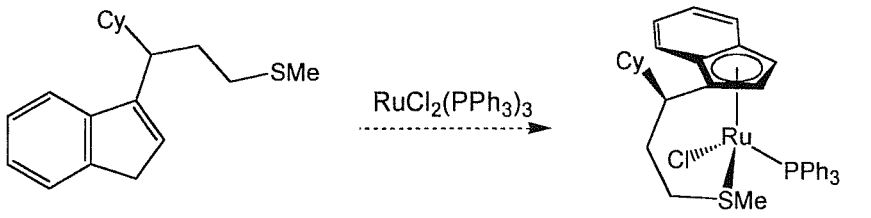

141 **152**
(not fully characterised)

Scheme 4.8

Unfortunately column chromatography of the resultant complex **152**, failed to provide clean material, with the ^{1}H NMR of the collected rust-red solid now indicating the presence of three very broad resonances at δ 3.92, 3.68 and 2.64 ppm. C-H correlation NMR failed to reveal the origin of these broad signals, which may belong to a diastereoisomer of **152**, or to the Cp-thiomethyl tether protons.

Complex **152** has so far resisted recrystallisation, and time constraints have precluded any further attempts at purification of this interesting compound.

4.2.7 Stability of Ruthenium complexes

It was noticed when preparing solutions of **147** for NMR analysis, that this complex appeared unstable to storage in chloroform solution, while remaining unaffected in benzene solution. In the hope of finding out more information about the stability of the complexes and in particular their planar- and metal-centred chiralities, a set of experiments were carried out to probe the affect of heating of complexes **147**, **149**, **150a**, **150b** and **151** in solution.

Chloroform solutions of complexes **147** (74 % d.e.), **149** (82 % d.e.), **150a** (single isomer), **150b** (single isomer) and **151** (66 % d.e.) were therefore heated at 60 °C for 24 hours, with monitoring by ^{1}H and ^{31}P NMR. Over the course of these experiments, all the

solutions darkened in colour, with the light brown solutions of **147** and **149** and the red solutions of **150a**, **150b** and **151** all resulting in dark brown solutions after 24 hours of heating.

The ^{1}H and ^{31}P NMR of complexes **150a** and **150b** (containing the three-carbon tethered Cp-phosphine ligand) showed very little change during the reaction, with only some very slight broadening of their ^{1}H NMR resonances noticeable after 24 hours. Equally, little change was seen with the metal-centred chiral complex **151** (containing the three-carbon bridged axially-chiral ligand) – demonstrating that the chirality of these complexes remains relatively stable under these vigorous conditions.

However, the complexes of the two-carbon Cp-phosphine tethered ligands proved to be less stable. The ^{1}H and ^{31}P NMR signals for the major isomer of **147** appeared to broaden dramatically over the reaction timescale. After six hours, the major isomer was barely visible by ^{1}H NMR, and by 24 hours only the resonances resulting from the minor isomer were visible in the ^{1}H and ^{31}P spectra (although these resonances had now become broad). Similarly the ^{1}H NMR signals of complex **149** became broad after six hours, and by 24 hours, the baseline noise now swamped the key Cp-H and alkyl-tether signals of complex **149**. This demonstrates the instability of these two ruthenium complexes to chloroform solution. In the case of complex **147**, the rapid broadening of only the major isomer's resonances, in the presence of the minor isomer's signals, may appear to suggest some interconversion from the major to the minor isomer could be occurring. However the intensities of the ^{1}H and ^{31}P spectra became weaker over the course of the reaction, which suggests loss or decomposition of the major isomer, rather than interconversion to the minor isomer.

An important general observation from these experiments, was that despite the probable decomposition of complexes **147** and **149**, no appearance of a second set of isomers, as a result of epimerisation at the metal-centre, was seen for any of the above complexes, by either ^{31}P NMR or ^{1}H NMR. This suggests that these complexes, particularly the more stable three-carbon Cp-phosphine complexes, contain stable chiral environments – ideal for use as asymmetric catalysts.

4.3 Synthesis of Rhodium complexes

Reaction of two equivalents of the anion of a cyclopentadienyl-containing ligand with one equivalent of the rhodium dimer $[RhCl(L)_2]_2$ (where L = CO, C_2H_4, COD) is a very common method of preparing rhodium(I) mono-cyclopentadienyl complexes. Takahashi has used this method in the preparation of the first enantiopure planar-chiral rhodium complex,[12] Poilblanc prepared the first rhodium complexes of Cp-phosphine tethered ligands by this route[20] and more recently Tani has used this method to prepare complexes of chiral indenyl-phosphine bridged ligands.[9,41]

Importantly for this research, previous workers within the Whitby group have used this technique to effect the complexation of indenyl-ligands to rhodium. In particular, Brookings has complexed the *beta*-substituted indene-phosphine ligand **59** to $[RhCl(CO)_2]_2$,[29] with some degree of induction of planar-chirality, Scheme 4.9 (for an explanation of this unexpected induction of planar-chirality, see Section 1.4.1, Figure 1.7 and associated discussion). Comparison with past results and literature compounds therefore makes this complexation route an appropriate reaction to perform with the indenyl ligands prepared in Chapters 2 and 3.

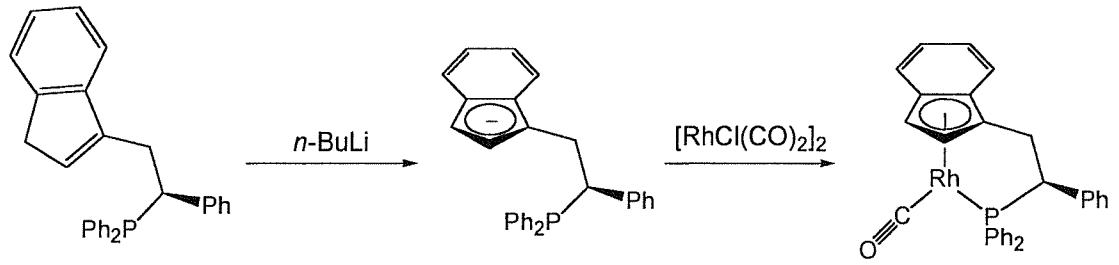

59 Li-**59** **153** 50 % d.e.

Scheme 4.9

4.3.1 Complexation of cyclohexyl-substituted two-carbon bridged ligand 121

Complexation of the enantiopure ligand (2*R*)-**121** (Section 2.3) with the rhodium carbonyl dimer $[RhCl(CO)_2]_2$ was performed by first deprotonating this ligand using *n*-butyl lithium in THF, at –78 °C, then transferring the anion solution dropwise into a solution of $[RhCl(CO)_2]_2$ in THF, at –78 °C. The solution was then warmed slowly to room temperature and stirred for 16 hours, Scheme 4.10. ^{1}H NMR analysis of the crude

showed a 78 : 22 ratio of diastereoisomers of complex **154** had formed, with the major diastereoisomer Cp-H resonances at δ 6.20 and 6.14 ppm, and the minor Cp-H resonances at δ 6.03 and 5.90 ppm. Purification of **154** was achieved by chromatography through Al_2O_3 to provide the complex as an orange powder, in 68 % yield and unchanged ratio of diastereoisomers.

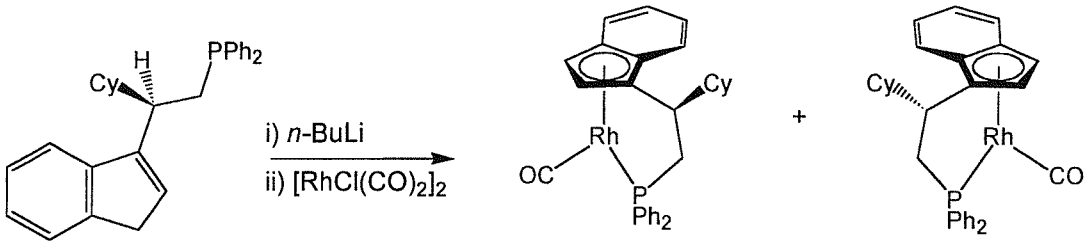

major 78:22 (56 % d.e.) minor

121 **154a** **154b**

Scheme 4.10

Unlike the ruthenium complexations discussed above (Section 4.2) the diastereoisomers formed on complexation of our indenyl-phosphine ligands with $[RhCl(CO)_2]_2$ can only form as a result of the planar-chirality induced on complexation, because the metal centre is not chiral in these complexes. This means the 78 : 22 ratio of diastereoisomers (56 % d.e.) seen on complexation of ligand (2*R*)-**121** is due the induction of planar-chirality on formation of complex **154**. Interestingly when this complexation was performed using the racemic ligand *rac*-**121**, a slightly lower 72 : 28 ratio of diastereoisomers resulted (44 % d.e.). The reason for this small but significant change in face-selectivity when going from enantiopure-**121** to racemic-**121** is not immediately obvious, however a good explanation can be given by examining the proposed key intermediate in the mechanism of complexation of Cp-phosphine ligands to $[RhCl(CO)_2]_2$, Scheme 4.11.

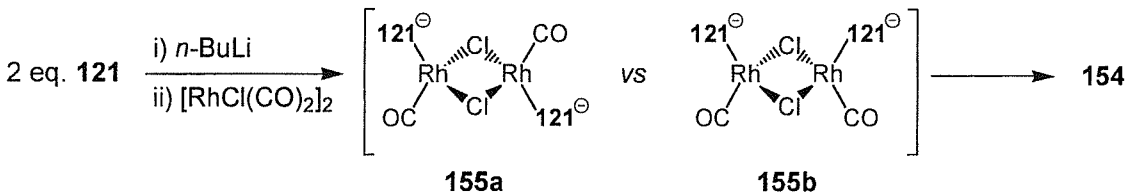

155a **155b**

Scheme 4.11

Poilblanc *et. al.* have carried out a study of mechanism of the complexation of an unsubstituted two-carbon Cp-phosphine tethered ligand and the rhodium dimers $[RhCl(L)_2]_2$ where L = CO, C_2H_4 and COD.[20] The mechanism is proposed to occur by initial complexation the ligand's tethered phosphine group to the rhodium dimer, prior to chloride displacement by the incoming indenyl group. Importantly two ligand molecules are suggested to bind to the rhodium dimer prior to chloride displacement, which would result in the diastereoisomers **155a** and **155b**. Therefore complexation of an enantioenriched ligand may result in a slightly different preference for one of the two diastereoisomers of **155** compared to the racemic ligand, owing to the differences in remote stereocontrol achieved by the chiral or racemic nature of the mono-complexed precursor to **155**, as the second ligand complexes to the dimer.

A similar difference in face-selectivity was noticed by Brookings during the complexation of chiral and racemic ligand **59** (Scheme 4.9) to $[RhCl(CO)_2]_2$ (50 % d.e. for enantiopure **59** *vs.* 43 % d.e. for racemic **59**). The fact that this level of face-selectivity was achieved for this *beta*-substituted complex **59** (which does not fulfil the 'favoured rotamer' design) is also likely to be as a result of the diastereomeric intermediates formed during its complexation (see Section 1.4.1, Scheme 1.17 and discussion).

Recrystallisation complex *rac*-**154** from diethyl ether/hexane, at –30 °C provided the major diastereoisomer *rac*-**154a** as red crystals suitable for X-ray analysis, Figure 4.10.

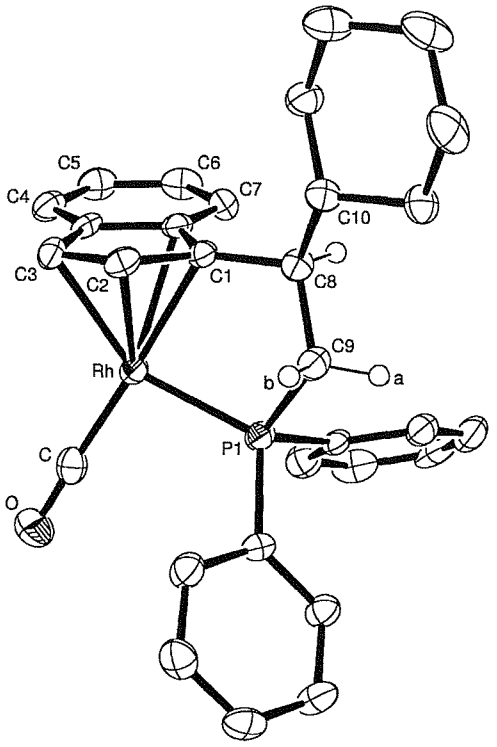

Figure 4.10

ORTEP view of *rac*-154a, thermal ellipsoids shown at 50 % probability, H-atoms shown only for C8 and C9. See Appendix 11 for full details.

A list of selected bond lengths and torsion angles is given for complexes **154a** and **153a** in Table 4.5. From these data, as with the ruthenium complexes (Section 4.2), we can calculate the 'slip parameter' Δ which shows the degree of η^3-distortion for these indenyl complexes.[95] (see Section 4.2.1).

For complex **154a**: Δ = (2.414 – 2.222) = 0.19 Å

For complex **153a**: Δ = (2.415 – 2.226) = 0.19 Å

These values of Δ show a large degree of η^3 distortion of the indenyl ligands in these complexes. The value of Δ for complex **154a** is almost twice that of the related ruthenium complex of ligand **121** (Δ_{121} = 0.10 Å), indeed of all the ruthenium complexes discussed in Section 4.2, only the minor isomer of complex **150** achieves the same Δ = 0.19 Å η^3-distortion seen with these rhodium complexes.

	alpha-Cy Complex **154a**	*beta*-Ph complex **153a** [45]
Rh-C1	2.179(3)	2.171(5)
Rh-C2	2.227(3)	2.240(5)
Rh-C3	2.261(3)	2.267(5)
Rh-C3a	2.433(3)	2.448(5)
Rh-C7a	2.395(3)	2.381(5)
Rh-P	2.223(1)	2.241(1)
Rh-CO	1.836(4)	1.843(6)
$Cp_{centroid}$-Rh-P	116.91	118.0
$Cp_{centroid}$-Rh-CO	144.67	-
Rh-P-C9-H9a	162.9(2)	-
P-C9-C8-C10	166.9(2)	-
P-C9-C8-H8	74.57(3)	-

Table 4.5

Selected bond lengths (Å) (with esds) and torsion angles (degrees) for complexes 154a, and 153a.

The ^{13}C NMR for complex the major isomer of complex **154a** has been fully assigned, and tabulated for comparison against that of the related major isomer of complex **153a**,[45] see Table 4.6.

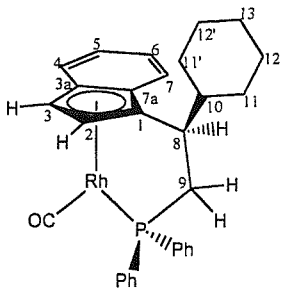

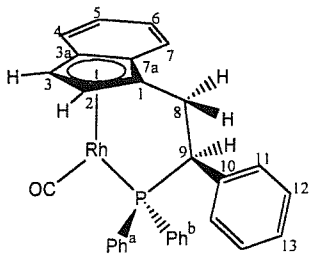

Complex **154a**				Complex **153a**			
Assignment[†††]	δ_C	J_{CP}	J_{CRh}	Assignment	δ_C	J_{CP}	J_{CRh}
CO	191.26	17.9	88.4	*CO*	190.26	17	89
o-Ph	134.48	13.8	1.0	*o*-Ph[a]	137.53	13.5	1
i-Ph	134.42	38.4	1.0	*i*-Ph	135.30	39.5	1
o-Ph	131.72	11.6	1.2	*o*-Ph[b]	131.95	10.5	-
p-Ph	130.52	2.4	-	*p*-Ph[a]	131.05	2.2	-
i-Ph	136.25	44.6	3.5	*i*-Ph	130.00	42.1	3.2
p-Ph	129.82	2.4	-	*p*-Ph[b]	129.64	2.8	-
m-Ph	128.50	10.4	-	*m*-Ph[b]	128.48	10	-
m-Ph	128.44	10.6	-	*m*-Ph[a]	127.61	11.5	-
6	124.37	0.7	-	6	124.31	-	-
5	121.09	-	-	5	121.91	-	-
3a	116.41	2.3	1.4	3a	120.95	1.0	-
4	117.92	1.2	-	4	118.46	1.6	-
7	117.42	-	-	7	117.13	-	-
7a	116.08	1.1	0.9	7a	116.10	2.1	1.6
2	91.36	5.6	3.1	2	98.40	5.6	4.0
1	103.32	5.0	3.8	1	92.10	4.8	3.7
3	76.09	10.6	3.6	3	72.40	10.8	3.2
9	52.60	29.7	-	9	67.77	18.4	-
8	39.37	4.8	-	8	30.46	9	-
10	42.95	22.4	-	10	137.8	9.5	1
11/11'	33.56	-	-	12	128.36	3.0	-
11/11'	31.17	-	-	11	128.20	2.2	-
12/12'/13	26.58	-	-	13	127.37	2.2	-
12/12'/13	26.42	-	-				
12/12'/13	26.25	-	-				

Table 4.6 100 MHz ^{13}C NMR data (in C_6D_6) for complexes 154a and 153a.

[†††] Assignments are based on results from ^1H, ^{13}C, DEPT and 2D COSY H-H and C-H correlation experiments. Where the signals could not be unambiguously assigned, all possible assignments are given.

4.3.2 Complexation of cyclohexyl-substituted three-carbon bridged ligand 129

Following the same complexation procedure as used for ligand **121** (Section 4.3.1) the three-carbon bridged ligand *rac*-**129** (Section 3.2.2) was deprotonated with *n*-butyl lithium in THF, and the resulting anion solution added dropwise to a THF solution of $[RhCl(CO)_2]_2$ at –78 °C, Scheme 4.12. ^{1}H NMR of the resulting crude material confirmed the presence of the desired complex and ^{31}P NMR confirmed complex **155** had formed as a 74 : 26 ratio of diastereoisomers (48 % d.e.).

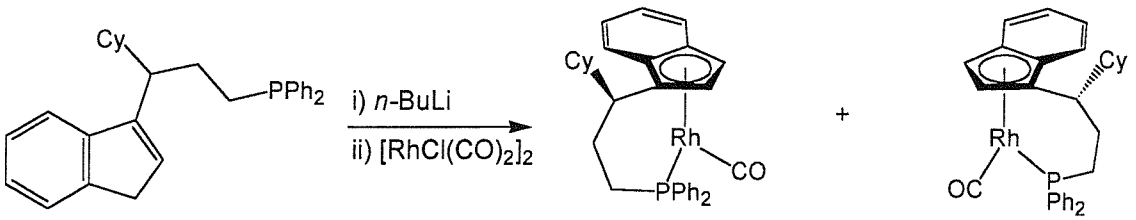

major 74:26 (48 % d.e.) minor

rac-**129** **155a** **155b**

Scheme 4.12

Purification of complex **155** by column chromatography through Al_2O_3 resulted in a very low yield of complex **155** (16 %) as a yellow film and unchanged 74 : 26 ratio of diastereoisomers (48 % d.e.). ^{1}H NMR showed the major Cp-H protons at δ 6.04 and 5.96 ppm, and the minor Cp-H protons at δ 6.00 and 5.95 ppm.

The 48 % d.e. face-selectivity shows a small improvement over the 44 % d.e. seen on formation of the racemic complex *rac*-**154** (Section 4.3.1) and for the reasons detailed in Section 4.3.1, we may therefore expect complexation of an enantiopure form of ligand **129** to show an improved d.e. on the 56 % d.e. seen on complexation of the enantiopure form of ligand **121**.

Unfortunately this compound has so far resisted all attempts to recrystallise it from a variety of solvents.

4.4 Conclusions

- The successful complexation of ligands (2*R*)-**121**, *rac*-**128** and *rac*-**129** with $RuCl_2(PPh_3)_3$ has been achieved to form complexes **147**, **149** and **150** respectively. In each case a high induction of planar-chirality is seen, **147**: 60 %, **149**: 74 %, and **150**: 66 % d.e. and complete (**147** and **150**) or very good (87 % d.e., **149**) induction of metal-centred chirality.

- The axially-chiral ligand and *rac*-**145** has been complexed with $RuCl_2(PPh_3)_3$ to provide the metal-centred chiral ruthenium complex **151**, with a high induction of metal-centred chirality (72 % d.e.).

- Complexes **147**, **149**, **150** and **151** have been found to have thermally stable chiral environments, with no epimerisation at the metal-centre seen after prolonged (24 hours) heating in chloroform (although decomposition eventually resulted in the case of complexes **147** and **149**).

- Ruthenium complex **147** has been hydrogenated to the its tetrahydroindenyl complex **148**, in order to provide a Cp-analogue of these indenyl complexes.

- The rhodium-carbonyl complex (–)-**154** and has been prepared in 56 % d.e. by reaction of the lithium salt of its ligand (2*R*)-**121** with $[RhCl(CO)_2]_2$. Complexation of the racemic ligand *rac*-**121** provided complex *rac*-**154** in 44 % d.e. These results have been published.[45]

- The rhodium-carbonyl complex *rac*-**155** has been prepared in 48 % d.e. on complexation of its ligand *rac*-**129** with $[RhCl(CO)_2]_2$.

Overall, complexation of the ligands reported in Chapters 2 and 3 has been very successful. Importantly the 'favoured rotamer' ligand design concept (Section 2.1.2) has proven a great success, with high inductions of planar-chirality seen on complexation of all the above ligands.

The results of the attempted application of ruthenium complex **147** (containing the two-carbon bridged ligand **121**) to catalytic processes are discussed in Chapter 5.

5. Chapter 5: Application of ruthenium complex 147 to the catalytic 'reconstitutive condensation' reaction.

5.1 Introduction

Having devised an optimised synthetic route to enantiopure ligand (2*R*)-**121** (Chapter 2) and formed its chiral ruthenium complex (–)-**147** (Chapter 4) it was now appropriate to perform catalytic trails of this complex in the recently reported ruthenium-Cp catalysed 'reconstitutive condensation' reaction.[‡‡‡]

5.1.1 The 'Reconstitutive condensation' reaction

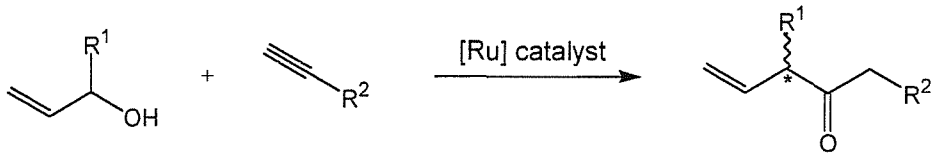

Scheme 5.1

Trost's investigations of the reconstitutive condensation reaction, Scheme 5.1 (see review in Chapter 1, Section 1.7) provides us with a wealth of data from the various examples of Cp-phosphine tethered ruthenium complexes used as catalysts for this reaction.[23] Of particular note, are the chiral complexes examined by Trost as asymmetric catalysts – complexes **90**, **62**, **64**, **67** and **69** (see Chapter 1). Although none of these complexes were prepared in diastereomerically pure form, all achieved some degree of enantioinduction in the product of the condensation reaction shown in Scheme 5.2 (see below). The best result for enantioinduction achieved in the reconstitutive condensation reaction has been reported by Hidai.[25] In this case the Cp-phosphine bridged complex **86** (see Chapter 1, Scheme 1.39) induced a 65 % e.e. in the product of the reaction, although this was only achieved when the reaction was performed stoichiometrically.

[‡‡‡] It should be made clear that the catalytic reactions and studies performed in this chapter were carried out *before* our ligand design was extended to include the three-carbon tethered ligands of Chapter 3. For this reason only complex **147** (both racemic and enantiopure) was available for use at the time of these studies. Where the use of later complexes such as **148-151** may be of benefit to the reactions detailed in this Chapter, the reasons behind this will be discussed.

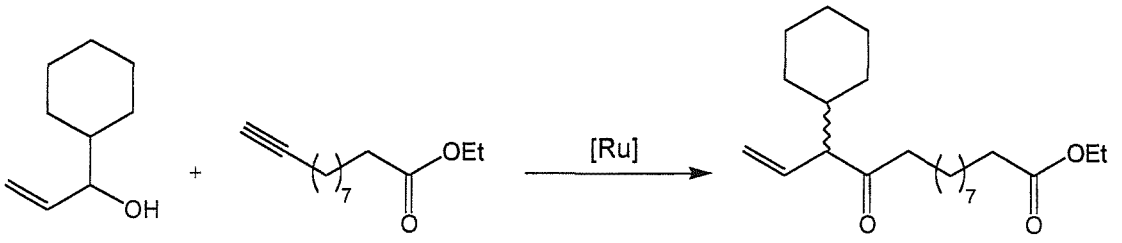

97 **98** **99**

Scheme 5.2

Trost has also reported the results of the reconstitutive condensation reaction performed using several non-chiral Cp-phosphine tethered complexes with varying lengths of Cp-phosphine tethers, Figure 5.1.

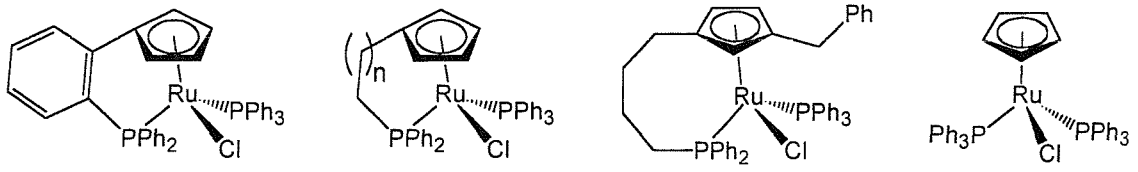

100 **101**: n = 1 **102**: n = 2 **103**: n = 3 **94** **156**

Figure 5.1

Table 5.1 details the results of the reconstitutive condensation reaction shown in Scheme 5.2, catalysed by complexes **100-103** and **94**, Figure 5.1. These results show that all the Cp-phosphine tethered complexes have reduced reactivity in this reaction compared to the original catalyst **156** (reaction 1). The loss in reactivity is particularly apparent for the complexes containing a two or three-carbon linked tether (reactions 2-4), which also showed the formation of additional side-products in the reaction. Comparison of the activity of complexes **100** and **101** suggest that part of the loss in reactivity may be due to the change from a triarylphosphine to an alkyldiarylphosphine. The four-carbon tethered complex **103** showed the highest activity of these reactions, however four-carbon tethered racemic planar-chiral complex **94** showed a much lower activity, probably owing to steric demands of the extra substitution on the Cp ring.

Reaction	Complex	% consumption alkyne	% Yield (GC) [conversion]
1	**156** no linker	100	78
2	**100** C-2 linker	41	(26) [63] + by-products
3	**101** C-2 linker	23	(11) [48] + by-products
4	**102** C-3 linker	56	(30) [54] + by-products
5	**103** C-4 linker	95	59 [62]
6	**94** C-4 linker	33	20 [61]

Table 5.1

As yet there has been no direct literature precedent for use of indenyl-ruthenium complexes to catalyse the reconstitutive condensation reaction, however we may expect indenyl-complexes to achieve far greater catalytic activity owing to the 'indenyl ligand effect'[62] (Section 1.7). This effect along with the wide range of results published from the use of chiral Cp-phosphine complexes, makes the 'reconstitutive condensation' reaction one of the most important reactions for us to study using our enantiopure complex **147**.

5.2 Catalytic application of ruthenium complex 147

5.2.1 'Reconstitutive condensation' literature conditions

In order to make a valid comparison between the original catalyst **156** for the reconstitutive condensation reaction and the ruthenium complex **147**, it was important to repeat and monitor the course of the reaction using the original catalyst and reaction substrates.[23] To this end the complex **156** was prepared according to the literature,[97] alcohol **97** was synthesised from cyclohexanecarboxaldehyde and vinylmagnesium bromide, and alkyne **98** prepared by esterification of its commercially available acid. The reaction co-catalyst, indium triflate, was obtained commercially.

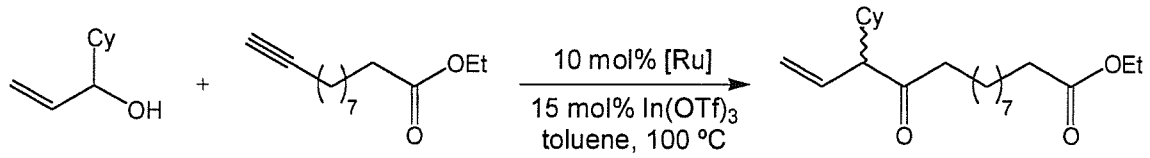

97 **98** **99**

Scheme 5.3

Performing the reaction shown in Scheme 5.3, using the literature catalyst **156** under the exact conditions reported in the literature, provided the expected β,γ-unsaturated ketone **99**. The same GC conversion and complete consumption of alkyne **98** was seen, as had been reported. A second reaction, using substrates similar to those used in the initial report of this reaction; 1-heptyne and 3-buten-2-ol,[46] also progressed as intended to give the product **161**, Scheme 5.4.

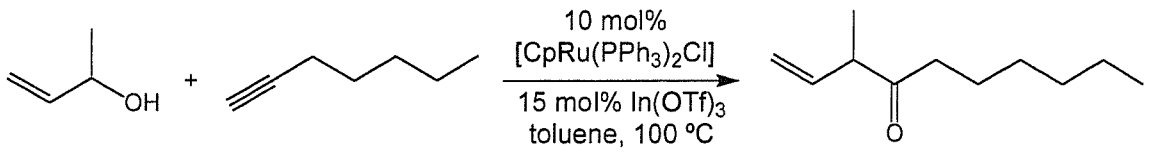

159 **160** **161**

Scheme 5.4

5.2.2 'Reconstitutive condensation' using complex 147

Initial trial reactions using complex **147** were performed under the conditions successful with the original catalyst, for both the substrate combinations shown in Schemes 5.3 and 5.4. GC monitoring of the reactions using **147** however showed no trace of the expected product being formed, but instead showed a large number of by-products forming rapidly upon heating to 100 °C. GC analysis of the reactions also indicated total consumption of the alcohol substrate with only part consumption of the alkyne substrate after six hours at this temperature.

These results were interesting in that with the original catalyst **156**, the alkyne substrate (**160** or **98**) had in each case been totally consumed within six hours of reaction time, while the alcohol substrate (**159** or **97**) remained only one third consumed after that time (having been in a three-fold excess at the start of the reaction). Complex **147** appeared to be showing the reverse of this and, with none of the intended product detected, this suggests that the alcohol substrates may be reacting or isomerising in some way under these conditions. Ruthenium is known to isomerise allyl alcohols,[61] therefore presence of complex **147** in the reaction mixture may be catalysing an isomerisation in preference to the desired catalytic cycle.

Control reactions with and without reaction catalyst and/or co-catalyst were performed to determine whether the by-products seen for this reaction were formed in the presence of complex **147** alone. The results showed that the reaction substrates were in fact stable to these conditions with only the ruthenium complex present (no co-catalyst), however, the substrates were rapidly consumed in the presence of indium triflate, to produce the range of by-products seen above. Ammonium hexaflurophosphate was therefore investigated as an alternative to the indium triflate co-catalyst (which is used to abstract the chloride ligand and form the proposed catalytically active cationic ruthenium species),[23] this less reactive co-catalyst resulted in much reduced formation of by products, however still no catalytic turnover was seen with complex **147**.

Trost and Hidai have also reported the presence of by-products in their reactions,[23,25] but usually alongside the intended product of the reaction. Importantly Trost reports that these by-products were only seen for the Cp-phosphine tethered complexes containing a

two or three-carbon tether, with complexes containing either a four-carbon tether or no tether at all, effecting clean conversion to the desired product (see Table 5.1). Hidai's report of by-products when using complex **86** ties in with Trost's observations, as complex **86** contains a three-carbon Cp-phosphine tether (see Scheme 1.39, Chapter 1).

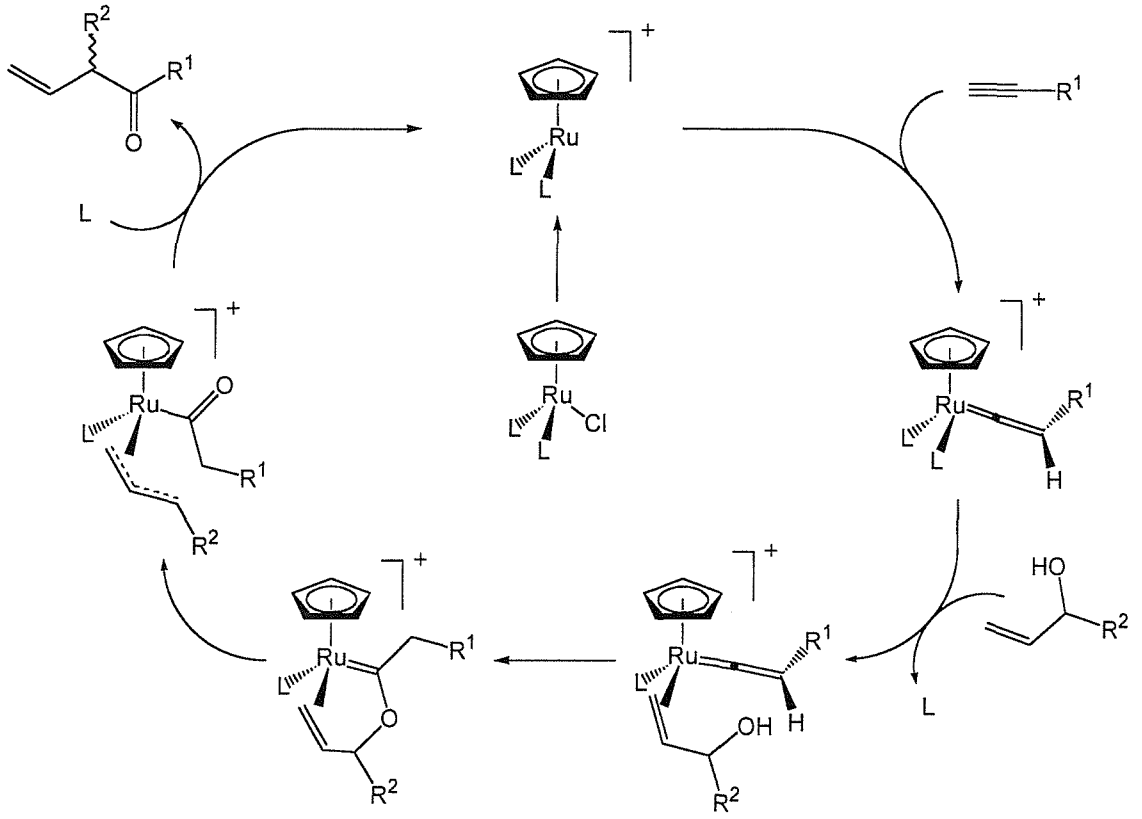

Scheme 5.5

The initial stage of the catalytic cycle proposed by Trost, Scheme 5.5,[23] is the formation of the cationic ruthenium species followed by reaction with the alkyne substrate to form a vinylidene complex. Although usually performed under slightly different conditions, the formation of ruthenium vinylidene complexes by abstraction of halide ligands is a well known literature procedure.[97] Hidai managed to avoid formation of by-products in the reconstitutive condensation reaction by pre-forming this vinylidene complex stoichiometrically and subsequently reacting it with the alcohol substrate.[25] This technique also led to an improved yield and e.e. in the reaction, so therefore would be a useful procedure to attempt with complex **147**.

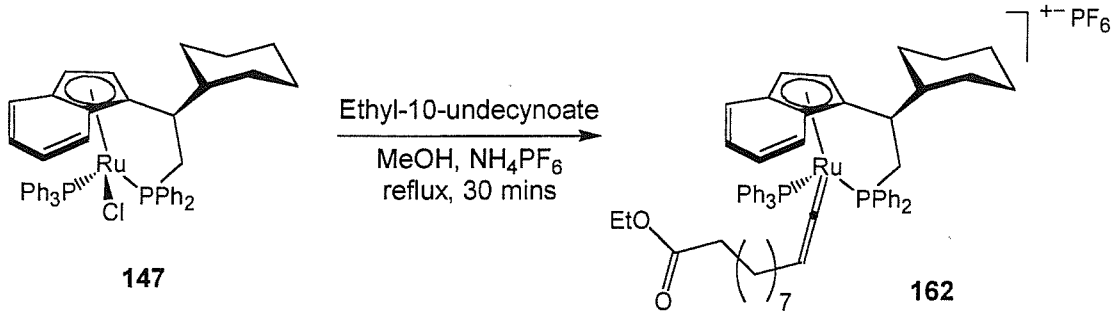

Scheme 5.6

Reaction of **147** with ethyl-10-undecynoate (alkyne substrate **98**) and ammonium hexaflurophosphate in refluxing methanol, for 30 minutes[97] provided the crude vinylidene complex **162** as a light orange solid, in *ca.* 45 % yield (unfortunately full characterisation of this complex was not achieved). The ease of which this vinylidene complex has formed suggests that the initial step in the reconstitutive condensation reaction should also be proceeding to form this complex. (Some evidence for this was gained by the presence of a TLC component at the same R_f as vinylidene complex **162**, seen in the TLC of a failed reconstitutive condensation mixture).

The final stage in the stoichiometric reconstitutive condensation reaction[25] is the reaction of the vinylidene complex **162** with alcohol substrate **159**. This was attempted by heating a sample of complex **162** in a toluene solution of alcohol substrate **159** – in the absence of any co-catalyst, with monitoring by GC. Unfortunately regular GC monitoring of this reaction showed no formation of the desired product **99** at any stage and after six hours the appearance of by-products was seen to occur. These results show that although complex **147** is successful in achieving the first step of the reconstitutive condensation reaction's catalytic cycle, the second, coupling step, is not achieved.

5.3 Conclusions

Overall these results proved very disappointing, especially when considering the precedent for this reaction being catalysed by several Cp-analogues of complex **147**. With hindsight there are many reasons why this reaction may have not have been successful with complex **147**. The obvious difference between complex **147** and the catalytically active Cp-phosphine tethered complex **101** (Figure 5.1) is the presence of an indenyl group on **147**. It had been hoped that this would lead to greater catalytic activity than the Cp-analogues,[63] however there are two important reasons why this may not be the case. Firstly, the size of the indene group may well be affecting the complex's ability to take part in this reaction. Trost reported a large decrease in reactivity when two substituents are present on the Cp-ring, *cf.* complex **94** (Figure 5.1).[23] Complex **147** contains three Cp-substituents, so steric crowding of the catalyst may well be a factor. The indene ligand of **147** may also act as an 'electron reservoir'[63] donating charge towards the catalytically-active (and electron deficient) cationic ruthenium species. This may account for a lower reactivity of this intermediate compared to the Cp-analogue.

Another possible cause of the poor reactivity of **147** in this reaction is the two-carbon length of its Cp-phosphine tether. When comparing ruthenium complexes of Cp-phosphine tethered ligands, Trost found that a two-carbon Cp-*diaryl*phosphine tether gave the lowest yield of all the various tether lengths tested (see Table 5.1).

5.3.1 Possible modifications to complex 147

The problems encountered with this catalytic cycle are by no means terminal. The low reactivity of the indenyl vinylidene complex **162**, and the use of harsh chloride scavenger reagents as co-catalysts, have compounded to give the poor catalytic results detailed above. Thankfully the flexibility of our design of complex allows many modifications to combat both of these areas.

The first obvious change which could improve reactivity of the vinylidene complex, would be to prepare a cyclopentadienyl equivalent of our indenyl complex. Without any new chemistry this has been achieved simply by reducing the indene ring on the complex to the corresponding tetrahydroindenyl system (Chapter 4). The resulting

tetrahydroindene complex **148** is a cyclopentadienyl system, and will more closely match the electronic characteristics of the catalysts used by Trost, so should now show the required reactivity to achieve turnover in this reaction.

The Cp-phosphine tether length is crucial in this reaction, and following recent reports,[49,71] we may expect it to be so for other catalytic reactions. A variety of complexes containing various different lengths of Cp-phosphine tether would be ideal when screening for catalytic activity in a range of reactions and work towards this has begun with the design and synthesis of a new three-carbon Cp-phosphine tethered ligand **129** (Chapter 3), which has now been complexed to ruthenium and rhodium (Chapter 4).

With a view to removing the need for a reactive co-catalyst, there is recent precedent for reactions of ruthenium cyclopentadienyl systems containing acetonitrile ligands, rather than chloride ligands, which can achieve reactive intermediates without use of co-catalysts.[37] Cationic complexes containing labile acetonitrile ligands may be transformed into reactive vinylidene intermediates, similar to those required for the reconstitutive condensation reaction, by gently heating with an alkyne at 40-50 °C.[37]

With the expanding range of known ruthenium catalysed reactions, the number of processes directly applicable to indenyl systems like complex **147** is rapidly increasing. Because of this, further work on the reconstitutive condensation reaction was not performed, it is however likely that this reaction will be investigated again by future researchers.

6. Chapter 6: Conclusions and further work

6.1 Conclusions

At the outset of this Ph.D. research the aims were set to develop and apply a series of chiral ligands based on the successful 'favoured rotamer' complexation model (Chapter 2). This model allows the design of chiral ligands intended to induce planar-chirality upon complexation to transition metals *via* face-selectivity and hence form diastereomerically pure complexes without the need for resolution. The ligands were targeted at late transition metals such as ruthenium and rhodium, with the intention of applying their complexes as novel chiral catalysts of organic transformations. Therefore as well as the 'favoured rotamer' feature, the ligand design incorporated features intended to create a stable and yet accessible chiral environment at the metal centre – based on the successful 'Roof' and 'Wall' catalyst model mastered by previous researchers (Chapter 2).[17]

Over the course of this research, the synthesis of three novel ligands (2*R*)-**121**, *rac*-**128** and *rac*-**129**, based upon the 'favoured rotamer' and 'Roof' and 'Wall' models has been achieved and these have been successfully complexed to rhodium and/or ruthenium with the desired high degree of induction of planar-chirality seen in each case. These results serve as a clear demonstration of the effectiveness of the 'favoured rotamer' model – which will undoubtedly go on to form the basis of future ligands from the laboratories of the Whitby group.

Although the application of ruthenium complex **147** as a catalyst of the 'reconstitutive condensation' reaction[23] has given somewhat disappointing results, the rapidly increasing number of reported catalytic reactions of related complexes[16] give much hope that this and the other complexes prepared herein shall find catalytic applications in the near future.

The synthesis of an axially-chiral (but racemic) ligand *rac*-**145** has also been achieved, in collaboration with Rob Baker (University of Sydney, Australia) and complexed to ruthenium, showing good control of the induction of metal-centred chirality.

6.2 Further work

Both the optimised synthesis of the enantiopure two-carbon tethered ligand and the synthesis of the racemic three-carbon tethered ligand offer the opportunity for modification of the tethered 'anchor' group, which should lead to interesting new series' of ligands.

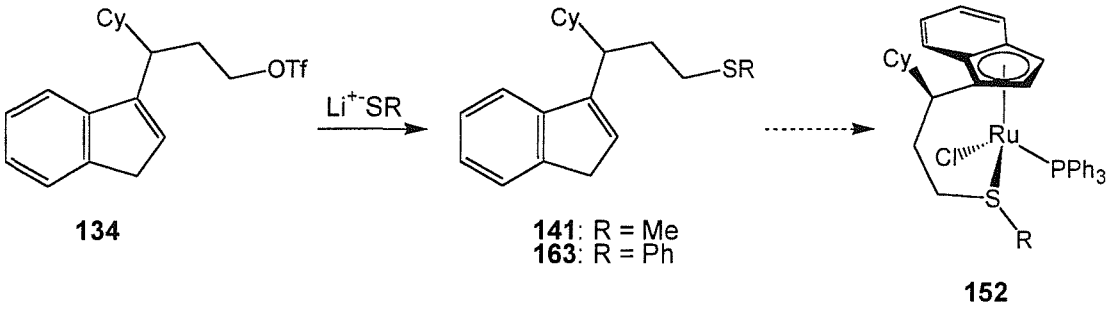

134 **141**: R = Me **163**: R = Ph **152**

Scheme 6.1

The chemistry used in the initial success of forming the thiomethyl ligand **141** from triflate **134** (Chapter 3) should allow access to other thioalkyl and thioaryl ligands. Complexation of **141** to ruthenium (Chapter 4) showed encouraging crude analysis, but the complex has yet to be isolated cleanly.

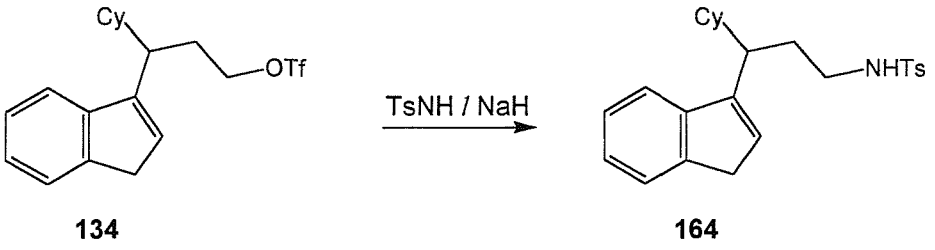

134 **164**

Scheme 6.2

Modifications of the 'anchor' group to include amine functionality should also be possible and will allow their complexes to become involved in different catalytic cycles. In particular hydrogen transfer catalysis is an important goal. Suitable amine functionality on the tether-chain of these ligands will bring their complexes (for example complex **164** or **166**) closer in structure to the successful Cp-rhodium hydrogen transfer catalysts **167** (Avecia, CATHy catalysts) and **168** developed by Noyori and Ikariya.[98]

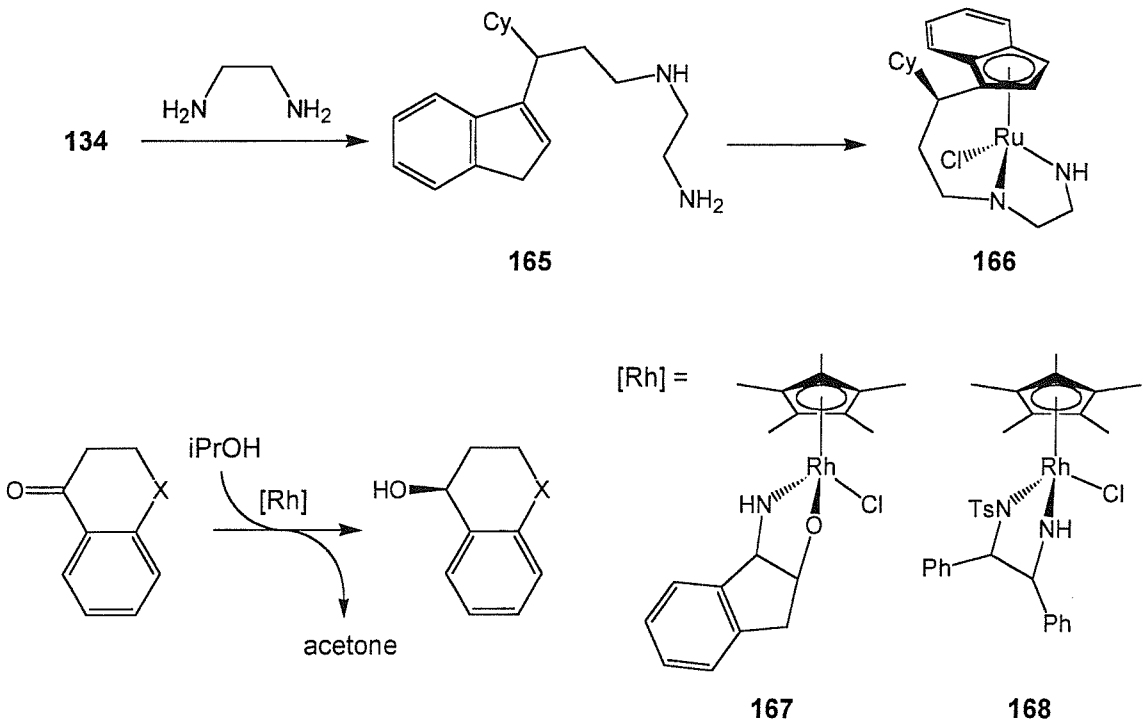

Scheme 6.3

Extension of the indene-phosphine tether chain to four or five atoms is another important long-term target for this series of ligands. Following many reports of widely differing catalytic activities seen for similar complexes which differ only in their length of Cp-phosphine tether-chain, future research should not focus solely on ligands of a single tether-length. During the latter stages of this Ph.D., the focus of research turned to examining modifications of the successful three-carbon tethered ligand **129**, in order to provide a four-atom tethered ligand. This was achieved by reaction of the alcohol **133** with chlorodiphenylphosphine and triethylamine, to provide the four-atom tethered phosphinite ligand **169**. Unfortunately this ligand proved highly air-sensitive, and only crude analysis was possible. Complexation of **169** with $RuCl_2(PPh_3)_3$ appeared successful, however isolation of the complex **170** was problematic, and analysis other than crude NMR could not be obtained.

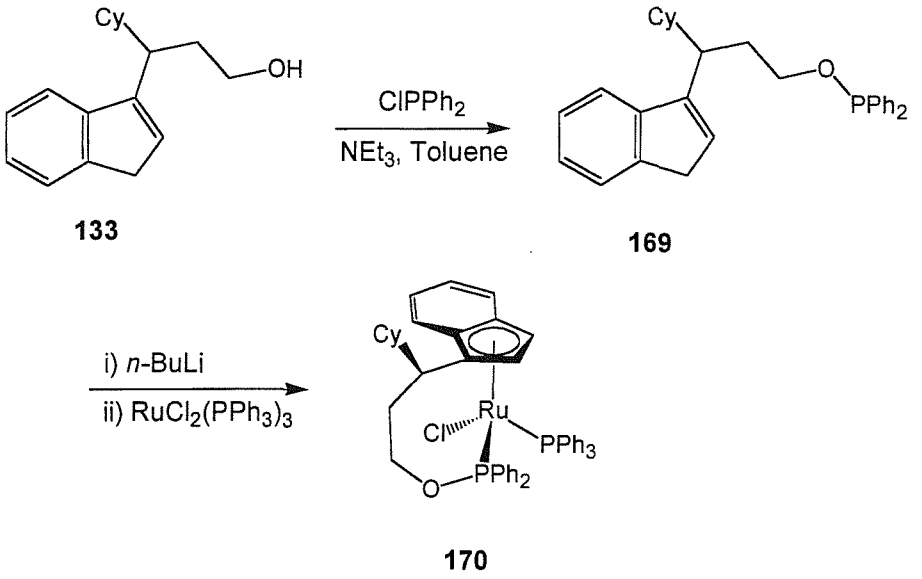

133 169 170

Scheme 6.4

This phosphinite series of ligands should be more easily handled as their air-stable borane-adducts and with more time, isolation and purification of their transition metal complexes should be achievable and provide an interesting novel series of complexes to explore.

Preparation of chiral transition metal catalysts remains a long-term goal of research within the Whitby group, and as such the development of a synthesis of the enantiopure form of the three-carbon tethered ligand **129** is an important target.

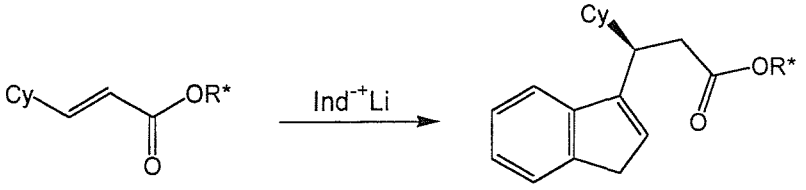

171: R* = auxiliary
131: R* = *t*-Bu

172: R* = auxiliary
132: R* = *t*-Bu

Scheme 6.5

Use of a chiral ester-auxiliary during the 1,4-addition of indenyl lithium to ester **171** is a promising method of achieving enantioenrichment in this ligand synthesis. Even if complete diastereocontrol cannot be gained by the use of an auxiliary, the resulting indene-ester compound **172** will be a mixture of diastereoisomers, and therefore fractional crystallisation could be employed to provide the diastereo-pure compound.

The slightly disappointing catalytic results of complex **147** (Chapter 5), should not be a cause of concern about this design of ligand/complex, as there are many opportunities to achieve catalysis in other recently reported reactions[16] and by simple modifications to the design of the complexes reported in Chapter 4.

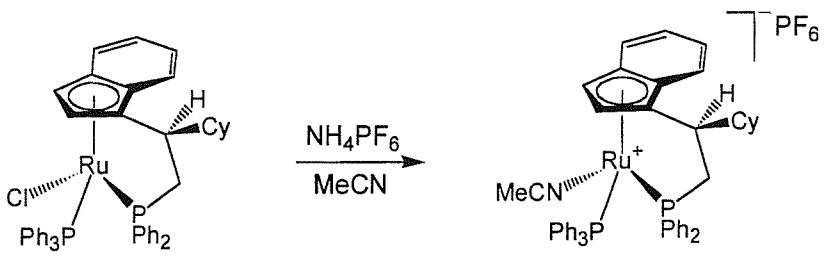

147 **173**

Scheme 6.6

During investigations into the poor catalytic results of complex **147** (Chapter 5) some derivatives of this complex were prepared on an 'NMR-tube' experiment scale (unfortunately full characterisation was not possible). Chapter 5 discusses the formation of the vinylidene complex **162** from **147**, in an effort to perform the 'reconstitutive condensation' reaction stoichiometrically. Another derivative which was examined was that of the cationic complex **173**, formed by abstraction of the chloride of **147**, using a 'chloride scavenger' reagent in the presence of a neutral ligand – in this case ammonium hexaflurophosphate in acetonitrile. Cationic complexes such as **173** would be expected to achieve catalysis in the recently reported reactions by Takahashi,[71] as well as in several other reactions known to be catalysed by cationic complexes, for example Diels-Alder reactions.[99]

In summary, the research detailed in this Ph.D. thesis has led to a wealth of new ideas many of which have yet to be investigated, these should offer a stimulating basis for future research in this area.

7. Chapter 7: Experimental

7.1 General Techniques

7.1.1 Air and moisture sensitive manipulations

All reactions and manipulations involving organometallic and phosphorous-containing compounds were performed under an argon atmosphere, using standard Schlenk, syringe and vacuum-line techniques. Reaction flasks, syringes, needles and canula were dried in a hot oven (>160 °C) for 12 hours prior to use and allowed to cool in a sealed desiccator, over silica gel.

7.1.2 Spectroscopic techniques

^{1}H, ^{13}C and ^{31}P NMR spectra were recorded on Brüker AM300, Brüker AC300 or Brüker DPX400 Fourier Transform spectrometers. The NMR spectra of moisture sensitive organometallics were recorded in deuterobenzene (stored over 4 Å molecular sieves) and referenced to the residual benzene signals at 7.18 ppm (^{1}H NMR) and 128.7 ppm (^{13}C NMR). Unless otherwise stated all other spectra were recorded in deuterochloroform (stored over K_2CO_3) and referenced to the residual chloroform signals at 7.27 ppm (^{1}H NMR) and 77.2 ppm (^{13}C NMR). Phosphorous-31 spectra were externally referenced to an H_3PO_4 solution. Chemical shifts are given in units of ppm on the δ scale. The following abbreviations are used to denote multiplicity and shape of signal and may be compounded: s = singlet, d = doublet, t = triplet, q = quartet, m = multiplet, br = broad, fs = fine splitting. Coupling constants *J* are reported in Hz. Carbon-13 spectra were proton decoupled and signals reported as C, CH, CH_2, CH_3 depending on the number of directly attached protons (0, 1, 2, 3 respectively), this being determined by DEPT experiments. Assignments of ^{13}C spectra containing carbon signals split by nuclei other than hydrogen e.g. boron, rhodium and/or phosphorus, include multiplicities and coupling constants, reported using the same system of 's', 'd', 't', etc. abbreviations used for the proton assignments. 2D COSY spectra (H-H and C-H correlation) were routinely used to conclusively assign signals from ^{1}H and ^{13}C spectra and have not been specifically documented. Assignments of ^{1}H and ^{13}C NMR resonances are listed using the numbering schemes shown in the title diagrams of the compounds (unless otherwise stated).

Mass spectra, including accurate masses, were recorded on a VG Analytical 70-250-SE double focusing mass spectrometer using, Electron Impact Ionisation (EI^+) at 70 eV. Electrospray (ES^+) and Atmospheric Pressure Chemical Ionisation (APCI, AP^+) spectra were recorded on a VG Platform quadrupole spectrometer in acetonitrile. M/z values are reported as values in atomic mass units followed by the peak intensity relative to the base peak. AP^+ spectra of organic compounds generally gave MH^+ as the only significant peak.

Infra-red spectra were recorded on Perkin Elmer 1600 FT-IR or Nicolet Impact 400 spectrometers as films between sodium chloride plates, dichloromethane solutions, or directly – using a Spectra-Tech Thunderdome accessory. Absorptions are given in wavenumbers (cm^{-1}) and peaks are described as 's' (strong), 'm' (medium), 'w' (weak) and may be compounded with 'br' (broad).

Optical rotations were measured in an AA-100 Polarimeter (Optical Activity Limited) or a PolAAr 2001 polarimeter (Optical Activity Limited), and are uncorrected.

7.1.3 Reagent purification

Unless otherwise indicated materials were obtained from commercial sources and used without further purification. Specific purifications were carried out according to standard procedures.[100] *n*-Butyl lithium (2.5 M solution in hexanes), *sec*-butyl lithium (1.3 M solution in cyclohexane), *tert*-butyl lithium (1.7 M solution in pentane) and methyl lithium (1.0 M solution in diethyl ether) were purchased from Aldrich and their titre checked regularly. Potassium diphenylphosphide (0.5 M solution in THF) was purchased from Aldrich.

Diethyl ether, di-isopropyl ether, tetrahydrofuran and toluene were freshly distilled from dark purple solutions of sodium/benzophenone ketyl under an argon atmosphere. Dichloromethane, hexane, pyridine, triethylamine, diethylamine and hexamethylphosphoramide (HMPA) were dried over, and distilled from, calcium hydride. Petrol refers to the fraction of petroleum ether which boils between 40 and 60 °C, and was redistilled before use.

Tetracarbonylbis(μ-chloro)dirhodium(I) was prepared from rhodium trichloride trihydrate and re-sublimed before use.[101] Tris(triphenylphosphine)dichloro-ruthenium(II) was prepared from ruthenium trichloride trihydrate and triphenylphosphine.[102] (*R*)-2-Cyclohexylethane-1,2-diol **115**, was prepared by Sharpless asymmetric dihydroxylation of vinylcyclohexane using the $(DHQD)_2PYR$ ligand[78] to give an 85 % yield of material of 97 % e.e. as determined by HPLC resolution of its benzaldehyde acetal. (*R*)-2-Cyclohexyloxirane **116** was prepared in 77 % yield by the Sharpless method[79] from (*R*)-2-Cyclohexylethane-1,2-diol **115** and had spectroscopic properties and optical rotations in accord with those previously reported.

7.1.4 Chromatography

Thin layer chromatography was carried out on 0.25 mm POLYGRAM® SIL G / UV_{254} and 0.20 mm POLYGRAM® ALOX N / UV_{254} pre-coated plates and were visualised with a 254 nm UV lamp, followed by phosphomolybdinic acid (12 g in 150 mL ethanol), sulphuric acid (5 % v/v in methanol), potassium permanganate (10 % w/v in water) or iodine (on SiO_2). Column chromatography of organic compounds was performed on silica 60 (230-400 mesh), under slight positive pressure. Air-sensitive compounds were purified by chromatography under argon atmosphere, using degassed solvents. Chromatography of organometallic complexes was performed under argon using degassed solvents, through neutral alumina (Brockman grade III, prepared from commercial grade I deactivated with 6 % w/w distilled water). Chromatography solvent mixtures are described as % volumes prior to mixing.

Routine monitoring of reactions was carried out using gas chromatography on a Hewlett Packard 6890 instrument with auto-sampler, using helium as the carrier gas, a flame ionisation detector and passing through a 5 % phenyl methyl siloxane column with the oven programmed to 50 °C to 250 °C over 10 minutes. Chiral HPLC was carried out using a Hewlett Packard 1050 series instrument, with UV detection at 254 nm, using normal phase elution through 250 mm × 4.6 mm Chiralcel OD-H, OB-H or Bakerbond Chiralpak AD columns. GC and HPLC peak size analysis was carried out using HP ChemStation software.

7.1.5 Miscellaneous

Elemental analyses were performed by MEDAC Ltd., Egham, Surrey, and the University of Strathclyde Microanalysis Service. Melting points were measured on a Gallenkamp type apparatus and are uncorrected.

7.2 Experimental for Chapter 2

7.2.1 Synthesis of two-carbon tethered ligands

7.2.1.1 (2*R*)-2-(3*H*-Inden-1-yl)-2-phenylethanol (110) and (1*S*)-2-(3*H*-Inden-1-yl)-1-phenylethanol (111)

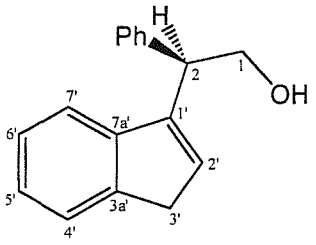

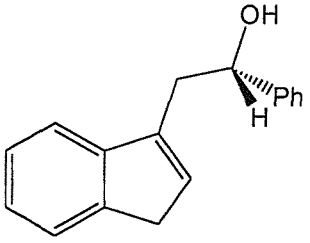

A solution of indene (5.8 g, 50 mmol), in di-*iso*-propylether (70 mL) was cooled to –78 °C and *n*-BuLi (20.0 mL, 2.5 M solution in hexanes, 50 mmol) added dropwise. The resulting yellow suspension was stirred at –78 °C for 15 min then warmed to room temperature and stirred for 2 h. The red suspension was cooled to 0 °C and *R*-(+)-styrene oxide (5.0 g, 41.6 mmol) added dropwise maintaining the internal temperature at 0 °C. The mixture was allowed to stir at 0 °C for 6 h and room temperature for a further 16 h. A saturated solution of ammonium chloride (100 mL) was added and the product extracted into diethyl ether (3 × 75 mL). The combined organic layers were washed with brine (2 × 50 mL), dried over $MgSO_4$ and the solvents removed *in vacuo*. Column chromatography (5 % diethyl ether/toluene) gave the title alcohols **111** (2.40 g, 24 %) followed by **110** (3.70 g, 37 %) as pale yellow viscous oils. In the racemic series **110** was obtained as a white crystalline solid from pentane at 0 °C (mp 61-63 °C). The proton NMR of **111** is consistent with that reported for **110** by Rieger.[76,77]

Although the synthesis of these two compounds has been reported previously,[29] full analysis has now been obtained and is given here.

Alcohol **110**:

$[\alpha]_D^{20}$ –13.5 (c = 0.96, $CHCl_3$).

^{1}H NMR (400 MHz, $CDCl_3$): δ 7.46 (1H, m), 7.37-7.30 (4H, m), 7.24 (1H, m), 7.20-7.15 (3H, m), 6.48 (1H, ddd, *J* = 2.0, 2.0, 1.3 Hz, *H2'*), 4.24-4.21 (2H, m, *H2 & H1-a*), 4.11 (1H, ddd, *J* = 13.1, 9.6, 6.4 Hz, *H1-b*), 3.46 (2H, br s, *H3'*), 1.58 (1H, t, *J* = 6.4 Hz, *OH*) ppm.

^{13}C NMR (75 MHz, $CDCl_3$): δ 144.80 (C), 144.46 (C), 143.82 (C), 140.16 (C), 128.97 (CH), 128.91 (2 × CH) 128.64 (2 × CH), 127.23 (CH), 126.23 (CH), 125.02 (CH), 123.94 (CH), 119.99 (CH, *C2'*), 66.13, (CH_2, *C1*), 47.54 (CH, *C2*), 38.25 (CH_2, *C3'*) ppm.

IR (thin film): 3554 (s), 3399 (bs), 3060 (s), 2880 (s), 1602 (s), 1582 (m), 1493 (s), 1452 (s), 1393 (s), 1180 (bm), 1052 (bs) cm^{-1}.

LRMS (EI^+): *m/z* 236 (M^+, 35 %), 218 ($(M–OH_2)^+$, 24), 205 ($(M–CH_2OH)^+$, 100), 189 (9), 128 (24), 91 (21).

Anal. Calcd. for $C_{17}H_{16}O$: C, 86.40; H, 6.82. Found: C, 86.13; H, 6.71.

Alcohol **111**:

$[\alpha]_D^{25}$ –19.1 (c = 2, $CHCl_3$).

^{1}H NMR (300 MHz, $CDCl_3$): δ 7.47 (1H, ddt, *J* = 7.8, 0.9, 0.9 Hz), 7.44-7.41 (2H, m), 7.40 (1H, dt, *J* = 7.5, 0.9 Hz), 7.38-7.26 (4H, m), 7.22 (1H, td, *J* = 7.5, 1.3 Hz), 6.33 (1H, ddd, *J* = 3.4, 2.1, 1.3 Hz, *H2'*), 5.03 (1H, ddd, *J* = 7.9, 5.3, 2.5 Hz, *H1*), 3.36 (2H, br. s, *H3'*), 3.01-2.97 (2H, m, *H2*), 2.15 (1H, d, *J*= 2.6 Hz, *OH*) ppm.

^{13}C NMR (75 MHz, $CDCl_3$): δ 144.84 (C), 144.39 (C), 144.07 (C), 140.72 (C), 131.03 (CH), 128.43 (2 × CH), 127.58 (CH), 126.11 (CH), 125.79 (2 × CH), 124.83 (CH), 123.87 (CH), 119.03 (CH, *C2'*), 72.49 (CH, *C1*), 38.31 (CH_2, *C2*), 37.31 (CH_2, *C3'*) ppm.

IR (thin film): 3400 (bs, OH), 3062 (m), 3028 (m), 2895 (m), 1606 (m), 1493 (m), 1455 (s), 1395 (s), 1201 (s), 1040 (bs), 970 (s), 913 (s), 873 (m) cm^{-1}.

LRMS (EI^+): *m/z* 236 (M^+, 5 %), 130 (M^+–PhCHO, 100), 107 ($PhCH=O^+H$, 31), 79 (26), 77 (15).

7.2.1.2 (2*R*)-Toluene-4-sulfonic Acid 2-(3*H*-Inden-1-yl)-2-phenylethyl Ester (112)

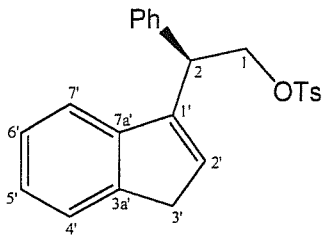

To a solution of (2*R*)-2-(3*H*-inden-1-yl)-2-phenylethanol **110** (3.55 g, 15 mmol) and dry pyridine (2.4 mL, 30 mmol) in dichloromethane (20 mL) was added *p*-toluenesulfonyl chloride (3.35 g, 16.6 mmol) portionwise at 0 °C. The reaction mixture was then stirred at 0 °C for 3 h and at room

temperature for 15 h before cooling to 0 °C and adding diethyl ether (50 mL) followed by hydrochloric acid (50 mL, 2M). The organic layer was separated then washed with 5 % aqueous sodium bicarbonate (45 mL) and water (45 mL) and dried over anhydrous magnesium sulphate. Removal of solvent *in vacuo* gave crude tosylate as an off white solid. Recrystallisation from hot ethanol afforded the title compound **112** as a white crystalline solid (4.32 g, 74 %). Mp 90-91 °C (sealed tube, under argon) (racemate mp 95-96 °C).

The NMR data were consistent with those reported previously.[29]

^{1}H NMR (400 MHz, $CDCl_3$): δ 7.61 (2H, d, *J* = 8.3 Hz), 7.40 (1H, m), 7.25-7.08 (9H, m), 6.99 (1H, m), 6.31 (1H, br.d, *J* = 1.4 Hz, *H2'*), 4.57 (1H, dd, *J* = 9.7, 7.0 Hz, *H1-a*), 4.39 (1H, dd, *J* = 9.7, 7.0 Hz, *H1-b*), 4.29 (1H, td, *J* = 7.0, 1.1 Hz, *H2*), 3.37 (2H, br.s, *H3'*), 2.40 (3H, s, CH_3) ppm.

^{13}C NMR (75 MHz, $CDCl_3$): δ 144.8 (C), 144.2 (C), 142.0 (C), 144.0 (C), 138.3 (C), 132.9 (C), 129.9 (2 × CH), 129.7 (CH), 128.9 (2 × CH), 128.5 (2 × CH), 128.0 (2 × CH), 127.5 (CH), 126.2 (CH), 125.0 (CH), 123.9 (CH), 119.7 (CH, *C2'*), 72.1 (CH_2, *C1*), 44.1 (CH, *C2*), 38.2 (CH_2, *C3'*), 21.8 (CH_3, *OTs*) ppm.

7.2.1.3 (1*S*)-[2-(3*H*-Inden-1-yl)-1-phenylethyl]diphenyl-phosphine (59)

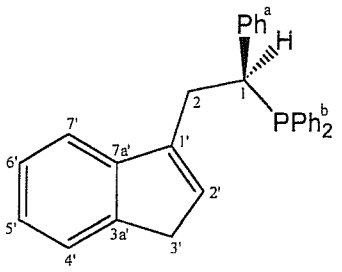

To a solution of tosylate **112** (1.56 g, 4 mmol), in THF (50 mL) at –78 °C was added dropwise *via* syringe potassium diphenylphosphide (8.8 mL of a 0.5 M solution in THF, 4.4 mmol). After addition was complete the reaction was stirred at –78 °C for 30 min before being warmed slowly to room temperature and stirred overnight, the colour changing from bright red to orange. Degassed ethanol (5 mL) was added to quench the reaction then approximately half the volume of solvent was removed *via* vacuum transfer. Toluene (50 mL) was added and the bright orange suspension filtered through silica under argon on an inline sinter (eluent toluene) to give a pale green solution. The solvents were removed to give the title phosphine as a white air sensitive solid (1.15 g, 70 %). Mp 98-99 °C.

Although the synthesis of this compound has been reported previously,[29] full analysis and detailed NMR assignments have now been obtained and are given here.

$[\alpha]_D^{18}$ –114.9 (c = 2.1, $CHCl_3$).

^{1}H NMR (300 MHz, C_6D_6): δ 7.89 (2H, t+fs, *J* = 7.5 Hz), 7.36 (2H, m), 7.05-7.30 (11H, m), 6.98-7.03 (4H, m), 5.85 (1H, br s, *H2'*), 4.03 (1H, apparent dt, *J* = 8.7, 6.2 Hz, *H1*. In $CDCl_3$ where the adjacent CH_2 protons are not degenerate it appears as a ddd J_{HH} = 11.0, 3.3 Hz, J_{PH} = 6.3 Hz), 3.26 (2H, app. t+fs, J_{HH} = 6.7 Hz, J_{PH} = 6.7Hz, *H2*), 2.99 (1H, d, *J* = 16.0 Hz, *H3'-a*), 2.91 (1H, d, *J* = 16.0 Hz, *H3'-b*) ppm.

^{13}C NMR (100 MHz, C_6D_6): δ 145.65 (C, *C7a'*), 144.50 (C, *C3a'*), 142.20 (C, d, J_{CP} = 13.2 Hz, *C1'*), 141.8 (C, d, J_{CP} = 8.3 Hz, *i-Ph*^{a}), 138.0 (C, d, J_{CP} = 17.5 Hz, *i-Ph*^{b}), 137.65 (C, d, J_{CP} = 15.6 Hz, *i-Ph*^{b}), 134.6 (2 × CH, d, J_{CP} = 20.4 Hz, *o-Ph*^{b}), 133.75 (2 × CH, d, J_{CP} = 18.5 Hz, *o-Ph*^{b}), 130.13 (CH, *C2'*), 129.56 (2 × CH, d, J_{CP} = 7.6 Hz, *m-Ph*^{b}), 129.51 (CH, *p-Ph*^{b}), 128.86 (2 × CH, d, J_{CP} = 7.3 Hz. *m-Ph*^{b}), 128.49 (CH, *p-Ph*^{b}), 128.38 (2 × CH, *m-Ph*^{a}), 128.12 (2 × CH, d, J_{CP} = 6.3 Hz, *o-Ph*^{a}), 126.38 (CH, d, J_{CP} = 2 Hz, *p-Ph*^{a}), 126.26 (CH, *C4'/5'/6'/7'*), 124.80 (CH, *C4'/5'/6'/7'*), 123.93 (CH, *C4'/5'/6'/7'*), 119.20 (CH, *C4'/5'/6'/7'*), 44.77 (CH, d, J_{CP} = 14.4 Hz, *C1*), 37.84 (CH_2, *C3'*), 32.34 (CH_2, d, J_{CP} = 24.7 Hz, *C2*) ppm.

^{31}P NMR (120 MHz, $CDCl_3$): δ 1.07 (s) ppm.

IR (CH_2Cl_2 solution): 3040 (bs), 2900 (bm), 1600 (bm), 1492 (s), 1453 (s), 1436 (s), 1280 (s), 1117 (m), 1019 (m), 895 (s), 775 (s), 603 (s) cm^{-1}.

LRMS (EI$^+$): *m/z* 404 (M^+, 100 %), 275 (Ph_2P^+=CHPh, 70), 219 ($(M–PPh_2)^+$, 53), 202 (87), 183 (35), 128 (70), 115 (50), 91 (84), 77 (61).

Anal. Determined for BH_3 adduct **123** (see Section 7.2.1.4).

7.2.1.4 (1*S*)-[2-(3*H*-Inden-1-yl)-1-phenylethyl]diphenyl-phosphine-Borane Complex (123)

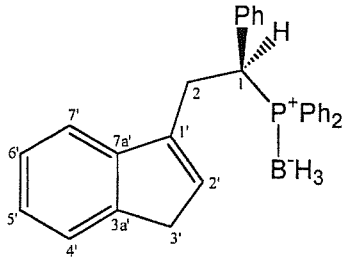

Crude (1*S*)-[2-(3*H*-Inden-1-yl)-1-phenylethyl]diphenyl-phosphine ligand **59** (1.0 eq, ~2.0 mmol, 809 mg) was dissolved in THF and cooled to 0 °C, under argon. Borane-methyl sulphide complex (2.0 M solution in toluene, 2.6 eq, 5.2 mmol, 2.6 mL) was then added dropwise and the reaction stirred at 0 °C for 1 h.

Ice-water (50 mL) was then added slowly at 0 °C, to quench the reaction (vigorous gas evolution). Ethyl acetate (50 mL) was added to the mixture and the aqueous phase separated and extracted with ethyl acetate (3 × 50 mL). The combined organics were washed with brine (50 mL), dried over $MgSO_4$ and concentrated *in vacuo* to give a pale green solid. Column chromatography (10 % ethyl acetate/petrol) gave the protected ligand as a white solid (0.70 g, 1.7 mmol, 83 % over two steps). Mp 150-152 °C.

$[\alpha]_D^{21}$ –86.5 (c = 0.1, CH_2Cl_2).

^{1}H NMR (300 MHz, $CDCl_3$): δ 8.03-7.94 (2H, t+fs, *J* = 8.1 Hz), 7.61-7.49 (3H, m), 7.40-7.10 (12H, m), 7.07 (1H, d+fs, *J* = 6.6 Hz), 5.86 (1H, br.s, *H2'*), 4.09 (1H, ddd, *J* = 15.8, 11.1, 3.2 Hz, *H1*), 3.37 (1H, m, *H2-a*), 3.15 (1H, m, *H2-b*), 3.09 (2H, m, *H3'*), 1.70-0.60 (3H, v.br.q, BH_3) ppm.

^{13}C NMR (75 MHz, $CDCl_3$): δ 145.00 (C, s, *C7a'*), 144.36 (C, s, *C3a'*), 141.04 (C, d, J_{CP} = 13.5 Hz, *i-Ph*^{a}), 136.21 (C, d, J_{CP} = 1.4 Hz, *C1'*), 133.40 (2 × CH, d, J_{CP} = 8.4 Hz, *o-Ph*^{b}), 133.00 (2 × CH, d, J_{CP} = 8.4 Hz, *o-Ph*^{b}), 131.79 (CH, d, J_{CP} = 2.5 Hz, *p-Ph*^{b}), 131.10 (CH, d, J_{CP} = 2.5 Hz, *p-Ph*^{b}), 130.68 (CH, s, *C4'/5'/6'/7'*), 130.15 (2 × CH, d, J_{CP} = 4.8 Hz, *m-Ph*^{a}), 129.13 (2 × CH, d, J_{CP} = 9.6 Hz, *m-Ph*^{b}), 128.58 (C, s, *i-Ph*^{b}), 128.38 (2 × CH, d, J_{CP} = 9.8 Hz, *m-Ph*^{b}), 128.12 (2 × CH, d, J_{CP} = 2.3 Hz, *o-Ph*^{a}), 127.89 (C, s, *i-Ph*^{b}), 127.37 (CH, d, J_{CP} = 2.5 Hz, *p-Ph*^{a}), 126.21 (CH, s, *C4'/5'/6'/7'*), 124.86 (CH, s, *C4'/5'/6'/7'*), 123.97 (CH, s, *C4'/5'/6'/7'*), 118.89 (CH, s, *C2'*), 42.13 (CH, d, J_{CP} = 30.0 Hz, *C1*), 38.03 (CH_2, s, *C3'*), 28.90 (CH_2, d, J_{CP} = 6.2 Hz, *C2*) ppm.

^{31}P NMR (121 MHz, $CDCl_3$): δ 24.72 (v. br. s) ppm.

IR (NaCl, thin film): 3057 (m), 2906 (w), 2398 (s), 1494 (m), 1454 (m), 1436 (s), 1265 (w), 1105 (m), 1068 (s), 770 (s), 738 (s) cm^{-1}.

Anal. Calcd. for $C_{29}H_{28}BP$: C, 83.27; H, 6.75. Found: C, 83.19; H, 6.76.

7.2.1.5 *rac*-(*R*,*R*)-Spiro[(2-phenylcyclopropane)-1,1′-indene] (114)

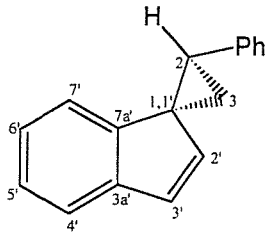

A solution of the racemic tosylate *rac*-**112** (0.78 g, 2 mmol) in THF (25 mL) was cooled to –78 °C and *n*-BuLi (0.96 mL of a 2.5 M solution in hexanes, 2.4 mmol, 1.2 eq) added dropwise. After stirring at –78 °C for 15 min and room temperature for 2 h, the reaction was quenched with water (20 mL) and the product extracted into diethyl ether (30 mL). The organic layer was washed with brine (20 mL) then dried over $MgSO_4$. Concentration *in vacuo*, followed by recrystallisation from hot ethanol provided the spirocycle **114** (0.30 g, 69 %) as white crystals, mp 79-81 °C. The crystals were suitable for X-ray crystallography which confirmed the relative stereochemistry of **114** (see Appendix 1).

^{1}H NMR (300 MHz, $CDCl_3$): δ 7.35 (1H, d, *J* = 7.2 Hz), 7.02-7.29 (8H, m), 6.73 (1H, d, *J* = 5.7 Hz, *H2'/3'*), 5.92 (1H, d, *J* = 5.5 Hz, *H2'/3'*), 3.15 (1H, dd, *J* = 8.7, 7.2 Hz, *H2*), 2.26 (1H, dd, *J* = 7.2, 5.0 Hz, *H3-a*), 1.94 (1H, dd, *J* = 8.7, 5.0 Hz, *H3-b*) ppm.

^{13}C NMR (100 MHz, $CDCl_3$): δ 147.9 (C), 143.4 (C), 139.3 (C), 137.6 (CH), 129.9 (CH), 128.5 (2 × CH), 128.4 (2 × CH), 126.9 (CH), 126.0 (CH), 124.6 (CH), 121.6 (CH), 117.7 (CH), 41.1 (C, *C1,1'*), 33.3 (CH, *C2*), 19.5 (CH_2, *C3*) ppm.

IR (thin film): 3044 (w), 1601 (m), 1497 (m), 1453 (s), 1200 (m), 1076 (m), 1048(m), 1018 (m), 983 (s), 905 (m), 882 (m), 756 (s), 728 (s) cm^{-1}.

LRMS (AP^+): *m/z* 218 (M^+, 100 %).

Anal. Calcd. for $C_{17}H_{14}$: C, 93.54; H, 6.46. Found: C, 93.44; H, 6.48.

7.2.1.6 *rac*-[2-(3*H*-Inden-1-yl)-1-phenylethyl]diphenylphosphine (59) from *rac*-(*R*,*R*)-Spiro[(2-phenylcyclopropane)-1,1'-indene] (114)

To a solution of spirocycle **114** (0.218 g, 1 mmol) in THF (13 mL) at –78 °C, was added dropwise potassium diphenylphosphide (2.2 mL of a 0.5 M solution in THF, 1.1 mmol). The reaction was stirred at –78 °C for 30 min and room temperature for 2 h then quenched with degassed ethanol (1 mL). The solution was concentrated to approximately half volume, diluted with toluene (30 mL) and filtered through a bed of silica gel, under argon. Removal of solvent gave *rac*-**59** as a white solid (0.29 g, 71 %), >90 % pure by ^{1}H NMR.

NMR data were consistent with those reported for (*1S*)-**59**, Section 7.2.1.3.

7.2.1.7 (*S*)-1-Cyclohexyl-2-(3*H*-inden-1-yl)ethanol (117)

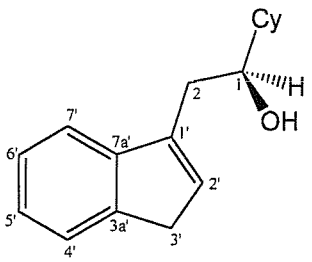

A solution of indene (5.6 mL, 48 mmol) in THF (70 mL), was cooled to –78 °C, and *n*-BuLi (19.2 mL of a 2.5 M solution in hexanes, 48 mmol) added dropwise. The resulting yellow suspension was stirred for 20 min at –78 °C, before being allowed to warm to room temperature and stirred for 2 h. The anion solution was then cooled to –5 °C and (*R*)-cyclohexyloxirane (5.05 g, 40 mmol) in THF (20 mL) was added dropwise and the mixture stirred at room temperature for 16 h. Saturated ammonium chloride solution (100 mL) was added and the product extracted into diethyl ether (3 × 100 mL). The combined organic layers were then washed with brine (100 mL), dried over $MgSO_4$, and the solvents removed *in vacuo* to yield a yellow solid. Column chromatography (10 % ethyl acetate/petrol) gave the title alcohol **117** as a white crystalline solid, (6.93 g, 72 %). Recrystallisation from ethanol gave fine needles mp 69-71 °C of >99 % e.e. by HPLC (250 × 5 mm Chiracel OD-H column, eluting with 0.7 % isopropyl alcohol in hexane, 1 mL/min, R_t 17.5 min (*R*)-enantiomer, R_t 21.0 min (*S*)-enantiomer). The racemate had mp 60-62 °C.

$[\alpha]_D^{26}$ –34.9 (c = 0.75, $CHCl_3$)

^{1}H NMR (300 MHz, $CDCl_3$): δ 7.49 (1H, d+fs, *J* = 7.3 Hz), 7.38 (1H, d+fs, *J* = 7.2 Hz), 7.31 (1H, td, *J* = 7.3, 1.1 Hz), 7.25 (1H, td, *J* = 7.2, 1.5 Hz), 6.38 (1H, br. s, *H2'*), 3.73 (1H, ddd, *J* = 9.7, 5.6, 3.1 Hz, *H1*), 3.40 (2H, br. s, *H3'*), 2.88 (1H, dtd, *J* = 14.4, 3.3, 1.8 Hz, *H2-a*), 2.61 (1H, ddd, *J* = 14.4, 9.8, 1.1 Hz, *H2-b*), 1.10-1.90 (12H, m) ppm.

^{13}C NMR (75 MHz, $CDCl_3$): δ 145.2 (C), 144.7 (C), 141.8 (C), 130.7 (CH), 126.3 (CH), 125.0 (CH), 124.1 (CH), 119.3 (CH), 73.9 (CH), 43.6 (CH), 38.1 (CH_2), 33.2 (CH_2), 29.4 (CH_2), 28.3 (CH_2), 26.8 (CH_2), 26.5 (CH_2), 26.4 (CH_2) ppm.

IR (Nujol® mull): 3368 (bs), 2720 (m), 1580 (w), 1104 (m), 1026 (m), 991 (m), 966 (m), 914 (m), 891 (m) cm^{-1}.

LRMS (AP^+): *m/z* 225 ($(M–OH)^+$, 19 %), 224 ($(M–H_2O)^+$, 13), 131 ($(M–CyCH_2OH)^+$, 100).

Anal. Calcd. for $C_{17}H_{22}O$: C, 84.25; H, 9.15. Found: C, 84.54; H, 9.21.

7.2.1.8 *rac*-Toluenesulfonic Acid 1-Cyclohexyl-2-(3*H*-inden-1-yl)ethyl Ester (118)

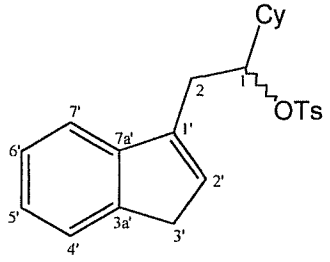

To a stirred solution of 1-cyclohexyl-2-(1*H*-3-indenyl)-1-ethanol *rac*-**117** (3.64 g, 15 mmol, 1 eq) in dichloromethane (60 mL), at 0 °C, was added pyridine (2.43 mL, 30 mmol, 2 eq), DMAP (20 mg, catalytic) and tosyl chloride (3.43 g, 18 mmol, 1.2 eq). The reaction was stirred for 15 minutes at 0 °C, then at room temperature for 48 h.

After this time, TLC indicated the reaction remained incomplete, so workup was performed. Diethyl ether (180 mL) was added to the reaction, followed by water (50 mL) and HCl (2 M, 180 mL) at 0 °C. The organic phase was separated and washed with 5 % sodium bicarbonate solution (80 mL) and water (80 mL), then dried over $MgSO_4$ and concentrated *in vacuo*. Flash silica gel chromatography (10 % ethyl acetate/petrol) was performed, and the product tosylate **118** collected as an off-white solid (1.78 g, ~30 %, with some co-elution of unreacted tosyl chloride, by ^{1}H NMR). Unreacted tosyl chloride was recovered as a white crystalline solid (2.22 g, 11.6 mmol, 65 %), and unreacted alcohol **117** as a yellow crystalline solid (2.01 g, 8.3 mmol, 55 %).

Recrystallisation from hot ethanol was required to obtain the pure product tosylate **118** as a white crystalline solid (1.35 g, 3.41 mmol, 23 %) which was found to be light/temperature sensitive, and seen to decompose to black crystals when left standing at room temperature for 2 h. Mp 68-70 °C (dec.).

^{1}H NMR (300 MHz, $CDCl_3$): δ 7.60 (2H, d, *J* = 8.2 Hz, *o/m-Ph*), 7.39 (1H, d, *J* = 7.2 Hz, *indene ArH*), 7.15-7.25 (3H, m, *indene ArH*), 7.05 (2H, d, *J* = 8.2 Hz, *o/m-Ph*), 6.19 (1H, br. s, *H2'*), 4.76 (1H, ddd, *J* = 6.7, 6.7, 3.7 Hz, *H1*), 3.20 (1H, d, *J* = 23.1 Hz, *H2-a*), 3.10 (1H, d, *J* = 23.1 Hz, *H2-b*), 2.88 (2H, d, *J* = 6.7 Hz, *H3'*), 2.36 (3H, s, CH_3), 1.60-1.90 (7H, m, *Cy*), 1.10-1.30 (4H, m, *Cy*) ppm.

^{13}C NMR (75 MHz, $CDCl_3$): δ 145.0 (C, *C1'*), 143.9 (C, *C3a'/7a'*), 144.5 (C, *C3a'/7a'*), 139.3 (C, *i-Ph*), 134.9 (C, *i-Ph*), 131.5 (CH, *C4'/5'/6'/7'*), 129.3 (2 × CH, *o/m-Ph*), 127.5 (2 × CH, *o/m-Ph*), 126.1 (CH, *C4'/5'/6'/7'*), 124.7 (CH, *C4'/5'/6'/7'*), 123.7 (CH, *C4'/5'/6'/7'*), 119.0 (CH, *C2'*), 86.3 (CH, *C1*), 41.2 (CH, *Cy*), 37.9 (CH_2, *C3'*), 29.6 (CH_2, *C2*), 28.3 (CH_2, *Cy*), 27.6 (CH_2, *Cy*), 26.3 (CH_2, *Cy*), 26.2 (2 × CH_2, *Cy*), 21.6 (CH_3, *OTs*) ppm.

IR (NaCl, thin film): 2928 (s), 2854 (m), 1598 (w), 1451 (m), 1359 (s), 1187 (m), 1175 (s), 1097 (m), 973 (w), 902 (s), 813 (m), 770 (m).

LRMS (ES^+): *m/z* 414 ($(M+NH_4)^+$, 15 %), 435 ($(M+K)^+$, 100), 815 ($(2M+Na)^+$, 25), 832 ($(2M+K)^+$, 15).

7.2.1.9 (*S*)-Methanesulfonic Acid 1-Cyclohexyl-2-(3*H*-inden-1-yl)ethyl Ester (119)

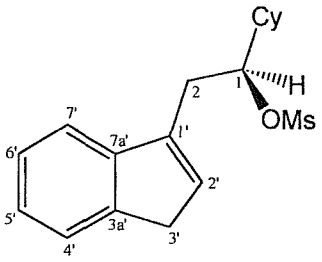

To a stirred solution of alcohol **117** (5.94 g, 24.5 mmol) and triethylamine (8.5 mL, 6.2 g, 61.2 mmol) in dichloromethane (130 mL) at –30 °C, was added dropwise mesyl chloride (2.5 mL, 3.7 g, 31.9 mmol). After stirring at –20 °C for 2 h the solution was filtered, and the organic phase washed with water (90 mL) and brine (90 mL), then dried over $MgSO_4$ and concentrated *in vacuo* yielding the crude product as a brown solid (6.63 g, ~21 mmol, ~84 % crude) which was used immediately in the formation of the spirocycle **120**.

^{1}H NMR (300 MHz, $CDCl_3$): δ 7.48 (1H, d, *J* = 7.2 Hz), 7.43 (1H, d, *J* = 7.5 Hz), 7.34 (1H, t, *J* = 7.2 Hz), 7.24 (1H, t, *J* = 7.5 Hz), 6.39 (1H, br. s, *H2'*), 5.85 (1H, ddd, *J* = 6.7, 6.7, 4.2 Hz, *H1*), 3.37 (2H, br. s, *H3'*), 2.99 (2H, d, *J* = 6.7 Hz, *H2*), 2.62 (3H, s, CH_3), 1.60-1.95 (7H, m, *Cy*), 1.20-1.40 (4H, m, *Cy*) ppm.

7.2.1.10 (*R*)-Methanesulfonic Acid 1-Cyclohexyl-2-((methanesulfonyl)oxy)-ethyl Ester (122)

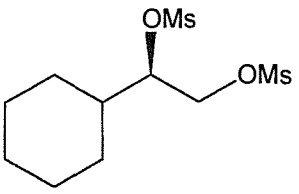

A stirred solution of (1*R*)-1-cyclohexyl-1,2-ethanediol **115** (6.49 g, 45 mmol) in dichloromethane (340 mL) was cooled to –30 °C, under argon. Triethylamine (22 mL, 158 mmol) was then added, followed by dropwise addition of mesyl chloride (8.7 mL, 113 mmol), causing the precipitation of a white solid. A further portion of dichloromethane (245 mL) was added to enable efficient stirring. The reaction was stirred at –30 °C to –20 °C for 2 h then filtered cold (–20 °C) and the residue washed with cold dichloromethane (120 mL, –20 °C). Water (300 mL) was then added to the collected filtrate, and the aqueous layer separated and extracted with dichloromethane (3 × 180 mL). The combined organic layers were dried over $MgSO_4$, and concentrated *in vacuo* to yield the crude dimesylate as an off-white solid (14.8 g, ~109 %). Recrystallisation from dichloromethane/hexane at 5 °C gave 3 crops of the title compound **122** as white crystals (13.1 g, 97 %). All 3 crops retained the 97 % e.e. of the diol starting material as judged from their independent conversion into spiro-cyclopropane **120** of 97 % e.e. Mp 114-116 °C. X-ray structure analysis confirmed the stereochemistry was as expected (see Appendix 2).

$[\alpha]_D^{25}$ –17.2 (c = 1, $CHCl_3$).

^{1}H NMR (400 MHz, $CDCl_3$): δ 4.68 (1H, ddd, *J* = 6.6, 6.6, 2.6 Hz), 4.47 (1H, dd, *J* = 11.4, 2.6 Hz), 4.36 (1H, dd, *J* = 11.7, 6.6 Hz), 3.12 (3H, s), 3.10 (3H, s), 1.67-1.91 (6H, m), 1.03-1.37 (5H, m) ppm.

^{13}C NMR (100 MHz, $CDCl_3$): δ 82.8 (CH), 67.3 (CH_2), 37.9 (CH_3), 37.8 (CH_3), 36.7 (CH), 27.5 (CH_2), 27.2 (CH_2), 24.8 (CH_2), 24.6 (CH_2), 24.5 (CH_2) ppm.

IR (thin film): 3029 (w), 2958 (m), 2929 (m), 2857 (w), 1452 (w), 1355 (s), 1344 (s), 1332 (s), 1175 (s), 1034 (m), 979 (s), 904 (s), 844 (s), 792 (s) cm^{-1}.

LRMS (AP^+): *m/z* 300 (M^+, 100 %).

Anal. Calcd. for $C_{10}H_{20}O_6S_2$: C, 39.99; H, 6.71. Found: C, 39.99; H, 6.74.

7.2.1.11 (+)-Spiro-[(2-cyclohexylcyclopropane)-1,1′-indene] (120)

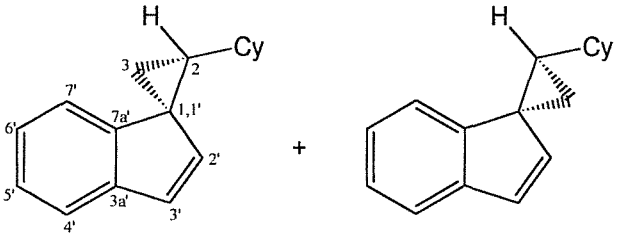

*i. From mesylate **119**.* To a solution of the crude mesylate **119** (6.63 g, ~21 mmol) in THF (130 mL) at –78 °C under argon was added *n*-BuLi (11.9 mL, 2.5 M solution in hexanes, 29.7 mmol). The reaction was stirred at –78 °C for 15 min, then room temperature for 2 h before quenching with water (40 mL). Diethyl ether (45 mL) was added, and the organic layer separated, washed with brine (40 mL), then dried over $MgSO_4$. Concentration *in vacuo*, followed by chromatography (100 % petrol), provided the title product as a clear oil (3.45 g, 83 % from **117**) and a 1 : 1 mixture of diastereoisomers.

*ii. From bis-mesylate **122**.* A solution of indene (5.3 mL, 45 mmol) in THF (50 mL) was cooled to –78 °C and *n*-BuLi (18 mL of a 2.5 M solution in hexanes, 45 mmol) added dropwise, in the dark. The resulting yellow suspension was stirred at –78 °C for 15 min, then warmed to room temperature and stirred for 1.5 h. The anion mixture was cooled to 0 °C, diluted with THF (90 mL) and dimesylate **122** (5.6 g, 18.8 mmol) added portionwise over 2 min. The mixture was stirred at 0 °C for 15 min then allowed to warm to room temperature overnight (*ca.* 17 h). The reaction was quenched with water (150 mL) and extracted with diethyl ether (4 × 75 mL). The combined organic layers were washed with saturated sodium bicarbonate solution (150 mL), then dried over $MgSO_4$ and concentrated *in vacuo*. Chromatography (100 % petrol) gave the desired product contaminated with a small amount of indene which was removed by evaporation under vacuum (0.3 mmHg) for 24 h at room temperature, to yield the clean spirocycle **120** as a white solid (3.56 g, 84 %) and a 9 : 2 mixture of diastereoisomers. Chiral HPLC (250 × 5 mm Chiracel OD-H column, eluting with 1 % isopropyl alcohol in hexane, 1 mL/min, R_t = 4.7 min (minor isomer, (+)-enantiomer), R_t = 4.9 min (major isomer, (+)-enantiomer),

R_t = 5.4 min (major isomer, (–)-enantiomer), R_t = 7.3 min (minor isomer, (–)-enantiomer)) showed the product has retained chirality (97 % e.e.) from the diol **115**. Recrystallisation from hot ethanol afforded the enantiopure major isomer as clear crystals mp 79-80 °C, X-ray structure analysis confirmed the structure and stereochemistry (see Appendix 3).

$[\alpha]_D^{25}$ +216.0 (c = 0.5, $CHCl_3$) (major isomer).

^{1}H NMR (400 MHz, major diastereoisomer, $CDCl_3$): δ 7.44 (1H, dt, *J* = 7.4, 0.9 Hz), 7.25 (1H, td, *J* = 7.4, 1.1 Hz), 7.18 (1H, td, *J* = 7.4, 0.9 Hz), 6.97 (1H, dt, *J* = 7.4, 0.9 Hz), 6.97 (1H, d, *J* = 5.7 Hz, *H2'/3'*), 6.41 (1H, d, *J* = 5.7 Hz, *H2'/3'*), 2.00 (1H, m, *Cy*), 2.00-1.50 (5H, m, *Cy*), 1.72 (1H, dd, *J* = 8.5, 4.3 Hz, *H3-a*), 1.61 (1H, dd, *J* = 7.2, 4.3 Hz, *H3-b*), 1.37-1.12 (4H, m, *Cy*), 1.24 (1H, dd, *J* = 11.1, 8.6 Hz, *H2*), 0.94 (1H, m, *Cy*) ppm.

^{13}C NMR (100 MHz, major diastereoisomer, $CDCl_3$): δ 148.94 (C), 143.09 (C), 138.01 (CH), 129.38 (CH), 125.40 (CH), 124.34 (CH), 121.42 (CH, *C2'/C3'*), 117.56 (CH, *C2'/3'*), 42.15 (CH, *C2*), 38.08 (C, *C1,1'*), 37.04 (CH, *Cy*), 33.56 (CH_2), 33.28 (CH_2), 26.65 (CH_2), 26.56 (CH_2), 26.31 (CH_2), 21.60 (CH_2) ppm.

IR (thin film): 3029 (w), 2958 (m), 2929 (m), 2857 (w), 1452 (m), 1355 (s), 1344 (s), 1332 (s), 1175 (s), 1034 (m), 979 (s), 904 (bs), 844 (s), 793 (s), 762 (m), 739 (m) cm^{-1}.

LRMS (AP$^+$): *m/z* 225 ($(M+H)^+$, 42 %), 224 (M^+, 100), 181 (9), 168 (11).

Anal. Calcd. for $C_{17}H_{20}$: C, 91.01; H, 8.99. Found: C, 91.16; H, 9.02.

7.2.1.12 [(2*R*)-2-Cyclohexyl-2-(3*H*-Inden-1-yl)ethyl]diphenyl-phosphine (121)

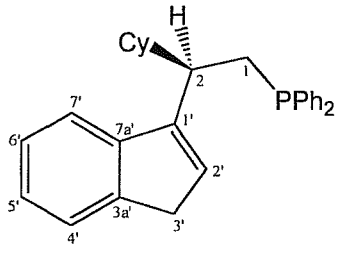

To a solution of spiro-[(2-cyclohexylcyclopropane)-1,1'-indene] **120** (2.02 g, 9.0 mmol) and 18-crown-6 (48 mg, 2 mol%) in THF (45 mL) at 0 °C, was added dropwise a deep red solution of potassium diphenylphosphide (21.6 mL of a 0.5 M solution in THF, 10.8 mmol). The reaction mixture was stirred at room temperature for 48 h before quenching with degassed ethanol (10 mL). Approximately half the THF was removed by vacuum transfer, the residue diluted with toluene (30 mL) and the mixture filtered through a 3 cm bed of silica under argon, washing through with more toluene (60 mL). Removal of solvent, and chromatography of

the crude product (0-3 % ethyl acetate/hexane) under argon gave the title compound as white cloudy air sensitive oil (3.26 g, 88 %), with no oxidised product present in the mass spectrum.

$[\alpha]_D^{26}$ + 23.0 (c = 1.0, $CHCl_3$).

^{1}H NMR (400 MHz, $CDCl_3$): δ 7.12-7.41 (14H, m), 6.12 (1H, t, *J* = 1.8 Hz, *H2'*), 3.24 (2H, d, *J* = 1.8 Hz, *H3'*), 2.64 (1H, dddd, J_{HH} = 10.2, 6.2, 4.2 Hz, J_{HP} = 10.2 Hz, *H2*), 2.55 (1H, ddd, J_{HH} = 13.6, 4.2 Hz, J_{HP} = 3.0 Hz, *H1-a*), 2.40 (1H, ddd, J_{HH} = 13.6, 10.2 Hz, J_{HP} = 2.0 Hz, *H1-b*), 1.53-1.89 (6H, m, *Cy*), 0.85-1.23 (5H, m, *Cy*) ppm.

^{13}C NMR (100 MHz, $CDCl_3$): δ 146.46 (C, d, J_{CP} = 3.9 Hz, *C1'*), 145.65 (C, *C3a'/7a'*), 144.94 (C, *C3a'/7a'*), 139.99 (C, d, J_{CP} = 13.5 Hz, *i-Ph*), 139.15 (C, d, J_{CP} = 15.0 Hz, *i-Ph*), 133.49 (2 × CH, d, J_{CP} = 19.3 Hz, *o-Ph*), 132.69 (2 × CH, d, J_{CP} = 18.3 Hz, *o-Ph*), 129.89 (CH, d, J_{CP} = 1.5 Hz, *C2'*), 128.84 (CH, *p-Ph*), 128.54 (2 × CH, d, J_{CP} = 6.8 Hz, *m-Ph*), 128.32 (2 × CH, d, J_{CP} = 6.3 Hz, *m-Ph*), 128.27 (CH, *p-Ph*), 125.91 (CH, *C4'/5'/6'/7'*), 124.52 (CH, *C4'/5'/6'/7'*), 123.98 (CH, *C4'/5'/6'/7'*), 119.96 (CH, *C4'/5'/6'/7'*), 42.47 (CH, d, J_{CP} = 8.2 Hz, *Cy*), 41.68 (CH, d, J_{CP} = 14.0 Hz, *C2*), 37.91 (CH_2, *C3'*), 31.05 (2 × CH_2, d, J_{CP} = 6.3 Hz, *Cy*), 30.76 (CH_2, d, J_{CP} = 12.1 Hz, *C1*), 26.78 (2 × CH_2, *Cy*), 26.75 (CH_2, *Cy*) ppm.

^{31}P NMR (120 MHz, $CDCl_3$): δ = –17.9 (s) ppm.

IR (thin film): 3068 (w), 2923 (bs), 2850 (bm), 1585 (w), 1480 (w), 1448 (m), 1433 (m), 1393 (w), 1263 (w), 1095 (m), 1026 (m), 969 (m), 915 (w), 845 (w), 769 (s), 738 (s), 696 (s) cm^{-1}.

LRMS (ES^+): *m/z* 411 ($(M+H)^+$, 100 %), (fully oxidised by air when in solution: *m/z* 427, ($(M+O+H)^+$, 100 %)).

Anal. determined for BH_3 derivative **124** (Section 7.2.1.13)

7.2.1.13 [(2*R*)-2-Cyclohexyl-2-(3*H*-Inden-1-yl)ethyl]diphenylphosphine-Borane Complex (124)

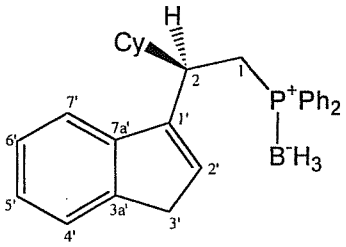

*i. From addition of borane to ligand **121**.* A solution of cyclohexyl substituted ligand **121** (180 mg, 0.44 mmol) was prepared in THF (10 mL) under argon, and cooled to 0 °C. A solution of borane-methyl sulphide complex (0.05 mL, 0.53 mmol) in THF (1 mL) was then added dropwise. The clear reaction mixture was stirred at 0 °C for 30 min before quenching by addition of ice-water (10 mL) at 0 °C and extraction of the product into ethyl acetate (4 × 20 mL). The combined organic layers were washed with brine (20 mL), dried over $MgSO_4$ then concentrated *in vacuo*. Recrystallisation of the crude product from hexane at –30 °C gave the title compound as a white air-stable solid (125 mg, 68 %).

*ii. By ring opening of spirocycle **120** with $[Ph_2PBH_3]^-Li^+$.* A solution of lithium diphenylphosphide-borane complex[85] (4 mL of a 0.25M solution in THF, 1.0 mmol) and HMPA (0.14 mL, 0.83 mmol) was prepared and cooled to 0 °C, under argon. A solution of spiro-[(2-cyclohexylcyclopropane)-1,1'-indene] **120** (186 mg, 0.83 mmol) in THF (1 mL) was then added dropwise. The reaction mixture was stirred for 15 min at 0 °C, then warmed to room temperature, and stirred for 24 h. The reaction was quenched with water (2 mL), and the product extracted with ethyl acetate (3 × 10 mL). The combined organic layers were washed with brine (10 mL), dried over $MgSO_4$ then concentrated *in vacuo*. The product was purified by column chromatography (10 % ethyl acetate/petrol), and isolated as a white solid (212 mg, 61 %). Mp 124-126 °C (enantiopure).

$[\alpha]_D^{25}$ –14.0 (c = 0.5, $CHCl_3$).

^{1}H NMR (400 MHz, $CDCl_3$): δ 7.61 (2H, t+fs, *J* = 8.3 Hz), 7.35-7.41 (6H, m), 7.33 (1H, d, *J* = 7.4 Hz), 7.24 (2H, br t, *J* = 8.8 Hz), 7.19 (1H, tq, *J* = 7.4, 1.4 Hz), 7.13 (1H, td, *J* = 7.4, 1.0 Hz), 7.05 (2H, tq, *J* = 7.7, 2.0 Hz), 5.94 (1H, t, *J* = 2.0 Hz, *H2'*), 3.19 (1H, dddd, *J* = 12.7, 10.3, 7.5, 2.6 Hz, *H2*), 2.71-2.92 (3H, m, *H3' & H1-a*), 2.58 (1H, ddd, *J* = 14.2, 9.4, 2.8 Hz, *H1-b*), 1.93 (1H, br. d, *J* = 12.5 Hz, *Cy*), 1.51-1.79 (5H, m, *Cy*), 0.85-1.25 (8H, m, *Cy & BH_3*) ppm.

^{13}C NMR (100 MHz, $CDCl_3$): δ 144.83 (C, s, *C1'/7a'/3a'*), 144.71 (C, s, *C1'/7a'/3a'*), 144.62 (C, s, *C1'/7a'/3a'*), 132.74 (2 × CH, d, J_{CP} = 9.2 Hz, *o-Ph*), 132.00 (2 × CH, d, J_{CP} = 8.7 Hz, *o-Ph*), 131.67 (CH, br.d, J_{CP}* = 11.4 Hz, *C2'*), 131.06 (CH, br.d, J_{CP}* = 21.8 Hz, *i-Ph*), 130.96 (CH, d, J_{CP} = 2.2 Hz, *p-Ph*), 130.72 (CH, d, J_{CP} = 2.4 Hz, *p-Ph*), 128.85 (2 × CH, d, J_{CP} = 9.7 Hz, *m-Ph*), 128.83 (C, d, J_{CP}* = 33.8 Hz, *i-Ph*), 127.96 (2 × CH, d, J_{CP} = 9.9 Hz, *m-Ph*), 125.82 (CH, s, *C7'/4'/6'/5'*), 124.49 (CH, s, *C7'/4'/6'/5'*), 123.85 (CH, s, *C7'/4'/6'/5'*), 120.23 (CH, s, *C7'/4'/6'/5'*), 42.39 (CH, br. d, J_{CP}* = 9.2 Hz, *Cy*), 39.87 (CH, br.s,* *C2*), 37.64 (CH_2, s, *C3'*), 31.27 (CH_2, s, *Cy*), 30.74 (CH_2, s, *Cy*), 27.35 (CH_2, br.d, J_{CP}* = 36.0 Hz, *C1*), 26.66 (CH_2, s, *Cy*), 26.59 (CH_2, s, *Cy*), 26.58 (CH_2, s, *Cy*) ppm. * – these signals and coupling constants were difficult to distinguish owing to borane-broadening of the ^{13}C resonances.

LRMS (AP^+): *m/z* 464 ($(M–H+CH_3CN)^+$, 72 %), 423 ($(M–H)^+$, 100), 411 ($(M–BH_3+H)^+$, 67).

IR (thin film): 2933 (bm), 2914 (bm), 2848 (m), 1458 (m), 1436 (s), 1107 (m), 1064 (s), 965 (m), 870 (m), 791 (m), 767 (s), 747 (m), 727 (s) cm^{-1}.

Anal. Calcd. for $C_{29}H_{34}BP$: C, 82.08; H, 8.08; P, 7.30. Found: C, 82.22; H, 8.18; P, 7.37.

7.2.1.14 Deprotection of Borane Complex (124)

Borane protected phosphine ligand **124** (50 mg, 0.12 mmol) was treated with neat diethylamine (1 mL), under argon, and warmed to 50 °C. The reaction was stirred with monitoring by TLC (10 % ethyl acetate/petrol) for 3 h. After this time TLC showed the deprotected phosphine ligand present at R_f 0.6, along with remaining borane protected phosphine at R_f 0.4. The reaction was allowed to cool, and then evacuated to dryness, in order to remove remaining diethylamine and the diethylamine-borane complex. Fresh diethylamine (1 mL) was then added to the mixture of starting material and product, and the reaction heated again to 50 °C overnight. After this time, TLC showed only the free phosphine present. The reaction was then cooled and evacuated to dryness, leaving the ligand **121** as an air-sensitive oil (48 mg, 99 %).

^{1}H NMR was identical to that of **121** prepared above (Section 7.2.1.12).

7.2.2 Synthesis of two-carbon disubstituted ligands

7.2.2.1 *rac*-1,2-Diphenyl-2-(3*H*-inden-1-yl)ethanol (125)

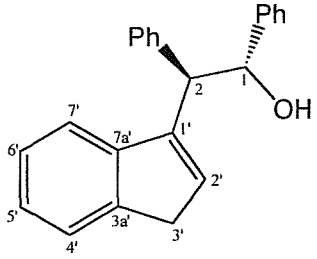

A solution of indene (1.2 eq, 60 mmol, 7.0 mL) in THF (70 mL), was cooled to –78 °C, and *n*-BuLi (2.3 M solution in hexanes, 1.2 eq, 60 mmol, 26.1 mL) added dropwise. The resulting yellow suspension was stirred for 15 minutes at –78 °C, before warming to room temperature and stirring for 2 h. The anion solution was then cooled to –5 °C and a solution of racemic *trans*-stilbene oxide (1.0 eq, 50 mmol, 9.81 g) in THF (20 mL) added dropwise. The reaction was stirred at 0 °C for 6 h, then warmed to room temperature and stirred for 16 h.

Saturated ammonium chloride solution (100 mL) was added to the reaction and the product extracted with ether (3 × 75 mL). The combined organic layers were then washed with brine (2 × 50 mL), dried over $MgSO_4$, and the solvents removed *in vacuo* to yield a yellow/brown solid. Column chromatography (15 % ethyl acetate/petrol) gave the title product **125** as a viscous yellow oil (9.37 g, 30.0 mmol, 60 %) which proved difficult to effectively dry for analysis.

^{1}H NMR (300 MHz, $CDCl_3$): δ 7.10-7.45 (14H, m, *ArH*), 6.65 (1H, br. s, *H2'*), 5.46 (1H, d, *J* = 6.6 Hz, *H1*), 4.40 (1H, d, *J* = 6.6 Hz, *H2*), 3.40 (2H, s, *H3'*), 2.10 (1H, br. s, *OH*) ppm.

^{13}C NMR (75 MHz, $CDCl_3$): δ 144.9 (C, *C1*), 144.1 (C), 144.0 (C), 142.9 (C), 138.5 (C), 130.2 (CH), 129.7 (2 × CH), 128.6 (2 × CH), 128.3 (2 × CH), 127.7 (CH), 127.4 (CH), 126.9 (2 × CH), 126.1 (CH), 124.7 (CH), 123.8 (CH) (*aromatic Cs*), 119.7 (CH, *C2'*), 76.2 (CH, *C1*), 52.4 (CH, *C2*), 38.3 (CH_2, *C3'*) ppm.

IR (CH_2Cl_2 solution): 3680 (m), 3588 (s, OH), 3053 (s), 2892 (m), 1702 (m), 1602 (s), 1493 (s), 1459 (s), 1394 (s), 1186 (m), 1067 (m), 1029 (s), 915 (w) cm^{-1}

LRMS (AP$^+$): *m/z* 295 ((M–OH)$^+$, 100 %), 217 ((M–OH–PhH)$^+$, 75), 206 (52).

Anal. Calcd. for $C_{23}H_{20}O$ + ⅓H_2O: C, 86.76; H, 6.54. Found: C, 86.59; H, 6.28.

7.2.2.2 *rac*-Methanesulfonic Acid 1,2-Diphenyl-2-(3*H*-inden-1-yl)ethyl Ester (126)

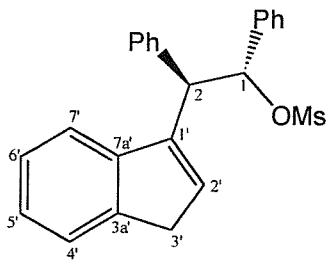

To a stirred solution of alcohol **125** (1.0 eq, 30 mmol, 9.37 g) in dichloromethane (150 mL) at –5 °C, was added triethylamine (2.5 eq, 75 mmol, 10.5 mL) and mesyl chloride (1.3 eq, 39 mmol, 3.0 mL) dropwise. Once addition was completed, a white precipitate had begun to form in the reaction mixture and this suspension was stirred for 3 h at –2 °C.

The suspension was then filtered, washed with water (1 × 80 mL) and brine (1 × 80 mL), then dried over $MgSO_4$ and concentrated *in vacuo*, to yield the crude product as a brown foam (11.99 g, ~100 %). No further purification was carried out and the crude material used immediately in the next step; formation of the spirocycle **127**. ^{1}H NMR of the crude (included below) clearly showed the mesylate had been formed with no trace of starting material present.

^{1}H NMR (300 MHz, $CDCl_3$, crude): δ 7.10-7.45 (14H, m, *ArH*), 6.51 (1H, br. s, *H2'*), 6.19 (1H, d, *J* = 9.1 Hz, *H1*), 4.61 (1H, d, *J* = 8.9 Hz, *H2*), 3.30 (2H, d, *J* = 9.9 Hz, *H3'*), 2.25 (3H, s, CH_3) ppm.

^{13}C NMR (75 MHz, $CDCl_3$, crude): δ 144.30 (C), 143.87 (C), 141.97 (C), 138.68 (C), 137.71 (C), 130.49 (CH), 129.63 (2 × CH), 129.28 (CH), 128.80 (2 × CH), 128.70 (2 × CH), 127.89 (2 × CH), 127.68 (CH), 126.14 (CH), 125.00 (CH), 123.84 (CH), 119.48 (CH, *C2'*), 86.70 (CH, *C1*), 50.16 (CH, *C2*), 38.60 (CH_3, *OMs*), 38.40 (CH_2, *C3'*).

LRMS (AP^+): *m/z* 390 ($(M)^+$, 100 %).

7.2.2.3 *rac*-Spiro-[(2,3-diphenylcyclopropane)-1,1´-indene] (127)

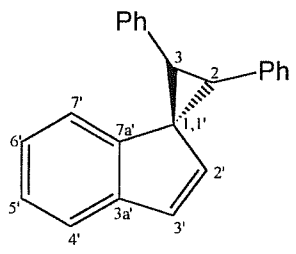

The crude mesylate **126** (1.0 eq, ~30 mmol, 11.72 g) was dissolved in THF (150 mL), and cooled to –78 °C. To this solution was added *n*-BuLi (2.5 M solution in hexanes, 1.1 eq, 33 mmol, 13.2 mL) dropwise, and the reaction warmed to room temperature, and stirred for 2 h.

The reaction was then quenched with water (50 mL), and diluted with diethyl ether (100 mL). The organic layer was then separated, washed with brine (1 × 50 mL), and dried over $MgSO_4$, then concentrated *in vacuo* to gave a dark solid. Purification was achieved by passing the crude material through a short silica gel column (100 % hexane), and subsequent recrystallisation from hot ethanol. The product spirocycle **127** was isolated as a white crystalline solid (6.29 g, 21.4 mmol, 71 %). Mp 106-108 °C. X-ray analysis confirmed the structure was as shown (see Appendix 4).

^{1}H NMR (300 MHz, $CDCl_3$): δ 7.21-7.39 (11H, m, *ArH*), 7.18 (1H, t, *J* = 7.4 Hz, *ArH*), 6.87 (1H, t, *J* = 7.4 Hz, *ArH*), 6.86 (1H, d, *J* = 5.2 Hz, *H2'/3'*), 6.25 (1H, d, *J* = 7.7 Hz, *deshielded H7'*), 6.13 (1H, d, *J* = 5.5 Hz, *H2'/3'*), 4.01 (1H, d, *J* = 7.9 Hz, *cyclopropane H2/3*), 3.72 (1H, d, *J* = 7.9 Hz, *cyclopropane H2/3*) ppm.
^{13}C NMR (75 MHz, $CDCl_3$): δ 144.0 (C), 143.8 (C), 139.1 (C), 137.7 (CH), 137.0 (C), 130.0 (2 × CH), 129.5 (CH), 128.6 (2 × CH), 128.5 (CH), 128.3 (2 × CH), 127.1 (2 × CH), 127.0 (CH), 125.6 (CH), 123.7 (CH) (*aromatic*), 121.4 (CH, *C2'/3'*) 120.6 (CH, *C2'/3'*), 46.8 (C, *C1,1'*), 37.8 (CH, *C2/3*), 35.7 (CH, *C2/3*) ppm.
IR (NaCl, thin film): 3058 (s), 3027 (s), 1602 (s), 1497 (s), 1447 (s), 1266 (m), 1195 (m), 1074 (m), 1028 (m), 990 (s) cm^{-1}.
LRMS (AP^+): *m/z* 295 ($(M+H)^+$, 100 %), 294 (M^+, 88), 217 ($(M-Ph)^+$, 63).
Anal. Calcd. for $C_{23}H_{18}$: C, 93.84; H, 6.16. Found: C, 93.47; H, 6.22.

7.2.2.4 Lithium *rac*-[1,2-Diphenyl-2-(3*H*-inden-1-yl)ethyl] diphenylphosphide (Li-128)

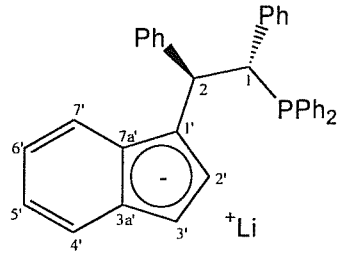

To a solution of diphenylphosphine (2.4 mmol, 0.42 mL) in THF (4.5 mL), at –40 °C, was added *n*-BuLi (2.4 mmol, 0.96 mL), and the reaction stirred at –40 °C for 15 minutes, then at 0 °C for 2 h. To the resulting dark red mixture, at 0 °C, was added a concentrated solution of 2,3-diphenylspiro<cyclopropane-1,1'-indene> **127** (2 mmol, 589 mg) in THF (0.5 mL). The reaction was stirred at 0 °C for 15 minutes, then at 20 °C for 72 h. After this time ^{1}H NMR of a small quantity of quenched material confirmed the ligand product **128** was

present, with only trace amounts of spirocycle **127** and diphenylphosphide starting materials.

Attempts to isolated the ligand, by quenching the reaction mixture, and performing column chromatography (under argon) failed to yield clean material, owing to the sensitivity of this ligand to air-oxidation. The crude ligand anion solution was therefore used directly in the complexation reaction with ruthenium (Section 4.2.3).

^{1}H NMR (300 MHz, $CDCl_3$, crude*): δ 7.37-7.74 (11H, m, *ArH*), 7.07-7.26 (11H, m, *ArH*), 7.01 (1H, d, J = 7.7 Hz, *ArH*), 6.94 (1H, d, J = 7.1 Hz, *ArH*), 6.34 (1H, t, J = 1.9 Hz, *H2'*), 5.31 (1H, dd, J_{HH} = 10.7 Hz, J_{PH} = 10.7 Hz, *H1*), 4.53 (1H, dd, J_{HH} = 10.5 Hz, J_{PH} = 6.5 Hz, *H2*), 2.74 (2H, dd, J = 6.8, 1.5 Hz, *H3'*) ppm.
LRMS (AP^+): *m/z* major (oxidised during analysis) 497 ($(M+O+H)^+$, 90 %), 481 ($(M+H)^+$, 10).

*-Note that the resonances for protons H2' and H3' display coupling not seen for the same protons in the spectra of the previous phosphine ligands **59** and **121**, however similar couplings were seen with the phosphine oxides of ligands **59** and **121**. It is likely therefore, that the above ligand has oxidised prior to the collection of the crude ^{1}H NMR data and thus the data reported above is that of the phosphine-oxide, rather than the free phosphine ligand. The mass spectrum is also in accordance with the phosphine oxide of this ligand.

7.3 Experimental for Chapter 3

7.3.1 Synthesis of the three-carbon tethered phosphine ligand

7.3.1.1 3-Cyclohexyl-acrylic acid (130)

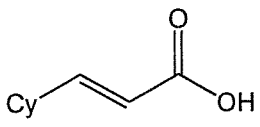

To a solution of malonic acid (41.6 g, 0.40 M) in pyridine (50.5 mL, 0.63 M), was added cyclohexanecarboxaldehyde (56.1 g, 0.50 M) and piperidine (cat. 3.2 mL, 32 mmol). The reaction was stirred for 72 h at room temperature, after which time the mixture was poured cautiously into cold H_2SO_4 (50 % solution, 150 mL). Diethyl ether (50 mL) was added, and the layers separated, then the product was extracted with diethyl ether (3 × 50 mL). The combined organics were washed with water (50 mL) and brine (50 mL), then dried over $MgSO_4$, and concentrated *in vacuo*, to give an off-white solid. Pure material was obtained by recrystallisation from ethanol, at 4 °C, to yield white crystals (54.6 g, 0.35 M, 89 %). ^{1}H NMR data were consistent with literature data.[103]

^{1}H NMR (300 MHz, $CDCl_3$): δ 7.05 (1H, dd, J = 15.8, 6.6 Hz), 5.77 (1H, d, J = 15.8 Hz), 2.11-2.26 (1H, m), 1.73-1.86 (4H, m), 1.64-1.73 (1H, m), 1.08-1.42 (5H, m) ppm.

7.3.1.2 3-Cyclohexyl-acrylic acid *tert*-butyl ester (131)

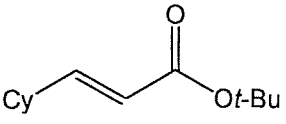

3-cyclohexyl-acrylic acid **130** (9.3 g, 60 mmol) was dissolved in dichloromethane (50 mL, dry), in a pressure-tube, and the mixture cooled to –20 °C. Excess isobutylene (13.5 g, ~240 mmol) was then added, followed by a catalytic amount concentrated sulphuric acid (6 drops), under counterflow of argon. The pressure-tube was then sealed, and allowed to warm to room temperature, in the dark. The reaction was stirred for 48 h, then cooled to –78 °C and opened. The flask was warmed to –15 °C and poured on saturated $NaHCO_3$ solution (40 mL).

The product was then extracted with dichloromethane (3 × 60 mL), which was then dried over $MgSO_4$, and concentrated *in vacuo* to yield a thick oil. Column chromatography (2.5

% ethyl acetate/petrol) gave the clean product **131** as a white solid (9.80 g, 47 mmol, 78 %). ^{1}H NMR data were consistent with literature values.[104]

^{1}H NMR (400 MHz, $CDCl_3$): δ 6.81 (1H, dd, J = 15.7, 6.6 Hz), 5.68 (1H, dd, 15.7, 1.4 Hz), 2.06-2.15 (1H, m), 1.72-1.80 (4H, m), 1.63-1.71 (1H, m), 1.48 (9H, s), 1.08-1.36 (5H, m) ppm.

^{13}C NMR (100 MHz, $CDCl_3$): δ 166.97 (C), 153.43 (CH), 120.97 (CH), 80.34 (C), 40.67 (CH), 32.18 (2 × CH_2), 28.57 (3 × CH_3), 26.38 (CH_2), 26.17 (2 × CH_2) ppm.

7.3.1.3 *rac*-3-Cyclohexyl-3-(3H-inden-1-yl)-propionic acid *tert*-butyl ester (132)

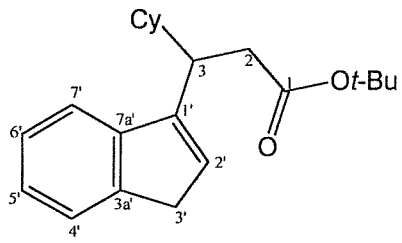

To a well stirred solution of indene (14 mL, 120 mmol) and 3-cyclohexyl-acrylic acid *tert*-butyl ester **131** (8.4 g, 40 mmol) in THF (200 mL) under argon, was added *sec*-BuLi (1.4 M solution in cyclohexane, 34 mL, 48 mmol), dropwise *via* canula, over 10-12 minutes, at room temperature. During this exothermic reaction, the internal temperature was maintained within the range 15 °C to 25 °C, by cooling the reaction flask in ice-water. GC monitoring indicated complete consumption of starting material **131** five minutes after addition of the base. The reaction was quenched with water (80 mL), then diethyl ether (80 mL) added and the organics separated. The aqueous phase was extracted with diethyl ether (3 × 80 mL) and the combined organics were then washed with brine (30 mL), dried over $MgSO_4$ and concentrated *in vacuo* to give *ca.* 99 % conversion (by ^{1}H NMR) to the expected 1,4-addition product. The crude mixture (~20 g, still containing excess indene) was used without further purification in the reduction to alcohol **133** below (Section 7.3.1.5).

On a 5 mmol (scaled-down) reaction, the title compound was isolated from the crude mixture by first applying high vacuum (0.05 mmHg) to remove excess indene, then performing flash column chromatography (3 % diethyl ether/petrol) to yield a white solid (1.39 g, 4.3 mmol, 85 %). Recrystallisation from ethanol at –20 °C gave analytically pure white crystals. Mp 47-49 °C.

^{1}H NMR (400 MHz, $CDCl_3$): δ 7.45 (1H, d, *J* = 6.5 Hz, *H7'/ 4'*), 7.43 (1H, d, *J* = 7.0 Hz, *H7'/4'*), 7.29 (1H, t, *J* = 7.5 Hz, *H5'/6'*), 7.19 (1H, t, *J* = 7.5 Hz, *H5'/6'*), 6.21 (1H, br. s, *H2'*), 3.33 (2H, br. s, *H3'*), 3.14 (1H, dt, *J* = 9.9, 5.7 Hz, *H3*), 2.68 (1H, dd, *J* = 14.9, 5.7 Hz, *H2-a*), 2.55 (1H, dd, *J* = 14.9, 9.9 Hz, *H2-b*), 1.56-1.83 (5H, m, *Cy-ring*), 1.25 (9H, s, *t-Bu*), 0.84-1.23 (6H, m, *Cy-ring*) ppm.

^{13}C NMR (100 MHz, $CDCl_3$): δ 172.66 (C, *C1*), 146.50 (C, *C1'/3a'/7a'*), 145.84 (C, *C1'/3a'/7a'*), 144.56 (C, *C1'/3a'/7a'*), 128.74 (CH, *C4'/5'/6'/7'*), 126.08 (CH, *C4'/5'/6'/7'*), 124.63 (CH, *C4'/5'/6'/7'*), 123.89 (CH, *C4'/5'/6'/7'*), 119.95 (CH, *C2'*), 80.19 (C, *t-Bu*), 41.81 (CH, *C3/Cy*), 40.57 (CH, *C3/Cy*), 38.29 (CH_2, *C2*), 37.95 (CH_2, *C3'*), 31.41 (CH_2, *Cy*), 30.66 (CH_2, *Cy*), 28.09 (3 × CH_2, *t-Bu*), 26.83 (2 × CH_2, *Cy*), 26.73 (CH_2, *Cy*) ppm.

IR (NaCl, thin film): 2975 (m), 2926 (s), 2851 (m), 1729 (s), 1450 (m), 1392 (m), 1367 (m), 1257 (m), 1150 (s), 972 (w), 951 (w), 848 (w), 769 (s), 720 (m) cm^{-1}.

Anal. Calcd. for $C_{22}H_{30}O_2$: C, 80.94; H, 9.26. Found: C, 80.84; H, 9.35.

During the initial development of this synthesis the by-product dimer **135** was formed preferentially to the 1,4-addition product **132**, therefore it's preparation and spectroscopic properties are described below (Section 7.3.1.4).

7.3.1.4 *rac*-3-Cyclohexyl-2-[cyclohexyl-(3H-inden-1-yl)-methyl]-pentanedioic acid di-*tert*-butyl ester (135)

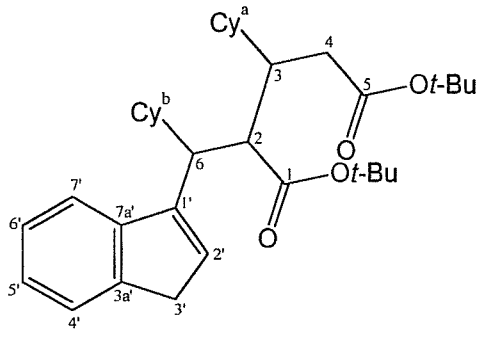

To a stirred solution of indene (0.13 mL, 1.1 mmol) in THF (2.5 mL), at –78 °C, was added *n*-BuLi (2.5 M solution in hexanes, 0.44 mL, 1.1 mmol), dropwise. The reaction was then stirred at –78 °C for 15 minutes and at room temperature for 2 h. After this time the indenyl anion solution was cooled to –78 °C and to this was added a THF (5 mL) solution of 3-cyclohexyl-acrylic acid *tert*-butyl ester **131** (210 mg, 1.0 mmol), dropwise. The mixture was stirred at –78 °C for 15 minutes, then at room temperature for 16 h.

After this time, crude ^{1}H NMR, indicated a 5 : 3 ratio of double-addition **135** to mono-addition **132** products formed from the reaction. The reaction was quenched with water

(10 mL) and extracted with diethyl ether (3 × 20 mL). The combined organics were then dried over $MgSO_4$, and concentrated *in vacuo*. Purification of the double-addition product **135** was achieved by column chromatography (3 % diethyl ether/petrol), to give a yellow oil (144 mg, 0.27 mmol, 24 %) which crystallised on cooling, mp 114-116 °C. X-ray structure analysis was used to confirm the structure and relative stereochemistry of **135** (see Appendix 5).

^{1}H NMR (400 MHz, $CDCl_3$): δ 7.47 (1H, d, *J* = 7.5 Hz, *H7'/4'*), 7.41 (1H, d, *J* = 7.3 Hz, *H7'/4'*), 7.28 (1H, td, *J* = 7.5, 0.9 Hz, *H6'/5'*), 7.17 (1H, td, *J* = 7.3, 1.0 Hz, *H6'/5'*), 6.25 (1H, t, *J* = 2.1 Hz, *H2'*), 3.38 (1H, dd, *J* = 23.2, 1.9 Hz, *H3'-a*), 3.30 (1H, dd, *J* = 11.5, 4.2 Hz, *H2-a*), 3.24 (1H, dd, *J* = 23.3, 2.0 Hz, *H3'-b*), 3.00 (1H, dd, *J* = 11.6, 4.3 Hz, *H2-b*), 2.40 (1H, dd, *J* = 15.9, 8.7 Hz, *H4/6*), 2.33 (1H, dd, *J* = 15.8, 5.5 Hz, *H4/6*), 2.25-2.28 (1H, m, *H3*), 1.53-1.84 (9H, m, *Cy-rings*), 1.47 (9H, s, *t-Bu*), 1.09-1.44 (7H, m, *Cy-rings*), 1.05 (9H, s, *t-Bu*), 0.79-1.03 (6H, m, *Cy-rings*) ppm.

^{13}C NMR (75 MHz, $CDCl_3$): δ 173.43 (C, *C1/5*), 173.11 (C, *C1/5*), 147.50 (C, *C1'/3a'/7a'*), 145.15 (C, *C1'/3a'/7a'*), 143.64 (C, *C1'/3a'/7a'*), 130.24 (CH, v. br., *C4'/5'/6'/7'*), 125.96 (CH, *C4'/5'/6'/7'*), 124.41 (CH, *C4'/5'/6'/7'*), 123.56 (CH, *C4'/5'/6'/7'*), 120.19 (CH, v. br., *C2'*), 80.26 (C, *t-Bu*), 80.17 (C, *t-Bu*), 50.85 (CH, *C2*), 40.74 (CH_2, v. br., *C3'*), 39.45 (CH, *C6/3*), 39.07 (CH, *C6/3*), 38.06 (CH_2, *C4*), 37.05 (2 × CH, *Cy*), 35.60 (CH_2, *Cy*), 34.43 (CH_2, *Cy*), 33.32 (CH_2, *Cy*), 28.95 (CH_2, *Cy*), 28.35 (3 × CH_3, *t-Bu*), 27.71 (3 × CH_3, *t-Bu*), 27.54 (CH_2, *Cy*), 27.33 (CH_2, *Cy*), 26.94 (CH_2, *Cy*), 26.76 (CH_2, *Cy*), 26.65 (CH_2, *Cy*), 26.60 (CH_2, *Cy*) ppm.

IR (NaCl, thin film): 2975 (s), 2925 (s), 2951 (s), 1727 (s), 1450 (m), 1391 (m), 1366 (s), 1304 (m), 1246 (m), 1151 (s), 849 (m), 771 (m), 738 (m), 721 (m) cm^{-1}.

LRMS (AP^+): *m/z* 425 ($(M+2H-2t\text{-}Bu)^+$, 25 %), 407 ($(M+H-Ot\text{-}Bu-t\text{-}Bu)^+$, 100), 389 ($(M-2Ot\text{-}Bu)^+$, 33).

HRMS (EI^+): $C_{35}H_{52}O_4$ requires *m/z* 536.38656, found *m/z* 536.38675.

Anal. Calcd. for $C_{35}H_{52}O_4$: C, 78.31; H, 9.76. Found: C, 77.86; H, 9.77.

7.3.1.5 *rac*-3-(3*H*-Inden-1-yl)-3-cyclohexylpropanol (133)

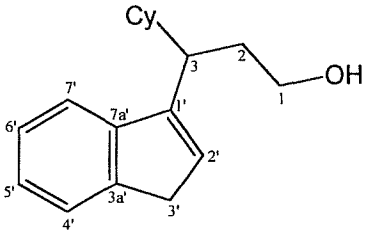

Crude *rac*-3-cyclohexyl-3-(3H-inden-1-yl)-propionic acid *tert*-butyl ester **132** (~40 mmol), still containing excess indene from the previous 1,4-addition reaction (Section 7.3.1.3) was dissolved in diethyl ether (165 mL) and added carefully, *via* canula, to a solution of lithium aluminium hydride (4.6 g, 120 mmol) in diethyl ether (220 mL) at 0 °C, under argon. After the addition was complete, the reaction was warmed to room temperature and stirred for 3.5 h. Complete consumption of the starting ester **132** had occurred after this time, so the mixture was cooled to 0 °C and water (5 mL) added very cautiously (vigorous evolution of hydrogen gas). Sodium hydroxide (15 % aqueous solution, 5 mL) was then added slowly, followed by further water (15.1 mL). The dark coloured quenched mixture was stirred at room temperature for 30 minutes, resulting in a pale yellow suspension. The suspension was filtered through celite (washed through with diethyl ether), then dried over $MgSO_4$ and concentrated *in vacuo*, to give a clear oil (10.5 g, ~102 % crude).
Purification was achieved by flash chromatography (40 % diethyl ether/petrol) to yield a pale yellow oil, which solidified on standing (8.62 g, 34 mmol, 84 %). Recrystallisation of **133** from hot hexane gave analytically pure white crystals. Mp 62-63 °C.

^{1}H NMR (400 MHz, $CDCl_3$): δ 7.48 (1H, d, *J* = 7.5 Hz, *H4'/7'*), 7.43 (1H, d, *J* = 7.5 Hz, *H7'/4'*), 7.30 (1H, t, *J* = 7.4 Hz, *H5'/6'*), 7.21 (1H, t, *J* = 7.3 Hz, *H6'/5'*), 6.22 (1H, br. s, *H2'*), 3.59 (1H, dd, *J* = 7.2, 5.1 Hz, *H1-a*), 3.53 (1H, dd, *J* = 9.0, 7.2 Hz, *H1-b*), 3.37 (2H, br. s, *H3'*), 2.70 (1H, ddd, *J* = 11.0, 6.8, 4.0 Hz, *H3*), 2.05 (1H, ddt, *J* = 13.3, 7.7, 3.9 Hz, *H2-a*), 1.86-1.99 (2H, m, *Cy* + *H2-b*), 1.59-1.79 (5H, m, *Cy*), 1.33 (1H, br. s, *OH*), 0.85-1.25 (5H, m, *Cy*) ppm.
^{13}C NMR (100 MHz, $CDCl_3$): δ 146.59 (C, *C7a'/3a'/1'*), 145.70 (C, *C7a'/3a'/1'*), 144.99 (C, *C7a'/3a'/1'*), 129.05 (CH, *C7'/6'/5'/4'*), 126.13 (CH, *C7'/6'/5'/4'*), 124.74 (CH, *C7'/6'/5'/4'*), 124.08 (CH, *C7'/6'/5'/4'*), 119.95 (CH, *C2'*), 62.15 (CH_2, *C1*), 41.64 (CH, *C3/Cy*), 41.18 (CH, *C3/Cy*), 37.93 (CH_2, *C3'*), 33.91 (CH_2, *C2*), 31.57 (CH_2, *Cy*), 30.95 (CH_2, *Cy*), 26.85 (CH_2, *Cy*), 26.83 (2 × CH_2, *Cy*) ppm.
IR (NaCl, thin film): 3334 (br), 2924 (s), 2850 (m), 1449 (m), 1395 (w), 1055 (m), 1039 (m), 1019 (m), 968 (w), 769 (m), 720 (m) cm^{-1}.

LRMS (AP$^+$): *m/z* 239 ((M–OH)$^+$, 10 %), 212 ((M–C_2H_4OH+H)$^+$, 7), 157 ((M–Cy–OH+H)$^+$, 10), 130 ((M–Cy–C_2H_4OH+H)$^+$, 10), 116 ((M–CH(Cy)C_2H_4OH+H)$^+$, 100).
Anal. Calcd. for $C_{18}H_{24}O$: C, 84.32; H, 9.43. Found: C, 84.34; H, 9.54.

7.3.1.6 *rac*-Trifluro-methanesulfonic Acid 3-Cyclohexyl-3-(3*H*-inden-1-yl)-propyl Ester (134)

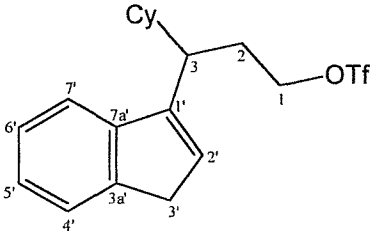

To a stirred solution of triflic anhydride (3.9 mL, 23 mmol) in dichloromethane (40 mL) at 0 °C, under argon, was added a solution of *rac*-3-(3*H*-inden-1-yl)-3-cyclohexylpropanol **133** (5.1 g, 20 mmol) and pyridine (1.8 mL, 22 mmol) in dichloromethane (5 mL), slowly. The reaction was stirred at 0 °C for 30 minutes, after which time TLC indicated complete consumption of starting material (note: this product is unstable on silica TLC plates, and hydrolyses back to the starting material if the TLC plate is not run immediately). The reaction was quenched with water (25 mL), then dichloromethane (25 mL) added, and the organics extracted into dichloromethane (2 × 25 mL). The combined organics were dried over $MgSO_4$ and concentrated *in vacuo*, to give the crude product **134** as a pale-green oil (7.0 g, 18 mmol, 90 % crude).
No further purification was attempted, as this intermediate was found to be unstable to silica chromatography, and was found to be unstable to storage at –20 °C for more than 72 h. It was also found that solutions of this crude reactive intermediate in THF were unstable, forming a solid polymeric material on standing for more than 20 minutes at room temperature (presumably owing to the action of trace triflic acid on the solvent).

^{1}H NMR (400 MHz, $CDCl_3$): δ 7.50 (1H, d, *J* = 7.3 Hz, *H4'/7'*), 7.39 (1H, d, *J* = 7.3 Hz, *H7'/4'*), 7.31 (1H, t, *J* = 7.2 Hz, *H5'*), 7.24 (1H, td, *J* = 7.3, 1.1 Hz, *H6'*), 6.25 (1H, br. s, *H2'*), 4.52 (1H, ddd, *J* = 9.8, 7.5, 4.3 Hz, *H1-a*), 4.39 (1H, ddd, *J* = 9.2, 9.2, 6.8 Hz, *H1-b*), 3.40 (2H, br. s, *H3'*), 2.72 (1H, ddd, *J* = 11.4, 7.2, 3.7 Hz, *H3*), 2.34 (1H, ddd, *J* = 14.1, 8.0, 3.5 Hz, *H2-a*), 2.18 (1H, dddd, *J* = 14.0, 11.5, 6.8, 4.5 Hz, *H2-b*), 1.89 (1H, br. d, *J* = 12.8 Hz, *Cy*), 1.76 (1H, br. d, *J* = 12.8 Hz, *Cy*), 1.54-1.73 (4H, m, *Cy*), 0.87-1.29 (5H, m, *Cy*) ppm.

^{13}C NMR (100 MHz, $CDCl_3$): δ 145.02 (C, *C7a'/3a'/1'*), 144.77 (C, *C7a'/3a'/1'*), 144.71 (C, *C7a'/3a'/1'*), 130.14 (CH, *C7'/6'/5'/4'*), 126.29 (CH, *C7'/6'/5'/4'*), 125.13 (CH, *C7'/6'/5'/4'*), 124.30 (CH, *C7'/6'/5'/4'*), 119.84 (CH, *C2'*), 77.02 (CH_2, *C1*), 41.30 (CH, *C3/Cy*), 40.85 (CH, *C3/Cy*), 38.03 (CH_2, *C3'*), 31.51 (CH_2, *Cy*), 30.81 (CH_2, *Cy*), 30.56 (CH_2, *C2*), 26.67 (CH_2, *Cy*), 26.66 (CH_2, *Cy*), 26.65 (CH_2, *Cy*) ppm.

7.3.1.7 *rac*-[3-Cyclohexyl-3-(3*H*-inden-1-yl)propyl]-diphenyl-phosphine (129)

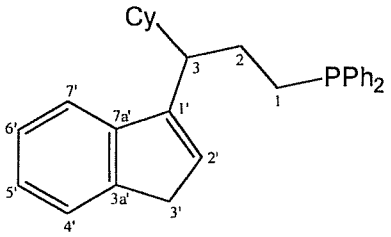

To a cold (–40 °C) solution of diphenylphosphine (1.0 mL, 6.0 mmol) in diethyl ether (17 mL), was added *n*-BuLi (2.5 M solution in hexanes, 2.2 mL, 5.5 mmol), under argon. The reaction was stirred at –40 °C for 15 minutes, then at 20 °C for 2 h. The resulting yellow suspension was then cooled to –5 °C and a solution of *rac*-trifluro-methanesulfonic acid 3-cyclohexyl-3-(3*H*-inden-1-yl)-propyl ester **134** (1.9 g, 5.0 mmol), in diethyl ether (3 mL), added dropwise – causing the suspension to clear. The reaction was stirred for 15 minutes at –5 °C, then 18 h at 20 °C. After this time, the reaction was quenched with degassed ethanol (2 mL), and concentrated *in vacuo*, to give a yellow air-sensitive oil. Purification of the ligand **129** was achieved by first filtering the mixture through a pad of silica (eluting with diethyl ether), followed by column chromatography under argon (0-2.5 % ethyl acetate/petrol) to yield a pale yellow oil which partially solidified on storage at –20 °C (1.81 g, 4.3 mmol, 85 %). (note: column fractions were kept under argon whenever possible; on exposure to air these solutions rapidly clouded as the ligand oxidised).

^{1}H NMR (400 MHz, $CDCl_3$): δ 7.47 (1H, d, J = 7.2 Hz, *H4/7*), 7.23-7.37 (12H, m, *Ar*), 7.19 (1H, t, J = 7.2 Hz, *H5/6*), 6.07 (1H, br.s, *H2*), 3.35 (2H, br.s, *H3*), 2.63-2.70 (1H, m, *H8*), 1.99-2.06 (1H, m, *Cy/H9/H10*), 1.72-1.94 (4H, m, *Cy/H9/H10*), 1.52-1.71 (5H, m, *Cy/H9/H10*), 0.83-1.20 (5H, m, *Cy/H9/H10*) ppm.

^{13}C NMR (100 MHz, $CDCl_3$): δ 146.22 (C, s, *C1*), 145.97 (C, s, *C3a/7a*), 144.97 (C, s, *C3a/7a*), 139.45 (C, d, J = 12.6 Hz, *i-Ph*), 138.57 (C, d, J = 12.9 Hz, *i-Ph*), 133.29 (2 × CH, J = 18.5 Hz, *o-Ph*), 132.59 (2 × CH, d, J = 17.7 Hz, *o-Ph*), 129.18 (CH, s, *C2*), 128.82 (CH, s, *p-Ph*), 128.54 (2 × CH, d, J = 6.6 Hz, *m-Ph*), 128.50 (2 × CH, d, J = 6.3

Hz, *m-Ph*), 128.44 (CH, s, *p-Ph*), 126.07 (CH, s, *5/6*), 124.59 (CH, s, *5/6*), 123.99 (CH, s, *4/7*), 119.99 (CH, s, *4/7*), 46.15 (CH, d, J = 12.4 Hz, *C8*), 41.56 (CH, s, *Cy*), 37.93 (CH_2, s, *C3*), 31.50 (CH_2, s, *Cy*), 30.93 (CH_2, s, *Cy*), 27.03 (CH_2, d, J = 17.3 Hz, *C10*), 26.85 (CH_2, s, *Cy*), 26.81 (2 × CH_2, s, *Cy*), 26.47 (CH_2, d, J = 10.4 Hz, *C9*) ppm.

^{31}P NMR (121 MHz, $CDCl_3$): δ –14.96 (s) ppm.

IR (NaCl, thin film): 3053 (w), 2923 (s), 2849 (m), 1706 (w), 1448 (m), 1436 (s), 1262 (w), 1183 (m), 1119 (m), 1026 (w), 770 (m), 739 (s), 720 (s), 696 (s).

LRMS (AP^+): *m/z* 425 ($(M+H)^+$, 100 %), 441 ($(M+O+H)^+$, 8), 466 ($(M+MeCN+H)^+$, 25).

Anal. determined for BH_3 derivative **139** (Section 7.3.1.8)

7.3.1.8 *rac*-[3-Cyclohexyl-3-(3*H*-inden-1-yl)propyl]-diphenyl-phosphine-Borane Complex (139)

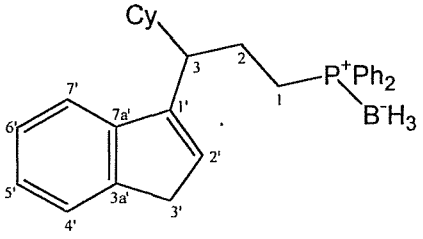

A solution of *rac*-[3-Cyclohexyl-3-(3*H*-inden-1-yl)propyl]diphenyl-phosphane **129** (424 mg, 1.0 mmol) was prepared in THF (20 mL) under argon, and cooled to 0 °C. A solution of borane-methyl sulphide complex (0.22 mL, 1.2 mmol) in THF (1.2 mL) was then added dropwise to the phosphine ligand and the reaction mixture stirred at 0 °C for 30 min before quenching at 0 °C, by addition of ice-water (10 mL). The product was extracted into ethyl acetate (4 × 20 mL), then the combined organic layers washed with brine (20 mL), dried over $MgSO_4$ and concentrated *in vacuo*.

Purification was achieved by column chromatography (2.5 % ethyl acetate/petrol), to provide the title compound **139** as a white solid (260 mg, 0.59 mmol, 59 %). Recrystallisation from hexane at 5 °C gave white crystals, mp 105-108 °C.

^{1}H NMR (300 MHz, $CDCl_3$): δ 7.45-7.62 (7H, m, *Ar*), 7.34-7.44 (4H, m, *Ar*), 7.21-7.33 (3H, m, *Ar*), 6.12 (1H, v.br.t, J = 1.8 Hz, *H2*), 3.47 (2H, v.br.d, J = 1.3 Hz, *H3*), 2.63 (1H, ddd, J = 9.8, 7.0, 3.6 Hz, *H8*), 1.52-2.35 (10H, m, *Cy+BH$_3$+H9+H10*), 0.84-1.38 (8H, m, *Cy*) ppm.

^{13}C NMR (75 MHz, $CDCl_3$): δ 145.62 (C, s, *C1*), 145.52 (C, s, *C3a/7a*), 144.88 (C, s, *C3a/7a*), 132.45 (2 × CH, d, J = 9.0 Hz, *o-Ph*), 132.07 (2 × CH, d, J = 8.9 Hz, *o-Ph*),

131.31 (C, d, J = 2.5 Hz, *i-Ph*), 131.15 (C, d, J = 2.4 Hz, *i-Ph*), 129.52 (CH, s, *C2*), 128.96 (2 × CH, s, *m-Ph*), 128.83 (2 × CH, s, *m-Ph*), 126.14 (CH, s, *C5/6*), 124.76 (CH, s, *C5/6*), 124.06 (CH, s, *C4/7*), 119.87 (CH, s, *C4/7*), 45.88 (CH, d, J = 12.7 Hz, *C8*), 41.57 (CH, s, *Cy*), 37.97 (CH_2, s, *C3*), 31.38 (CH_2, s, *Cy*), 30.77 (CH_2, s, *Cy*), 26.74 (CH_2, s, *C9*), 26.69 (CH_2, s, *Cy*), 26.64 (CH_2, s, *Cy*), 24.02 (CH_2, d, J = 37.4 Hz, *C10*), 23.98 (CH_2, s, *Cy*) ppm. Note: 2×para-Ph CH carbons (*ca.* 128.8 ppm) could not be unambiguously distinguished from baseline noise, owing to broadening of their signals in this compound.

^{31}P NMR (121 MHz, $CDCl_3$): δ 16.57 (br. s) ppm.

IR (NaCl, thin film): 3078 (m), 3056 (m), 3017 (w), 2924 (s), 2850 (m), 2380 (s), 2335 (m), 1484 (w), 1449 (m), 1437 (s), 1389 (w), 1264 (m), 1108 (m), 1061 (s), 1025 (m), 973 (w), 772 (s), 736 (s), 693 (s) cm^{-1}.

Anal. Calcd. for $C_{30}H_{36}BP$: C, 82.19; H, 8.28. Found: C, 82.47; H, 8.57.

7.3.1.9 *rac*-Spiro-[(2-cyclohexylcyclobutane)-1,1′-indene] (138)

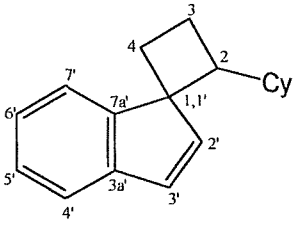

A solution of *rac*-trifluro-methanesulfonic acid 3-cyclohexyl-3-(3*H*-inden-1-yl)-propyl ester **137** (172 mg, 0.44 mmol), in THF (5 mL), was cooled to –78 °C and treated with *n*-BuLi (2.5 M solution in hexanes, 0.21 mL, 0.53 mmol). The reaction was then warmed to room temperature and stirred for 2 h. Water (10 mL) was added to quench the reaction, and the product extracted with hexane (3 × 10 mL). The combined organics were dried over $MgSO_4$ and concentrated *in vacuo* to give the crude as an off-white solid. Crude ^{1}H NMR showed the spirocycle had formed as a 7 : 3 mixture of diastereoisomers. Column chromatography (100 % petrol) provided the product as a white solid, and 7 : 3 mixture of isomers (77 mg, 0.32 mmol, 73 %).

^{1}H NMR (note: complicated by 7 : 3 mixture of diastereoisomers – only clearly identifiable major and minor resonances identified, 400 MHz, $CDCl_3$): δ 7.65 ('1H' *minor*, dd, J = 7.1, 0.9 Hz, *ArH*), 7.43-7.49 (1H, m, *ArH*), 7.17-7.65 (3H, m, *ArH's*), 6.86 (1H, d, J = 5.5 Hz, *major H2'/3'*), 6.74 (1H, d, J = 5.6 Hz, *major H2'/3'*), 6.55 ('1H' *minor*, d, J = 5.4 Hz, *minor H2'/3'*), 6.39 ('1H' *minor*, d, J = 5.4 Hz, *minor H2'/3'*), 1.90-

2.67 (4H, m, *cyclobutyl-ring*), 0.54-1.72 (11H, m, *Cy*), 0.16-0.42 (1H, m, *cyclobutyl-ring*) ppm.

^{13}C NMR (major isomer – all resonances clearly identified from the spectrum of the 7 : 3 mixture, 100 MHz, $CDCl_3$): δ 150.7 (C), 143.05 (C), 140.37 (CH), 129.70 (CH), 126.58 (CH), 125.12 (CH), 121.69 (CH), 120.99 (CH), 58.98 (C), 49.68 (CH), 42.83 (CH), 30.53 (CH_2), 30.09 (CH_2), 27.03 (CH_2), 26.79 (CH_2), 26.21 (CH_2), 25.85 (CH_2), 22.74 (CH_2) ppm.

^{13}C NMR (minor isomer – all resonances clearly identified from the spectrum of the 7 : 3 mixture, 100 MHz, $CDCl_3$): δ 149.27 (C), 145.32 (CH), 144.28 (C), 128.19 (CH), 126.46 (CH), 124.66 (CH), 122.98 (CH), 121.18 (CH), 58.66 (C), 47.26 (CH), 40.90 (CH), 30.13 (CH_2), 29.56 (CH_2), 26.79 (CH_2), 26.60 (CH_2), 26.04 (CH_2), 25.60 (CH_2), 24.06 (CH_2) ppm.

IR (NaCl, thin film): 3059 (w), 2922 (s), 2850 (m), 1457 (m), 1447 (m), 778 (m), 748 (m), 730 (w) cm^{-1}.

LRMS (AP^+): *m/z* 238 ($(M)^+$, 19 %), 155 ($(M–Cy)^+$, 100).

7.3.2 Synthesis of three-carbon tethered sulphur ligand

7.3.2.1 *rac*-3-(1-Cyclohexyl-3-methylsulfany-propyl)-1H-indene (141)

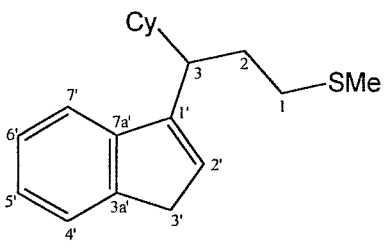

To a cold (–78 °C) solution of dimethyl disulphide (0.18 mL, 2.0 mmol) in THF (7 mL), was added *n*-BuLi (2.5 M solution in hexanes, 0.75 mL, 1.9 mmol), dropwise. The solution was stirred at –78 °C for 15 minutes, then at room temperature for 1 h, forming a white suspension. This suspension was cooled to –78 °C and a solution of crude *rac*-trifluro-methanesulfonic acid 3-cyclohexyl-3-(3*H*-inden-1-yl)-propyl ester **134** (486 mg, 1.25 mmol) in THF (3 mL) prepared and added to the cold anion solution. The reaction was then stirred at –78 °C for 15 minutes, and room temperature for 16 h.

After this time, water (10 mL) was added to quench the pale yellow reaction mixture, and the product extracted with diethyl ether (3 × 10 mL). The combined organics were washed with brine (10 mL), then dried over $MgSO_4$, and concentrated *in vacuo*.

Purification of the product was achieved by column chromatography (2.5 % ethyl acetate/petrol), to yield a light orange oil (284 mg, 1.0 mmol, 79 %).

^{1}H NMR (400 MHz, $CDCl_3$): δ 7.48 (1H, d, *J* = 7.3 Hz, *H4'/7'*), 7.43 (1H, d, *J* = 7.5 Hz, *H7'/4'*), 7.30 (1H, t, *J* = 7.4 Hz, *H5'/6'*), 7.21 (1H, t, *J* = 7.4 Hz, *H6'/5'*), 6.21 (1H, s, *H2'*), 3.38 (2H, s, *H3'*), 2.71 (1H, ddd, *J* = 10.4, 6.3, 4.3 Hz, *H3*), 2.47 (1H, ddd, *J* = 12.7, 9.2, 5.1 Hz, *H2-a*), 2.33 (1H, ddd, *J* = 12.7, 9.3, 6.9 Hz, *H2-b*), 2.05 (3H, s, *SMe*), 1.89-2.05 (2H, m, *H1-a & H1-b*), 1.56-1.71 (5H, m, *Cy*), 0.92-1.26 (6H, m, *Cy*) ppm.
^{13}C NMR (100 MHz, $CDCl_3$): δ 146.25 (C, *C7a'/3a'/1'*), 145.84 (C, *C7a'/3a'/1'*), 144.97 (C, *C7a'/3a'/1'*), 129.07 (CH, *C2'*), 126.11 (CH, *C5'/6'*), 124.67 (CH, *C6'/5'*), 124.03 (CH, *C4'/7'*), 119.92 (CH, *C7'/4'*), 43.90 (CH, *C3/Cy*), 41.61 (CH, *Cy/C3*), 37.95 (CH_2, *C3'*), 33.09 (CH_2, *C2*), 31.57 (CH_2, *Cy*), 30.98 (CH_2, *Cy*), 30.52 (CH_2, *C1*), 26.85 (CH_2, *Cy*), 26.82 (2 × CH_2, *Cy*), 15.72 (CH_3, *SMe*) ppm.
IR (NaCl, thin film): 2922 (s), 2850 (m), 1448 (m), 1394 (w), 968 (w), 769 (m), 720 (m) cm^{-1}.
LRMS (AP^+): *m/z* 287 ($(M+H)^+$, 100 %).
HRMS (EI^+): $C_{19}H_{26}S$ requires *m/z* 286.17552, found *m/z* 286.17544.

7.3.3 Synthesis of axially-chiral indenyl-naphthalene phosphine ligand

7.3.3.1 *rac*-[1-(2-Methyl-1H-inden-3-yl)-naphthalen-2-ylmethyl]diphenyl-phosphine (145)

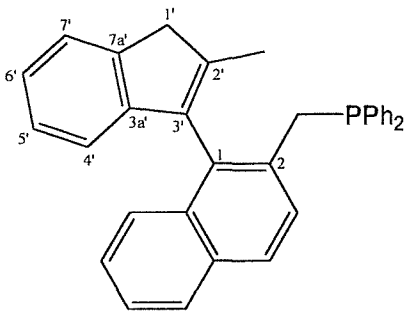

A solution of *rac*-2-chloromethyl-1-(2-Methyl-1H-inden-3-yl)-naphthalene **144** (0.91 g, 3.0 mmol, provided by Rob Baker (University of Sydney, Australia)) was prepared in THF (12 mL), and cooled to –78 °C, under argon. This was then treated with potassium diphenylphosphide (0.5 M solution in THF, 6.6 mL, 3.3 mmol), dropwise, and the reaction stirred at –78 °C for 15 minutes, then at room temperature for 16 h. After this time, degassed water (1.0 M solution in THF, 3.5 mL, 3.5 mmol) was added to quench the reaction, and the solvents removed by vacuum transfer. The resulting crude material was purified by column chromatography (2.5 %

ethyl acetate/petrol) under argon, using degassed solvents, to provide the title compound **145** as a white, air-sensitive solid (559 mg, 1.2 mmol, 41 %), mp 115-118 °C.

^{1}H NMR (400 MHz, $CDCl_3$): δ 7.84 (1H, d, J = 8.0 Hz), 7.71 (1H, d, J = 8.5 Hz), 7.58 (1H, d, J = 8.4 Hz), 7.51 (1H, d, J = 7.2 Hz), 7.42 (1H, t, J = 7.5 Hz), 7.32 (3H, t, J = 8.3 Hz), 7.15-7.29 (10H, m), 7.13 (1H, t, J = 7.0 Hz), 6.70 (1H, d, J = 7.2 Hz), 3.63 (1H, d, J = 22.6 Hz), 3.53 (1H, d, J = 22.6 Hz), 3.51 (1H, d, J = 13.4 Hz), 3.45 (1H, dd, J = 13.6, 2.8 Hz), 1.84 (3H, s) ppm.

^{13}C NMR (100 MHz, $CDCl_3$): δ 147.29 (C, s), 144.01 (C, s), 142.69 (C, s), 139.35 (C, d, J = 16.8 Hz), 138.86 (C, d, J = 16.8 Hz), 136.51 (C, s), 135.10 (C, d, J = 9.2 Hz), 134.22 (C, d, J = 16.8 Hz), 133.40 (2 × CH, d, J = 19.4 Hz), 132.79 (2 × CH, d, J = 18.7 Hz), 132.78 (C, d, J = 1.7 Hz), 132.55 (C, d, J = 2.2 Hz), 131.80 (CH, d, J = 5.3 Hz), 128.84 (CH, s), 128.55 (2 × CH, d, J = 6.3 Hz), 128.51 (2 × CH, d, J = 6.8 Hz), 128.41 (CH, s), 128.24 (CH, s), 127.64 (CH, s), 126.58 (CH, s), 126.29 (CH, s), 126.16 (CH, s), 125.35 (CH, s), 124.18 (CH, s), 123.51 (CH, s), 120.06 (CH, s), 43.12 (CH_2, s), 34.85 (CH_2, d, J = 17.0 Hz), 15.65 (CH_3, d, J = 3.9 Hz) ppm.

^{31}P NMR (121 MHz, $CDCl_3$): δ –9.50 (s) ppm.

IR (NaCl, thin film): 3054 (m), 2987 (w), 2916 (m), 2849 (w), 1592 (w), 1506 (w), 1461 (m), 1434 (s), 1265 (s), 1200 (m), 1025 (m), 947 (w), 828 (m), 818 (m), 740 (s) cm^{-1}.

HRMS (EI^+): collected for BH_3 derivative **146** (Section 7.3.3.2)

7.3.3.2 *rac*-[1-(2-Methyl-1H-inden-3-yl)-naphthalen-2-ylmethyl]-diphenylphosphine-Borane Complex (146)

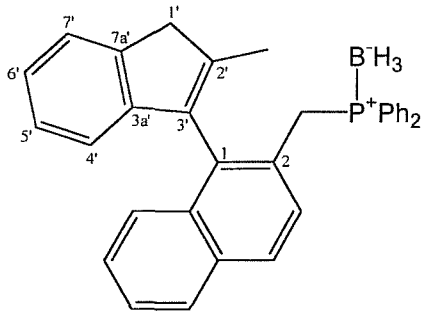

To a stirred solution of *rac*-[1-(2-methyl-1H-inden-3-yl)-naphthalen-2-ylmethyl]-diphenylphosphine **145** (155 mg, 0.34 mmol) in toluene (5 mL), at 0 °C, was added borane-methyl sulphide complex (2.0 M solution in diethyl ether, 0.21 mL, 0.41 mmol), under argon. The reaction was stirred at 0 °C for 45 minutes, then poured onto ice-water (15 mL). The product was extracted from this mixture with ethyl acetate (3 × 15 mL), then the combined organics washed with brine (15 mL), dried over $MgSO_4$ and concentrated *in vacuo*. The crude was purified by column

chromatography (10 % ethyl acetate/petrol) to give the product **146** as a white solid (115 mg, 0.25 mmol, 72 %), mp 177-179 °C.

^{1}H NMR (300 MHz, $CDCl_3$): δ 7.84 (1H, d, *J* = 8.0 Hz, *Ar*), 7.77 (1H, d, *J* = 8.6 Hz, *Ar*), 7.59 (1H, dd, *J* = 8.6, 1.1 Hz, *Ar*), 7.38-7.52 (8H, m, *Ar*), 7.21-7.37 (6H, m, *Ar*), 7.16 (1H, td, *J* = 7.3, 1.0 Hz, *Ar*), 7.07 (1H, td, *J* = 7.4, 0.9 Hz, *Ar*), 6.53 (1H, d, *J* = 7.3 Hz, *Ar*), 3.82 (1H, d, *J* = 12.3 Hz, *CH_2-Ha*), 3.80 (1H, d, *J* = 13.1 Hz, *CH_2-Hb*), 3.55 (1H, d, *J* = 22.7 Hz, *H1'-a*), 3.41 (1H, d, *J* = 22.7 Hz, *H1'-b*), 1.62 (3H, s, *CH_3*), 0.80-2.50 (3H, v.br.'q', *BH_3*) ppm.

^{13}C NMR (75 MHz, $CDCl_3$): δ 146.82 (C, s), 144.68 (C, d, *J* = 0.7 Hz), 142.41 (C, s), 135.81 (C, d, *J* = 1.4 Hz), 132.91 (C, d, *J* = 1.7 Hz, *i-Ph*), 132.68 (2 × CH, d, *J* = 2.5 Hz, *o-Ph*), 132.56 (2 × CH, d, *J* = 2.5 Hz, *o-Ph*), 132.51 (C, d, *J* = 3.5 Hz), 132.40 (C, d, *J* = 2.0 Hz, *i-Ph*), 131.26 (CH, s, *p-Ph*), 131.23 (CH, s, *p-Ph*), 130.07 (C, d, *J* = 15.3 Hz), 130.01 (C, d, *J* = 3.8 Hz), 129.35 (C, d, *J* = 15.1 Hz), 128.88 (2 × CH, d, *J* = 3.7 Hz, *m-Ph*), 128.80 (CH, d, *J* = 3.1 Hz), 128.75 (2 × CH, d, *J* = 3.8 Hz, *m-Ph*), 128.35 (CH, d, *J* = 1.3 Hz), 127.69 (CH, d, *J* = 1.8 Hz), 126.66 (CH, s, *C5'/6'*), 126.60 (CH, d, *J* = 1.1 Hz), 126.24 (CH, s), 125.83 (CH, d, *J* = 1.1 Hz), 124.30 (CH, s, *C5'/6'*), 123.53 (CH, s, *C4'/7'*), 120.02 (CH, s, *C4'/7'*), 43.03 (CH_2, s, *C1'*), 31.75 (CH_2, d, *J* = 32.5 Hz, *CH_2*), 15.41 (CH_3, s, *CH_3*) ppm.

^{31}P NMR (121 MHz, $CDCl_3$): δ 18.19 (br. s) ppm.

IR (NaCl, thin film): 3057 (m), 2902 (w), 2387 (s), 2340 (m), 1507 (w), 1460 (m), 1436 (s), 1392 (m), 1265 (w), 1106 (m), 1060 (m), 1026 (w), 999 (w), 828 (m), 765 (m), 738 (s) cm^{-1}.

LRMS (AP^+): *m/z* 468 ($(M+H)^+$, 15 %), 467 (M^+, 47), 455 ($(M–BH_3+H)^+$, 100).

HRMS (EI^+) $(M–BH_3)^+$ peak: $C_{33}H_{27}P$ requires *m/z* 454.18504, found *m/z* 454.18413.

7.4 Experimental for Chapter 4

7.4.1 Synthesis of Ruthenium complexes

7.4.1.1 (–)-(η^5:η^1-indenyl-CH(Cy)CH_2PPh_2)$Ru^{II}(PPh_3)Cl$ (147)

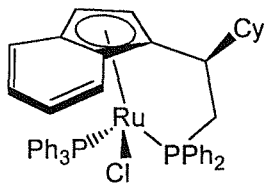

Chiral cyclohexyl-substituted ligand [(2*R*)-2-cyclohexyl-2-(1*H*-3-indenyl)ethyl] (diphenyl)phosphine **121** (1.0 eq, 3.0 mmol, 1.23 g) was dissolved in toluene (50 mL) and cooled under argon to –78 °C. *n*-BuLi (2.5 M solution in hexanes, 1.1 eq, 3.3 mmol, 1.3 mL) was then added dropwise to the stirred solution, with the exclusion of light. The reaction was stirred at –78 °C for 15 minutes, then allowed to warm slowly to room temperature, and stirred for 2 h.

Meanwhile a suspension of dichlorotris(triphenylphosphine)ruthenium(II) (1.1 eq, 3.3 mmol, 3.16 g) in toluene (45 mL) was prepared and cooled to –60 °C, under argon. The anion solution was then further diluted with toluene (30 mL) and added dropwise to the ruthenium solution, *via* canula. The resulting dark mixture was stirred at –60 °C for 15 minutes, then warmed gradually to 95 °C and stirred at this temperature for 17 h. After this time, the dark solution was cooled to room temperature and the solvents removed *in vacuo*, to give a brown solid. ^{1}H NMR of the crude showed an 80 : 20 mixture of diastereoisomers (60 % d.e.). The complex was purified by column chromatography (Al_2O_3, 50-60 % diethyl ether/petrol) using degassed solvents, to give a brown air-stable powder (1.72 g, 2.12 mmol, 71 %) and 87 : 13 mixture of diastereoisomers. Mp (chiral) 165-167 °C.

Crystals of the major isomer were obtained by slow diffusion of pentane into a benzene solution of the complex. X-ray crystallography confirmed the structure of the major isomer is as shown (see Appendix 6).

$[\alpha]_D^{21}$ –160 (c=0.05, $CHCl_3$)

^{1}H NMR (400 MHz, C_6D_6) Numbering as in Table 4.2: δ 8.29 (2H, dd, *J* = 10.0, 9.0 Hz, *Ar*), 7.84 (5H, br. m, *Ar*), 7.47 (1H, dd, *J* = 10.8, 4.8 Hz, *Ar*), 7.41 (1H, d, *J* = 8.0 Hz, *Ar*), 7.34 (2H, td, *J* = 7.5, 1.0 Hz, *Ar*), 7.23 (2H, m, *Ar*), 7.17 (2H, m, *Ar*), 7.05 (10H, br. m,

Ar), 6.94 (1H, td, J = 7.7, 1.5 Hz, *Ar*), 6.87 (1H, t+fs, J = 7.4 Hz, *Ar*), 6.75 (2H, td, J = 7.5, 1.2 Hz, *Ar*), 5.04 (1H, d, J = 1.3 Hz, *Cp-H3*), 3.47 (1H, ddd, J = 12.0, 12.0, 4.5 Hz, *H9-a*), 2.85 (1H, ddd, J = 13.0, 13.0, 4.9 Hz, *H9-b*), 2.46 (1H, dddd, J = 13.1, 8.7, 4.4, 4.4 Hz, *H8*), 2.28 (1H, dd, J = 1.9, 1.9 Hz, *Cp-H2*), 1.38-1.73 (5H, m, *Cy*), 1.10-1.20 (2H, m, *Cy*), 0.56-0.97 (4H, m, *Cy*) ppm.

^{13}C NMR (100 MHz, C_6D_6): See Table 4.2.

^{31}P NMR (121 MHz, C_6D_6): δ 50.16 (d, J = 28.5 Hz, *minor isomer*), 47.90 (d, J = 26.4 Hz, *major isomer*), 39.77 (d, J = 28.9 Hz, *minor isomer*), 38.91 (d, J = 26.4 Hz, *major isomer*) ppm.

IR (NaCl, thin film): 3050 (m), 2925 (s), 2850 (m), 1481 (m), 1433 (s), 1185 (w), 1090 (m), 812 (w), 739 (m), 695 (s) cm^{-1}.

LRMS (ES$^+$): *m/z* 808 ((M+H)$^+$, 100 %).

HRMS (EI$^+$): $C_{47}H_{45}ClP_2Ru$ requires *m/z* 808.17285, found *m/z* 808.17667.

Anal. Calcd. for $C_{47}H_{45}ClP_2Ru$: C, 69.84; H, 5.61; Cl, 4.39; P, 7.66. Found: C, 69.74; H, 5.64; Cl, 4.29; P, 7.61.

7.4.1.2 (–)-[(η^5:η^1-(4,5,6,7-tetrahydroindenyl)CH(Cy)CH$_2$PPh$_2$)]-Ru^{II}(PPh$_3$)Cl (148)

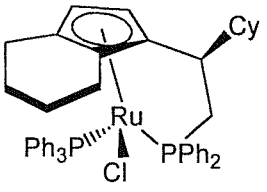

A suspension of platinum oxide (12 mg, 10 mol%) and (–)-(η^5:η^1-indenyl-CH(Cy)CH$_2$PPh$_2$)Ru^{II}(PPh$_3$)Cl **147** (74 % d.e., 404 mg, 0.5 mmol) was prepared in dry dichloromethane (20 mL), and the mixture degassed by repeatedly freezing in liquid nitrogen, applying vacuum, then sealing the system and warming to room temperature. The degassed mixture was transferred, under argon, to a stainless steel hydrogenation bomb with stirrer, and the bomb pressurised to 1800 psi of hydrogen, and warmed to 65 °C. The hydrogenation reaction was stirred under these conditions for 3 days. After this time, the bomb was depressurised and the mixture filtered through celite with dichloromethane (3 × 5 mL). Concentration of the filtrate gave an orange/brown solid (406 mg, 0.5 mmol, 99 %) corresponding to the hydrogenated material by crude ^{1}H NMR, with retained 74 % d.e.

Further purification was achieved by column chromatography (Al_2O_3, 30 % diethyl ether/petrol) to give a bright yellow/orange solid (164 mg, 0.2 mmol, 40 %), mp 157-159 °C.

$[\alpha]_D^{21}$ –120 (c=0.03, CH_2Cl_2).

^{1}H NMR (400 MHz, C_6D_6) Numbering as in Table 4.2: δ 8.67 (2H, dd, *J* = 9.9, 8.4 Hz, *Ar*), 7.67-7.91 (5H, v.br. s, *Ar*), 7.38 (2H, t+fs, *J* = 7.1 Hz, *Ar*), 7.19-7.26 (3H, m, *Ar*), 7.01-7.13 (10H, v.br. s, *Ar*), 6.87 (1H, t+fs, *J* = 7.5 Hz, *Ar*), 6.76 (2H, td, *J* = 7.6, 1.5 Hz, *Ar*), 4.53 (1H, d, *J* = 1.6 Hz, *Cp-H3*), 3.39 (1H, ddd, *J* = 11.8, 11.8, 4.4 Hz, *H9-a*), 3.28 (1H, ddd, *J* = 21.1, 10.7, 5.3 Hz, *tetrahydroindene*), 2.70 (1H, *J* = 12.6, 12.6, 4.8 Hz, *H9-b*), 2.68-2.76 (2H, m, *tetrahydroindene*), 2.47-2.55 (1H, m, *tetrahydroindene*), 2.39 (1H, d, *J* = 2.0 Hz, *Cp-H2*), 2.28-2.39 (2H, m, *tetrahydroindene*), 2.05 (1H, dddd, *J* = 13.3, 8.9, 4.4, 4.4 Hz, *H8*), 0.70-1.92 (13H, m, *Cy+tetrahydroindene*) ppm.

^{13}C NMR (100 MHz, C_6D_6): See Table 4.2.

^{31}P NMR (121 MHz, C_6D_6): δ 44.43 (d, *J* = 36.5 Hz, minor isomer), 43.76 (d, *J* = 39.1 Hz, major isomer), 37.74 (d, *J* = 36.3 Hz, minor isomer), 37.41 (d, *J* = 39.0 Hz, major isomer) ppm.

IR (CH_2Cl_2 solution): 3050 (m), 2926 (s), 2851 (m), 1481 (m), 1447 (w), 1433 (s), 1185 (w), 1090 (m), 1028 (w), 869 (w), 812 (w), 740 (m), 694 (s).

LRMS (ES^+): *m/z* 812 ($(M+H)^+$, 100 %).

HRMS (EI^+): $C_{47}H_{49}ClP_2Ru$ requires *m/z* 812.20415, found *m/z* 812.20597.

Anal. Calcd. for $C_{47}H_{49}ClP_2Ru$: C, 69.49; H, 6.08. Found: C, 69.44; H, 6.55.

7.4.1.3 *rac*-(η^5:η^1-Indenyl-CH(Ph)CH(Ph)PPh_2)Ru^{II}(PPh_3)Cl (149)

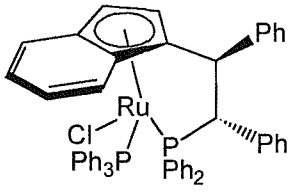

A solution of the crude lithium salt of *rac*-[2-(3*H*-inden-1-yl)-1,2-diphenylethyl]diphenyl-phosphine **128** (~1.0 mmol, 480 mg) was prepared in toluene (33 mL) and transferred slowly (over *ca.* 15 minutes) *via* syringe, to a suspension of dichlorotris-(triphenylphosphine)ruthenium(II) (1.2 mmol, 1.15 g) in toluene (19 mL) at –60 °C. The resulting dark mixture was stirred at –60 °C for 15 minutes, then warmed gradually to 95 °C and stirred at this temperature for 24 h.

After this time, the reaction was cooled to room temperature and the solvents removed *in vacuo*, to give a dark solid. ^{1}H NMR of the crude confirmed the title complex had been prepared as a 87 : 13 (^{1}H NMR) mixture of planar-chiral diastereoisomers with very high metal-centred diastereoselectivity – *ca.* 14 : 1 (by ^{31}P NMR).

The complex was purified by flushing an ethereal solution through a pad of deactivated Al_2O_3, in order to remove inorganic salts, then performing column chromatography (Al_2O_3, 50 % diethyl ether/petrol) using degassed solvents, to give a yellow/light brown powder (223 mg, 0.25 mmol, 25 % over two steps, from spirocycle 2,3-diphenylspiro-[cyclopropane-1,1'-indene] **127** precursor). ^{1}H NMR showed the chromatographed material to be a 91 : 9 mixture of planar-chiral diastereoisomers and ^{31}P NMR showed a 23 : 1 ratio of metal-centred diastereoisomers. Mp 154-157 °C (dec).

Successful crystallisation of the major isomer was achieved by slow diffusion of pentane into a benzene solution of the complex, at 5 °C. X-ray structure analysis has confirmed the structure to be as shown above (see Appendix 7).

^{1}H NMR (400 MHz, C_6D_6, major isomer): δ 7.93 (2H, t, *J* = 7.9 Hz, *Ar*), 7.81 (1H, d, *J* = 8.5 Hz, *Ar*), 7.55-7.76 (5H, v.br.s, *Ar*), 7.48 (2H, t, *J* = 8.0 Hz, *Ar*), 7.43 (1H, t, *J* = 7.7 Hz, *Ar*), 7.12-7.33 (7H, m, *Ar*), 6.99-7.12 (9H, v.br.s, *Ar*), 6.97 (3H, t, *J* = 7.7 Hz, *Ar*), 6.67-6.90 (9H, m, *Ar*), 5.25 (1H, dd, *J* = 13.3, 5.5 Hz, *benzylic CH*), 4.88 (1H, br.s, *Cp-H*), 4.82 (1H, dd, *J* = 13.3, 5.5 Hz, *benzylic CH*), 3.47 (1H, d, *J* = 2.5 Hz, *Cp-H*) ppm.

^{1}H NMR (400 MHz, C_6D_6, minor isomer, clearly identifiable resonances only): δ 6.15 (1H, dd, *J* = 13.9, 8.9 Hz, *benzylic CH*), 5.11 (1H, br. s, *Cp-H*), 4.09 (1H, dd, *J* = 13.8, 6.0 Hz, *benzylic CH*), 3.76 (1H, br. s, *Cp-H*) ppm.

^{13}C NMR (100 MHz, $CDCl_3$) Numbering as in Figure 4.6: δ 141.50 (C, d, *J* = 22.6 Hz, *i-Ph*), 141.04 (3 × C, d, *J* = 23.1 Hz, *i-Ph* (PPh_3)), 138.48 (CH, d, *J* = 10.0 Hz, *o-Ph*), 137.61 (C, d, *J* = 6.8 Hz, *i-Ph*), 135.95 (C, d, *J* = 24.5 Hz, *i-Ph*), 135.78 (C, d, *J* = 32.1 Hz, *i-Ph*), 134.37 (3 × CH, br. d, *J* = 8.0 Hz, *o-Ph* (PPh_3)), 132.54 (CH, d, *J* = 8.3 Hz, *o-Ph*), 130.40 (CH, s, *p-Ph*), 130.03 (CH, s, *p-Ph*), 128.95 (3 × CH, s, *p-Ph* (PPh_3)), 128.66 (CH, *p-Ph*), 128.29 (CH, d, *J* = 1.0 Hz), 127.82 (CH, s, *p-Ph*), 127.77 (3 × CH, d, *J* = 17.5 Hz, *m-Ph* (PPh_3)), 127.64 (CH, d, *J* = 13.1 Hz, *m-Ph*), 127.63 (CH, d, *J* = 24.5 Hz, *m-Ph*), 127.44 (CH, d, *J* = 8.0 Hz, *m-Ph*), 127.11 (CH, *J* = 9.2 Hz, *m-Ph*), 126.79 (CH, s, *C4/5/6/7*), 126.54 (CH, s, *C4/5/6/7*), 124.25 (CH, s, *C4/5/6/7*), 124.15 (CH, s, *C4/5/6/7*),

101.86 (C, s, *C3a*), 100.60 (C, d, J = 6.8 Hz, *C7a*), 97.19 (C, d, J = 10.0 Hz, *C1*), 79.64 (CH, d, J = 1.9 Hz, *Cp-H*), 66.87 (CH, d, J = 23.6 Hz, *C9*), 63.11 (CH, s, *Cp-H*), 44.03 (CH, d, J = 11.2 Hz, *C8*) ppm. * - note: two o-Ph signals could not be assigned, owing to the complex overlapping of aromatic resonances in this spectrum.

^{31}P NMR (121 MHz, C_6D_6, planar-chiral diastereoisomers): δ 79.66 (d, J = 23.4 Hz, *minor isomer*), 71.57 (d, J = 20.8 Hz, *major isomer*), 48.27 (d, J = 23.7 Hz, *minor isomer*), 46.01 (d, J = 20.6 Hz, *major isomer*) ppm.

^{31}P NMR (121 MHz, C_6D_6, metal-centred diastereoisomers): δ 75.84 (d, J = 37.8 Hz, *major isomer*), 71.88 (d, J = 35.3 Hz, *minor isomer*), 46.77 (d, J = 34.7 Hz, *minor isomer*), 41.82 (d, J = 37.8 Hz, *major isomer*) ppm.

IR (CH_2Cl_2 solution): 3054 (m), 1600 (w), 1585 (w), 1495 (w), 1480 (m), 1434 (s), 1265 (m), 1186 (m), 1157 (w), 1090 (s), 1028 (m), 738 (s), 695 (s) cm^{-1}.

LRMS (EI$^+$): *m/z* 878 (M^+, 10 %), 842 ($(M–Cl)^+$, 55), 616 ($(M–PPh_3)^+$, 100).

HRMS (EI$^+$): $C_{53}H_{43}ClP_2Ru$ requires *m/z* 878.15720, found *m/z* 878.15835.

Anal. Calcd. for $C_{53}H_{43}ClP_2Ru$: C, 72.47; H, 4.93. Found: C, 72.10; H, 5.06.

7.4.1.4 *rac*-(η^5:η^1-Indenyl-CH(Cy)$CH_2CH_2PPh_2$)$Ru^{II}(PPh_3)Cl$ (150)

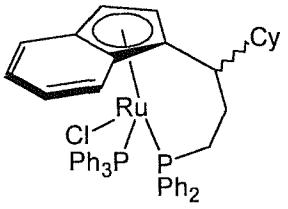

Ligand *rac*-[3-Cyclohexyl-3-(3*H*-inden-1-yl)propyl]diphenylphosphine **129** (425 mg, 1.0 mmol) was dissolved in toluene (33 mL) and cooled to –78 °C. *n*-BuLi (2.5 M solution in hexanes, 0.44 mL, 1.1 mmol) was added dropwise, in the dark, and the reaction stirred at –78 °C for 15 minutes. The resulting cloudy suspension was then warmed slowly to room temperature and stirred for 2 h, to give a yellow solution. This solution was transferred slowly (over *ca.* 10 minutes) *via* syringe, to a suspension of dichlorotris(triphenylphosphine)ruthenium(II) (1.1 mmol, 1.1 g) in toluene (19 mL) at –60 °C.

The dark mixture was stirred at –60 °C for 15 minutes, then warmed to reflux for 24 h. After this time, the reaction was cooled to room temperature and the solvents removed under vacuum. ^{1}H NMR of the crude material indicated the expected complex had been formed as a 83 : 17 mixture of planar-chiral diastereoisomers, with complete metal-centre control (no further diastereoisomer resonances seen).

Inorganics were removed from the crude by redissolving the material in diethyl ether/toluene and flushing the mixture through a short pad of deactivated Al_2O_3. Final purification of the complex was achieved by column chromatography (Al_2O_3, 30-40 % diethyl ether/petrol, using degassed solvents) which provided both diastereoisomers of the complex. The major isomer **150a** was collected as a dark-red solid (454 mg, 0.55 mmol, 55 %, R_f 0.4 in 40 % diethyl ether/petrol) mp 168-171 °C (dec), the minor isomer **150b** was collected as a red/brown solid (70 mg, 0.08 mmol, 9 %, R_f 0.1 in 40 % diethyl ether/petrol) mp 179-182 °C (dec).

The minor isomer crystallised from a solution in diethyl ether on standing at room temperature for 3 h. The major isomer was crystallised by slow diffusion of pentane into a solution in benzene, over 2 weeks at 4 °C. X-ray crystallography has confirmed the structures of the major and minor isomers (see Appendices 8 (major isomer **150a**) and 9 (minor isomer **150b**)).

Major diastereoisomer **150a**:

^{1}H NMR (400 MHz, C_6D_6) Numbering as in Table 4.4: δ 7.75 (1H, d, *J* = 8.5 Hz), 7.61 (1H, d, *J* = 7.6 Hz), 7.59 (2H, dd, *J* = 9.8, 2.0 Hz), 7.57 (4H, dd, *J* = 9.8, 4.0 Hz), 7.34 (2H, dd, *J* = 8.4, 8.4 Hz), 7.28 (1H, d, *J* = 7.8 Hz), 7.24 (2H, dd+fs, *J* = 7.6, 7.6 Hz), 7.18 (2H, dd, *J* = 7.5, 7.5 Hz), 6.95-7.03 (10H, m), 6.88 (1H, dd, *J* = 7.4, 7.4 Hz), 6.83 (1H, d, *J* = 7.3 Hz), 6.71 (2H, dd+fs, *J* = 7.3, 7.3 Hz), 4.65 (1H, s+fs), 3.90 (1H, dddd, *J* = 13.3, 13.3, 7.3, 1.5 Hz), 3.60 (1H, d+fs, *J* = 12.1 Hz), 3.36 (1H, br.s), 2.65 (1H, ddd, *J* = 14.4, 14.4, 5.6 Hz), 2.09 (1H, dddd, *J* = 36.0, 14.6, 2.9, 2.9, Hz), 1.48-1.75 (6H, m), 0.88-1.20 (6H, m) ppm.

^{13}C NMR (100 MHz, C_6D_6): See Table 4.4.

^{31}P NMR (121 MHz, C_6D_6): δ 48.76 (d, *J* = 35.9 Hz), 38.70 (d, *J* = 35.9 Hz) ppm.

IR (NaCl, thin film): 3052 (m), 2923 (s), 2851 (m), 1581(w), 1567 (w), 1481 (m), 1449 (m), 1434 (s), 1330 (m), 1185 (w), 1092 (s), 1028 (w), 811 (m), 741 (s), 696 (s) cm^{-1}.

LRMS (EI$^+$): *m/z* 822 (M^+, 9 %), 560 ($(M–PPh_3)^+$, 100).

HRMS (EI$^+$): $C_{48}H_{47}ClP_2Ru$ requires *m/z* 822.18850, found *m/z* 822.18697.

Anal. Calcd. for $C_{48}H_{47}ClP_2Ru$: C, 70.11; H, 5.76. Found: C, 70.11; H, 5.96.

Minor diastereoisomer **150b**:

^{1}H NMR (400 MHz, C_6D_6) Numbering as in Table 4.4: δ 7.76 (1H, dd, J = 8.9, 8.9 Hz), 7.65-7.73 (6H, m), 7.56 (1H, d, J = 8.5 Hz), 7.33 (1H, dd, J = 7.4, 7.4 Hz), 7.19-7.35 (6H, m), 6.97-7.09 (10H, m), 6.81 (1H, dd, J = 8.5, 8.5 Hz), 6.79 (1H, dd, J = 7.8, 7.8 Hz), 6.59 (1H, dd, J = 8.5, 8.5 Hz), 6.54 (1H, d, J = 8.3 Hz), 4.90 (1H, s+fs), 4.38 (1H, s+fs), 2.69 (1H, ddd, J = 14.1, 14.1, 5.3 Hz), 2.12 (1H, dddd, J = 35.3, 14.2, 2.7, 2.7), 1.97 (1H, dd, J = 12.3, 12.3 Hz), 1.88 (1H, br.d, J = 13.6 Hz), 1.79 (1H, dddd, J = 13.8, 13.8, 2.4, 2.4 Hz), 1.76 (1H, d+fs, J = 14.3 Hz), 1.59 (1H, d+fs, J = 12.1 Hz), 1.18-1.54 (4H, m), 1.06 (1H, ddddd, J = 12.3, 12.3, 12.3, 3.2, 3.2 Hz), 0.82-1.02 (3H, m), 0.71 (1H, dddd, J = 12.1, 12.1, 12.1, 3.1 Hz) ppm.

^{13}C NMR (100 MHz, C_6D_6): See Table 4.4.

^{31}P NMR (121 MHz, C_6D_6): δ 57.32 (d, J = 41.2 Hz), 26.75 (d, J = 41.2 Hz) ppm.

IR (NaCl, thin film): 3049 (m), 2922 (s), 2849 (m), 1587 (w), 1571 (w), 1480 (m), 1433 (s), 1330 (w), 1186 (w), 1090 (s), 813 (w), 740 (m), 696 (s) cm^{-1}.

Anal. Obtained for major isomer, see above.

7.4.1.5 *rac*-[η^5:η^1-1-(2-methylindenyl)-naphthalen-2-yl-(CH_2PPh_2)]Ru^{II} (PPh_3)Cl (151)

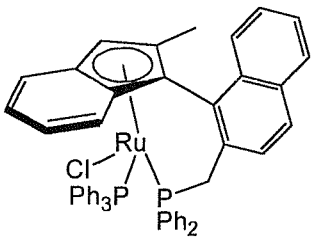

A toluene solution (25 mL) of ligand *rac*-[1-(2-methyl-3H-inden-1-yl)-naphthalen-2-ylmethyl]-diphenylphosphine **145** (341 mg, 0.75 mmol) was prepared and cooled to –78 °C. *n*-BuLi (2.5 M solution in hexanes, 0.33 mL, 0.83 mmol) was added dropwise, in the dark, and the dark yellow mixture stirred at –78 °C for 15 minutes. The resulting suspension was then warmed slowly to room temperature and stirred for 2 h, to give a yellow/orange solution. This solution was transferred over 10 minutes, *via* syringe, to a suspension of dichlorotris(triphenylphosphine)ruthenium(II) (0.86 g, 0.9 mmol) in toluene (14 mL) at –60 °C.

The dark mixture was stirred at –60 °C for 15 minutes, then warmed to reflux for 16 h. After the reaction was cooled to room temperature and the solvents removed under vacuum. ^{31}P NMR of the crude material indicated the expected complex had been formed as an 86 : 14 mixture of diastereoisomers.

Purification of the complex was achieved by column chromatography (Al_2O_3, 30-40 % diethyl ether/petrol, using degassed solvents) to yield a brick-red solid, with 83 : 17 mixture of diastereoisomers (246 mg, 0.29 mmol, 38 %, R_f 0.4 in 40 % diethyl ether/petrol). Mp 176-177 °C (dec).

X-ray quality crystals of the major isomer **151a** were obtained by slow diffusion of pentane into a solution in benzene, over 1 week at 4 °C. Crystallographic analysis has confirmed the structure is as shown (see Appendix 10).

^{1}H NMR (400 MHz, C_6D_6): Numbering as in Figure 4.9: δ 7.55 (1H, d, J = 8.5 Hz), 7.52 (1H, d, J = 8.4 Hz), 7.48 (2H, t, J = 7.9 Hz), 7.33 (1H, d, J = 8.5 Hz), 6.88-7.18 (23H, m), 6.83 (2H, t, J = 6.9 Hz), 6.76 (2H, t, J = 6.7 Hz), 6.50 (1H, dd, J = 7.8, 7.0 Hz), 6.17 (1H, d, J = 8.5 Hz), 5.94 (1H, d, J = 8.5 Hz), 5.01 (1H, d, J = 4.3 Hz, *Cp-H*), 4.94 (1H, dd, J = 14.1, 8.4 Hz), 4.12 (1H, t, J = 14.1 Hz), 1.86 (3H, s, *CH_3*) ppm.
^{13}C NMR (100 MHz, C_6D_6): Numbering as in Figure 4.9: δ 141.94 (C, d, J = 28.2 Hz), 138.83 (3 × CH, v.br.s, *i-Ph (PPh$_3$)*), 136.77 (C, d, J = 36.9 Hz), 136.02 (C, s), 135.55 (C, s), 134.98 (2 × CH, d, J = 10.9 Hz, *o-Ph*), 134.65 (CH, d, J = 10.2 Hz), 134.32 (6 × CH, d, J = 10.4 Hz, *o-Ph (PPh$_3$)*), 134.05 (CH, s), 133.60 (C, d, J = 2.4 Hz), 133.42 (2 × CH, d, J = 8.0 Hz, *o-Ph*), 133.26 (C, d, J = 1.2 Hz), 132.23 (CH, s), 130.09 (CH, d, J = 7.3 Hz), 129.20 (CH, d, J = 1.7 Hz), 128.82 (3 × CH, s, *p-Ph (PPh$_3$)*), 128.45 (2 × CH, d, J = 11.2 Hz, *m-Ph*), 128.29 (CH, s), 127.72 (CH, s), 127.18 (6 × CH, d, J = 9.2 Hz, *m-Ph (PPh$_3$)*), 126.94 (2 × CH, d, J = 9.5 Hz, *m-Ph*), 126.59 (CH, s), 126.05 (CH, s), 125.37 (CH, s), 122.72 (CH, s), 121.27 (CH, s), 107.63 (C, d, J = 6.1 Hz, *C7a*), 105.99 (C, s, *C3a*), 87.91 (C, d, J = 2.2 Hz, *C2*), 86.04 (C, dd, J = 10.4, 1.5 Hz, *C1*), 72.22 (CH, d, J = 11.7 Hz, *C3*), 40.44 (CH_2, d, J = 28.4 Hz, *CH_2*), 11.84 (CH_3, s, *CH_3*) ppm.
^{31}P NMR (121 MHz, C_6D_6): δ / ppm = 46.73 (d, J = 30.2 Hz, *minor isomer*), 44.46 (d, J = 35.9 Hz, *major isomer*), 43.15 (d, J = 30.2 Hz, *minor isomer*), 41.88 (d, J = 36.0 Hz, *major isomer*).
IR (NaCl, thin film): 3053 (m), 1481 (m), 1433 (s), 1265 (m), 1185 (w), 1092 (s), 1028 (m), 852 (m), 811 (m), 740 (s), 695 (s) cm^{-1}.
Anal. Calcd. for $C_{51}H_{41}ClP_2Ru$: C, 71.87; H, 4.85. Found: C, 71.97; H, 4.98.

7.4.2 Synthesis of Rhodium complexes

7.4.2.1 Synthesis of (–)-(η^5:η^1-indenyl-CH(Cy)CH_2PPh_2)Rh^ICO (154)

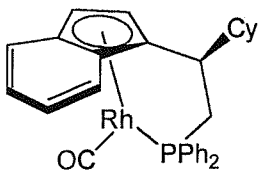

To a solution of chiral ligand **121** (0.41 g, 1 mmol) in THF (20 mL) under argon at –78 °C, was added slowly *n*-BuLi (0.4 mL of a 2.5 M solution in hexanes, 1.0 mmol), and the reaction stirred at –78 °C for 30 min, then allowed to warm to room temperature and stirred for a further 2 h. The dark red ligand anion solution was then cooled to –78 °C and added *via* canula dropwise over *ca.* 20 min to a solution of $[Rh^I(\mu\text{-Cl})(CO)_2]_2$ (194 mg, 0.5 mmol) in THF (20 mL) at –78 °C, immediately forming a dark brown solution. This solution was allowed to stir at –78 °C for 2 h before being warmed slowly to room temperature, overnight (16 h). The solvents were then removed *in vacuo*, to give a brown foamy solid. ^{1}H NMR spectroscopy showed the desired complex formed as a 78 : 22 mixture of **154a** : **154b** (using the racemic ligand the ratio was typically 72 : 28). The crude material was purified by column chromatography (Al_2O_3, 30-50 % toluene/petrol) to afford the product as an orange powder (367 mg, 68 %). There was no change in isomer ratios from the crude product on chromatography. Recrystallisation from diethyl ether/hexane at –30 °C afforded the major diastereoisomer **154a** as clear red crystals (195 mg, 36 %). Mp (chiral) decomposes 168 °C (sealed tube). Mp (racemic) decomposes 170 °C (sealed tube). The X-ray structure of the major isomer **154a** has been obtained (see Appendix 11).

$[\alpha]_D^{21}$ –75.6 (c = 1, $CHCl_3$).

^{1}H NMR (400 MHz, C_6D_6) Numbering as in Table 4.6: δ 7.75-7.68 (2H, m, *o-Ph*), 7.59 (2H, ddd, J_{HP} = 11.7 Hz, J_{HH} = 7.8, 1.7 Hz, *o-Ph*), 7.38 (1H, d+fs, J_{HH} = 8.0 Hz, *H4*), 7.21-7.17 (4H, m, *m-Ph* + *p-Ph* + *H6*), 7.12-7.08 (3H, m, *m-Ph* + *p-Ph*), 7.07 (1H, ddd, J_{HH} = 8.0, 7.0, 1.0 Hz, *H5*), 6.98 (1H, d+fs, J_{HH} = 8.0 Hz, *H7*), 6.20 (1H, dd, J_{HH} = 2.8 Hz, J_{HP}* = 2.7 Hz, *H3*), 6.14 (1H, dd, J_{HH} = 2.8 Hz, J_{HP}* = 2.5 Hz, *H2*), 3.30 (1H, dddd, J_{HP} = 13.3 Hz, J_{HH} = 13.3, 4.6 Hz, J_{HRh} = 2.5 Hz, *H9*), 2.93 (1H, ddd, J_{HH} = 13.6, 13.3 Hz, J_{HP} = 7.0 Hz, *H9*), 2.63 (1H, dddd, J_{HH} = 13.6, 4.6, 4.6 Hz, J_{HP} = 9.0 Hz, *H8*), 1.80-0.72 (11H, m, *Cy*) ppm. * – could be coupling to Rh.

^{13}C NMR (100 MHz, C_6D_6): See Table 4.6.

^{31}P NMR (121 MHz, C_6D_6): δ 57.33 (d, J = 212.0 Hz, major isomer), 53.69 (d, J = 210.7 Hz, minor isomer) ppm.

IR (CH_2Cl_2 solution): 2929 (m), 2853 (m), 1939 (s, CO), 1479 (w), 1436 (w), 1095 (w) cm^{-1}.

LRMS (AP^+): *m/z* 554 ($(M+CH_3CN+H-CO)^+$, 100 %), 553 ($(M+CH_3CN-CO)^+$, 46), 541 ($(M+H)^+$, 33), 513 ($(M+H-CO)^+$, 10), 512 ($(M-CO)^+$, 4).

Anal. Calcd. for $C_{30}H_{30}OPRh$: C, 66.67; H, 5.60; P, 5.73. Found: C, 66.71; H, 5.67; P, 5.67.

7.4.2.2 Synthesis of *rac*-(η^5:η^1-Indenyl-CH(Cy)$CH_2CH_2PPh_2$)Rh^ICO (155)

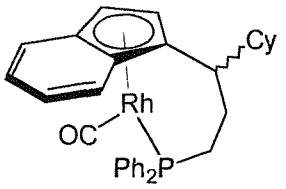

Ligand *rac*-[3-Cyclohexyl-3-(3*H*-inden-1-yl)propyl]diphenylphosphane **129** (212 mg, 0.5 mmol) was dissolved in THF (5 mL) and cooled to –78 °C, under argon. *n*-BuLi (2.5 M solution in hexanes, 0.22 mL, 0.55 mmol) was added to the cold ligand solution, in the dark. The reaction was stirred at –78 °C for 30 minutes, then warmed to room temperature and stirred for 2 h. The ligand anion solution was then cooled to –78 °C, and added slowly *via* canula, to a –78 °C solution of $[Rh^I(\mu\text{-}Cl)(CO)_2]_2$ (107 mg, 0.27 mmol) in THF (5 mL). The resulting dark red suspension was stirred at –78 °C for a further 30 minutes, then warmed slowly to room temperature over 14 h. Solvents were now removed *in vacuo*, to give a crude reddish-brown solid. ^{31}P NMR showed complex **155** had formed as a 74 : 26 mixture of diastereoisomers. The crude material was purified by column chromatography (Al_2O_3, 4-6 % diethyl ether/petrol) to give a yellow film (44.9 mg, 0.08 mmol, 16 %), which was shown by ^{31}P NMR to contain the same 74 : 26 mixture of diastereoisomers as the crude material.

^{1}H NMR (400 MHz, C_6D_6, major isomer): δ 7.64 (2H, ddd, J = 11.1, 8.1, 1.3 Hz), 7.38-7.44 (3H, m), 6.97-7.19 (9H, m), 6.04 (1H, dd, J = 3.8, 3.1 Hz, *Cp-H*), 5.96 (1H, dd, J = 2.7, 2.4 Hz, *Cp-H*), 2.42 (1H, ddd, J = 14.3, 14.3, 6.4 Hz), 2.11 (1H, ddd, J = 9.8, 9.8, 2.1 Hz), 1.84 (1H, dd, J = 36.2, 12.6 Hz), 1.51-1.83 (5H, m), 1.09-1.50 (5H, m), 0.83-1.05 (3H, m) ppm.

^{1}H NMR (400 MHz, C_6D_6, minor isomer, clearly identifiable resonances only): δ 7.47 (2H, ddd, *J* = 11.1, 7.9, 1.5 Hz), 7.34 (1H, dd, *J* = 11.1, 1.7 Hz), 7.33 (1H, dd, *J* = 11.2, 2.3 Hz), 6.90 (1H, t, *J* = 7.8 Hz), 6.72 (1H, d, *J* = 8.2 Hz), 6.00 (1H, dd, *J* = 4.1, 3.1 Hz, *Cp-H*), 5.95 (1H, dd, *J* = 2.7, 2.4 Hz, *Cp-H*) ppm.

^{13}C NMR (100 MHz, C_6D_6): δ 193.15 (C, dd, *J* = 88.8, 20.3 Hz, *C=O*), 139.30 (C, dd, *J* = 47.4, 2.7 Hz, *i-Ph*), 137.98 (C, d, *J* = 44.5 Hz, *i-Ph*), 133.48 (2 × CH, d, *J* = 12.6 Hz, *o-Ph*), 132.21 (2 × CH, d, *J* = 10.7 Hz, *o-Ph*), 129.83 (CH, d, *J* = 2.4 Hz, *p-Ph*), 129.46 (CH, *J* = 2.2 Hz, *p-Ph*), 128.90 (2 × CH, d, *J* = 9.3 Hz, *m-Ph*), 128.17 (2 × CH, d, *J* = 8.6 Hz, *m-Ph*), 123.51 (CH, s, *C5/6*), 121.07 (CH, s, *C5/6*), 118.09 (CH, s, *C4/7*), 118.58 (CH, s, *C3a/7a*), 117.97 (C, d, *J* = 1.2 Hz, *C3a/7a*), 116.61 (CH, s, *C4/7*), 92.94 (C, dd, *J* = 5.7, 2.1 Hz, *C2*), 90.58 (C, d, *J* = 3.2 Hz, *C3*), 73.43 (C, dd, *J* = 10.2, 3.9 Hz, *C1*), 43.90 (CH_2, s, *C10*), 42.07 (CH, s, *Cy*), 32.03 (CH_2, s, *Cy*), 31.28 (CH, dd, *J* = 9.5, 1.0 Hz, *C8*), 31.09 (CH_2, s, *Cy*), 29.32 (CH_2, d, *J* = 28.2 Hz, *C9*), 26.82 (CH_2, s, *Cy*), 26.80 (CH_2, s, *Cy*), 26.75 (CH_2, d, *J* = 1.2 Hz, *Cy*) ppm.

^{31}P NMR (121 MHz, C_6D_6): δ 48.20 (d, *J* = 202.5 Hz, *major isomer*), 46.70 (d, *J* = 196.7 Hz, *minor isomer*) ppm.

IR (NaCl, thin film): 3051 (w), 2924 (s), 2851 (m), 2035 (w), 1944 (s), 1448 (m), 1435 (m), 1324 (m), 1263 (w), 1175 (w), 1098 (m), 1027 (w), 812 (w), 795 (w), 741 (m), 694 (m) cm^{-1}.

LRMS (EI^+): *m/z* 554 (M^+, 75 %), 526 ($(M–CO)^+$, 100).

HRMS (EI^+): $C_{31}H_{32}OPRh$ requires *m/z* 554.12458, found *m/z* 554.12527.

8. Chapter 8: References

(1) Kealy, T. J.; Pauson, P. L. *Nature* **1951**, *168*, 1039-1040.

(2) Schlogl, K. *Topics in Stereochemistry* **1967**, *1*, 39-91.

(3) Halterman, R. L. *Chem. Rev.* **1992**, *92*, 965-994.

(4) Willoughby, C. A.; Buchwald, S. L. *J. Am. Chem. Soc.* **1992**, *114*, 7562-7564.

(5) Willoughby, C. A.; Buchwald, S. L. *J. Org. Chem* **1993**, *58*, 7627-7629.

(6) Willoughby, C. A.; Buchwald, S. L. *J. Am. Chem. Soc.* **1994**, *116*, 8952-8965.

(7) Willoughby, C. A.; Buchwald, S. L. *J. Am. Chem. Soc.* **1994**, *116*, 11703-11714.

(8) Cesarotti, E.; Kegan, H. B.; Goddard, R.; Krüger, C. *J. Organomet. Chem.* **1978**, *162*, 297-309.

(9) Kataoka, Y.; Saito, Y.; Nagata, K.; Kitamura, K.; Shibahara, A.; Tani, K. *Chem. Lett.* **1995**, 833-834.

(10) Komatsuzaki, N.; Uno, M.; Kikuchi, H.; Takahashi, S. *Chem. Lett.* **1996**, 677-678.

(11) Grossman, R. B.; Doyle, R. A.; Buchwald, S. L. *Organometallics* **1991**, *10*, 1501-1505.

(12) Uno, M.; Ando, K.; Komatsuzaki, N.; Takahashi, S. *J. Chem. Soc.-Chem. Commun.* **1992**, 964-965.

(13) Komatsuzaki, N.; Uno, M.; Shirai, K.; Tanaka, T.; Sawada, M.; Takahashi, S. *J. Organomet. Chem.* **1995**, *498*, 53-61.

(14) Jaquith, J. B.; Gaun, J.; Wang, S.; Collins, S. *Organometallics* **1995**, *14*, 1079-1081.

(15) Morken, J. P.; Diduik, M. T.; Hoveyda, A. H. *J. Am. Chem. Soc.* **1993**, *115*, 6997-6998.

(16) Naota, T.; Takaya, H.; Murahashi, S.-I. *Chem. Rev.* **1998**, *98*, 2599-2660.

(17) Bell, L.; Whitby, R. J. *Tetrahedron Lett.* **1996**, *37*, 7139-7142.

(18) Bell, L.; Brookings, D. C.; Dawson, G. J.; Whitby, R. J. *Tetrahedron* **1998**, *54*, 14617-14634.

(19) Butenschön, H. *Chem. Rev.* **2000**, *100*, 1527-1564.

(20) Lee, I.; Dahan, F.; Maisonnat, A.; Poilblanc, R. *Organometallics* **1994**, *13*, 2743-2750.

(21) Kauffmann, T.; Olbrich, J. *Tetrahedron Lett.* **1984**, *25*, 1967-1970.

(22) Salwin, A. M. Z.; Williams, D. L.; Crosby, J.; Ramsden, J. A.; White, C. *J. Chem. Soc., Dalton Trans.* **1988**, 2491-2494.

(23) Trost, B. M.; Vidal, B.; Thommen, M. *Chem.-Eur. J.* **1999**, *5*, 1055-1069.

(24) Lefort, L.; Crane, T. W.; Farwell, M. D.; Baruch, D. M.; Kaeuper, J. A.; Lachicotte, R. J.; Jones, W. D. *Organometallics* **1998**, *17*, 3889-3899.

(25) Nishibayashi, Y.; Takei, I.; Hidai, M. *Organometallics* **1997**, *16*, 3091-3093.

(26) Marquarding, D.; Klusacek, H.; Gokel, G.; Hoffmann, P.; Ugi, I. *J. Am. Chem. Soc.* **1970**, *92*, 5389-5393.

(27) Gokel, G. W.; Marquarding, D.; Ugi, I. *J. Org. Chem.* **1972**, *37*, 3052-3058.

(28) Ciruelos, S.; Englert, U.; Salzer, A.; Bolm, C.; Maischak, A. *Organometallics* **2000**, *19*, 2240-2242.

(29) Brookings, D. C. B. Ph.D. Thesis, The University of Southampton, 1999.

(30) Kataoka, Y. S., Y.; Shibahara, A.; Tani, K. *Chem. Lett.* **1997**, 621-622.

(31) Rerek, M. E.; Basolo, F. *J. Am. Chem. Soc.* **1984**, *106*, 5908-5912.

(32) Katayama, T.; Morimoto, Y.; Yuge, M.; Uno, M.; Takahashi, S. *Organometallics* **1999**, *18*, 3087-3095.

(33) Morimoto, Y.; Ando, K.; Uno, M.; Takahashi, S. *Chem. Lett.* **1996**, 887-888.

(34) Gill, T. P.; Mann, K. R. *Organometallics* **1982**, *1*, 485-488.

(35) Matsushima, E.; Komatsuzaki, N.; Ajioka, Y.; Yamamoto, M.; Kikuchi, H.; Takata, Y.; Dodo, N.; Onitsuka, K.; Uno, M.; Takahashi, S. *Bull. Chem. Soc. Jpn.* **2001**, *74*, 527-537.

(36) Dodo, N.; Matsushima, Y.; Uno, M.; Onitsuka, K.; Takahashi, S. *J. Chem. Soc.-Dalton Trans.* **2000**, 35-41.

(37) Ajioka, Y.; Matsushima, Y.; Onitsuka, K.; Yamazaki, H.; Takahashi, S. *J. Organomet. Chem.* **2001**, *617*, 601-615.

(38) Paley, R. S. *Chem. Rev.* **2002**, *102*, 1493-1523.

(39) Rupert, K. C.; Liu, C. C.; Nguyen, T. T.; Whitener, M. A.; Sowa, J. R. *Organometallics* **2002**, *21*, 144-149.

(40) Liu, C.; Sowa, J. R., Jr. *Tetrahedron Lett.* **1996**, *37*, 7241-7244.

(41) Kataoka, Y.; Iwato, Y.; Yamagata, T.; Tani, K. *Organometallics* **1999**, *18*, 5423-5425.

(42) Schumann, H.; Stenzel, O.; Dechert, S.; Girgsdies, F.; Halterman, R. L. *Organometallics* **2001**, *20*, 2215-2225.

(43) Weast, R. C.; Astle, M. J.; Eds. *Handbook of Chemistry and Physics*; CRC Press: Boca Raton, FL, 1981.

(44) Komatsuzaki, N.; Kikuchi, H.; Yamamoto, M.; Uno, M.; Takahashi, S. *Chem. Lett.* **1998**, 445-446.

(45) Brookings, D. C.; Harrison, S. A.; Whitby, R. J.; Crombie, B.; Jones, R. V. H. *Organometallics* **2001**, *20*, 4574-4583.

(46) Trost, B. M.; Kulawiec, R. J. *J. Am. Chem. Soc.* **1992**, *114*, 5579-5584.

(47) Brunner, H.; Valerio, C.; Zabel, M. *New J. Chem.* **2000**, *24*, 275-279.

(48) van der Zeijden, A. A. H.; Jimenez, J.; Mattheis, C.; Wagner, C.; Merzweiler, K. *Eur. J. Inorg. Chem.* **1999**, 1919-1930.

(49) Kataoka, Y. S., A.; Saito, Y.; Yamagata, T.; Tani, K. *Organometallics* **1998**, *17*, 4338-4340.

(50) Kataoka, Y.; Shibahara, A.; Yamagata, T.; Tani, K. *Organometallics* **2001**, *20*, 2431-2433.

(51) Kataoka, Y.; Iwato, Y.; Shibahara, A.; Yamagata, T.; Tani, K. *Chem. Commun.* **2000**, 841-842.

(52) Katayama, T.; Matsushima, Y.; Onitsuka, K.; Takahashi, S. *Chem. Commun.* **2000**, *2*, 2337-2338.

(53) Morimoto, Y.; Ando, K.; Uno, M.; Takahashi, S. *Chem. Commun.* **1997**, 1795-1796.

(54) Onitsuka, K.; Dodo, N.; Matsushima, Y.; Takahashi, S. *Chem. Commun.* **2001**, 521-522.

(55) Onitsuka, K.; Ajioka, Y.; Matsushima, Y.; Takahashi, S. *Organometallics* **2001**, *20*, 3274-3282.

(56) Kaulen, C.; Pala, C.; Hu, C. H.; Ganter, C. *Organometallics* **2001**, *20*, 1614-1619.

(57) Matsushima, Y.; Onitsuka, K.; Takahashi, S. *Chem. Lett.* **2000**, 760-761.

(58) Tutusaus, O.; Delfosse, S.; Demonceau, A.; Noels, A. F.; Núñez, R.; Viñas, C.; Teixidor, F. *Tetrahedron Lett.* **2002**, *43*, 983-987.

(59) Schumann, H.; Stenzel, O.; Dechert, S.; Girgsdies, F.; Blum, J.; Gelman, D.; Halterman, R. L. *Eur. J. Inorg. Chem.* **2002**, 211-219.

(60) Schumann, H.; Stenzel, O.; Dechert, S.; Girgsdies, F.; Halterman, R. L. *Organometallics* **2001**, *20*, 5360-5368.

(61) Trost, B. M.; Kulawiec, R. J. *J. Am. Chem. Soc.* **1993**, *115*, 2027-2036.

(62) Kakkar, A. K.; Taylor, N. J.; Marder, T. B.; Shen, J. K.; Hallinan, N.; Basolo, F. *Inorg. Chim. Acta* **1992**, *200*, 219-231 and references within.

(63) Gamasa, M. P.; Gimeno, J.; GonzalezBernardo, C.; MartinVaca, B. M.; Monti, D.; Bassetti, M. *Organometallics* **1996**, *15*, 302-308.

(64) Habib, A.; Tanke, R. S.; Holt, E. M.; Crabtree, R. H. *Organometallics* **1989**, *8*, 1225-1231.

(65) Rerek, M. E.; Ji, L. N.; Basolo, F. *J. Chem. Soc. Chem. Commun.* **1983**, 1208-1209.

(66) Jones, D. J.; Mawby, R. J. *Inorg. Chim. Acta.* **1972**, *4*, 157-160.

(67) Garrett, C. E.; Fu, G. C. *J. Org. Chem.* **1998**, *63*, 1370-1371.

(68) Marder, T. B.; Roe, C. D.; Milstein, D. *Organometallics* **1988**, *7*, 1451-1453.

(69) Borrini, A.; Diversi, P.; Ingrosso, G.; Luccherini, A.; Serra, G. *J. Mol. Catal.* **1985**, *30*, 181-195.

(70) Trost, B. M.; Kulawiec, R. J.; Hammes, A. *Tetrahedron Lett.* **1993**, *34*, 587-590.

(71) Matsushima, Y.; Onitsuka, K.; Kondo, T.; Mitsudo, T.; Takahashi, S. *J. Am. Chem. Soc.* **2001**, *123*, 10405-10406.

(72) Koh, J. H.; Jeong, H. M.; Park, J. *Tetrahedron Lett.* **1998**, *39*, 5545-5548.

(73) Koh, J. H.; Jung, H. M.; Kim, M. J.; Park, J. *Tetrahedron Lett.* **1999**, *40*, 6281-6284.

(74) Kündig, E. P.; Saudan, M. C.; Alezra, V.; Viton, F.; Bernardinelli, G. *Angew. Chem.-Int. Edit.* **2001**, *40*, 4481-4485.

(75) Erker, G.; Aulbach, M.; Knickmeier, M.; Wingbermuhle, D.; Kruger, C.; Nolte, M.; Werner, S. *J. Am. Chem. Soc.* **1993**, *115*, 4590-4601.

(76) Reiger, B.; Jany, G.; Fawzi, R.; Steimann, M. *Organometallics* **1994**, *13*, 647-653.

(77) Rieger reports[76] obtaining just the alcohol **110** in 67 % yield, although the proton NMR data he gives is only consistent with **111**.

(78) Crispino, G. A.; Jeong, K.-S.; Kolb, H. C.; Wang, Z.-M.; Xu, D.; Sharpless, K. B. *J. Org. Chem.* **1993**, *58*, 3785-3786.

(79) Klob, H. C.; Sharpless, K. B. *Tetrahedron* **1992**, *48*, 10515-10530.

(80) Ready, J. M.; Jacobsen, E. N. *J. Am. Chem. Soc.* **1999**, *121*, 6086-6087.

(81) Tokunaga, M.; Larrow, J. F.; Kakiuchi, F.; Jacobsen, E. N. *Science* **1997**, *277*, 936-938.

(82) Bensley, D. M.; Mintz, E. A.; Sussangkarn, S. J. *J. Org. Chem.* **1988**, *53*, 4417-4419.

(83) Segall, Y.; Granoth, I.; Kalir, A. *J. Chem. Soc.-Chem. Commun.* **1974**, 501-502.

(84) Tani, K.; Suwa, K.; Tanigawa, E.; Ise, T.; Yamagata, T.; Tatsuno, Y.; Otsuka, S. *J. Organomet. Chem.* **1989**, *370*, 203-221.

(85) Brisset, H.; Gourdel, Y.; Pellon, P.; Le Corre, M. *Tetrahedron Lett.* **1993**, *34*, 4523-4526.

(86) Imamoto, T.; Oshiki, T.; Onozanwa, T.; Kusumoto, T.; Sato, K. *J. Am. Chem. Soc.* **1990**, *112*, 5244-5252.

(87) Langer, F.; Püntener, K.; Stürmer, R.; Knochel, P. *Tetrahedron: Asym.* **1997**, *8*, 715-738.

(88) Pellon, P.; Le Goaster, C.; Toupet, L. *Tetrahedron Lett.* **1996**, *37*, 4713-4716.

(89) Nelson, A.; Warren, S. *J. Chem. Soc., Perkin Trans. 1* **1999**, 1963-1982.

(90) Lawrence, N. J.; Muhammad, F. *Tetrahedron* **1998**, *54*, 15345-15360.

(91) Peterson, D. J. *J. Organomet. Chem.* **1967**, *8*, 199-208.

(92) Krause, N.; Hoffmann-Röder, A. *Synthesis* **2001**, *2*, 171-196.

(93) Baker, R. W.; Hambley, T. W.; Turner, P. *J. Chem. Soc.-Chem. Commun.* **1995**, 2509-2510.

(94) Baker, R. W.; Wallace, B. J. *Chem. Commun.* **1999**, 1405-1406.

(95) Westcott, S. A.; Kakkar, A. K.; Stringer, G.; Taylor, N. J.; Marder, T. B. *J. Organomet. Chem.* **1990**, *394*, 777-794.

(96) Gansow, O. A.; Burke, A. R.; Vernon, W. D. *J. Am. Chem. Soc.* **1976**, *98*, 5817-5826.

(97) Bruce, M. I.; Hameister, C.; Swincer, A. G.; Wallis, R. C. *Inorg. Synth.* **1982**, *21*, 78-80.

(98) Murata, K.; Ikariya, T.; Noyori, R. *J. Org. Chem.* **1999**, *64*, 2186-2187.

(99) Faller, J. W.; Smart, C. J. *Tetrahedron Lett.* **1989**, *30*, 1189-1192.

(100) Perrin, D. D.; Armarego, W. L. F. *Purification of Laboratory Chemicals*; 3rd Edition ed.; Pergammon Press: Oxford, 1988.

(101) McCleverty, J. A.; Wilkinson, G. *Inorg. Synth.* **1966**, *8*, 211-214.

(102) Hallman, P. S.; Stephenson, T. A.; Wilkinson, G. *Inorg. Synth.* **1970**, *12*, 237-240.

(103) Outurquin, F.; Paulmier, C. *Synthesis* **1989**, 690-691.

(104) Sato, Y.; Takeuchi, S. *Synthesis* **1983**, 734-735.

9. Appendices

Appendix 1 **X-ray Structure of Spiro-cyclopropane (114)**
Appendix 2 **X-ray Structure of Bis-mesylate (122)**
Appendix 3 **X-ray Structure of Spiro-cyclopropane (120)**
Appendix 4 **X-ray Structure of Spiro-cyclopropane (127)**
Appendix 5 **X-ray Structure of Bis-*tert*-butyl-ester Compound (135)**
Appendix 6 **X-ray Structure of Ruthenium Complex (147)**
Appendix 7 **X-ray Structure of Ruthenium Complex (149)**
Appendix 8 **X-ray Structure of Ruthenium Complex (150a)-major**
Appendix 9 **X-ray Structure of Ruthenium Complex (150b)-minor**
Appendix 10 **X-ray Structure of Ruthenium Complex (151)**
Appendix 11 **X-ray Structure of Rhodium Complex (154)**

Please note: the atom-numbering system used for the X-ray structures given in Appendices 1-11 may differ from that used for the same compound throughout the remainder of this Thesis. For this reason, a fully numbered ORTEP view of each X-ray structure is given at the start of the individual appendices, and the reader is encouraged to consult these diagrams before seeking information from the associated X-ray data tables.

All X-ray structure solutions by S. Harrison and S. Harrison/R. Whitby. Thanks to Simon Coles and Peter Wright for collection of the X-ray crystal data.

University of Southampton · Department of Chemistry

Crystallography Service

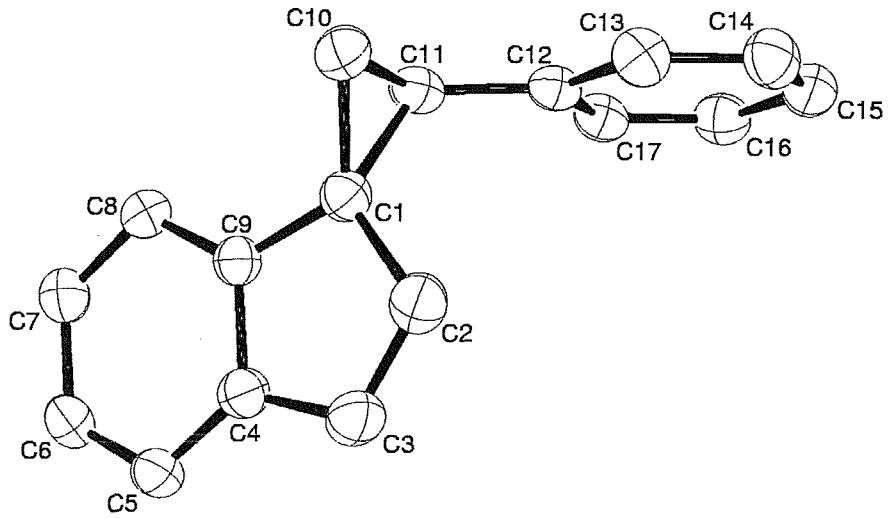

Table 1. Crystal data and structure refinement.

Compound name	***rac*-(*R*,*R*)-Spiro[(2-phenylcyclopropane)-1,1′-indene]**	
Empirical formula	$C_{17}H_{14}$	
Formula weight	218.28	
Temperature	150(2) K	
Wavelength	0.71073 Å	
Crystal system	Monoclinic	
Space group	$P2_1/c$	
Unit cell dimensions	a = 6.9761(14) Å	α = 90°
	b = 12.498(3) Å	β = 93.36(3)°
	c = 14.135(3) Å	γ = 90°
Volume	1230.3(4) Å^3	
Z	4	
Density (calculated)	1.178 Mg / m^3	
Absorption coefficient	0.066 mm^{-1}	
F(000)	464	
Crystal	Needle; colourless	
Crystal size	0.30 × 0.04 × 0.04 mm^3	
θ range for data collection	3.26 – 27.50°	
Index ranges	$-8 \le h \le 8$, $-15 \le k \le 16$, $-18 \le l \le 18$	
Reflections collected	9975	
Independent reflections	2790 [R_{int} = 0.0458]	
Completeness to θ = 27.50°	98.9 %	
Absorption correction	Semi–empirical from equivalents	
Max. and min. transmission	0.9973 and 0.9804	
Refinement method	Full-matrix least-squares on F^2	
Data / restraints / parameters	2790 / 0 / 155	
Goodness-of-fit on F^2	1.020	
Final R indices [$F^2 > 2\sigma(F^2)$]	$R1$ = 0.0490, $wR2$ = 0.1195	
R indices (all data)	$R1$ = 0.0777, $wR2$ = 0.1357	
Largest diff. peak and hole	0.237 and –0.164 e Å^{-3}	

Diffractometer: *Enraf Nonius KappaCCD* area detector (ϕ scans and ω scans to fill *Ewald* sphere). **Data collection and cell refinement**: *Denzo* (Z. Otwinowski & W. Minor, *Methods in Enzymology* (1997) Vol. **276**: *Macromolecular Crystallography*, part A, pp. 307–326; C. W. Carter, Jr. & R. M. Sweet, Eds., Academic Press). **Absorption correction**: *SORTAV* (R. H. Blessing, Acta Cryst. A**51** (1995) 33–37; R. H. Blessing, J. Appl. Cryst. **30** (1997) 421–426). **Program used to solve structure**: *SHELXS97* (G. M. Sheldrick, Acta Cryst. (1990) A**46** 467–473). **Program used to refine structure**: *SHELXL97* (G. M. Sheldrick (1997), University of Göttingen, Germany).
Further information: http://www.soton.ac.uk/~xservice/strat.htm

Table 2. Atomic coordinates [× 10^4], equivalent isotropic displacement parameters [$Å^2$ × 10^3] and site occupancy factors. U_{eq} is defined as one third of the trace of the orthogonalized U^{ij} tensor.

Atom	*x*	*y*	*z*	U_{eq}	*S.o.f.*
C1	1516(2)	−1033(1)	3113(1)	30(1)	1
C2	−41(2)	−601(1)	3662(1)	37(1)	1
C3	−638(2)	−1349(1)	4261(1)	39(1)	1
C4	461(2)	−2320(1)	4157(1)	32(1)	1
C5	460(2)	−3294(1)	4629(1)	36(1)	1
C6	1741(2)	−4081(1)	4386(1)	40(1)	1
C7	2999(2)	−3910(1)	3676(1)	41(1)	1
C8	3016(2)	−2936(1)	3203(1)	36(1)	1
C9	1757(2)	−2140(1)	3451(1)	30(1)	1
C10	1919(2)	−691(1)	2116(1)	37(1)	1
C11	3304(2)	−351(1)	2902(1)	31(1)	1
C12	3495(2)	761(1)	3250(1)	30(1)	1
C13	2350(2)	1602(1)	2906(1)	36(1)	1
C14	2591(2)	2625(1)	3263(1)	39(1)	1
C15	3987(2)	2836(1)	3975(1)	38(1)	1
C16	5141(2)	2013(1)	4325(1)	37(1)	1
C17	4903(2)	987(1)	3963(1)	33(1)	1

Table 3. Bond lengths [Å] and angles [°].

C1–C9	1.470(2)
C1–C2	1.475(2)
C1–C10	1.5141(19)
C1–C11	1.5541(19)
C2–C3	1.344(2)
C3–C4	1.448(2)
C4–C5	1.388(2)
C4–C9	1.4033(19)
C5–C6	1.385(2)
C6–C7	1.389(2)
C7–C8	1.388(2)
C8–C9	1.385(2)
C10–C11	1.491(2)
C11–C12	1.477(2)
C12–C13	1.391(2)
C12–C17	1.395(2)
C13–C14	1.381(2)
C14–C15	1.383(2)
C15–C16	1.380(2)
C16–C17	1.386(2)
C9–C1–C2	104.30(11)
C9–C1–C10	123.02(12)
C2–C1–C10	124.68(13)
C9–C1–C11	120.07(11)
C2–C1–C11	121.60(13)
C10–C1–C11	58.12(9)
C3–C2–C1	109.98(14)
C2–C3–C4	109.52(13)
C5–C4–C9	120.04(14)
C5–C4–C3	132.18(13)
C9–C4–C3	107.75(13)
C6–C5–C4	119.00(13)
C5–C6–C7	120.94(15)
C8–C7–C6	120.42(15)
C9–C8–C7	118.97(13)
C8–C9–C4	120.61(14)
C8–C9–C1	130.94(13)
C4–C9–C1	108.43(12)
C11–C10–C1	62.28(9)
C12–C11–C10	123.94(12)
C12–C11–C1	120.68(12)
C10–C11–C1	59.59(9)
C13–C12–C17	117.70(14)
C13–C12–C11	123.78(13)
C17–C12–C11	118.52(13)
C14–C13–C12	121.14(13)
C13–C14–C15	120.50(14)
C16–C15–C14	119.32(15)
C15–C16–C17	120.16(13)
C16–C17–C12	121.19(13)

Symmetry transformations used to generate equivalent atoms:

Table 4. Anisotropic displacement parameters [$Å^2 \times 10^3$]. The anisotropic displacement factor exponent takes the form: $-2\pi^2[h^2a^{*2}U^{11} + \cdots + 2\ h\ k\ a^*\ b^*\ U^{12}]$.

Atom	U^{11}	U^{22}	U^{33}	U^{23}	U^{13}	U^{12}
C1	29(1)	31(1)	30(1)	−2(1)	3(1)	−3(1)
C2	30(1)	37(1)	42(1)	−5(1)	2(1)	−1(1)
C3	32(1)	43(1)	42(1)	−6(1)	11(1)	−5(1)
C4	29(1)	37(1)	30(1)	−6(1)	3(1)	−8(1)
C5	39(1)	38(1)	34(1)	−3(1)	9(1)	−12(1)
C6	49(1)	30(1)	40(1)	1(1)	6(1)	−10(1)
C7	47(1)	32(1)	45(1)	−3(1)	11(1)	−2(1)
C8	42(1)	33(1)	34(1)	−4(1)	12(1)	−3(1)
C9	31(1)	31(1)	27(1)	−4(1)	2(1)	−7(1)
C10	47(1)	37(1)	29(1)	−1(1)	2(1)	−1(1)
C11	29(1)	33(1)	32(1)	5(1)	6(1)	0(1)
C12	27(1)	34(1)	29(1)	5(1)	6(1)	−2(1)
C13	33(1)	37(1)	37(1)	3(1)	−3(1)	1(1)
C14	38(1)	34(1)	45(1)	5(1)	3(1)	6(1)
C15	39(1)	35(1)	41(1)	−2(1)	10(1)	−5(1)
C16	33(1)	43(1)	35(1)	1(1)	1(1)	−6(1)
C17	28(1)	37(1)	33(1)	7(1)	2(1)	0(1)

University of Southampton · Department of Chemistry

Crystallography Service

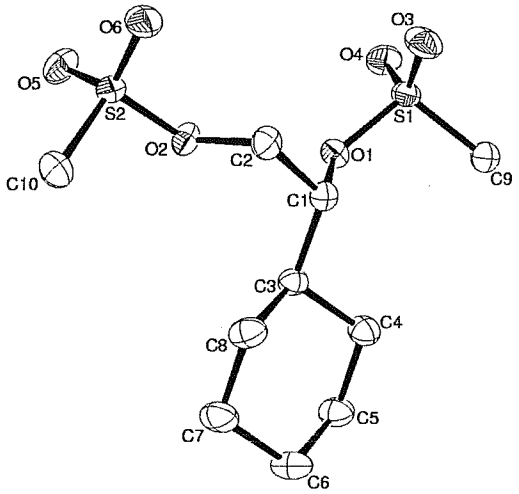

Table 1. Crystal data and structure refinement.

Compound name	**(*R*)-Methanesulfonic acid 1-cyclohexyl-2-((methane-sulfonyl)oxy)ethyl ester**	
Empirical formula	$C_{10}H_{20}O_6S_2$	
Formula weight	300.38	
Temperature	150(2) K	
Wavelength	0.71073 Å	
Crystal system	Orthorhombic	
Space group	$P2_12_12_1$	
Unit cell dimensions	a = 9.0329(18) Å	α = 90°
	b = 9.0501(18) Å	β = 90°
	c = 16.602(3) Å	γ = 90°
Volume	1357.2(5) Å^3	
Z	4	
Density (calculated)	1.470 Mg / m^3	
Absorption coefficient	0.409 mm^{-1}	
F(000)	640	
Crystal	Needle; colourless	
Crystal size	0.17 × 0.05 × 0.02 mm^3	
θ range for data collection	2.45 – 27.47°	
Index ranges	$-11 \le h \le 10$, $-11 \le k \le 11$, $-21 \le l \le 20$	
Reflections collected	15139	
Independent reflections	3108 [R_{int} = 0.0533]	
Completeness to θ = 27.47°	99.6 %	
Absorption correction	Semi–empirical from equivalents	
Max. and min. transmission	0.9919 and 0.9338	
Refinement method	Full-matrix least-squares on F^2	
Data / restraints / parameters	3108 / 0 / 164	
Goodness-of-fit on F^2	1.042	
Final R indices [$F^2 > 2\sigma(F^2)$]	$R1$ = 0.0324, $wR2$ = 0.0777	
R indices (all data)	$R1$ = 0.0369, $wR2$ = 0.0798	
Flack absolute structure parameter	x = -0.0003 (esd 0.0652)	
Largest diff. peak and hole	0.242 and –0.330 e Å^{-3}	

Diffractometer: *Enraf Nonius KappaCCD* area detector (ϕ scans and ω scans to fill *Ewald* sphere). **Data collection and cell refinement**: *Denzo* (Z. Otwinowski & W. Minor, *Methods in Enzymology* (1997) Vol. **276**: *Macromolecular Crystallography*, part A, pp. 307–326; C. W. Carter, Jr. & R. M. Sweet, Eds., Academic Press). **Absorption correction**: *SORTAV* (R. H. Blessing, Acta Cryst. A**51** (1995) 33–37; R. H. Blessing, J. Appl. Cryst. **30** (1997) 421–426). **Program used to solve structure**: *SHELXS97* (G. M. Sheldrick, Acta Cryst. (1990) A**46** 467–473). **Program used to refine structure**: *SHELXL97* (G. M. Sheldrick (1997), University of Göttingen, Germany).
Further information: http://www.soton.ac.uk/~xservice/strat.htm

Table 2. Atomic coordinates [$\times 10^4$], equivalent isotropic displacement parameters [$Å^2 \times 10^3$] and site occupancy factors. U_{eq} is defined as one third of the trace of the orthogonalized U^{ij} tensor.

Atom	*x*	*y*	*z*	U_{eq}	*S.o.f.*
C1	8117(2)	8278(2)	−356(1)	22(1)	1
C2	7684(2)	7317(2)	344(1)	26(1)	1
C3	8893(2)	9737(2)	−163(1)	22(1)	1
C4	8869(2)	10742(2)	−906(1)	29(1)	1
C5	9662(2)	12199(2)	−751(1)	32(1)	1
C6	9061(2)	12991(2)	−12(1)	33(1)	1
C7	9106(3)	11975(2)	714(1)	37(1)	1
C8	8246(2)	10543(2)	562(1)	31(1)	1
C9	8299(2)	7748(2)	−2351(1)	30(1)	1
C10	8328(3)	7509(2)	2355(1)	37(1)	1
O1	9179(1)	7445(1)	−856(1)	23(1)	1
O2	9001(1)	7056(1)	841(1)	25(1)	1
O3	7326(2)	5710(2)	−1389(1)	37(1)	1
O4	9948(2)	5644(2)	−1794(1)	36(1)	1
O5	10169(2)	5536(2)	1820(1)	35(1)	1
O6	7517(2)	5198(2)	1548(1)	33(1)	1
S1	8660(1)	6469(1)	−1591(1)	24(1)	1
S2	8757(1)	6158(1)	1641(1)	23(1)	1

Table 3. Bond lengths [Å] and angles [°].

C1–O1	1.475(2)
C1–C2	1.503(2)
C1–C3	1.529(2)
C2–O2	1.467(2)
C3–C8	1.525(2)
C3–C4	1.533(2)
C4–C5	1.522(3)
C5–C6	1.521(3)
C6–C7	1.517(3)
C7–C8	1.531(3)
C9–S1	1.7433(19)
C10–S2	1.746(2)
O1–S1	1.5777(13)
O2–S2	1.5730(13)
O3–S1	1.4267(14)
O4–S1	1.4233(14)
O5–S2	1.4255(14)
O6–S2	1.4257(13)
O1–C1–C2	107.95(14)
O1–C1–C3	105.14(13)
C2–C1–C3	117.21(14)
O2–C2–C1	108.51(14)
C8–C3–C1	113.79(14)
C8–C3–C4	110.29(15)
C1–C3–C4	109.75(13)
C5–C4–C3	111.78(15)
C6–C5–C4	112.17(16)
C7–C6–C5	110.21(15)
C6–C7–C8	111.63(16)
C3–C8–C7	109.93(15)
C1–O1–S1	121.86(10)
C2–O2–S2	116.43(10)
O4–S1–O3	119.60(9)
O4–S1–O1	103.56(7)
O3–S1–O1	109.79(7)
O4–S1–C9	109.20(9)
O3–S1–C9	109.40(10)
O1–S1–C9	104.09(8)
O5–S2–O6	119.02(8)
O5–S2–O2	104.77(7)
O6–S2–O2	109.44(7)
O5–S2–C10	109.48(10)
O6–S2–C10	109.06(10)
O2–S2–C10	103.99(9)

Symmetry transformations used to generate equivalent atoms:

Table 4. Anisotropic displacement parameters [$Å^2 \times 10^3$]. The anisotropic displacement factor exponent takes the form: $-2\pi^2[h^2a^{*2}U^{11} + \cdots + 2\,h\,k\,a^*\,b^*\,U^{12}]$.

Atom	U^{11}	U^{22}	U^{33}	U^{23}	U^{13}	U^{12}
C1	19(1)	24(1)	23(1)	0(1)	1(1)	2(1)
C2	19(1)	29(1)	29(1)	2(1)	−2(1)	−1(1)
C3	20(1)	20(1)	27(1)	−1(1)	0(1)	1(1)
C4	32(1)	26(1)	27(1)	0(1)	2(1)	−7(1)
C5	39(1)	24(1)	32(1)	1(1)	6(1)	−3(1)
C6	39(1)	21(1)	38(1)	−2(1)	13(1)	−2(1)
C7	54(1)	26(1)	30(1)	−7(1)	9(1)	4(1)
C8	38(1)	24(1)	30(1)	1(1)	11(1)	4(1)
C9	38(1)	28(1)	24(1)	1(1)	−3(1)	−2(1)
C10	53(1)	32(1)	26(1)	−7(1)	−4(1)	4(1)
O1	21(1)	24(1)	24(1)	−4(1)	0(1)	0(1)
O2	22(1)	28(1)	24(1)	7(1)	−1(1)	−1(1)
O3	41(1)	34(1)	36(1)	−1(1)	1(1)	−19(1)
O4	41(1)	26(1)	39(1)	−7(1)	2(1)	10(1)
O5	36(1)	31(1)	39(1)	10(1)	−5(1)	7(1)
O6	37(1)	29(1)	32(1)	2(1)	2(1)	−13(1)
S1	29(1)	19(1)	25(1)	−2(1)	0(1)	−3(1)
S2	28(1)	19(1)	23(1)	2(1)	−1(1)	−2(1)

University of Southampton · Department of Chemistry
Crystallography Service

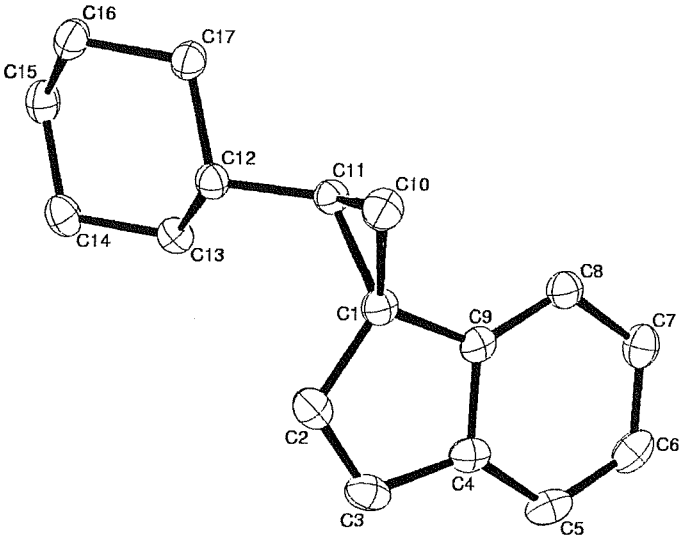

Table 1. Crystal data and structure refinement.

Compound name	**(+)-Spiro-[(2-cyclohexylcyclopropane)-1,1′-indene]**	
Empirical formula	$C_{17}H_{20}$	
Formula weight	224.33	
Temperature	120(2) K	
Wavelength	0.71073 Å	
Crystal system	Orthorhombic	
Space group	*P*222	
Unit cell dimensions	$a = 6.4985(2)$ Å	$\alpha = 90°$
	$b = 9.3237(4)$ Å	$\beta = 90°$
	$c = 21.1066(7)$ Å	$\gamma = 90°$
Volume	1278.85(8) Å^3	
Z	4	
Density (calculated)	1.165 Mg / m^3	
Absorption coefficient	0.065 mm^{-1}	
F(000)	488	
Crystal	Needle; colourless	
Crystal size	0.70 × 0.30 × 0.30 mm^3	
θ range for data collection	2.92 – 27.48°	
Index ranges	$-8 \le h \le 8$, $-12 \le k \le 12$, $-25 \le l \le 25$	
Reflections collected	2684	
Independent reflections	2684 [$R_{int} = 0.0000$]	
Completeness to $\theta = 27.48°$	96.6 %	
Absorption correction	Semi–empirical from equivalents	
Max. and min. transmission	0.9935 and 0.9935	
Refinement method	Full-matrix least-squares on F^2	
Data / restraints / parameters	2684 / 0 / 235	
Goodness-of-fit on F^2	1.039	
Final *R* indices [$F^2 > 2\sigma(F^2)$]	$R1 = 0.0360$, $wR2 = 0.0846$	
R indices (all data)	$R1 = 0.0433$, $wR2 = 0.0888$	
Flack absolute structure parameter	$x = 0.00001$	
Largest diff. peak and hole	0.159 and –0.153 e Å^{-3}	

Diffractometer: *Enraf Nonius KappaCCD* area detector (ϕ scans and ω scans to fill *Ewald* sphere). **Data collection and cell refinement**: *Denzo* (Z. Otwinowski & W. Minor, *Methods in Enzymology* (1997) Vol. **276**: *Macromolecular Crystallography*, part A, pp. 307–326; C. W. Carter, Jr. & R. M. Sweet, Eds., Academic Press). **Absorption correction**: *SORTAV* (R. H. Blessing, Acta Cryst. A**51** (1995) 33–37; R. H. Blessing, J. Appl. Cryst. **30** (1997) 421–426). **Program used to solve structure**: *SHELXS97* (G. M. Sheldrick, Acta Cryst. (1990) A**46** 467–473). **Program used to refine structure**: *SHELXL97* (G. M. Sheldrick (1997), University of Göttingen, Germany).
Further information: http://www.soton.ac.uk/~xservice/strat.htm

Table 2. Atomic coordinates [$\times 10^4$], equivalent isotropic displacement parameters [$Å^2 \times 10^3$] and site occupancy factors. U_{eq} is defined as one third of the trace of the orthogonalized U^{ij} tensor.

Atom	*x*	*y*	*z*	U_{eq}	*S.o.f.*
C1	10744(2)	10233(2)	2606(1)	21(1)	1
C2	8734(2)	10757(2)	2837(1)	25(1)	1
C3	8486(2)	10393(2)	3448(1)	27(1)	1
C4	10287(2)	9609(2)	3669(1)	23(1)	1
C5	10810(2)	9039(2)	4257(1)	28(1)	1
C6	12693(2)	8366(2)	4328(1)	29(1)	1
C7	14054(2)	8248(2)	3823(1)	28(1)	1
C8	13545(2)	8816(2)	3232(1)	24(1)	1
C9	11670(2)	9497(2)	3159(1)	21(1)	1
C10	12096(2)	11079(2)	2142(1)	25(1)	1
C11	11117(2)	9719(2)	1927(1)	20(1)	1
C12	9429(2)	9741(2)	1437(1)	20(1)	1
C13	7777(2)	8615(2)	1562(1)	24(1)	1
C14	6141(2)	8615(2)	1045(1)	28(1)	1
C15	7110(2)	8371(2)	396(1)	27(1)	1
C16	8757(2)	9479(2)	260(1)	26(1)	1
C17	10383(2)	9517(2)	782(1)	24(1)	1

Table 3. Bond lengths [Å] and angles [°].

C1–C2	1.4776(19)
C1–C9	1.4818(18)
C1–C11	1.5289(17)
C1–C10	1.5336(19)
C2–C3	1.345(2)
C3–C4	1.456(2)
C4–C5	1.393(2)
C4–C9	1.4063(18)
C5–C6	1.383(2)
C6–C7	1.389(2)
C7–C8	1.395(2)
C8–C9	1.3826(19)
C10–C11	1.4889(19)
C11–C12	1.5085(18)
C12–C13	1.5243(19)
C12–C17	1.5289(18)
C13–C14	1.5232(19)
C14–C15	1.524(2)
C15–C16	1.515(2)
C16–C17	1.5279(18)
C2–C1–C9	104.61(11)
C2–C1–C11	123.57(11)
C9–C1–C11	121.90(12)
C2–C1–C10	123.12(13)
C9–C1–C10	120.56(11)
C11–C1–C10	58.18(9)
C3–C2–C1	109.82(13)
C2–C3–C4	109.72(12)
C5–C4–C9	119.89(13)
C5–C4–C3	132.25(13)
C9–C4–C3	107.84(11)
C6–C5–C4	119.02(13)
C5–C6–C7	121.08(13)
C6–C7–C8	120.34(14)
C9–C8–C7	118.89(13)
C8–C9–C4	120.78(12)
C8–C9–C1	131.20(12)
C4–C9–C1	108.01(11)
C11–C10–C1	60.75(9)
C10–C11–C12	120.52(12)
C10–C11–C1	61.07(9)
C12–C11–C1	121.55(11)
C11–C12–C13	112.55(11)
C11–C12–C17	108.88(10)
C13–C12–C17	110.38(11)
C14–C13–C12	111.54(11)
C13–C14–C15	110.81(12)
C16–C15–C14	111.17(12)
C15–C16–C17	111.53(11)
C16–C17–C12	112.01(11)

Symmetry transformations used to generate equivalent atoms:

Table 4. Anisotropic displacement parameters [$Å^2 \times 10^3$]. The anisotropic displacement factor exponent takes the form: $-2\pi^2[h^2a^{*2}U^{11} + \cdots + 2\,h\,k\,a^*\,b^*\,U^{12}]$.

Atom	U^{11}	U^{22}	U^{33}	U^{23}	U^{13}	U^{12}
C1	21(1)	21(1)	21(1)	−1(1)	0(1)	−3(1)
C2	21(1)	21(1)	32(1)	−6(1)	−1(1)	−1(1)
C3	24(1)	24(1)	31(1)	−8(1)	6(1)	−3(1)
C4	27(1)	19(1)	24(1)	−5(1)	4(1)	−6(1)
C5	39(1)	23(1)	22(1)	−3(1)	6(1)	−7(1)
C6	44(1)	23(1)	21(1)	1(1)	−4(1)	−5(1)
C7	30(1)	25(1)	29(1)	−1(1)	−6(1)	−2(1)
C8	23(1)	26(1)	23(1)	−2(1)	−1(1)	−4(1)
C9	23(1)	18(1)	21(1)	−2(1)	0(1)	−5(1)
C10	25(1)	24(1)	24(1)	2(1)	−1(1)	−5(1)
C11	20(1)	21(1)	20(1)	1(1)	0(1)	1(1)
C12	20(1)	20(1)	21(1)	0(1)	−1(1)	2(1)
C13	22(1)	24(1)	26(1)	0(1)	0(1)	0(1)
C14	21(1)	26(1)	35(1)	−3(1)	−4(1)	−1(1)
C15	26(1)	26(1)	29(1)	−3(1)	−7(1)	1(1)
C16	28(1)	29(1)	21(1)	0(1)	−5(1)	1(1)
C17	22(1)	27(1)	21(1)	2(1)	−2(1)	−3(1)

University of Southampton · Department of Chemistry

Crystallography Service

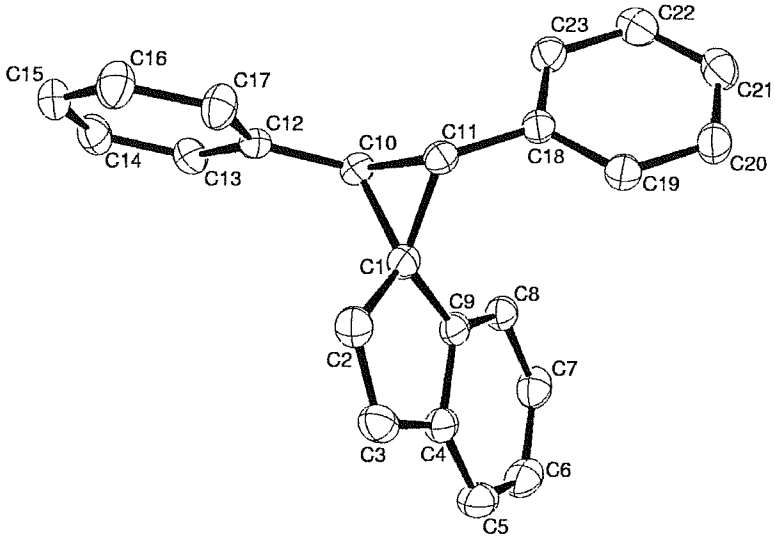

Table 1. Crystal data and structure refinement.

Compound name	***rac*-Spiro-[(2,3-diphenylcyclopropane)-1,1′-indene]**	
Empirical formula	$C_{23}H_{18}$	
Formula weight	294.37	
Temperature	120(2) K	
Wavelength	0.71073 Å	
Crystal system	P2	
Space group	Monoclinic	
Unit cell dimensions	a = 15.0885(5) Å	α = 90°
	b = 6.1161(2) Å	β = 104.8550(10)°
	c = 18.2311(8) Å	γ = 90°
Volume	1626.19(10) Å^3	
Z	4	
Density (calculated)	1.202 Mg / m^3	
Absorption coefficient	0.068 mm^{-1}	
F(000)	624	
Crystal	Rod; colourless	
Crystal size	0.60 × 0.10 × 0.10 mm^3	
θ range for data collection	2.99 – 27.47°	
Index ranges	$-19 \le h \le 19$, $-7 \le k \le 7$, $-23 \le l \le 23$	
Reflections collected	6567	
Independent reflections	3693 [R_{int} = 0.0418]	
Completeness to θ = 27.47°	99.5 %	
Absorption correction	Semi–empirical from equivalents	
Max. and min. transmission	0.9932 and 0.9932	
Refinement method	Full-matrix least-squares on F^2	
Data / restraints / parameters	3693 / 0 / 281	
Goodness-of-fit on F^2	0.976	
Final R indices [$F^2 > 2\sigma(F^2)$]	$R1$ = 0.0460, $wR2$ = 0.0943	
R indices (all data)	$R1$ = 0.0917, $wR2$ = 0.1092	
Largest diff. peak and hole	0.189 and –0.197 e Å^{-3}	

Diffractometer: *Enraf Nonius KappaCCD* area detector (ϕ scans and ω scans to fill *Ewald* sphere). **Data collection and cell refinement**: *Denzo* (Z. Otwinowski & W. Minor, *Methods in Enzymology* (1997) Vol. **276**: *Macromolecular Crystallography*, part A, pp. 307–326; C. W. Carter, Jr. & R. M. Sweet, Eds., Academic Press). **Absorption correction**: *SORTAV* (R. H. Blessing, Acta Cryst. A**51** (1995) 33–37; R. H. Blessing, J. Appl. Cryst. **30** (1997) 421–426). **Program used to solve structure**: *SHELXS97* (G. M. Sheldrick, Acta Cryst. (1990) A**46** 467–473). **Program used to refine structure**: *SHELXL97* (G. M. Sheldrick (1997), University of Göttingen, Germany).
Further information: http://www.soton.ac.uk/~xservice/strat.htm

Table 2. Atomic coordinates [$\times 10^4$], equivalent isotropic displacement parameters [$Å^2 \times 10^3$] and site occupancy factors. U_{eq} is defined as one third of the trace of the orthogonalized U^{ij} tensor.

Atom	*x*	*y*	*z*	U_{eq}	*S.o.f.*
C1	3010(1)	7328(2)	3651(1)	24(1)	1
C2	3478(1)	5260(2)	3939(1)	28(1)	1
C3	3133(1)	4436(2)	4485(1)	30(1)	1
C4	2429(1)	5911(2)	4621(1)	27(1)	1
C5	1916(1)	5855(3)	5150(1)	35(1)	1
C6	1338(1)	7586(3)	5184(1)	38(1)	1
C7	1270(1)	9363(3)	4696(1)	33(1)	1
C8	1778(1)	9429(2)	4158(1)	27(1)	1
C9	2354(1)	7699(2)	4120(1)	23(1)	1
C10	3506(1)	9244(2)	3370(1)	22(1)	1
C11	2822(1)	7923(2)	2807(1)	23(1)	1
C12	4514(1)	9160(2)	3464(1)	22(1)	1
C13	5075(1)	10520(2)	4000(1)	26(1)	1
C14	6019(1)	10504(2)	4114(1)	31(1)	1
C15	6424(1)	9089(2)	3704(1)	31(1)	1
C16	5877(1)	7716(2)	3175(1)	34(1)	1
C17	4931(1)	7768(2)	3050(1)	30(1)	1
C18	1901(1)	8768(2)	2391(1)	23(1)	1
C19	1150(1)	7389(2)	2287(1)	28(1)	1
C20	288(1)	8059(3)	1878(1)	34(1)	1
C21	166(1)	10128(3)	1558(1)	34(1)	1
C22	911(1)	11524(2)	1667(1)	33(1)	1
C23	1771(1)	10859(2)	2085(1)	27(1)	1

Table 3. Bond lengths [Å] and angles [°].

C1–C2	1.4776(18)
C1–C9	1.480(2)
C1–C11	1.5353(19)
C1–C10	1.5466(18)
C2–C3	1.336(2)
C3–C4	1.462(2)
C4–C5	1.384(2)
C4–C9	1.4110(19)
C5–C6	1.383(2)
C6–C7	1.391(2)
C7–C8	1.392(2)
C8–C9	1.3831(19)
C10–C12	1.4886(19)
C10–C11	1.4916(19)
C11–C18	1.4951(19)
C12–C17	1.391(2)
C12–C13	1.3919(19)
C13–C14	1.387(2)
C14–C15	1.384(2)
C15–C16	1.382(2)
C16–C17	1.387(2)
C18–C19	1.3863(19)
C18–C23	1.389(2)
C19–C20	1.385(2)
C20–C21	1.386(2)
C21–C22	1.384(2)
C22–C23	1.387(2)
C2–C1–C9	104.84(12)
C2–C1–C11	120.44(12)
C9–C1–C11	124.25(12)
C2–C1–C10	122.57(12)
C9–C1–C10	121.78(11)
C11–C1–C10	57.89(9)
C3–C2–C1	110.16(14)
C2–C3–C4	109.44(13)
C5–C4–C9	120.34(14)
C5–C4–C3	131.54(14)
C9–C4–C3	108.01(13)
C6–C5–C4	118.91(15)
C5–C6–C7	120.94(16)
C6–C7–C8	120.63(15)
C9–C8–C7	118.71(14)
C8–C9–C4	120.45(13)
C8–C9–C1	131.94(12)
C4–C9–C1	107.51(12)
C12–C10–C11	124.53(12)
C12–C10–C1	120.18(11)
C11–C10–C1	60.68(9)
C10–C11–C18	123.38(12)
C10–C11–C1	61.43(9)
C18–C11–C1	119.95(12)
C17–C12–C13	118.03(13)
C17–C12–C10	123.32(12)
C13–C12–C10	118.64(12)
C14–C13–C12	121.11(14)
C15–C14–C13	120.20(14)
C16–C15–C14	119.27(15)
C15–C16–C17	120.48(15)
C16–C17–C12	120.88(14)
C19–C18–C23	118.62(13)

C19–C18–C11	118.71(12)
C23–C18–C11	122.65(13)
C20–C19–C18	121.06(14)
C19–C20–C21	120.08(15)
C22–C21–C20	119.22(15)
C21–C22–C23	120.57(15)
C22–C23–C18	120.43(14)

Symmetry transformations used to generate equivalent atoms:

Table 4. Anisotropic displacement parameters [$Å^2 \times 10^3$]. The anisotropic displacement factor exponent takes the form: $-2\pi^2[h^2a^{*2}U^{11} + \cdots + 2\,h\,k\,a^*\,b^*\,U^{12}]$.

Atom	U^{11}	U^{22}	U^{33}	U^{23}	U^{13}	U^{12}
C1	22(1)	24(1)	25(1)	1(1)	6(1)	−1(1)
C2	27(1)	25(1)	32(1)	0(1)	6(1)	0(1)
C3	33(1)	26(1)	29(1)	4(1)	4(1)	−2(1)
C4	26(1)	31(1)	22(1)	0(1)	4(1)	−8(1)
C5	39(1)	40(1)	24(1)	3(1)	8(1)	−10(1)
C6	37(1)	54(1)	25(1)	−6(1)	14(1)	−12(1)
C7	28(1)	41(1)	31(1)	−8(1)	10(1)	−2(1)
C8	24(1)	32(1)	24(1)	−2(1)	6(1)	−3(1)
C9	21(1)	28(1)	20(1)	−2(1)	4(1)	−5(1)
C10	23(1)	21(1)	25(1)	0(1)	8(1)	−1(1)
C11	23(1)	24(1)	22(1)	−1(1)	8(1)	0(1)
C12	21(1)	22(1)	23(1)	5(1)	6(1)	0(1)
C13	26(1)	28(1)	23(1)	−1(1)	3(1)	1(1)
C14	26(1)	33(1)	29(1)	−1(1)	−1(1)	−2(1)
C15	20(1)	38(1)	32(1)	5(1)	3(1)	0(1)
C16	26(1)	40(1)	37(1)	−5(1)	10(1)	2(1)
C17	24(1)	34(1)	32(1)	−9(1)	7(1)	−4(1)
C18	21(1)	30(1)	19(1)	−3(1)	7(1)	1(1)
C19	26(1)	34(1)	23(1)	0(1)	7(1)	−2(1)
C20	24(1)	50(1)	27(1)	−5(1)	6(1)	−6(1)
C21	26(1)	49(1)	26(1)	−2(1)	6(1)	9(1)
C22	35(1)	36(1)	29(1)	1(1)	10(1)	9(1)
C23	25(1)	31(1)	27(1)	−1(1)	9(1)	0(1)

University of Southampton · Department of Chemistry

Crystallography Service

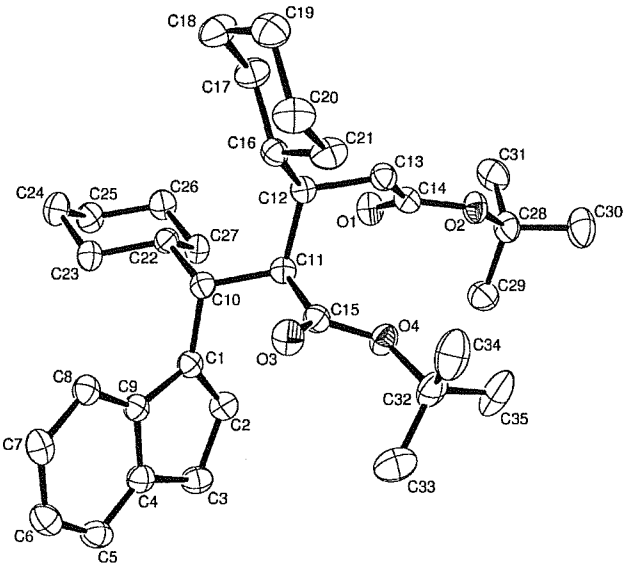

Table 1. Crystal data and structure refinement.

Compound name	***rac*-3-Cyclohexyl-2-[cyclohexyl-(3H-inden-1-yl)-methyl]-pentanedioic acid di-*tert*-butyl ester**	
Empirical formula	$C_{35}H_{52}O_4$	
Formula weight	536.77	
Temperature	120(2) K	
Wavelength	0.71073 Å	
Crystal system	Monoclinic	
Space group	$P2_1/c$	
Unit cell dimensions	$a = 11.7812(2)$ Å	$\alpha = 90°$
	$b = 28.4782(6)$ Å	$\beta = 114.2870(10)°$
	$c = 10.6209(2)$ Å	$\gamma = 90°$
Volume	3248.02(11) Å^3	
Z	4	
Density (calculated)	1.098 Mg / m^3	
Absorption coefficient	0.070 mm^{-1}	
F(000)	1176	
Crystal	Block; yellow	
Crystal size	0.15 x 0.05 x 0.04 mm^3	
θ range for data collection	3.01 – 27.08°	
Index ranges	$-15 \le h \le 15$, $-36 \le k \le 36$, $-11 \le l \le 13$	
Reflections collected	34155	
Independent reflections	6924 [$R_{int} = 0.0635$]	
Completeness to $\theta = 27.08°$	97.0 %	
Absorption correction	Semi–empirical from equivalents	
Max. and min. transmission	0.9931 and 0.9931	
Refinement method	Full-matrix least-squares on F^2	
Data / restraints / parameters	6924 / 0 / 353	
Goodness-of-fit on F^2	1.023	
Final R indices [$F^2 > 2\sigma(F^2)$]	$R1 = 0.0536$, $wR2 = 0.1133$	
R indices (all data)	$R1 = 0.0908$, $wR2 = 0.1280$	
Largest diff. peak and hole	0.245 and –0.204 e Å^{-3}	

Diffractometer: *Enraf Nonius KappaCCD* area detector (ϕ scans and ω scans to fill *Ewald* sphere). **Data collection and cell refinement**: *Denzo* (Z. Otwinowski & W. Minor, *Methods in Enzymology* (1997) Vol. **276**: *Macromolecular Crystallography*, part A, pp. 307–326; C. W. Carter, Jr. & R. M. Sweet, Eds., Academic Press). **Absorption correction**: *SORTAV* (R. H. Blessing, Acta Cryst. A**51** (1995) 33–37; R. H. Blessing, J. Appl. Cryst. **30** (1997) 421–426). **Program used to solve structure**: *SHELXS97* (G. M. Sheldrick, Acta Cryst. (1990) A**46** 467–473). **Program used to refine structure**: *SHELXL97* (G. M. Sheldrick (1997), University of Göttingen, Germany).
Further information: http://www.soton.ac.uk/~xservice/strat.htm

Table 2. Atomic coordinates [$\times 10^4$], equivalent isotropic displacement parameters [$Å^2 \times 10^3$] and site occupancy factors. U_{eq} is defined as one third of the trace of the orthogonalized U^{ij} tensor.

Atom	*x*	*y*	*z*	U_{eq}	*S.o.f.*
C1	−1668(2)	754(1)	5814(2)	25(1)	1
C2	−620(2)	504(1)	6431(2)	30(1)	1
C3	−422(2)	358(1)	7864(2)	33(1)	1
C4	−1521(2)	573(1)	8018(2)	28(1)	1
C5	−1844(2)	578(1)	9127(2)	33(1)	1
C6	−2905(2)	820(1)	9007(2)	33(1)	1
C7	−3642(2)	1049(1)	7792(2)	32(1)	1
C8	−3327(2)	1042(1)	6669(2)	28(1)	1
C9	−2260(2)	805(1)	6784(2)	24(1)	1
C10	−2184(2)	970(1)	4389(2)	24(1)	1
C11	−1135(2)	1221(1)	4143(2)	24(1)	1
C12	−1559(1)	1463(1)	2709(2)	24(1)	1
C13	−455(2)	1631(1)	2418(2)	27(1)	1
C14	430(2)	1247(1)	2445(2)	27(1)	1
C15	−494(2)	1564(1)	5316(2)	26(1)	1
C16	−2550(2)	1854(1)	2433(2)	26(1)	1
C17	−3492(2)	1855(1)	927(2)	35(1)	1
C18	−4513(2)	2221(1)	642(2)	42(1)	1
C19	−3983(2)	2709(1)	1099(2)	39(1)	1
C20	−3060(2)	2704(1)	2602(2)	40(1)	1
C21	−2031(2)	2348(1)	2839(2)	36(1)	1
C22	−2917(1)	610(1)	3245(2)	25(1)	1
C23	−3969(2)	382(1)	3520(2)	30(1)	1
C24	−4758(2)	60(1)	2338(2)	36(1)	1
C25	−3962(2)	−319(1)	2094(2)	35(1)	1
C26	−2890(2)	−104(1)	1848(2)	34(1)	1
C27	−2115(2)	228(1)	3014(2)	29(1)	1
C28	2559(2)	1121(1)	2645(2)	33(1)	1
C29	2947(2)	792(1)	3878(2)	41(1)	1
C30	3575(2)	1478(1)	2821(2)	48(1)	1
C31	2170(2)	860(1)	1291(2)	44(1)	1
C32	1586(2)	1892(1)	6700(2)	39(1)	1
C33	1629(2)	1734(1)	8074(2)	64(1)	1
C34	1204(2)	2398(1)	6389(2)	56(1)	1
C35	2818(2)	1803(1)	6612(2)	60(1)	1
O1	180(1)	834(1)	2310(1)	33(1)	1
O2	1537(1)	1428(1)	2619(1)	31(1)	1
O3	−999(1)	1790(1)	5893(1)	35(1)	1
O4	733(1)	1584(1)	5604(1)	31(1)	1

Table 3. Bond lengths [Å] and angles [°].

C1–C2	1.340(2)
C1–C9	1.469(2)
C1–C10	1.511(2)
C2–C3	1.501(2)
C3–C4	1.501(2)
C4–C5	1.379(2)
C4–C9	1.404(2)
C5–C6	1.385(2)
C6–C7	1.386(2)
C7–C8	1.388(2)
C8–C9	1.387(2)
C10–C11	1.540(2)
C10–C22	1.553(2)
C11–C15	1.518(2)
C11–C12	1.555(2)
C12–C13	1.532(2)
C12–C16	1.552(2)
C13–C14	1.505(2)
C14–O1	1.2057(19)
C14–O2	1.3430(19)
C15–O3	1.2021(19)
C15–O4	1.3497(19)
C16–C21	1.524(2)
C16–C17	1.526(2)
C17–C18	1.524(2)
C18–C19	1.519(3)
C19–C20	1.518(3)
C20–C21	1.521(2)
C22–C27	1.524(2)
C22–C23	1.530(2)
C23–C24	1.523(2)
C24–C25	1.520(2)
C25–C26	1.520(2)
C26–C27	1.528(2)
C28–O2	1.4776(19)
C28–C31	1.512(3)
C28–C29	1.520(2)
C28–C30	1.522(3)
C32–O4	1.474(2)
C32–C34	1.505(3)
C32–C33	1.508(3)
C32–C35	1.513(3)
C2–C1–C9	108.48(14)
C2–C1–C10	128.11(14)
C9–C1–C10	123.37(14)
C1–C2–C3	111.76(15)
C4–C3–C2	102.47(13)
C5–C4–C9	120.61(16)
C5–C4–C3	130.60(16)
C9–C4–C3	108.77(14)
C4–C5–C6	118.81(16)
C5–C6–C7	121.03(16)
C6–C7–C8	120.42(16)
C9–C8–C7	118.98(15)
C8–C9–C4	120.14(15)
C8–C9–C1	131.32(14)
C4–C9–C1	108.50(14)
C1–C10–C11	109.79(13)
C1–C10–C22	112.25(13)
C11–C10–C22	113.60(12)

C15–C11–C10	108.85(13)
C15–C11–C12	111.72(12)
C10–C11–C12	114.47(13)
C13–C12–C16	111.83(12)
C13–C12–C11	112.25(13)
C16–C12–C11	114.57(12)
C14–C13–C12	114.01(13)
O1–C14–O2	124.51(15)
O1–C14–C13	125.02(15)
O2–C14–C13	110.46(13)
O3–C15–O4	124.83(15)
O3–C15–C11	125.41(15)
O4–C15–C11	109.76(13)
C21–C16–C17	109.16(13)
C21–C16–C12	115.21(13)
C17–C16–C12	111.44(13)
C18–C17–C16	112.60(14)
C19–C18–C17	112.01(15)
C20–C19–C18	110.53(15)
C19–C20–C21	110.89(15)
C20–C21–C16	111.67(15)
C27–C22–C23	109.42(13)
C27–C22–C10	114.55(13)
C23–C22–C10	111.37(13)
C24–C23–C22	111.45(14)
C25–C24–C23	110.94(14)
C24–C25–C26	110.97(14)
C25–C26–C27	111.79(14)
C22–C27–C26	111.68(13)
O2–C28–C31	110.26(14)
O2–C28–C29	109.56(13)
C31–C28–C29	112.53(15)
O2–C28–C30	101.64(13)
C31–C28–C30	111.07(15)
C29–C28–C30	111.25(16)
O4–C32–C34	110.51(16)
O4–C32–C33	109.14(15)
C34–C32–C33	112.71(18)
O4–C32–C35	102.16(14)
C34–C32–C35	110.80(18)
C33–C32–C35	111.00(19)
C14–O2–C28	120.88(12)
C15–O4–C32	121.51(13)

Symmetry transformations used to generate equivalent atoms:

Table 4. Anisotropic displacement parameters [$Å^2 \times 10^3$]. The anisotropic displacement factor exponent takes the form: $-2\pi^2[h^2a^{*2}U^{11} + \cdots + 2\,h\,k\,a^*\,b^*\,U^{12}]$.

Atom	U^{11}	U^{22}	U^{33}	U^{23}	U^{13}	U^{12}
C1	26(1)	21(1)	27(1)	−1(1)	10(1)	−2(1)
C2	30(1)	29(1)	31(1)	−2(1)	12(1)	2(1)
C3	35(1)	30(1)	29(1)	4(1)	9(1)	4(1)
C4	30(1)	25(1)	27(1)	−2(1)	10(1)	−4(1)
C5	41(1)	29(1)	25(1)	−1(1)	10(1)	−6(1)
C6	45(1)	30(1)	31(1)	−6(1)	21(1)	−7(1)
C7	35(1)	26(1)	40(1)	−4(1)	22(1)	−4(1)
C8	28(1)	24(1)	31(1)	0(1)	12(1)	−2(1)
C9	27(1)	21(1)	26(1)	−2(1)	11(1)	−4(1)
C10	24(1)	23(1)	27(1)	1(1)	11(1)	3(1)
C11	25(1)	22(1)	26(1)	0(1)	11(1)	2(1)
C12	25(1)	22(1)	26(1)	−1(1)	11(1)	0(1)
C13	27(1)	25(1)	30(1)	2(1)	12(1)	0(1)
C14	30(1)	29(1)	26(1)	1(1)	14(1)	0(1)
C15	27(1)	23(1)	28(1)	2(1)	11(1)	−1(1)
C16	27(1)	26(1)	28(1)	2(1)	14(1)	2(1)
C17	36(1)	32(1)	33(1)	0(1)	9(1)	6(1)
C18	34(1)	42(1)	38(1)	5(1)	5(1)	6(1)
C19	41(1)	34(1)	42(1)	8(1)	16(1)	12(1)
C20	50(1)	29(1)	40(1)	0(1)	16(1)	10(1)
C21	39(1)	27(1)	36(1)	0(1)	10(1)	5(1)
C22	24(1)	25(1)	26(1)	1(1)	9(1)	−1(1)
C23	27(1)	28(1)	37(1)	0(1)	15(1)	0(1)
C24	30(1)	33(1)	44(1)	−5(1)	15(1)	−7(1)
C25	37(1)	31(1)	36(1)	−6(1)	15(1)	−7(1)
C26	36(1)	33(1)	35(1)	−6(1)	17(1)	−4(1)
C27	27(1)	30(1)	33(1)	−5(1)	14(1)	−3(1)
C28	27(1)	33(1)	42(1)	5(1)	19(1)	6(1)
C29	35(1)	47(1)	41(1)	9(1)	16(1)	9(1)
C30	32(1)	44(1)	73(2)	10(1)	27(1)	4(1)
C31	49(1)	49(1)	45(1)	2(1)	30(1)	8(1)
C32	33(1)	44(1)	36(1)	−16(1)	10(1)	−11(1)
C33	60(2)	86(2)	34(1)	−13(1)	9(1)	−17(1)
C34	51(1)	38(1)	77(2)	−20(1)	25(1)	−16(1)
C35	30(1)	78(2)	64(2)	−32(1)	12(1)	−12(1)
O1	33(1)	27(1)	43(1)	−4(1)	20(1)	−1(1)
O2	26(1)	30(1)	41(1)	2(1)	18(1)	1(1)
O3	37(1)	33(1)	38(1)	−10(1)	19(1)	−2(1)
O4	26(1)	33(1)	31(1)	−8(1)	10(1)	−4(1)

University of Southampton · Department of Chemistry

Crystallography Service

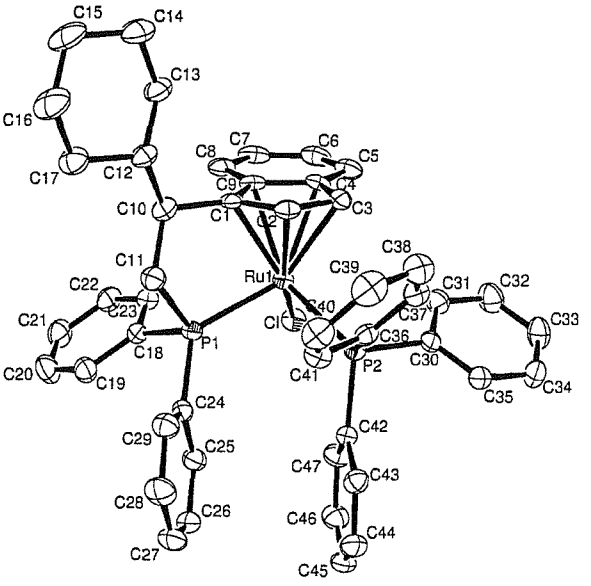

Note: Two solvent benzene molecules are present, numbered C48-C53 and C54-C59.

Table 1. Crystal data and structure refinement.

Compound name	***rac*-(η^5:η^1-indenyl-CH(Cy)CH_2PPh_2)Ru^{II}(PPh_3)Cl**	
Empirical formula	$C_{47}H_{45}ClP_2Ru$	
Formula weight	808.33	
Temperature	150(2) K	
Wavelength	0.71073 Å	
Crystal system	Monoclinic	
Space group	$P2_1/c$	
Unit cell dimensions	a = 25.905(5) Å	α = 90°
	b = 15.323(3) Å	β = 94.73(3)°
	c = 12.178(2) Å	γ = 90°
Volume	4817.5(17) $Å^3$	
Z	4	
Density (calculated)	1.330 Mg / m^3	
Absorption coefficient	0.486 mm^{-1}	
F(000)	2008	
Crystal	Plate; Orange/red	
Crystal size	0.10 × 0.10 × 0.03 mm^3	
θ range for data collection	3.09 – 27.50°	
Index ranges	$-33 \le h \le 33$, $-19 \le k \le 18$, $-15 \le l \le 15$	
Reflections collected	46096	
Independent reflections	10769 [R_{int} = 0.0779]	
Completeness to θ = 27.50°	97.4 %	
Absorption correction	Semi–empirical from equivalents	
Max. and min. transmission	0.9856 and 0.9530	
Refinement method	Full-matrix least-squares on F^2	
Data / restraints / parameters	10769 / 0 / 569	
Goodness-of-fit on F^2	0.996	
Final R indices [$F^2 > 2\sigma(F^2)$]	$R1$ = 0.0433, $wR2$ = 0.0842	
R indices (all data)	$R1$ = 0.0876, $wR2$ = 0.0977	
Largest diff. peak and hole	0.719 and –0.819 e $Å^{-3}$	

Diffractometer: *Enraf Nonius KappaCCD* area detector (ϕ scans and ω scans to fill *Ewald* sphere). **Data collection and cell refinement**: *Denzo* (Z. Otwinowski & W. Minor, *Methods in Enzymology* (1997) Vol. **276**: *Macromolecular Crystallography*, part A, pp. 307–326; C. W. Carter, Jr. & R. M. Sweet, Eds., Academic Press). **Absorption correction**: *SORTAV* (R. H. Blessing, Acta Cryst. A**51** (1995) 33–37; R. H. Blessing, J. Appl. Cryst. **30** (1997) 421–426). **Program used to solve structure**: *SHELXS97* (G. M. Sheldrick, Acta Cryst. (1990) A**46** 467–473). **Program used to refine structure**: *SHELXL97* (G. M. Sheldrick (1997), University of Göttingen, Germany).
Further information: http://www.soton.ac.uk/~xservice/strat.htm

Table 2. Atomic coordinates [× 10^4], equivalent isotropic displacement parameters [$Å^2$ × 10^3] and site occupancy factors. U_{eq} is defined as one third of the trace of the orthogonalized U^{ij} tensor.

Atom	*x*	*y*	*z*	U_{eq}	*S.o.f.*
C1	2116(1)	4595(2)	8002(2)	21(1)	1
C2	2553(1)	4028(2)	7882(2)	23(1)	1
C3	2993(1)	4403(2)	8496(2)	25(1)	1
C4	2835(1)	5169(2)	9019(2)	23(1)	1
C5	3115(1)	5786(2)	9720(2)	32(1)	1
C6	2855(1)	6472(2)	10097(2)	35(1)	1
C7	2317(1)	6586(2)	9843(2)	33(1)	1
C8	2030(1)	6016(2)	9179(2)	29(1)	1
C9	2289(1)	5289(2)	8726(2)	24(1)	1
C10	1576(1)	4462(2)	7466(2)	27(1)	1
C11	1591(1)	4455(2)	6210(2)	27(1)	1
C12	1320(1)	3660(2)	7947(2)	27(1)	1
C13	1327(1)	3729(2)	9194(2)	35(1)	1
C14	1071(1)	2948(2)	9711(2)	44(1)	1
C15	532(1)	2791(2)	9194(3)	51(1)	1
C16	521(2)	2710(2)	7955(3)	50(1)	1
C17	773(1)	3486(2)	7439(2)	37(1)	1
C18	1585(1)	6316(2)	5810(2)	23(1)	1
C19	1204(1)	6484(2)	4946(2)	32(1)	1
C20	882(1)	7189(2)	4983(2)	40(1)	1
C21	925(1)	7756(2)	5874(2)	38(1)	1
C22	1302(1)	7603(2)	6723(2)	32(1)	1
C23	1628(1)	6892(2)	6685(2)	26(1)	1
C24	2049(1)	5199(2)	4332(2)	23(1)	1
C25	2243(1)	5880(2)	3737(2)	27(1)	1
C26	2289(1)	5807(2)	2617(2)	33(1)	1
C27	2152(1)	5039(2)	2081(2)	39(1)	1
C28	1964(1)	4356(2)	2655(2)	39(1)	1
C29	1909(1)	4434(2)	3780(2)	31(1)	1
C30	4003(1)	5110(2)	6728(2)	24(1)	1
C31	4064(1)	5623(2)	7676(2)	29(1)	1
C32	4553(1)	5853(2)	8119(2)	40(1)	1
C33	4985(1)	5582(2)	7627(3)	41(1)	1
C34	4932(1)	5069(2)	6681(2)	36(1)	1
C35	4443(1)	4842(2)	6237(2)	28(1)	1
C36	3331(1)	3671(2)	5994(2)	23(1)	1
C37	3629(1)	3147(2)	6725(2)	28(1)	1
C38	3533(1)	2256(2)	6772(2)	36(1)	1
C39	3149(1)	1875(2)	6079(3)	42(1)	1
C40	2859(1)	2393(2)	5323(2)	36(1)	1
C41	2948(1)	3281(2)	5288(2)	28(1)	1
C42	3431(1)	5263(2)	4712(2)	21(1)	1
C43	3524(1)	4736(2)	3817(2)	27(1)	1
C44	3621(1)	5119(2)	2823(2)	32(1)	1
C45	3634(1)	6009(2)	2708(2)	31(1)	1
C46	3551(1)	6538(2)	3594(2)	33(1)	1
C47	3446(1)	6166(2)	4588(2)	30(1)	1
P1	2015(1)	5355(1)	5816(1)	21(1)	1
P2	3350(1)	4862(1)	6103(1)	20(1)	1
Cl	2929(1)	6798(1)	7032(1)	27(1)	1
Ru1	2688(1)	5281(1)	7133(1)	18(1)	1
C48	4509(1)	1911(2)	4778(3)	49(1)	1
C49	4756(2)	2611(2)	5281(3)	53(1)	1
C50	5220(2)	2902(2)	4939(3)	56(1)	1
C51	5438(2)	2490(3)	4090(3)	58(1)	1
C52	5188(2)	1788(3)	3595(3)	62(1)	1
C53	4730(2)	1487(3)	3938(3)	54(1)	1
C54	576(2)	4948(2)	2504(3)	55(1)	1
C55	341(2)	4766(2)	3426(3)	59(1)	1
C56	−112(2)	4343(2)	3371(4)	66(1)	1
C57	−346(2)	4082(2)	2397(5)	69(1)	1
C58	−121(2)	4264(2)	1451(4)	67(1)	1

C59	351(2)	4696(2)	1503(3)	60(1)	1

Table 3. Bond lengths [Å] and angles [°].

C1–C9	1.430(3)
C1–C2	1.444(4)
C1–C10	1.508(4)
C1–Ru1	2.163(3)
C2–C3	1.432(4)
C2–Ru1	2.166(2)
C3–C4	1.412(4)
C3–Ru1	2.231(2)
C4–C5	1.430(4)
C4–C9	1.441(4)
C4–Ru1	2.304(2)
C5–C6	1.349(4)
C6–C7	1.413(4)
C7–C8	1.366(4)
C8–C9	1.434(4)
C9–Ru1	2.272(3)
C10–C11	1.533(4)
C10–C12	1.536(4)
C11–P1	1.850(3)
C12–C17	1.520(4)
C12–C13	1.521(4)
C13–C14	1.529(4)
C14–C15	1.504(5)
C15–C16	1.512(4)
C16–C17	1.519(4)
C18–C23	1.380(4)
C18–C19	1.404(4)
C18–P1	1.847(3)
C19–C20	1.370(4)
C20–C21	1.387(4)
C21–C22	1.383(4)
C22–C23	1.382(4)
C24–C29	1.385(4)
C24–C25	1.388(4)
C24–P1	1.832(3)
C25–C26	1.383(4)
C26–C27	1.378(4)
C27–C28	1.371(4)
C28–C29	1.395(4)
C30–C35	1.391(4)
C30–C31	1.394(4)
C30–P2	1.837(3)
C31–C32	1.381(4)
C32–C33	1.376(5)
C33–C34	1.391(4)
C34–C35	1.381(4)
C36–C37	1.385(4)
C36–C41	1.394(4)
C36–P2	1.829(3)
C37–C38	1.390(4)
C38–C39	1.381(4)
C39–C40	1.388(4)
C40–C41	1.381(4)
C42–C47	1.393(4)
C42–C43	1.393(4)
C42–P2	1.830(3)
C43–C44	1.387(4)
C44–C45	1.371(4)
C45–C46	1.380(4)
C46–C47	1.386(4)
P1–Ru1	2.2721(10)

P2–Ru1	2.2989(9)
Cl–Ru1	2.4125(8)
C48–C49	1.367(5)
C48–C53	1.375(5)
C49–C50	1.379(5)
C50–C51	1.372(5)
C51–C52	1.370(5)
C52–C53	1.370(5)
C54–C55	1.349(5)
C54–C59	1.362(5)
C55–C56	1.339(6)
C56–C57	1.347(6)
C57–C58	1.362(6)
C58–C59	1.388(6)

C9–C1–C2	107.5(2)
C9–C1–C10	126.9(2)
C2–C1–C10	125.6(2)
C9–C1–Ru1	75.37(15)
C2–C1–Ru1	70.64(15)
C10–C1–Ru1	120.14(16)
C3–C2–C1	107.6(2)
C3–C2–Ru1	73.49(15)
C1–C2–Ru1	70.40(14)
C4–C3–C2	108.7(2)
C4–C3–Ru1	74.69(14)
C2–C3–Ru1	68.54(14)
C3–C4–C5	131.9(3)
C3–C4–C9	108.0(2)
C5–C4–C9	120.1(2)
C3–C4–Ru1	69.07(13)
C5–C4–Ru1	125.43(18)
C9–C4–Ru1	70.42(14)
C6–C5–C4	118.4(3)
C5–C6–C7	122.1(3)
C8–C7–C6	121.9(3)
C7–C8–C9	118.3(3)
C1–C9–C8	133.0(3)
C1–C9–C4	108.0(2)
C8–C9–C4	119.0(2)
C1–C9–Ru1	67.10(14)
C8–C9–Ru1	126.37(17)
C4–C9–Ru1	72.88(15)
C1–C10–C11	109.5(2)
C1–C10–C12	111.0(2)
C11–C10–C12	114.9(2)
C10–C11–P1	108.54(18)
C17–C12–C13	110.7(2)
C17–C12–C10	113.7(2)
C13–C12–C10	110.7(2)
C12–C13–C14	112.7(2)
C15–C14–C13	111.9(3)
C14–C15–C16	111.8(3)
C15–C16–C17	112.1(3)
C16–C17–C12	112.8(3)
C23–C18–C19	118.0(2)
C23–C18–P1	119.73(19)
C19–C18–P1	122.3(2)
C20–C19–C18	120.8(3)
C19–C20–C21	120.7(3)
C22–C21–C20	119.0(3)
C23–C22–C21	120.4(3)
C18–C23–C22	121.2(3)

C29–C24–C25	118.3(2)
C29–C24–P1	123.9(2)
C25–C24–P1	117.8(2)
C26–C25–C24	121.3(3)
C27–C26–C25	119.8(3)
C28–C27–C26	119.9(3)
C27–C28–C29	120.3(3)
C24–C29–C28	120.4(3)
C35–C30–C31	118.8(3)
C35–C30–P2	121.3(2)
C31–C30–P2	119.9(2)
C32–C31–C30	120.4(3)
C33–C32–C31	120.3(3)
C32–C33–C34	120.2(3)
C35–C34–C33	119.5(3)
C34–C35–C30	120.9(3)
C37–C36–C41	118.6(2)
C37–C36–P2	121.5(2)
C41–C36–P2	119.1(2)
C36–C37–C38	120.3(3)
C39–C38–C37	120.8(3)
C38–C39–C40	119.2(3)
C41–C40–C39	120.1(3)
C40–C41–C36	121.0(3)
C47–C42–C43	118.9(2)
C47–C42–P2	116.11(19)
C43–C42–P2	124.7(2)
C44–C43–C42	119.5(3)
C45–C44–C43	121.2(3)
C44–C45–C46	119.8(3)
C45–C46–C47	119.8(3)
C46–C47–C42	120.8(3)
C24–P1–C18	100.32(11)
C24–P1–C11	103.68(12)
C18–P1–C11	102.98(13)
C24–P1–Ru1	126.35(9)
C18–P1–Ru1	118.03(8)
C11–P1–Ru1	102.52(9)
C36–P2–C42	105.83(11)
C36–P2–C30	104.74(12)
C42–P2–C30	98.19(12)
C36–P2–Ru1	107.55(9)
C42–P2–Ru1	123.95(9)
C30–P2–Ru1	114.78(9)
C1–Ru1–C2	38.96(10)
C1–Ru1–C3	63.75(10)
C2–Ru1–C3	37.97(10)
C1–Ru1–C9	37.53(9)
C2–Ru1–C9	62.93(9)
C3–Ru1–C9	61.69(10)
C1–Ru1–P1	81.56(7)
C2–Ru1–P1	101.55(7)
C3–Ru1–P1	139.44(7)
C9–Ru1–P1	103.10(8)
C1–Ru1–P2	134.70(7)
C2–Ru1–P2	97.80(8)
C3–Ru1–P2	90.16(8)
C9–Ru1–P2	151.60(7)
P1–Ru1–P2	101.10(3)
C1–Ru1–C4	62.58(10)
C2–Ru1–C4	62.18(9)
C3–Ru1–C4	36.24(9)
C9–Ru1–C4	36.70(10)

P1–Ru1–C4	139.63(8)
P2–Ru1–C4	116.97(8)
C1–Ru1–Cl	133.16(7)
C2–Ru1–Cl	157.93(7)
C3–Ru1–Cl	122.78(7)
C9–Ru1–Cl	100.14(7)
P1–Ru1–Cl	95.92(2)
P2–Ru1–Cl	91.89(3)
C4–Ru1–Cl	95.76(7)
C49–C48–C53	119.7(4)
C48–C49–C50	120.3(3)
C51–C50–C49	120.1(4)
C52–C51–C50	118.9(4)
C51–C52–C53	121.3(4)
C52–C53–C48	119.5(4)
C55–C54–C59	119.9(4)
C56–C55–C54	120.7(4)
C55–C56–C57	121.2(4)
C56–C57–C58	119.4(4)
C57–C58–C59	119.8(4)
C54–C59–C58	119.0(4)

Symmetry transformations used to generate equivalent atoms:

Table 4. Anisotropic displacement parameters [$Å^2 \times 10^3$]. The anisotropic displacement factor exponent takes the form: $-2\pi^2[h^2a^{*2}U^{11} + \cdots + 2\,h\,k\,a^*\,b^*\,U^{12}]$.

Atom	U^{11}	U^{22}	U^{33}	U^{23}	U^{13}	U^{12}
C1	26(2)	24(2)	15(1)	6(1)	5(1)	−5(1)
C2	32(2)	17(1)	19(1)	2(1)	6(1)	0(1)
C3	25(2)	27(2)	22(1)	7(1)	2(1)	6(1)
C4	33(2)	25(2)	12(1)	4(1)	1(1)	1(1)
C5	41(2)	35(2)	18(1)	1(1)	−2(1)	−5(2)
C6	53(2)	34(2)	18(1)	0(1)	0(1)	−9(2)
C7	60(2)	23(2)	18(1)	1(1)	11(1)	4(2)
C8	40(2)	24(2)	24(1)	9(1)	10(1)	7(1)
C9	36(2)	21(1)	14(1)	4(1)	9(1)	1(1)
C10	28(2)	26(2)	29(2)	1(1)	7(1)	−4(1)
C11	28(2)	27(2)	27(2)	1(1)	1(1)	−7(1)
C12	29(2)	21(2)	32(2)	3(1)	10(1)	−2(1)
C13	33(2)	41(2)	33(2)	5(1)	8(1)	−10(2)
C14	50(2)	43(2)	41(2)	14(2)	14(2)	−9(2)
C15	55(3)	49(2)	51(2)	2(2)	23(2)	−27(2)
C16	53(2)	49(2)	51(2)	−1(2)	13(2)	−27(2)
C17	38(2)	36(2)	37(2)	−1(1)	6(1)	−11(2)
C18	20(2)	25(2)	23(1)	3(1)	3(1)	1(1)
C19	29(2)	36(2)	29(2)	−3(1)	0(1)	3(1)
C20	35(2)	44(2)	39(2)	3(2)	−7(2)	10(2)
C21	32(2)	35(2)	46(2)	6(2)	5(2)	10(1)
C22	33(2)	31(2)	33(2)	−4(1)	8(1)	4(1)
C23	25(2)	30(2)	24(1)	3(1)	2(1)	0(1)
C24	21(2)	26(2)	22(1)	0(1)	0(1)	4(1)
C25	30(2)	29(2)	24(1)	2(1)	1(1)	2(1)
C26	29(2)	45(2)	24(2)	7(1)	5(1)	6(2)
C27	42(2)	54(2)	20(2)	−1(2)	2(1)	7(2)
C28	47(2)	41(2)	27(2)	−12(2)	−1(1)	−4(2)
C29	34(2)	30(2)	28(2)	0(1)	2(1)	−2(1)
C30	24(2)	23(2)	24(1)	7(1)	1(1)	2(1)
C31	30(2)	30(2)	27(2)	−3(1)	−2(1)	1(1)
C32	37(2)	44(2)	36(2)	−8(2)	−7(2)	0(2)
C33	25(2)	50(2)	48(2)	−4(2)	−8(2)	−5(2)
C34	23(2)	44(2)	41(2)	5(2)	6(1)	2(1)
C35	28(2)	30(2)	25(1)	2(1)	3(1)	−1(1)
C36	25(2)	22(1)	23(1)	−1(1)	8(1)	2(1)
C37	31(2)	25(2)	30(2)	0(1)	5(1)	2(1)
C38	46(2)	21(2)	42(2)	5(1)	8(2)	8(2)
C39	51(2)	24(2)	53(2)	−3(2)	12(2)	0(2)
C40	39(2)	31(2)	38(2)	−10(1)	7(1)	−7(2)
C41	34(2)	24(2)	26(2)	−3(1)	3(1)	2(1)
C42	21(2)	23(1)	19(1)	1(1)	2(1)	1(1)
C43	27(2)	27(2)	26(2)	−2(1)	3(1)	0(1)
C44	33(2)	41(2)	23(1)	−3(1)	5(1)	−1(1)
C45	32(2)	42(2)	20(1)	8(1)	2(1)	−4(1)
C46	39(2)	28(2)	33(2)	9(1)	2(1)	−1(1)
C47	40(2)	25(2)	26(2)	2(1)	2(1)	2(1)
P1	23(1)	21(1)	18(1)	2(1)	2(1)	−1(1)
P2	22(1)	19(1)	18(1)	0(1)	2(1)	1(1)
Cl	33(1)	19(1)	28(1)	−1(1)	3(1)	−2(1)
Ru1	23(1)	17(1)	16(1)	0(1)	2(1)	0(1)
C48	37(2)	60(2)	50(2)	−2(2)	5(2)	6(2)
C49	52(3)	45(2)	62(2)	−7(2)	12(2)	15(2)
C50	57(3)	36(2)	75(3)	−6(2)	6(2)	3(2)
C51	49(3)	65(3)	62(2)	5(2)	13(2)	−6(2)
C52	46(3)	90(3)	50(2)	−20(2)	8(2)	1(2)
C53	39(2)	66(2)	55(2)	−19(2)	−7(2)	−1(2)
C54	42(2)	56(2)	67(3)	−2(2)	4(2)	−8(2)
C55	78(3)	55(2)	42(2)	−1(2)	−4(2)	0(2)
C56	83(4)	40(2)	82(3)	9(2)	48(3)	10(2)

C57	32(2)	27(2)	147(5)	1(3)	6(3)	4(2)
C58	81(4)	40(2)	73(3)	−14(2)	−39(3)	11(2)
C59	92(4)	50(2)	43(2)	4(2)	29(2)	11(2)

University of Southampton · Department of Chemistry

Crystallography Service

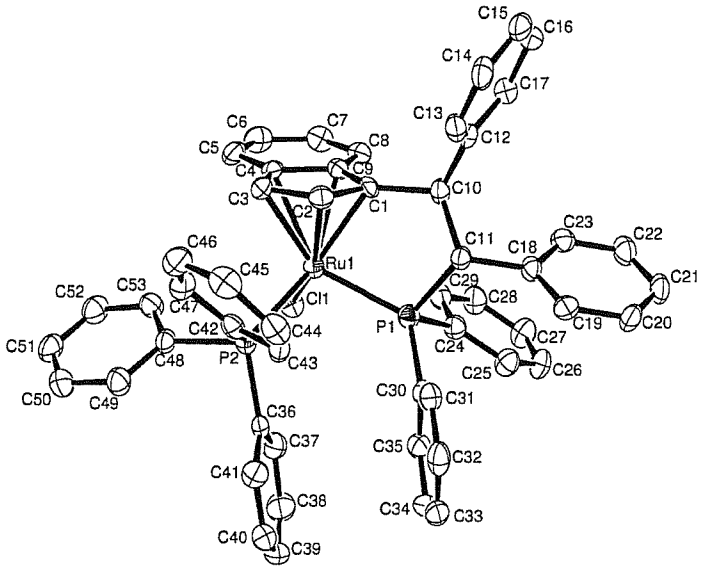

The second molecule in the structure is numbered as above+100, ie. C101-C153; solvent benzene is numbered C3xx and C4xx.

Table 1. Crystal data and structure refinement.

Compound name	***rac*-(η^5:η^1-Indenyl-CH(Ph)CH(Ph)PPh_2)Ru^{II}(PPh_3)Cl**	
Empirical formula	$C_{53}H_{43}ClP_2Ru$	
Formula weight	878.38	
Temperature	120(2) K	
Wavelength	0.71073 Å	
Crystal system	Triclinic	
Space group	*P*1	
Unit cell dimensions	a = 11.9689(4) Å	α = 112.1300(10)°
	b = 19.6049(6) Å	β = 93.9490(10)°
	c = 21.7880(9) Å	γ = 100.535(2)°
Volume	4602.5(3) Å^3	
Z	4	
Density (calculated)	1.382 Mg / m^3	
Absorption coefficient	0.508 mm^{-1}	
F(000)	1978	
Crystal	Block; red	
Crystal size	0.08 × 0.10 × 0.10 mm^3	
θ range for data collection	2.97 – 27.36°	
Index ranges	$-15 \le h \le 15$, $-24 \le k \le 25$, $-28 \le l \le 28$	
Reflections collected	33197	
Independent reflections	18122 [R_{int} = 0.1006]	
Completeness to θ = 27.36°	86.8 %	
Absorption correction	Semi–empirical from equivalents	
Max. and min. transmission	0.9509 and 0.9509	
Refinement method	Full-matrix least-squares on F^2	
Data / restraints / parameters	18122 / 0 / 1105	
Goodness-of-fit on F^2	0.967	
Final *R* indices [$F^2 > 2\sigma(F^2)$]	*R1* = 0.0626, *wR2* = 0.1058	
R indices (all data)	*R1* = 0.1572, *wR2* = 0.1292	
Largest diff. peak and hole	0.939 and –0.941 e Å^{-3}	

Diffractometer: *Enraf Nonius KappaCCD* area detector (ϕ scans and ω scans to fill *Ewald* sphere). **Data collection and cell refinement**: *Denzo* (Z. Otwinowski & W. Minor, *Methods in Enzymology* (1997) Vol. **276**: *Macromolecular Crystallography*, part A, pp. 307–326; C. W. Carter, Jr. & R. M. Sweet, Eds., Academic Press). **Absorption correction**: *SORTAV* (R. H. Blessing, Acta Cryst. A**51** (1995) 33–37; R. H. Blessing, J. Appl. Cryst. **30** (1997) 421–426). **Program used to solve structure**: *SHELXS97* (G. M. Sheldrick, Acta Cryst. (1990) A**46** 467–473). **Program used to refine structure**: *SHELXL97* (G. M. Sheldrick (1997), University of Göttingen, Germany).
Further information: http://www.soton.ac.uk/~xservice/strat.htm

Table 2. Atomic coordinates [$\times 10^4$], equivalent isotropic displacement parameters [$Å^2 \times 10^3$] and site occupancy factors. U_{eq} is defined as one third of the trace of the orthogonalized U^{ij} tensor.

Atom	*x*	*y*	*z*	U_{eq}	*S.o.f.*
Ru1	5983(1)	5334(1)	6880(1)	23(1)	1
Ru2	4896(1)	151(1)	6822(1)	22(1)	1
Cl1	6170(1)	4683(1)	7617(1)	31(1)	1
P102	3052(1)	309(1)	6750(1)	23(1)	1
Cl2	4468(1)	−491(1)	7564(1)	30(1)	1
P2	4264(1)	5587(1)	7236(1)	25(1)	1
P1	7266(1)	6446(1)	7538(1)	24(1)	1
P101	5791(1)	1282(1)	7661(1)	23(1)	1
C10	8085(4)	6069(3)	6319(3)	25(1)	1
C9	6985(4)	4705(3)	6096(3)	23(1)	1
C135	4549(4)	1964(3)	8650(3)	30(1)	1
C131	5000(4)	2630(3)	7950(3)	30(1)	1
C104	5279(4)	−839(3)	5919(3)	24(1)	1
C8	7863(4)	4347(3)	6209(3)	27(1)	1
C130	5069(4)	2023(3)	8116(3)	27(1)	1
C36	4193(4)	6190(3)	8103(3)	26(1)	1
C1	7004(4)	5455(3)	6133(3)	21(1)	1
C30	6836(4)	7288(3)	8085(3)	24(1)	1
C101	6401(4)	394(3)	6378(3)	21(1)	1
C2	5840(4)	5483(3)	5943(3)	26(1)	1
C149	763(4)	−526(3)	6335(3)	25(1)	1
C13	7720(4)	6502(3)	5375(3)	28(1)	1
C153	2175(4)	−1255(3)	6304(3)	24(1)	1
C11	7992(4)	6778(3)	6919(3)	24(1)	1
C12	8425(4)	6217(3)	5713(3)	25(1)	1
C148	1920(4)	−561(3)	6429(3)	22(1)	1
C31	6458(4)	7797(3)	7853(3)	28(1)	1
C118	7709(4)	2443(3)	7640(3)	23(1)	1
C113	7807(4)	1578(3)	5897(3)	30(1)	1
C110	7358(4)	1074(3)	6787(3)	20(1)	1
C111	6828(4)	1725(3)	7225(3)	22(1)	1
C112	8169(4)	1307(3)	6363(3)	23(1)	1
C117	9310(4)	1270(3)	6443(3)	25(1)	1
C48	3122(4)	4771(3)	7151(3)	24(1)	1
C134	3987(4)	2511(3)	9018(3)	41(2)	1
C132	4443(5)	3179(3)	8321(3)	39(2)	1
C103	4702(4)	−381(3)	5704(3)	24(1)	1
C147	2180(4)	318(3)	5504(3)	23(1)	1
C142	2832(4)	729(3)	6144(3)	21(1)	1
C144	3353(4)	1786(3)	5830(3)	30(1)	1
C16	9726(5)	6170(3)	4917(3)	36(2)	1
C35	6814(4)	7419(3)	8753(3)	32(1)	1
C136	2406(4)	841(3)	7468(3)	26(1)	1
C143	3414(4)	1461(3)	6292(3)	23(1)	1
C17	9424(4)	6050(3)	5470(3)	31(1)	1
C152	1296(4)	−1903(3)	6106(3)	28(1)	1
C146	2133(4)	644(3)	5047(3)	31(1)	1
C49	2019(4)	4871(3)	7289(3)	35(2)	1
C32	6108(4)	8419(3)	8277(3)	36(2)	1
C34	6461(4)	8044(3)	9180(3)	38(2)	1
C141	1962(4)	1466(3)	7524(3)	29(1)	1
C137	2258(5)	552(3)	7953(3)	39(2)	1
C116	10077(5)	1485(3)	6064(3)	33(1)	1
C108	7115(4)	−695(3)	6589(3)	26(1)	1
C106	5782(4)	−1911(3)	6021(3)	32(1)	1
C107	6840(4)	−1448(3)	6430(3)	32(1)	1
C15	9027(5)	6448(3)	4583(3)	38(2)	1
C145	2716(4)	1375(3)	5204(3)	31(1)	1
C5	5552(5)	3509(3)	5808(3)	32(1)	1
C114	8561(4)	1806(3)	5520(3)	29(1)	1
C119	7613(4)	3125(3)	7616(3)	32(1)	1
C109	6355(4)	−359(3)	6335(3)	23(1)	1

C102	5403(4)	373(3)	5967(3)	24(1)	1
C120	8389(5)	3785(3)	8002(3)	43(2)	1
C18	9133(4)	7364(3)	7210(3)	26(1)	1
C121	9296(4)	3779(3)	8417(3)	42(2)	1
C14	8035(5)	6622(3)	4818(3)	34(1)	1
C122	9424(4)	3103(3)	8441(3)	33(1)	1
C4	5805(4)	4280(3)	5896(3)	25(1)	1
C19	9162(4)	8129(3)	7467(3)	29(1)	1
C53	3333(4)	4057(3)	6984(3)	31(1)	1
C3	5122(4)	4771(3)	5818(3)	25(1)	1
C105	5014(4)	−1624(3)	5773(3)	30(1)	1
C150	−79(4)	−1165(3)	6131(3)	28(1)	1
C21	11209(4)	8444(3)	7741(3)	35(2)	1
C151	177(4)	−1859(3)	6019(3)	26(1)	1
C123	8651(4)	2438(3)	8052(3)	27(1)	1
C23	10179(4)	7144(3)	7218(3)	29(1)	1
C124	6735(4)	1266(3)	8346(3)	24(1)	1
C125	7191(4)	1915(3)	8929(3)	30(1)	1
C33	6118(4)	8542(3)	8937(3)	36(2)	1
C129	7124(4)	620(3)	8264(3)	29(1)	1
C7	7573(5)	3617(3)	6126(3)	34(1)	1
C20	10188(5)	8669(3)	7728(3)	37(2)	1
C128	7950(4)	605(3)	8742(3)	33(1)	1
C43	3934(4)	6746(3)	6834(3)	27(1)	1
C27	10547(5)	6421(3)	8768(3)	39(2)	1
C25	9241(4)	7116(3)	8529(3)	35(1)	1
C45	2842(4)	6550(3)	5798(3)	35(2)	1
C29	8847(4)	5774(3)	7958(3)	30(1)	1
C47	2822(4)	5519(3)	6136(3)	31(1)	1
C44	3541(4)	7030(3)	6387(3)	32(1)	1
C26	10247(4)	7097(3)	8872(3)	37(2)	1
C24	8528(4)	6444(3)	8062(3)	28(1)	1
C41	3601(4)	6768(3)	8298(3)	31(1)	1
C42	3583(4)	5984(3)	6711(3)	24(1)	1
C126	8003(4)	1905(3)	9411(3)	37(2)	1
C37	4720(4)	6020(3)	8599(3)	35(1)	1
C115	9705(4)	1760(3)	5608(3)	32(1)	1
C40	3559(4)	7163(3)	8964(3)	37(2)	1
C52	2481(5)	3462(3)	6970(3)	37(2)	1
C127	8373(5)	1251(3)	9308(3)	38(2)	1
C38	4641(5)	6412(3)	9264(3)	42(2)	1
C51	1415(5)	3577(3)	7110(3)	40(2)	1
C46	2470(4)	5793(3)	5671(3)	34(1)	1
C22	11200(4)	7679(3)	7485(3)	36(2)	1
C28	9847(4)	5761(3)	8312(3)	36(2)	1
C6	6402(5)	3202(3)	5926(3)	38(2)	1
C50	1189(5)	4275(3)	7259(3)	40(2)	1
C39	4067(4)	6989(3)	9452(3)	38(2)	1
C133	3950(5)	3124(3)	8848(3)	45(2)	1
C138	1662(5)	860(3)	8467(3)	50(2)	1
C139	1226(5)	1475(4)	8512(4)	55(2)	1
C140	1382(5)	1781(3)	8042(3)	45(2)	1
C310	9347(5)	9385(3)	9462(3)	40(2)	1
C312	10515(5)	9560(3)	9500(3)	42(2)	1
C311	8828(5)	9823(3)	9963(3)	41(2)	1
C301	5577(14)	494(8)	9740(12)	39(5)	0.522(4)
C300	4500(20)	11(10)	9412(9)	35(5)	0.522(4)
C302	6102(13)	484(9)	10334(9)	31(5)	0.522(4)
C321	1895(8)	4074(5)	9882(6)	95(6)	0.486(8)
C323	2396(10)	4520(7)	10542(5)	81(7)	0.486(8)
C325	3031(11)	5250(7)	10709(5)	85(6)	0.486(8)
C326	3166(11)	5534(5)	10216(6)	460(40)	0.486(8)
C324	2665(10)	5088(6)	9556(6)	107(7)	0.486(8)
C322	2030(8)	4358(5)	9389(4)	44(4)	0.486(8)
C401	2210(20)	4417(8)	10364(10)	185(14)	0.514(8)
C404	1134(19)	4429(11)	10087(12)	269(17)	0.514(8)

C402	994(12)	5037(14)	9931(12)	580(50)	0.514(8)
C403	1928(15)	5632(10)	10052(10)	208(13)	0.514(8)
C406	3002(12)	5620(7)	10329(7)	82(6)	0.514(8)
C405	3142(17)	5012(10)	10485(9)	211(15)	0.514(8)
C303	5280(20)	332(12)	9565(8)	39(5)	0.522(4)
C304	6002(18)	500(9)	10123(12)	41(5)	0.522(4)
C305	5764(14)	165(10)	10573(10)	40(6)	0.522(4)

Table 3. Bond lengths [Å] and angles [°].

Ru1–C1	2.159(5)
Ru1–C2	2.168(5)
Ru1–C3	2.227(5)
Ru1–C9	2.261(5)
Ru1–P1	2.2983(14)
Ru1–C4	2.313(5)
Ru1–P2	2.3201(14)
Ru1–Cl1	2.4198(13)
Ru2–C101	2.164(5)
Ru2–C102	2.166(5)
Ru2–C103	2.235(5)
Ru2–P101	2.2836(14)
Ru2–P102	2.2876(13)
Ru2–C109	2.295(5)
Ru2–C104	2.328(5)
Ru2–Cl2	2.4240(13)
P102–C142	1.827(5)
P102–C148	1.831(5)
P102–C136	1.835(5)
P2–C36	1.830(5)
P2–C42	1.830(5)
P2–C48	1.844(5)
P1–C30	1.824(5)
P1–C24	1.831(5)
P1–C11	1.900(5)
P101–C124	1.823(5)
P101–C130	1.826(5)
P101–C111	1.893(5)
C10–C1	1.509(6)
C10–C12	1.520(7)
C10–C11	1.537(7)
C9–C8	1.423(6)
C9–C1	1.438(6)
C9–C4	1.446(6)
C135–C130	1.390(7)
C135–C134	1.391(7)
C131–C130	1.381(7)
C131–C132	1.393(7)
C104–C103	1.415(6)
C104–C105	1.417(6)
C104–C109	1.457(6)
C8–C7	1.346(6)
C36–C37	1.391(7)
C36–C41	1.393(6)
C1–C2	1.443(6)
C30–C35	1.382(7)
C30–C31	1.404(7)
C101–C102	1.427(6)
C101–C109	1.434(6)
C101–C110	1.512(6)
C2–C3	1.416(6)
C149–C150	1.357(6)
C149–C148	1.403(6)
C13–C14	1.384(7)
C13–C12	1.402(7)
C153–C148	1.380(6)
C153–C152	1.393(6)
C11–C18	1.532(6)
C12–C17	1.384(7)
C31–C32	1.381(7)
C118–C119	1.382(6)

C118–C123	1.396(7)
C118–C111	1.510(6)
C113–C114	1.384(7)
C113–C112	1.391(7)
C110–C112	1.510(7)
C110–C111	1.550(6)
C112–C117	1.383(6)
C117–C116	1.389(7)
C48–C53	1.385(6)
C48–C49	1.406(7)
C134–C133	1.391(8)
C132–C133	1.357(8)
C103–C102	1.435(6)
C147–C146	1.373(7)
C147–C142	1.406(7)
C142–C143	1.380(6)
C144–C145	1.375(7)
C144–C143	1.384(7)
C16–C17	1.371(7)
C16–C15	1.383(7)
C35–C34	1.389(7)
C136–C137	1.380(7)
C136–C141	1.389(6)
C152–C151	1.363(6)
C146–C145	1.375(7)
C49–C50	1.366(7)
C32–C33	1.365(8)
C34–C33	1.382(7)
C141–C140	1.369(7)
C137–C138	1.373(8)
C116–C115	1.380(7)
C108–C107	1.352(6)
C108–C109	1.412(6)
C106–C105	1.342(7)
C106–C107	1.427(7)
C15–C14	1.374(7)
C5–C6	1.330(7)
C5–C4	1.420(6)
C114–C115	1.394(7)
C119–C120	1.371(7)
C120–C121	1.368(7)
C18–C19	1.382(6)
C18–C23	1.398(6)
C121–C122	1.382(7)
C122–C123	1.377(7)
C4–C3	1.419(6)
C19–C20	1.389(7)
C53–C52	1.390(7)
C150–C151	1.383(6)
C21–C20	1.375(7)
C21–C22	1.386(7)
C23–C22	1.381(7)
C124–C129	1.382(6)
C124–C125	1.401(7)
C125–C126	1.389(7)
C129–C128	1.397(7)
C7–C6	1.431(7)
C128–C127	1.372(7)
C43–C44	1.385(7)
C43–C42	1.390(6)
C27–C28	1.371(7)
C27–C26	1.377(7)
C25–C26	1.386(7)

C25–C24	1.398(7)
C45–C44	1.375(7)
C45–C46	1.382(7)
C29–C24	1.376(6)
C29–C28	1.388(7)
C47–C42	1.382(7)
C47–C46	1.386(7)
C41–C40	1.372(7)
C126–C127	1.377(7)
C37–C38	1.380(8)
C40–C39	1.370(7)
C52–C51	1.371(7)
C38–C39	1.376(7)
C51–C50	1.365(7)
C138–C139	1.372(8)
C139–C140	1.377(8)
C310–C312	1.366(7)
C310–C311	1.378(8)
C312–C311^{i}	1.383(7)
C311–C312^{i}	1.383(7)
C301–C300	1.41(2)
C301–C302	1.41(2)
C300–C302^{ii}	1.41(2)
C302–C300^{ii}	1.41(2)
C321–C323	1.3900
C321–C322	1.3900
C323–C325	1.3900
C325–C326	1.3900
C326–C324	1.3900
C324–C322	1.3900
C401–C404	1.3900
C401–C405	1.3900
C404–C402	1.3900
C402–C403	1.3900
C403–C406	1.3900
C406–C405	1.3900
C303–C304	1.34(2)
C303–C305^{ii}	1.37(2)
C304–C305	1.39(2)
C305–C303^{ii}	1.37(2)

C1–Ru1–C2	38.96(17)
C1–Ru1–C3	63.54(18)
C2–Ru1–C3	37.56(17)
C1–Ru1–C9	37.88(16)
C2–Ru1–C9	63.24(18)
C3–Ru1–C9	61.92(18)
C1–Ru1–P1	81.12(13)
C2–Ru1–P1	99.44(14)
C3–Ru1–P1	137.00(13)
C9–Ru1–P1	104.45(13)
C1–Ru1–C4	62.69(17)
C2–Ru1–C4	62.10(18)
C3–Ru1–C4	36.37(16)
C9–Ru1–C4	36.82(16)
P1–Ru1–C4	140.74(13)
C1–Ru1–P2	138.35(13)
C2–Ru1–P2	100.83(13)
C3–Ru1–P2	90.69(13)
C9–Ru1–P2	151.34(13)
P1–Ru1–P2	101.55(5)
C4–Ru1–P2	115.34(13)
C1–Ru1–Cl1	130.68(13)

C2–Ru1–Cl1	157.53(14)
C3–Ru1–Cl1	124.13(13)
C9–Ru1–Cl1	97.92(13)
P1–Ru1–Cl1	97.08(5)
C4–Ru1–Cl1	95.56(13)
P2–Ru1–Cl1	90.60(5)
C101–Ru2–C102	38.49(17)
C101–Ru2–C103	63.62(18)
C102–Ru2–C103	38.02(17)
C101–Ru2–P101	81.61(13)
C102–Ru2–P101	99.32(14)
C103–Ru2–P101	137.34(13)
C101–Ru2–P102	136.22(13)
C102–Ru2–P102	99.34(13)
C103–Ru2–P102	89.85(13)
P101–Ru2–P102	100.18(5)
C101–Ru2–C109	37.37(16)
C102–Ru2–C109	62.30(17)
C103–Ru2–C109	61.44(17)
P101–Ru2–C109	105.07(13)
P102–Ru2–C109	150.70(13)
C101–Ru2–C104	62.55(17)
C102–Ru2–C104	61.90(17)
C103–Ru2–C104	36.05(16)
P101–Ru2–C104	141.29(12)
P102–Ru2–C104	115.49(12)
C109–Ru2–C104	36.73(16)
C101–Ru2–Cl2	133.56(13)
C102–Ru2–Cl2	161.25(13)
C103–Ru2–Cl2	126.75(13)
P101–Ru2–Cl2	94.84(5)
P102–Ru2–Cl2	90.12(5)
C109–Ru2–Cl2	102.18(12)
C104–Ru2–Cl2	99.42(12)
C142–P102–C148	103.3(2)
C142–P102–C136	104.6(2)
C148–P102–C136	97.2(2)
C142–P102–Ru2	109.42(15)
C148–P102–Ru2	115.76(16)
C136–P102–Ru2	124.16(17)
C36–P2–C42	106.1(2)
C36–P2–C48	97.8(2)
C42–P2–C48	102.2(2)
C36–P2–Ru1	122.05(16)
C42–P2–Ru1	109.40(16)
C48–P2–Ru1	117.03(17)
C30–P1–C24	101.6(2)
C30–P1–C11	102.5(2)
C24–P1–C11	100.2(2)
C30–P1–Ru1	123.52(16)
C24–P1–Ru1	120.64(17)
C11–P1–Ru1	104.61(16)
C124–P101–C130	101.1(2)
C124–P101–C111	102.9(2)
C130–P101–C111	105.0(2)
C124–P101–Ru2	117.75(17)
C130–P101–Ru2	124.83(16)
C111–P101–Ru2	102.76(16)
C1–C10–C12	111.5(4)
C1–C10–C11	111.1(4)
C12–C10–C11	114.5(4)
C8–C9–C1	132.8(4)
C8–C9–C4	119.4(4)

C1–C9–C4	107.8(4)
C8–C9–Ru1	125.4(4)
C1–C9–Ru1	67.2(3)
C4–C9–Ru1	73.6(3)
C130–C135–C134	120.8(5)
C130–C131–C132	120.5(5)
C103–C104–C105	132.2(5)
C103–C104–C109	107.4(4)
C105–C104–C109	120.3(4)
C103–C104–Ru2	68.4(3)
C105–C104–Ru2	129.0(4)
C109–C104–Ru2	70.4(3)
C7–C8–C9	119.0(5)
C131–C130–C135	118.6(5)
C131–C130–P101	123.4(4)
C135–C130–P101	118.0(4)
C37–C36–C41	118.1(5)
C37–C36–P2	116.5(4)
C41–C36–P2	125.3(4)
C9–C1–C2	107.5(4)
C9–C1–C10	123.9(4)
C2–C1–C10	128.6(4)
C9–C1–Ru1	74.9(3)
C2–C1–Ru1	70.9(3)
C10–C1–Ru1	121.3(4)
C35–C30–C31	117.4(5)
C35–C30–P1	119.4(4)
C31–C30–P1	123.0(4)
C102–C101–C109	107.7(4)
C102–C101–C110	127.5(4)
C109–C101–C110	124.8(4)
C102–C101–Ru2	70.9(3)
C109–C101–Ru2	76.3(3)
C110–C101–Ru2	119.1(3)
C3–C2–C1	107.8(4)
C3–C2–Ru1	73.5(3)
C1–C2–Ru1	70.2(3)
C150–C149–C148	120.1(5)
C14–C13–C12	120.1(5)
C148–C153–C152	120.4(4)
C18–C11–C10	113.3(4)
C18–C11–P1	115.6(4)
C10–C11–P1	107.3(3)
C17–C12–C13	118.5(5)
C17–C12–C10	120.6(5)
C13–C12–C10	121.0(5)
C153–C148–C149	118.6(4)
C153–C148–P102	121.2(4)
C149–C148–P102	120.1(4)
C32–C31–C30	121.7(5)
C119–C118–C123	118.1(5)
C119–C118–C111	120.8(4)
C123–C118–C111	121.1(4)
C114–C113–C112	121.4(5)
C112–C110–C101	112.9(4)
C112–C110–C111	112.9(4)
C101–C110–C111	109.1(4)
C118–C111–C110	113.7(4)
C118–C111–P101	119.0(4)
C110–C111–P101	104.9(3)
C117–C112–C113	118.1(5)
C117–C112–C110	120.2(5)
C113–C112–C110	121.6(4)

C112–C117–C116	121.4(5)
C53–C48–C49	118.0(5)
C53–C48–P2	121.6(4)
C49–C48–P2	120.3(4)
C135–C134–C133	119.4(6)
C133–C132–C131	120.6(5)
C104–C103–C102	108.7(4)
C104–C103–Ru2	75.6(3)
C102–C103–Ru2	68.4(3)
C146–C147–C142	120.4(5)
C143–C142–C147	117.8(5)
C143–C142–P102	119.0(4)
C147–C142–P102	123.0(4)
C145–C144–C143	120.0(5)
C17–C16–C15	120.5(5)
C30–C35–C34	121.0(5)
C137–C136–C141	118.2(5)
C137–C136–P102	116.9(4)
C141–C136–P102	124.6(4)
C142–C143–C144	121.4(5)
C16–C17–C12	120.9(5)
C151–C152–C153	120.2(5)
C147–C146–C145	120.9(5)
C50–C49–C48	120.4(5)
C33–C32–C31	119.5(5)
C33–C34–C35	119.9(6)
C140–C141–C136	120.9(6)
C138–C137–C136	121.1(6)
C115–C116–C117	119.6(5)
C107–C108–C109	119.7(5)
C105–C106–C107	122.0(5)
C108–C107–C106	121.3(5)
C14–C15–C16	119.5(6)
C146–C145–C144	119.5(5)
C6–C5–C4	119.2(5)
C113–C114–C115	119.4(5)
C120–C119–C118	121.5(5)
C108–C109–C101	133.9(5)
C108–C109–C104	118.2(4)
C101–C109–C104	107.8(4)
C108–C109–Ru2	127.7(4)
C101–C109–Ru2	66.3(3)
C104–C109–Ru2	72.9(3)
C101–C102–C103	108.3(4)
C101–C102–Ru2	70.7(3)
C103–C102–Ru2	73.6(3)
C121–C120–C119	120.1(5)
C19–C18–C23	117.8(5)
C19–C18–C11	121.0(4)
C23–C18–C11	121.2(4)
C120–C121–C122	119.5(5)
C15–C14–C13	120.5(5)
C123–C122–C121	120.6(5)
C3–C4–C5	133.5(5)
C3–C4–C9	107.4(4)
C5–C4–C9	119.1(4)
C3–C4–Ru1	68.5(3)
C5–C4–Ru1	127.7(4)
C9–C4–Ru1	69.6(3)
C18–C19–C20	121.9(5)
C48–C53–C52	120.5(5)
C2–C3–C4	109.4(4)
C2–C3–Ru1	69.0(3)

C4–C3–Ru1	75.1(3)
C106–C105–C104	118.4(5)
C149–C150–C151	121.2(5)
C20–C21–C22	119.4(5)
C152–C151–C150	119.4(5)
C122–C123–C118	120.1(5)
C22–C23–C18	120.5(5)
C129–C124–C125	118.0(5)
C129–C124–P101	119.5(4)
C125–C124–P101	122.1(4)
C126–C125–C124	120.8(5)
C32–C33–C34	120.4(5)
C124–C129–C128	121.7(5)
C8–C7–C6	121.0(5)
C21–C20–C19	119.6(5)
C127–C128–C129	118.6(5)
C44–C43–C42	120.9(5)
C28–C27–C26	119.4(5)
C26–C25–C24	120.0(5)
C44–C45–C46	120.0(5)
C24–C29–C28	120.9(5)
C42–C47–C46	121.1(5)
C45–C44–C43	119.9(5)
C27–C26–C25	120.7(5)
C29–C24–C25	118.5(5)
C29–C24–P1	119.5(4)
C25–C24–P1	121.7(4)
C40–C41–C36	120.5(5)
C47–C42–C43	118.2(5)
C47–C42–P2	120.8(4)
C43–C42–P2	120.5(4)
C127–C126–C125	119.3(5)
C38–C37–C36	120.4(5)
C116–C115–C114	120.0(5)
C39–C40–C41	121.3(5)
C51–C52–C53	120.1(5)
C128–C127–C126	121.5(5)
C39–C38–C37	121.0(6)
C50–C51–C52	119.9(5)
C45–C46–C47	119.7(5)
C23–C22–C21	120.7(5)
C27–C28–C29	120.4(5)
C5–C6–C7	122.3(5)
C51–C50–C49	121.0(5)
C40–C39–C38	118.7(6)
C132–C133–C134	120.1(5)
C139–C138–C137	119.9(6)
C138–C139–C140	120.0(6)
C141–C140–C139	119.9(6)
C312–C310–C311	119.8(6)
C310–C312–C311^{i}	120.1(6)
C310–C311–C312^{i}	120.1(5)
C300–C301–C302	120.6(13)
C301–C300–C302^{ii}	122.1(13)
C300^{ii}–C302–C301	117.3(13)
C323–C321–C322	120.0
C321–C323–C325	120.0
C326–C325–C323	120.0
C325–C326–C324	120.0
C322–C324–C326	120.0
C324–C322–C321	120.0
C404–C401–C405	120.0
C402–C404–C401	120.0

C404–C402–C403	120.0
C406–C403–C402	120.0
C405–C406–C403	120.0
C406–C405–C401	120.0
C304–C303–C305[ii]	120.5(15)
C303–C304–C305	122.4(15)
C303[ii]–C305–C304	117.0(14)

Symmetry transformations used to generate equivalent atoms:
(i) –x+2,–y+2,–z+2 (ii) –x+1,–y,–z+2

Table 4. Anisotropic displacement parameters [$Å^2 \times 10^3$]. The anisotropic displacement factor exponent takes the form: $-2\pi^2[h^2a^{*2}U^{11} + \cdots + 2\,h\,k\,a^*\,b^*\,U^{12}]$.

Atom	U^{11}	U^{22}	U^{33}	U^{23}	U^{13}	U^{12}
Ru1	21(1)	22(1)	26(1)	10(1)	4(1)	4(1)
Ru2	18(1)	23(1)	25(1)	10(1)	3(1)	4(1)
Cl1	29(1)	32(1)	36(1)	19(1)	5(1)	9(1)
P102	18(1)	22(1)	29(1)	11(1)	2(1)	3(1)
Cl2	29(1)	33(1)	31(1)	19(1)	0(1)	1(1)
P2	22(1)	23(1)	31(1)	11(1)	4(1)	4(1)
P1	22(1)	24(1)	26(1)	10(1)	3(1)	5(1)
P101	19(1)	24(1)	23(1)	9(1)	1(1)	4(1)
C10	20(3)	19(3)	34(4)	10(3)	5(3)	2(2)
C9	21(3)	23(3)	24(3)	9(3)	7(2)	5(2)
C135	31(3)	34(3)	23(4)	11(3)	−1(3)	7(3)
C131	26(3)	30(3)	32(4)	9(3)	1(3)	8(3)
C104	19(3)	26(3)	32(4)	15(3)	10(3)	7(2)
C8	28(3)	28(3)	25(4)	10(3)	8(3)	7(3)
C130	19(3)	26(3)	23(4)	−1(3)	−4(3)	3(2)
C36	18(3)	29(3)	22(3)	6(3)	4(2)	−4(2)
C1	21(3)	21(3)	22(3)	11(2)	8(2)	2(2)
C30	19(3)	17(3)	26(4)	2(3)	2(3)	−2(2)
C101	23(3)	17(3)	20(3)	3(2)	7(2)	8(2)
C2	29(3)	30(3)	20(3)	11(3)	3(3)	6(3)
C149	25(3)	23(3)	28(4)	11(3)	3(3)	4(2)
C13	20(3)	24(3)	37(4)	11(3)	6(3)	2(2)
C153	21(3)	28(3)	23(3)	9(3)	3(2)	6(2)
C11	24(3)	22(3)	24(3)	9(3)	2(2)	0(2)
C12	25(3)	18(3)	25(4)	5(3)	1(3)	−5(2)
C148	18(3)	23(3)	22(3)	9(2)	1(2)	−1(2)
C31	20(3)	30(3)	33(4)	14(3)	2(3)	3(2)
C118	21(3)	24(3)	26(4)	11(3)	10(3)	4(2)
C113	26(3)	27(3)	36(4)	13(3)	4(3)	6(2)
C110	17(3)	23(3)	21(3)	11(3)	−1(2)	1(2)
C111	22(3)	27(3)	22(3)	14(3)	6(2)	9(2)
C112	26(3)	13(3)	23(3)	2(2)	3(2)	0(2)
C117	28(3)	19(3)	26(4)	9(3)	6(3)	3(2)
C48	24(3)	23(3)	24(3)	9(3)	2(2)	−2(2)
C134	29(3)	55(4)	29(4)	3(3)	3(3)	15(3)
C132	42(4)	28(3)	40(4)	5(3)	−7(3)	12(3)
C103	15(3)	30(3)	20(3)	4(3)	2(2)	−1(2)
C147	26(3)	17(3)	26(4)	9(3)	3(3)	6(2)
C142	11(3)	22(3)	33(4)	15(3)	5(2)	5(2)
C144	24(3)	26(3)	44(4)	20(3)	6(3)	7(2)
C16	32(3)	34(3)	31(4)	4(3)	11(3)	0(3)
C35	26(3)	28(3)	39(4)	9(3)	8(3)	6(2)
C136	17(3)	30(3)	25(4)	6(3)	4(2)	0(2)
C143	17(3)	26(3)	27(4)	13(3)	1(2)	3(2)
C17	29(3)	31(3)	32(4)	12(3)	6(3)	4(3)
C152	29(3)	22(3)	29(4)	9(3)	2(3)	1(3)
C146	29(3)	36(3)	22(4)	6(3)	4(3)	6(3)
C49	31(3)	25(3)	46(4)	11(3)	9(3)	4(3)
C32	22(3)	24(3)	61(5)	16(3)	4(3)	5(2)
C34	35(3)	41(4)	30(4)	5(3)	13(3)	8(3)
C141	22(3)	34(3)	28(4)	8(3)	3(3)	8(3)
C137	39(4)	32(3)	40(4)	9(3)	16(3)	0(3)
C116	29(3)	35(3)	31(4)	9(3)	8(3)	8(3)
C108	17(3)	37(3)	29(4)	18(3)	9(2)	7(2)
C106	32(3)	21(3)	41(4)	11(3)	14(3)	4(3)
C107	32(3)	36(3)	44(4)	28(3)	15(3)	16(3)
C15	45(4)	34(3)	25(4)	10(3)	3(3)	−13(3)
C145	30(3)	36(3)	42(4)	28(3)	12(3)	10(3)
C5	37(3)	24(3)	25(4)	5(3)	2(3)	−3(3)
C114	43(4)	24(3)	24(4)	13(3)	4(3)	8(3)
C119	26(3)	30(3)	40(4)	16(3)	2(3)	3(3)
C109	12(3)	34(3)	28(4)	18(3)	10(2)	3(2)

C102	22(3)	30(3)	25(3)	13(3)	15(3)	11(2)
C120	35(4)	25(3)	68(5)	21(3)	0(3)	1(3)
C18	20(3)	31(3)	24(4)	12(3)	−1(2)	0(2)
C121	29(3)	29(3)	53(5)	7(3)	−6(3)	−6(3)
C14	31(3)	29(3)	38(4)	17(3)	−2(3)	−7(3)
C122	30(3)	29(3)	34(4)	8(3)	−4(3)	3(3)
C4	31(3)	22(3)	16(3)	4(2)	6(3)	−1(2)
C19	29(3)	32(3)	22(4)	9(3)	2(3)	4(3)
C53	29(3)	30(3)	35(4)	13(3)	9(3)	8(3)
C3	22(3)	28(3)	19(3)	7(3)	0(2)	1(2)
C105	17(3)	24(3)	41(4)	7(3)	5(3)	1(2)
C150	16(3)	38(3)	27(4)	13(3)	5(2)	1(3)
C21	23(3)	40(4)	32(4)	13(3)	−4(3)	−11(3)
C151	32(3)	20(3)	20(3)	7(3)	2(3)	−6(2)
C123	27(3)	23(3)	30(4)	8(3)	9(3)	5(3)
C23	32(3)	26(3)	28(4)	11(3)	8(3)	7(3)
C124	16(3)	30(3)	28(4)	16(3)	4(2)	1(2)
C125	28(3)	39(3)	24(4)	12(3)	9(3)	9(3)
C33	29(3)	21(3)	48(5)	2(3)	14(3)	4(3)
C129	22(3)	36(3)	28(4)	15(3)	4(3)	2(3)
C7	37(4)	34(3)	36(4)	17(3)	8(3)	12(3)
C20	44(4)	26(3)	28(4)	5(3)	3(3)	−10(3)
C128	30(3)	43(4)	31(4)	18(3)	1(3)	13(3)
C43	20(3)	24(3)	31(4)	8(3)	2(3)	1(2)
C27	37(4)	35(4)	43(4)	15(3)	−4(3)	8(3)
C25	30(3)	35(3)	36(4)	12(3)	−2(3)	7(3)
C45	36(3)	44(4)	37(4)	24(3)	7(3)	16(3)
C29	24(3)	34(3)	31(4)	16(3)	3(3)	3(3)
C47	29(3)	20(3)	40(4)	8(3)	4(3)	7(2)
C44	31(3)	28(3)	45(4)	20(3)	13(3)	12(3)
C26	27(3)	36(4)	39(4)	11(3)	−8(3)	−3(3)
C24	25(3)	25(3)	33(4)	11(3)	6(3)	7(3)
C41	29(3)	29(3)	37(4)	12(3)	3(3)	11(3)
C42	21(3)	26(3)	32(4)	14(3)	9(3)	10(2)
C126	37(3)	41(4)	24(4)	8(3)	−2(3)	1(3)
C37	31(3)	40(3)	33(4)	14(3)	3(3)	9(3)
C115	32(3)	25(3)	33(4)	7(3)	16(3)	0(3)
C40	25(3)	37(4)	39(4)	7(3)	7(3)	4(3)
C52	44(4)	29(3)	37(4)	14(3)	4(3)	2(3)
C127	32(3)	61(4)	26(4)	23(3)	2(3)	8(3)
C38	43(4)	52(4)	29(4)	17(3)	2(3)	4(3)
C51	45(4)	29(3)	34(4)	10(3)	5(3)	−10(3)
C46	32(3)	31(3)	35(4)	8(3)	1(3)	11(3)
C22	25(3)	45(4)	37(4)	18(3)	1(3)	0(3)
C28	27(3)	28(3)	54(5)	15(3)	7(3)	11(3)
C6	52(4)	24(3)	39(4)	14(3)	11(3)	11(3)
C50	34(3)	36(4)	44(4)	12(3)	12(3)	1(3)
C39	33(3)	46(4)	24(4)	3(3)	8(3)	2(3)
C133	38(4)	46(4)	41(5)	1(4)	6(3)	22(3)
C138	58(4)	47(4)	40(5)	17(4)	21(4)	−6(3)
C139	35(4)	56(5)	59(6)	6(4)	23(4)	6(3)
C140	34(4)	51(4)	40(5)	4(4)	7(3)	19(3)
C310	41(4)	36(4)	38(4)	12(3)	−4(3)	8(3)
C312	49(4)	45(4)	28(4)	9(3)	4(3)	16(3)
C311	36(4)	44(4)	42(5)	17(4)	6(3)	8(3)

University of Southampton · Department of Chemistry

Crystallography Service

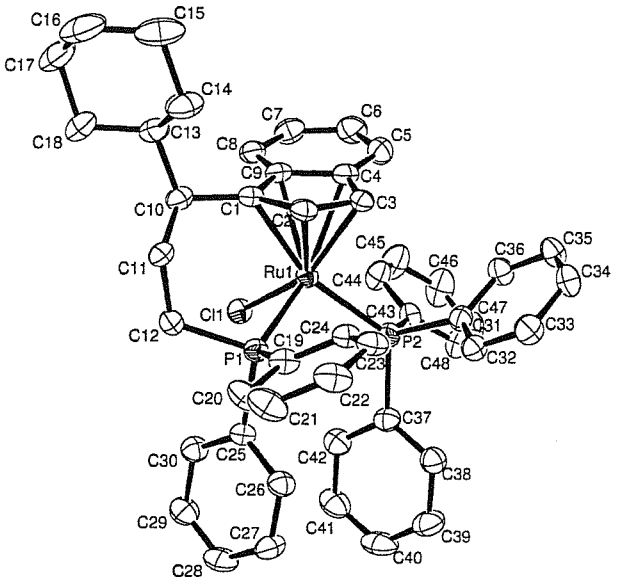

Major isomer. Note: solvent benzene is numbered C1xx and C2xx.

Table 1. Crystal data and structure refinement.

Compound name	***rac*-(η^5:η^1-Indenyl-CH(Cy)$CH_2CH_2PPh_2$)$Ru^{II}(PPh_3)Cl$**	
Empirical formula	$C_{48}H_{47}ClP_2Ru$	
Formula weight	822.36	
Temperature	120(2) K	
Wavelength	0.71069 Å	
Crystal system	Monoclinic	
Space group	*C*2	
Unit cell dimensions	$a = 31.476(5)$ Å	$\alpha = 90.000(5)°$
	$b = 20.240(5)$ Å	$\beta = 96.019(5)°$
	$c = 18.430(5)$ Å	$\gamma = 90.000(5)°$
Volume	11677(5) $Å^3$	
Z	4	
Density (calculated)	1.271 Mg / m^3	
Absorption coefficient	0.411 mm^{-1}	
F(000)	4592	
Crystal	Rod; red	
Crystal size	0.16 × 0.08 × 0.04 mm^3	
θ range for data collection	2.98 – 27.51°	
Index ranges	$-40 \le h \le 40$, $-24 \le k \le 26$, $-22 \le l \le 22$	
Reflections collected	23383	
Independent reflections	12999 [$R_{int} = 0.0653$]	
Completeness to $\theta = 27.51°$	96.7 %	
Absorption correction	Semi–empirical from equivalents	
Max. and min. transmission	0.9600 and 0.9600	
Refinement method	Full-matrix least-squares on F^2	
Data / restraints / parameters	12999 / 0 / 784	
Goodness-of-fit on F^2	0.980	
Final *R* indices [$F^2 > 2\sigma(F^2)$]	$R1 = 0.0571$, $wR2 = 0.1272$	
R indices (all data)	$R1 = 0.1201$, $wR2 = 0.1519$	
Largest diff. peak and hole	0.912 and –1.087 e $Å^{-3}$	

Diffractometer: *Enraf Nonius KappaCCD* area detector (ϕ scans and ω scans to fill *Ewald* sphere). **Data collection and cell refinement**: *Denzo* (Z. Otwinowski & W. Minor, *Methods in Enzymology* (1997) Vol. **276**: *Macromolecular Crystallography*, part A, pp. 307–326; C. W. Carter, Jr. & R. M. Sweet, Eds., Academic Press). **Absorption correction**: *SORTAV* (R. H. Blessing, Acta Cryst. A**51** (1995) 33–37; R. H. Blessing, J. Appl. Cryst. **30** (1997) 421–426). **Program used to solve structure**: *SHELXS97* (G. M. Sheldrick, Acta Cryst. (1990) A**46** 467–473). **Program used to refine structure**: *SHELXL97* (G. M. Sheldrick (1997), University of Göttingen, Germany).
Further information: http://www.soton.ac.uk/~xservice/strat.htm

Table 2. Atomic coordinates [× 10^4], equivalent isotropic displacement parameters [$Å^2$ × 10^3] and site occupancy factors. U_{eq} is defined as one third of the trace of the orthogonalized U^{ij} tensor.

Atom	*x*	*y*	*z*	U_{eq}	*S.o.f.*
C1	7655(1)	1752(2)	6588(2)	26(1)	1
C2	7845(1)	1338(2)	7166(2)	28(1)	1
C3	8288(1)	1460(2)	7287(2)	29(1)	1
C4	8378(1)	2020(2)	6829(2)	30(1)	1
C5	8747(1)	2401(2)	6775(2)	38(1)	1
C6	8730(1)	2920(2)	6299(2)	43(1)	1
C7	8351(1)	3065(2)	5851(2)	39(1)	1
C8	7986(1)	2711(2)	5881(2)	31(1)	1
C9	7986(1)	2188(2)	6398(2)	27(1)	1
C10	7188(1)	1786(2)	6320(2)	29(1)	1
C11	6969(1)	1103(2)	6336(2)	30(1)	1
C12	7119(1)	601(2)	5804(2)	30(1)	1
C13	6957(1)	2325(2)	6730(2)	33(1)	1
C14	6956(2)	2179(2)	7544(2)	45(1)	1
C15	6746(2)	2750(2)	7927(3)	64(2)	1
C16	6297(2)	2885(2)	7570(3)	66(2)	1
C17	6304(2)	3037(2)	6766(3)	54(1)	1
C18	6506(1)	2466(2)	6379(2)	41(1)	1
C19	7565(1)	−249(2)	6880(2)	28(1)	1
C20	7213(1)	−655(2)	6896(2)	38(1)	1
C21	7160(2)	−1008(2)	7526(2)	44(1)	1
C22	7454(1)	−964(2)	8128(2)	38(1)	1
C23	7806(1)	−569(2)	8111(2)	32(1)	1
C24	7861(1)	−210(2)	7484(2)	28(1)	1
C25	7651(1)	−424(2)	5374(2)	26(1)	1
C26	7813(1)	−1045(2)	5576(2)	31(1)	1
C27	7799(1)	−1554(2)	5067(2)	38(1)	1
C28	7628(1)	−1445(2)	4359(2)	42(1)	1
C29	7473(1)	−834(2)	4155(2)	38(1)	1
C30	7481(1)	−320(2)	4652(2)	31(1)	1
C31	9044(1)	345(2)	6972(2)	28(1)	1
C32	8921(1)	−184(2)	7387(2)	30(1)	1
C33	9099(1)	−273(2)	8101(2)	37(1)	1
C34	9396(1)	170(2)	8412(2)	35(1)	1
C35	9519(1)	699(2)	8011(2)	37(1)	1
C36	9347(1)	784(2)	7300(2)	32(1)	1
C37	8790(1)	−253(2)	5563(2)	30(1)	1
C38	9016(1)	−809(2)	5814(2)	36(1)	1
C39	9042(1)	−1358(2)	5369(3)	47(1)	1
C40	8851(2)	−1347(2)	4663(2)	49(1)	1
C41	8629(2)	−793(2)	4405(2)	46(1)	1
C42	8596(1)	−246(2)	4852(2)	35(1)	1
C43	9163(1)	985(2)	5631(2)	31(1)	1
C44	9062(1)	1609(2)	5341(2)	40(1)	1
C45	9371(2)	1973(2)	5026(3)	55(1)	1
C46	9770(2)	1712(3)	4981(3)	55(1)	1
C47	9867(1)	1075(2)	5245(2)	44(1)	1
C48	9567(1)	728(2)	5571(2)	34(1)	1
C100	6161(6)	−209(8)	7490(13)	118(10)	0.410(11)
C101	5894(5)	239(9)	7095(8)	116(8)	0.410(11)
C102	5790(5)	833(7)	7412(8)	117(8)	0.410(11)
C103	5953(6)	979(7)	8124(8)	109(9)	0.410(11)
C104	6220(7)	531(10)	8520(8)	420(60)	0.410(11)
C105	6324(7)	−63(10)	8203(12)	310(50)	0.410(11)
C110	6466(4)	−2065(6)	6341(5)	55(4)	0.57(2)
C111	6697(4)	−1946(5)	5752(8)	79(7)	0.57(2)
C112	6485(5)	−1781(6)	5077(6)	99(6)	0.57(2)
C113	6042(5)	−1734(8)	4991(6)	136(7)	0.57(2)
C114	5811(4)	−1853(6)	5580(8)	102(6)	0.57(2)
C115	6023(4)	−2018(5)	6255(6)	68(4)	0.57(2)
C140	9147(5)	4365(9)	5314(11)	260(30)	0.446(10)

C141	9201(5)	3820(8)	4873(11)	290(30)	0.446(10)
C142	9585(6)	3726(8)	4580(10)	280(30)	0.446(10)
C143	9916(4)	4177(10)	4728(9)	131(8)	0.446(10)
C144	9863(5)	4721(9)	5169(9)	156(10)	0.446(10)
C145	9478(6)	4815(7)	5462(10)	190(13)	0.446(10)
C150	5631(6)	−177(13)	7824(11)	860(80)	0.590(11)
C151	5529(4)	441(15)	8085(11)	620(60)	0.590(11)
C152	5852(7)	879(10)	8333(11)	1300(160)	0.590(11)
C153	6277(5)	699(9)	8320(8)	131(8)	0.590(11)
C154	6380(4)	82(10)	8059(10)	128(9)	0.590(11)
C155	6057(7)	−357(8)	7811(12)	480(50)	0.590(11)
C200	5000	3836(5)	7500	83(3)	1
C201	5055(2)	3494(4)	6888(4)	102(2)	1
C202	5000	2457(6)	7500	106(3)	1
C203	4944(3)	2772(4)	8120(4)	109(2)	1
P1	7648(1)	236(1)	6054(1)	25(1)	1
P2	8758(1)	521(1)	6073(1)	27(1)	1
Cl1	7973(1)	1245(1)	4879(1)	29(1)	1
Ru1	8124(1)	1075(1)	6187(1)	24(1)	1
C171	6193(6)	−1255(13)	5281(9)	120(10)	0.43(2)
C170	5963(5)	−1425(15)	5857(10)	158(14)	0.43(2)
C175	6140(5)	−1848(12)	6401(7)	105(10)	0.43(2)
C173	6549(6)	−2100(8)	6370(7)	136(14)	0.43(2)
C172	6780(5)	−1929(6)	5794(7)	89(10)	0.43(2)
C174	6602(5)	−1507(8)	5250(6)	71(5)	0.43(2)
C180	9438(7)	3979(10)	3917(9)	270(20)	0.554(10)
C181	9387(6)	3861(7)	4646(9)	370(30)	0.554(10)
C182	9161(5)	4307(11)	5032(9)	270(30)	0.554(10)
C184	8985(4)	4870(10)	4688(16)	590(60)	0.554(10)
C183	9036(7)	4988(10)	3959(17)	800(110)	0.554(10)
C185	9262(8)	4542(13)	3574(10)	610(80)	0.554(10)
C120	10000	2420(4)	7500	82(3)	1
C121	9949(3)	2692(7)	6876(6)	165(5)	1
C122	9882(5)	3248(10)	6697(13)	260(11)	1
C123	10162(6)	3663(6)	7420(40)	376(18)	1

Table 3. Bond lengths [Å] and angles [°].

C1–C2	1.435(5)
C1–C9	1.438(5)
C1–C10	1.501(5)
C1–Ru1	2.198(4)
C2–C3	1.411(5)
C2–Ru1	2.156(3)
C3–C4	1.458(5)
C3–Ru1	2.184(3)
C4–C5	1.407(5)
C4–C9	1.434(5)
C4–Ru1	2.345(4)
C5–C6	1.367(6)
C6–C7	1.409(6)
C7–C8	1.359(6)
C8–C9	1.425(5)
C9–Ru1	2.335(4)
C10–C11	1.546(5)
C10–C13	1.551(5)
C11–C12	1.521(5)
C12–P1	1.836(4)
C13–C18	1.524(6)
C13–C14	1.528(5)
C14–C15	1.539(6)
C15–C16	1.520(7)
C16–C17	1.516(7)
C17–C18	1.532(5)
C19–C24	1.378(5)
C19–C20	1.381(5)
C19–P1	1.854(3)
C20–C21	1.388(5)
C21–C22	1.372(6)
C22–C23	1.370(6)
C23–C24	1.391(5)
C25–C26	1.392(5)
C25–C30	1.397(5)
C25–P1	1.832(3)
C26–C27	1.390(5)
C27–C28	1.377(5)
C28–C29	1.367(6)
C29–C30	1.385(5)
C31–C36	1.393(5)
C31–C32	1.395(5)
C31–P2	1.835(4)
C32–C33	1.387(5)
C33–C34	1.377(5)
C34–C35	1.379(5)
C35–C36	1.376(5)
C37–C38	1.385(5)
C37–C42	1.387(5)
C37–P2	1.834(4)
C38–C39	1.389(6)
C39–C40	1.374(6)
C40–C41	1.379(7)
C41–C42	1.389(5)
C43–C48	1.388(5)
C43–C44	1.395(5)
C43–P2	1.842(4)
C44–C45	1.395(6)
C45–C46	1.374(6)
C46–C47	1.400(6)
C47–C48	1.366(5)

C100–C101	1.3900
C100–C105	1.3900
C101–C102	1.3900
C102–C103	1.3900
C103–C104	1.3900
C104–C105	1.3900
C110–C111	1.3900
C110–C115	1.3900
C111–C112	1.3900
C112–C113	1.3900
C113–C114	1.3900
C114–C115	1.3900
C140–C141	1.3900
C140–C145	1.3900
C141–C142	1.3900
C142–C143	1.3900
C143–C144	1.3900
C144–C145	1.3900
C144–C144^{i}	1.59(3)
C150–C151	1.3900
C150–C155	1.3900
C151–C152	1.3900
C152–C153	1.3900
C153–C154	1.3900
C154–C155	1.3900
C200–C201	1.350(9)
C200–C201^{ii}	1.350(9)
C201–C203^{ii}	1.462(10)
C202–C203	1.336(8)
C202–C203^{ii}	1.336(8)
C203–C201^{ii}	1.462(11)
P1–Ru1	2.2596(11)
P2–Ru1	2.3182(11)
Cl1–Ru1	2.4315(11)
C171–C170	1.3900
C171–C174	1.3900
C170–C175	1.3900
C175–C173	1.3900
C173–C172	1.3900
C172–C174	1.3900
C180–C181	1.3900
C180–C185	1.3900
C181–C182	1.3900
C182–C184	1.3900
C184–C183	1.3900
C183–C185	1.3900
C120–C121	1.270(11)
C120–C121^{iii}	1.270(11)
C121–C122	1.185(16)
C122–C123	1.74(6)
C122–C123^{iii}	1.85(5)
C123–C123^{iii}	1.09(3)
C123–C122^{iii}	1.85(5)

C2–C1–C9	106.4(3)
C2–C1–C10	126.0(3)
C9–C1–C10	127.0(3)
C2–C1–Ru1	69.2(2)
C9–C1–Ru1	76.8(2)
C10–C1–Ru1	125.9(2)
C3–C2–C1	110.1(3)
C3–C2–Ru1	72.09(19)
C1–C2–Ru1	72.35(19)

C2–C3–C4	107.0(3)
C2–C3–Ru1	69.96(19)
C4–C3–Ru1	77.3(2)
C5–C4–C9	119.9(3)
C5–C4–C3	132.7(4)
C9–C4–C3	107.3(3)
C5–C4–Ru1	130.7(3)
C9–C4–Ru1	71.8(2)
C3–C4–Ru1	65.32(19)
C6–C5–C4	119.4(4)
C5–C6–C7	120.6(4)
C8–C7–C6	122.3(4)
C7–C8–C9	118.6(4)
C8–C9–C4	119.1(3)
C8–C9–C1	132.1(4)
C4–C9–C1	108.8(3)
C8–C9–Ru1	126.3(2)
C4–C9–Ru1	72.5(2)
C1–C9–Ru1	66.41(19)
C1–C10–C11	112.1(3)
C1–C10–C13	111.4(3)
C11–C10–C13	112.7(3)
C12–C11–C10	114.5(3)
C11–C12–P1	116.2(3)
C18–C13–C14	110.9(3)
C18–C13–C10	112.9(3)
C14–C13–C10	113.0(3)
C13–C14–C15	110.5(4)
C16–C15–C14	111.1(4)
C17–C16–C15	110.6(4)
C16–C17–C18	110.6(4)
C13–C18–C17	110.9(4)
C24–C19–C20	119.5(3)
C24–C19–P1	119.4(3)
C20–C19–P1	121.1(3)
C19–C20–C21	119.5(4)
C22–C21–C20	120.8(4)
C23–C22–C21	120.0(4)
C22–C23–C24	119.6(4)
C19–C24–C23	120.6(4)
C26–C25–C30	118.9(3)
C26–C25–P1	120.3(3)
C30–C25–P1	120.9(3)
C27–C26–C25	120.3(3)
C28–C27–C26	120.2(4)
C29–C28–C27	119.9(4)
C28–C29–C30	121.1(4)
C29–C30–C25	119.7(4)
C36–C31–C32	118.0(3)
C36–C31–P2	121.1(3)
C32–C31–P2	120.4(3)
C33–C32–C31	120.8(4)
C34–C33–C32	119.9(4)
C33–C34–C35	120.0(3)
C36–C35–C34	120.2(4)
C35–C36–C31	121.1(4)
C38–C37–C42	118.9(3)
C38–C37–P2	125.2(3)
C42–C37–P2	115.8(3)
C37–C38–C39	120.9(4)
C40–C39–C38	119.9(4)
C39–C40–C41	119.7(4)
C40–C41–C42	120.6(4)

C37–C42–C41	120.0(4)
C48–C43–C44	118.9(4)
C48–C43–P2	121.8(3)
C44–C43–P2	119.4(3)
C45–C44–C43	119.8(4)
C46–C45–C44	120.2(4)
C45–C46–C47	120.1(4)
C48–C47–C46	119.4(4)
C47–C48–C43	121.6(4)
C101–C100–C105	120.0
C100–C101–C102	120.0
C103–C102–C101	120.0
C102–C103–C104	120.0
C103–C104–C105	120.0
C104–C105–C100	120.0
C111–C110–C115	120.0
C110–C111–C112	120.0
C113–C112–C111	120.0
C112–C113–C114	120.0
C113–C114–C115	120.0
C114–C115–C110	120.0
C141–C140–C145	120.0
C142–C141–C140	120.0
C141–C142–C143	120.0
C142–C143–C144	120.0
C143–C144–C145	120.0
C143–C144–C144^{i}	103(2)
C145–C144–C144^{i}	126(2)
C144–C145–C140	120.0
C151–C150–C155	120.0
C152–C151–C150	120.0
C151–C152–C153	120.0
C154–C153–C152	120.0
C153–C154–C155	120.0
C154–C155–C150	120.0
C201–C200–C201^{ii}	118.3(10)
C200–C201–C203^{ii}	121.5(7)
C203–C202–C203^{ii}	123.0(12)
C202–C203–C201^{ii}	117.9(8)
C25–P1–C12	100.97(17)
C25–P1–C19	100.71(16)
C12–P1–C19	102.48(17)
C25–P1–Ru1	124.93(12)
C12–P1–Ru1	107.35(13)
C19–P1–Ru1	117.28(12)
C37–P2–C31	104.49(17)
C37–P2–C43	97.50(17)
C31–P2–C43	101.63(17)
C37–P2–Ru1	123.58(13)
C31–P2–Ru1	110.94(12)
C43–P2–Ru1	115.82(13)
C2–Ru1–C3	37.95(14)
C2–Ru1–C1	38.48(13)
C3–Ru1–C1	64.34(13)
C2–Ru1–P1	87.32(11)
C3–Ru1–P1	117.30(10)
C1–Ru1–P1	92.52(10)
C2–Ru1–P2	128.70(10)
C3–Ru1–P2	97.71(10)
C1–Ru1–P2	161.25(10)
P1–Ru1–P2	101.14(4)
C2–Ru1–C9	61.47(13)
C3–Ru1–C9	61.98(13)

C1–Ru1–C9	36.83(13)
P1–Ru1–C9	127.64(10)
P2–Ru1–C9	131.21(10)
C2–Ru1–C4	61.50(13)
C3–Ru1–C4	37.36(13)
C1–Ru1–C4	61.79(13)
P1–Ru1–C4	148.68(9)
P2–Ru1–C4	100.92(10)
C9–Ru1–C4	35.70(13)
C2–Ru1–Cl1	137.76(10)
C3–Ru1–Cl1	150.77(11)
C1–Ru1–Cl1	100.17(9)
P1–Ru1–Cl1	86.57(3)
P2–Ru1–Cl1	93.47(3)
C9–Ru1–Cl1	90.49(9)
C4–Ru1–Cl1	113.93(9)
C170–C171–C174	120.0
C175–C170–C171	120.0
C170–C175–C173	120.0
C172–C173–C175	120.0
C174–C172–C173	120.0
C172–C174–C171	120.0
C181–C180–C185	120.0
C180–C181–C182	120.0
C184–C182–C181	120.0
C183–C184–C182	120.0
C184–C183–C185	120.0
C183–C185–C180	120.0
C121–C120–C121^{iii}	128.7(16)
C122–C121–C120	132(2)
C121–C122–C123	100.7(18)
C121–C122–C123^{iii}	102.4(18)
C123–C122–C123^{iii}	35.2(12)
C123^{iii}–C123–C122	78(5)
C123^{iii}–C123–C122^{iii}	67(5)
C122–C123–C122^{iii}	112.2(11)

Symmetry transformations used to generate equivalent atoms:
(i) –x+2,–y+1,–z+1 (ii) –x+1,y,–z+3/2 (iii) –x+2,y,–z+3/2

Table 4. Anisotropic displacement parameters [$Å^2 \times 10^3$]. The anisotropic displacement factor exponent takes the form: $-2\pi^2[h^2a^{*2}U^{11} + \cdots + 2\,h\,k\,a^*\,b^*\,U^{12}]$.

Atom	U^{11}	U^{22}	U^{33}	U^{23}	U^{13}	U^{12}
C1	35(2)	20(2)	22(2)	-4(1)	5(2)	0(2)
C2	38(2)	26(2)	20(2)	-4(2)	6(2)	0(2)
C3	35(2)	27(2)	25(2)	-9(2)	-1(2)	5(2)
C4	41(3)	22(2)	28(2)	-4(2)	6(2)	0(2)
C5	36(3)	31(2)	45(2)	0(2)	-1(2)	-1(2)
C6	42(3)	32(2)	54(3)	0(2)	9(2)	-11(2)
C7	52(3)	24(2)	44(2)	6(2)	11(2)	2(2)
C8	39(3)	25(2)	28(2)	-2(2)	5(2)	2(2)
C9	38(2)	18(2)	27(2)	-4(2)	5(2)	2(2)
C10	35(2)	27(2)	25(2)	-2(2)	6(2)	6(2)
C11	26(2)	29(2)	35(2)	-6(2)	6(2)	5(2)
C12	28(2)	30(2)	31(2)	-6(2)	1(2)	0(2)
C13	38(2)	23(2)	39(2)	-3(2)	11(2)	1(2)
C14	60(3)	42(3)	35(2)	-9(2)	15(2)	11(2)
C15	92(5)	51(3)	54(3)	-21(2)	34(3)	7(3)
C16	69(4)	40(3)	95(4)	-22(3)	40(3)	9(3)
C17	42(3)	35(3)	90(4)	-4(2)	26(3)	10(2)
C18	40(3)	35(2)	50(2)	1(2)	15(2)	10(2)
C19	39(2)	25(2)	20(2)	1(2)	11(2)	-2(2)
C20	46(3)	40(3)	27(2)	-6(2)	6(2)	-14(2)
C21	55(3)	42(3)	35(2)	-1(2)	12(2)	-22(2)
C22	61(3)	30(2)	25(2)	0(2)	11(2)	-6(2)
C23	49(3)	23(2)	24(2)	-5(2)	7(2)	-2(2)
C24	35(2)	23(2)	26(2)	-4(2)	5(2)	-1(2)
C25	33(2)	22(2)	24(2)	-3(2)	3(2)	-2(2)
C26	39(2)	30(2)	24(2)	-2(2)	4(2)	-1(2)
C27	53(3)	26(2)	35(2)	-4(2)	9(2)	9(2)
C28	56(3)	36(3)	33(2)	-18(2)	10(2)	-3(2)
C29	47(3)	42(3)	24(2)	-7(2)	-1(2)	0(2)
C30	37(2)	31(2)	25(2)	-2(2)	5(2)	1(2)
C31	27(2)	28(2)	28(2)	1(2)	3(2)	3(2)
C32	31(2)	29(2)	29(2)	-2(2)	3(2)	1(2)
C33	40(3)	35(2)	36(2)	6(2)	4(2)	0(2)
C34	35(2)	43(3)	26(2)	4(2)	-4(2)	-3(2)
C35	33(2)	41(3)	34(2)	-1(2)	-5(2)	-10(2)
C36	31(2)	33(2)	33(2)	4(2)	2(2)	-8(2)
C37	32(2)	27(2)	32(2)	-3(2)	8(2)	-1(2)
C38	31(2)	34(2)	42(2)	-8(2)	3(2)	-2(2)
C39	43(3)	34(3)	66(3)	-11(2)	14(2)	6(2)
C40	47(3)	43(3)	59(3)	-26(2)	24(2)	-8(2)
C41	46(3)	57(3)	38(2)	-18(2)	12(2)	-7(2)
C42	38(3)	37(2)	31(2)	-4(2)	7(2)	-3(2)
C43	30(2)	36(2)	26(2)	2(2)	1(2)	-2(2)
C44	33(3)	42(3)	46(2)	7(2)	7(2)	6(2)
C45	45(3)	43(3)	78(3)	25(2)	13(2)	-1(2)
C46	36(3)	62(3)	70(3)	26(3)	14(2)	-7(2)
C47	32(3)	55(3)	47(2)	13(2)	7(2)	3(2)
C48	32(2)	38(2)	34(2)	9(2)	5(2)	4(2)
C100	62(13)	55(12)	230(30)	-33(16)	-4(16)	15(10)
C101	100(20)	140(20)	106(15)	-33(15)	33(13)	-6(16)
C102	150(20)	89(14)	109(16)	9(12)	8(14)	9(14)
C103	150(20)	77(13)	91(15)	5(10)	-41(16)	28(14)
C104	260(50)	620(120)	430(90)	-380(90)	290(60)	-320(70)
C105	170(50)	530(120)	240(60)	-170(60)	10(40)	50(60)
C110	77(10)	45(10)	43(7)	-9(6)	2(6)	-29(7)
C111	59(8)	40(10)	142(18)	-51(10)	31(9)	-19(7)
C112	117(15)	59(10)	125(13)	13(9)	30(11)	8(10)
C113	180(20)	82(13)	146(16)	23(11)	12(15)	33(13)
C114	98(12)	87(11)	124(13)	34(9)	28(10)	15(8)

C115	83(10)	32(6)	84(9)	−7(6)	−13(7)	0(6)
C140	510(80)	60(15)	180(30)	−16(17)	−60(30)	−110(30)
C141	500(70)	150(30)	270(40)	120(30)	290(50)	200(40)
C142	300(50)	140(30)	450(60)	−40(30)	320(50)	−70(30)
C143	79(14)	160(20)	151(19)	13(17)	6(12)	28(14)
C144	130(20)	160(20)	200(20)	−10(18)	72(17)	−39(16)
C145	180(30)	94(18)	310(40)	10(20)	90(30)	24(18)
C150	290(40)	2000(200)	260(30)	280(60)	−70(30)	−770(80)
C151	360(50)	1190(140)	330(40)	450(70)	190(40)	520(80)
C152	2000(300)	1100(180)	570(100)	550(110)	−1000(160)	−1000(200)
C153	114(14)	210(20)	78(10)	−26(13)	57(10)	−84(15)
C154	130(20)	160(20)	103(16)	0(16)	40(15)	20(16)
C155	420(70)	250(40)	690(90)	260(50)	−260(60)	−220(40)
C200	64(6)	122(8)	65(5)	0	14(4)	0
C201	97(6)	116(6)	90(5)	3(5)	0(4)	1(5)
C202	102(8)	123(9)	95(7)	0	21(6)	0
C203	132(7)	98(6)	95(5)	−22(4)	0(5)	3(5)
P1	32(1)	23(1)	20(1)	−1(1)	4(1)	0(1)
P2	29(1)	26(1)	26(1)	0(1)	3(1)	1(1)
Cl1	38(1)	29(1)	21(1)	2(1)	4(1)	2(1)
Ru1	29(1)	21(1)	21(1)	0(1)	3(1)	1(1)
C171	101(16)	180(30)	77(13)	52(15)	−1(11)	36(17)
C170	87(16)	300(40)	87(15)	10(20)	−6(12)	20(20)
C175	124(19)	140(20)	45(10)	−4(11)	−3(10)	−92(17)
C173	110(20)	70(20)	240(40)	−60(20)	70(20)	−36(16)
C172	210(30)	20(11)	35(10)	14(7)	1(11)	−39(12)
C174	83(13)	55(12)	73(10)	1(8)	−3(8)	−22(9)
C180	380(50)	290(40)	140(20)	−60(20)	10(20)	−240(40)
C181	840(90)	41(10)	153(18)	33(11)	−270(30)	−140(20)
C182	30(10)	310(50)	440(50)	270(40)	−65(18)	−80(17)
C184	80(30)	930(170)	730(110)	−260(90)	−30(40)	−250(60)
C183	110(30)	290(60)	2000(300)	−380(120)	150(90)	−10(40)
C185	70(20)	610(130)	1200(200)	−350(140)	30(60)	−20(40)
C120	41(5)	62(6)	142(9)	0	1(6)	0
C121	93(7)	214(13)	186(10)	76(9)	11(7)	37(8)
C122	97(10)	250(20)	430(30)	180(20)	7(13)	19(15)
C123	135(16)	107(9)	900(60)	90(20)	130(30)	−35(8)

University of Southampton · Department of Chemistry

Crystallography Service

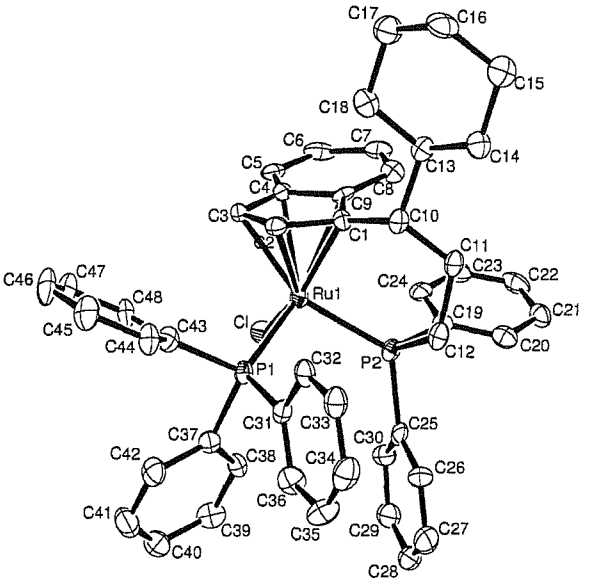

Minor isomer. Note diethyl ether solvent molecule is numbered C101-104 and O101.

Table 1. Crystal data and structure refinement.

Compound name	***rac*-(η^5:η^1-Indenyl-CH(Cy)$CH_2CH_2PPh_2$)$Ru^{II}(PPh_3)Cl$**	
Empirical formula	$C_{48}H_{47}ClP_2Ru$	
Formula weight	822.36	
Temperature	150(2) K	
Wavelength	0.71073 Å	
Crystal system	Orthorhombic	
Space group	*P*222	
Unit cell dimensions	$a = 11.2235(4)$ Å	$\alpha = 90°$
	$b = 22.4547(8)$ Å	$\beta = 90°$
	$c = 32.5552(16)$ Å	$\gamma = 90°$
Volume	8204.6(6) $Å^3$	
Z	8	
Density (calculated)	1.381 Mg / m^3	
Absorption coefficient	0.561 mm^{-1}	
F(000)	3531	
Crystal	Rod; red	
Crystal size	0.2 × 0.06 × 0.04 mm^3	
θ range for data collection	3.09 – 27.47°	
Index ranges	$-14 \le h \le 14$, $-28 \le k \le 29$, $-42 \le l \le 42$	
Reflections collected	11650	
Independent reflections	7360 [$R_{int} = 0.0716$]	
Completeness to $\theta = 27.47°$	78.2 %	
Absorption correction	Semi–empirical from equivalents	
Max. and min. transmission	0.952 and 0.742	
Refinement method	Full-matrix least-squares on F^2	
Data / restraints / parameters	7360 / 0 / 490	
Goodness-of-fit on F^2	0.941	
Final *R* indices [$F^2 > 2\sigma(F^2)$]	$R1 = 0.0513$, $wR2 = 0.0798$	
R indices (all data)	$R1 = 0.1271$, $wR2 = 0.0961$	
Largest diff. peak and hole	0.706 and –0.507 e $Å^{-3}$	

Diffractometer: *Enraf Nonius KappaCCD* area detector (ϕ scans and ω scans to fill *Ewald* sphere). **Data collection and cell refinement**: *Denzo* (Z. Otwinowski & W. Minor, *Methods in Enzymology* (1997) Vol. **276**: *Macromolecular Crystallography*, part A, pp. 307–326; C. W. Carter, Jr. & R. M. Sweet, Eds., Academic Press). **Absorption correction**: *SORTAV* (R. H. Blessing, Acta Cryst. A**51** (1995) 33–37; R. H. Blessing, J. Appl. Cryst. **30** (1997) 421–426). **Program used to solve structure**: *SHELXS97* (G. M. Sheldrick, Acta Cryst. (1990) A**46** 467–473). **Program used to refine structure**: *SHELXL97* (G. M. Sheldrick (1997), University of Göttingen, Germany).
Further information: http://www.soton.ac.uk/~xservice/strat.htm

Table 2. Atomic coordinates [× 10^4], equivalent isotropic displacement parameters [$Å^2$ × 10^3] and site occupancy factors. U_{eq} is defined as one third of the trace of the orthogonalized U^{ij} tensor.

Atom	*x*	*y*	*z*	U_{eq}	*S.o.f.*
C101	5482(11)	4419(5)	2580(4)	74(4)	0.480(4)
C102	4654(14)	4858(7)	2460(5)	119(6)	0.480(4)
C103	7698(14)	4159(7)	2682(5)	126(6)	0.480(4)
C104	8464(13)	4579(6)	2540(5)	103(5)	0.480(4)
O101	6738(14)	4661(7)	2546(5)	240(7)	0.480(4)
C1	7595(3)	3563(2)	1181(1)	18(1)	1
C2	7231(3)	3514(2)	1598(1)	20(1)	1
C3	6121(3)	3829(2)	1664(1)	20(1)	1
C5	4928(4)	4517(2)	1172(2)	24(1)	1
C6	4959(4)	4785(2)	801(2)	31(1)	1
C7	5893(3)	4671(2)	517(1)	27(1)	1
C8	6768(3)	4272(2)	603(1)	23(1)	1
C10	8782(3)	3374(2)	1009(1)	19(1)	1
C11	8679(3)	3030(2)	606(1)	22(1)	1
C12	7989(3)	2437(2)	620(1)	23(1)	1
C13	9623(3)	3921(2)	962(1)	23(1)	1
C14	10879(3)	3748(2)	827(1)	26(1)	1
C15	11720(3)	4276(2)	800(2)	32(1)	1
C16	11743(3)	4628(2)	1198(2)	35(1)	1
C17	10507(3)	4827(2)	1322(1)	34(1)	1
C18	9672(3)	4293(2)	1352(1)	27(1)	1
C9	6764(3)	3986(2)	993(1)	18(1)	1
C4	5871(3)	4127(2)	1287(1)	18(1)	1
C19	6030(3)	2888(2)	159(1)	18(1)	1
C20	6587(4)	2705(2)	−205(2)	27(1)	1
C21	6338(4)	2994(2)	−572(1)	28(1)	1
C22	5533(4)	3457(2)	−581(2)	34(1)	1
C23	4955(4)	3630(2)	−227(2)	30(1)	1
C24	5204(3)	3345(2)	140(1)	24(1)	1
C25	5821(4)	1783(2)	536(1)	22(1)	1
C26	6518(4)	1277(2)	549(1)	30(1)	1
C27	6050(5)	726(2)	447(2)	47(2)	1
C28	4861(5)	678(2)	341(1)	43(1)	1
C29	4148(4)	1175(2)	333(1)	35(1)	1
C30	4629(4)	1722(2)	425(1)	26(1)	1
C31	7168(3)	1759(2)	1638(1)	21(1)	1
C32	8339(3)	1960(2)	1673(1)	24(1)	1
C33	9284(4)	1570(2)	1656(1)	28(1)	1
C34	9093(4)	969(2)	1591(1)	34(1)	1
C35	7939(4)	760(2)	1545(2)	39(1)	1
C36	6980(4)	1151(2)	1574(1)	32(1)	1
C37	4657(3)	1784(2)	1740(2)	22(1)	1
C38	3882(3)	1663(2)	1417(1)	23(1)	1
C39	2937(4)	1269(2)	1475(2)	33(1)	1
C40	2736(4)	1003(2)	1853(2)	35(1)	1
C41	3499(4)	1121(2)	2175(2)	40(1)	1
C42	4449(4)	1503(2)	2116(2)	32(1)	1
C43	6039(3)	2555(2)	2209(1)	24(1)	1
C44	6941(4)	2403(2)	2480(1)	29(1)	1
C45	6935(4)	2605(2)	2883(1)	33(1)	1
C46	6034(4)	2973(2)	3016(1)	38(1)	1
C47	5124(4)	3121(2)	2750(1)	30(1)	1
C48	5135(3)	2925(2)	2351(1)	25(1)	1
P1	5928(1)	2294(1)	1675(1)	20(1)	1
P2	6379(1)	2530(1)	655(1)	21(1)	1
Cl	3763(1)	3042(1)	1127(1)	27(1)	1
Ru1	5913(1)	3073(1)	1228(1)	18(1)	1

Table 3. Bond lengths [Å] and angles [°].

C101–C102	1.410(16)
C101–O101	1.516(16)
C102–C104^{i}	1.476(17)
C103–C104	1.358(17)
C103–O101	1.622(18)
C104–C102^{ii}	1.476(17)
C1–C2	1.422(5)
C1–C9	1.465(5)
C1–C10	1.506(5)
C1–Ru1	2.191(4)
C2–C3	1.449(5)
C2–Ru1	2.150(4)
C3–C4	1.428(5)
C3–Ru1	2.225(4)
C5–C6	1.351(6)
C5–C4	1.424(5)
C6–C7	1.420(6)
C7–C8	1.359(5)
C8–C9	1.423(5)
C10–C11	1.527(5)
C10–C13	1.558(5)
C11–C12	1.540(5)
C12–P2	1.822(3)
C13–C18	1.521(5)
C13–C14	1.526(5)
C14–C15	1.518(5)
C15–C16	1.519(6)
C16–C17	1.512(5)
C17–C18	1.525(5)
C9–C4	1.420(5)
C9–Ru1	2.387(4)
C4–Ru1	2.374(4)
C19–C24	1.384(5)
C19–C20	1.401(5)
C19–P2	1.845(4)
C20–C21	1.386(5)
C21–C22	1.378(5)
C22–C23	1.379(6)
C23–C24	1.384(6)
C25–C26	1.379(5)
C25–C30	1.393(5)
C25–P2	1.833(4)
C26–C27	1.386(5)
C27–C28	1.383(6)
C28–C29	1.374(6)
C29–C30	1.375(5)
C31–C32	1.393(5)
C31–C36	1.398(5)
C31–P1	1.841(4)
C32–C33	1.377(5)
C33–C34	1.382(5)
C34–C35	1.386(5)
C35–C36	1.391(5)
C37–C38	1.391(5)
C37–C42	1.397(6)
C37–P1	1.842(4)
C38–C39	1.394(5)
C39–C40	1.386(6)
C40–C41	1.379(6)
C41–C42	1.382(5)
C43–C44	1.386(5)

C43–C48	1.389(5)
C43–P1	1.841(5)
C44–C45	1.386(6)
C45–C46	1.376(5)
C46–C47	1.379(5)
C47–C48	1.374(5)
P1–Ru1	2.2758(12)
P2–Ru1	2.2895(12)
Cl–Ru1	2.4358(10)

C102–C101–O101	110.0(13)
C101–C102–C104^{i}	107.4(12)
C104–C103–O101	81.0(12)
C103–C104–C102^{ii}	150.3(15)
C101–O101–C103	110.4(13)
C2–C1–C9	105.4(3)
C2–C1–C10	125.9(4)
C9–C1–C10	126.3(4)
C2–C1–Ru1	69.3(2)
C9–C1–Ru1	78.8(2)
C10–C1–Ru1	130.3(3)
C1–C2–C3	110.6(4)
C1–C2–Ru1	72.5(2)
C3–C2–Ru1	73.5(2)
C4–C3–C2	105.6(4)
C4–C3–Ru1	77.7(2)
C2–C3–Ru1	67.9(2)
C6–C5–C4	119.3(4)
C5–C6–C7	121.4(4)
C8–C7–C6	121.2(4)
C7–C8–C9	118.6(4)
C1–C10–C11	113.3(3)
C1–C10–C13	110.5(3)
C11–C10–C13	111.1(3)
C10–C11–C12	116.8(3)
C11–C12–P2	113.7(3)
C18–C13–C14	110.2(3)
C18–C13–C10	111.8(4)
C14–C13–C10	112.7(3)
C15–C14–C13	113.1(3)
C14–C15–C16	111.6(4)
C17–C16–C15	111.4(4)
C16–C17–C18	110.4(3)
C13–C18–C17	113.6(4)
C4–C9–C8	120.2(4)
C4–C9–C1	108.2(4)
C8–C9–C1	131.5(4)
C4–C9–Ru1	72.1(2)
C8–C9–Ru1	132.4(3)
C1–C9–Ru1	64.2(2)
C9–C4–C5	119.0(4)
C9–C4–C3	109.7(4)
C5–C4–C3	131.3(4)
C9–C4–Ru1	73.1(2)
C5–C4–Ru1	127.3(3)
C3–C4–Ru1	66.3(2)
C24–C19–C20	118.5(4)
C24–C19–P2	120.2(3)
C20–C19–P2	121.2(3)
C21–C20–C19	120.1(4)
C22–C21–C20	120.2(5)
C21–C22–C23	120.2(5)
C22–C23–C24	119.7(4)

C23–C24–C19	121.1(4)
C26–C25–C30	118.2(4)
C26–C25–P2	123.6(3)
C30–C25–P2	118.2(3)
C25–C26–C27	120.9(4)
C28–C27–C26	119.7(4)
C29–C28–C27	120.3(4)
C28–C29–C30	119.5(4)
C29–C30–C25	121.5(4)
C32–C31–C36	118.0(4)
C32–C31–P1	119.8(3)
C36–C31–P1	122.2(3)
C33–C32–C31	121.2(4)
C32–C33–C34	120.5(4)
C33–C34–C35	119.4(4)
C34–C35–C36	120.2(4)
C35–C36–C31	120.6(4)
C38–C37–C42	118.0(4)
C38–C37–P1	121.2(4)
C42–C37–P1	120.8(4)
C37–C38–C39	119.8(4)
C40–C39–C38	121.2(5)
C41–C40–C39	119.4(4)
C40–C41–C42	119.5(5)
C41–C42–C37	122.1(4)
C44–C43–C48	118.0(4)
C44–C43–P1	124.9(3)
C48–C43–P1	117.0(3)
C45–C44–C43	121.2(4)
C46–C45–C44	119.9(4)
C45–C46–C47	119.5(4)
C48–C47–C46	120.6(4)
C47–C48–C43	120.8(4)
C43–P1–C31	102.59(19)
C43–P1–C37	98.1(2)
C31–P1–C37	100.83(18)
C43–P1–Ru1	111.07(14)
C31–P1–Ru1	117.75(14)
C37–P1–Ru1	123.10(15)
C12–P2–C25	102.73(18)
C12–P2–C19	101.87(19)
C25–P2–C19	98.17(18)
C12–P2–Ru1	109.79(14)
C25–P2–Ru1	125.51(14)
C19–P2–Ru1	115.67(14)
C2–Ru1–C1	38.22(13)
C2–Ru1–C3	38.62(12)
C1–Ru1–C3	64.60(14)
C2–Ru1–P1	89.48(11)
C1–Ru1–P1	115.10(11)
C3–Ru1–P1	100.22(11)
C2–Ru1–P2	122.99(11)
C1–Ru1–P2	90.77(11)
C3–Ru1–P2	154.46(10)
P1–Ru1–P2	96.30(4)
C2–Ru1–C4	60.61(14)
C1–Ru1–C4	61.43(13)
C3–Ru1–C4	35.99(13)
P1–Ru1–C4	135.66(11)
P2–Ru1–C4	126.91(11)
C2–Ru1–C9	60.56(15)
C1–Ru1–C9	37.01(13)
C3–Ru1–C9	60.53(15)

P1–Ru1–C9	149.55(10)
P2–Ru1–C9	95.99(11)
C4–Ru1–C9	34.70(12)
C2–Ru1–Cl	140.42(11)
C1–Ru1–Cl	149.15(11)
C3–Ru1–Cl	102.25(10)
P1–Ru1–Cl	94.14(4)
P2–Ru1–Cl	95.80(4)
C4–Ru1–Cl	91.15(9)
C9–Ru1–Cl	112.18(10)

Symmetry transformations used to generate equivalent atoms:
(i) x–1/2,y,–z+1/2 (ii) x+1/2,y,–z+1/2

Table 4. Anisotropic displacement parameters [$Å^2 \times 10^3$]. The anisotropic displacement factor exponent takes the form: $-2\pi^2[h^2a^{*2}U^{11} + \cdots + 2\,h\,k\,a^*\,b^*\,U^{12}]$.

Atom	U^{11}	U^{22}	U^{33}	U^{23}	U^{13}	U^{12}
C1	15(2)	23(3)	16(3)	0(2)	−1(2)	−2(2)
C2	21(2)	18(3)	21(3)	−1(2)	−3(2)	−2(2)
C3	22(3)	20(2)	16(3)	−4(2)	6(2)	−7(2)
C5	21(3)	15(3)	37(3)	−7(3)	2(2)	−3(2)
C6	22(3)	15(3)	56(4)	3(3)	−7(3)	−1(2)
C7	27(3)	21(3)	34(3)	−1(2)	−8(3)	−8(2)
C8	18(2)	27(3)	25(3)	2(2)	−4(2)	−1(2)
C10	16(2)	22(2)	19(3)	1(2)	0(2)	8(2)
C11	19(2)	26(3)	20(3)	−1(2)	4(2)	7(2)
C12	24(2)	31(3)	15(3)	0(2)	−3(2)	8(2)
C13	23(2)	25(3)	20(3)	0(2)	−3(2)	2(2)
C14	22(2)	30(3)	26(3)	0(2)	0(2)	1(2)
C15	20(2)	33(3)	45(4)	0(3)	3(2)	9(2)
C16	21(3)	30(3)	55(4)	−2(3)	4(3)	−7(2)
C17	32(3)	32(3)	37(4)	−1(3)	1(2)	0(2)
C18	18(2)	33(3)	29(3)	4(3)	0(2)	3(2)
C9	19(2)	14(2)	21(3)	−7(2)	−6(2)	−1(2)
C4	11(2)	18(2)	24(3)	−5(2)	4(2)	−2(2)
C19	15(2)	21(3)	18(3)	0(2)	−4(2)	−3(2)
C20	24(3)	28(3)	28(3)	4(3)	−5(2)	−5(2)
C21	34(3)	33(3)	17(3)	3(3)	−1(2)	−9(2)
C22	42(3)	32(3)	27(3)	15(3)	−10(3)	−14(2)
C23	29(3)	25(3)	36(4)	9(3)	−9(3)	−3(2)
C24	30(3)	22(3)	21(3)	−5(2)	−6(2)	−9(2)
C25	33(3)	23(3)	10(2)	−1(2)	2(2)	3(2)
C26	38(3)	17(3)	34(3)	2(2)	5(3)	1(2)
C27	66(4)	27(3)	49(4)	3(3)	26(3)	14(3)
C28	73(4)	33(3)	22(3)	−10(3)	9(3)	−19(3)
C29	49(3)	34(3)	23(3)	0(3)	0(3)	−8(3)
C30	36(3)	22(3)	19(3)	3(2)	−6(2)	−2(2)
C31	23(2)	23(3)	16(3)	−1(2)	2(2)	3(2)
C32	26(3)	30(3)	16(3)	4(2)	1(2)	4(2)
C33	27(3)	37(3)	20(3)	3(3)	0(2)	6(2)
C34	35(3)	38(3)	30(3)	−1(3)	0(3)	15(2)
C35	44(3)	25(3)	46(4)	−6(3)	−1(3)	8(3)
C36	30(3)	32(3)	34(4)	4(3)	−1(2)	4(2)
C37	23(2)	19(3)	24(3)	3(2)	1(2)	7(2)
C38	23(3)	26(3)	20(3)	5(2)	2(2)	2(2)
C39	29(3)	33(3)	37(4)	0(3)	−10(3)	2(2)
C40	32(3)	35(3)	38(4)	0(3)	5(3)	−7(2)
C41	45(3)	44(3)	30(4)	7(3)	7(3)	−7(3)
C42	35(3)	41(3)	19(3)	0(3)	−5(2)	−3(2)
C43	17(2)	29(3)	25(3)	−2(2)	3(2)	1(2)
C44	27(3)	42(3)	17(3)	0(3)	2(3)	2(2)
C45	27(3)	51(3)	21(3)	0(3)	−6(2)	1(2)
C46	33(3)	66(4)	15(3)	−9(3)	2(3)	−4(3)
C47	28(3)	41(3)	21(3)	−7(3)	6(2)	5(2)
C48	21(2)	39(3)	14(3)	2(3)	3(2)	−1(2)
P1	20(1)	24(1)	15(1)	1(1)	−1(1)	2(1)
P2	23(1)	24(1)	15(1)	−2(1)	−2(1)	3(1)
Cl	18(1)	27(1)	35(1)	3(1)	−3(1)	2(1)
Ru1	18(1)	23(1)	15(1)	−1(1)	−1(1)	2(1)

University of Southampton · Department of Chemistry

Crystallography Service

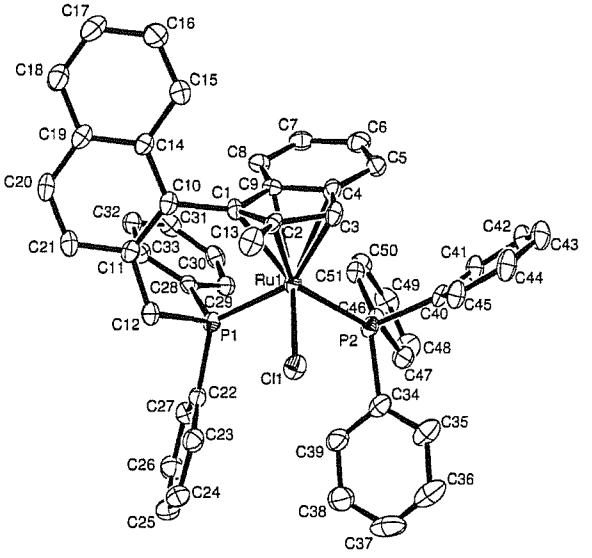

The second molecule in the structure is numbered as above+100, ie. C101-C151; two solvent benzenes are numbered C3xx and C4xx.

Table 1. Crystal data and structure refinement.

Compound name	***rac*-[η^5:η^1-2-methyl-(2-(CH_2PPh_2)naphthyl)indene]Ru^{II}(PPh_3)Cl**	
Empirical formula	$C_{51}H_{41}ClP_2Ru$	
Formula weight	852.34	
Temperature	150(2) K	
Wavelength	0.71073 Å	
Crystal system	Triclinic	
Space group	*P*1	
Unit cell dimensions	a = 9.9909(3) Å	α = 90.555(2)°
	b = 15.5888(5) Å	β = 92.423(2)°
	c = 28.2679(8) Å	γ = 94.8650(10)°
Volume	4382.4(2) $Å^3$	
Z	4	
Density (calculated)	1.410 Mg / m^3	
Absorption coefficient	0.531 mm^{-1}	
F(000)	1920	
Crystal	Block; red	
Crystal size	0.10 × 0.08 × 0.04 mm^3	
θ range for data collection	2.91 – 27.52°	
Index ranges	$-12 \le h \le 12$, $-20 \le k \le 20$, $-34 \le l \le 35$	
Reflections collected	33687	
Independent reflections	18714 [R_{int} = 0.0716]	
Completeness to θ = 27.52°	92.9 %	
Absorption correction	Semi–empirical from equivalents	
Max. and min. transmission	0.952 and 0.742	
Refinement method	Full-matrix least-squares on F^2	
Data / restraints / parameters	18714 / 0 / 1100	
Goodness-of-fit on F^2	0.972	
Final R indices [$F^2 > 2\sigma(F^2)$]	$R1$ = 0.0577, $wR2$ = 0.1016	
R indices (all data)	$R1$ = 0.1213, $wR2$ = 0.1183	
Largest diff. peak and hole	0.711 and –0.599 e $Å^{-3}$	

Diffractometer: *Enraf Nonius KappaCCD* area detector (ϕ scans and ω scans to fill *Ewald* sphere). **Data collection and cell refinement**: *Denzo* (Z. Otwinowski & W. Minor, *Methods in Enzymology* (1997) Vol. **276**: *Macromolecular Crystallography*, part A, pp. 307–326; C. W. Carter, Jr. & R. M. Sweet, Eds., Academic Press). **Absorption correction**: *SORTAV* (R. H. Blessing, Acta Cryst. A**51** (1995) 33–37; R. H. Blessing, J. Appl. Cryst. **30** (1997) 421–426). **Program used to solve structure**: *SHELXS97* (G. M. Sheldrick, Acta Cryst. (1990) A**46** 467–473). **Program used to refine structure**: *SHELXL97* (G. M. Sheldrick (1997), University of Göttingen, Germany).
Further information: http://www.soton.ac.uk/~xservice/strat.htm

Table 2. Atomic coordinates [$\times 10^4$], equivalent isotropic displacement parameters [$Å^2 \times 10^3$] and site occupancy factors. U_{eq} is defined as one third of the trace of the orthogonalized U^{ij} tensor.

Atom	*x*	*y*	*z*	U_{eq}	*S.o.f.*
C1	7420(4)	7150(3)	4287(1)	18(1)	1
C2	6242(4)	6855(3)	4009(1)	19(1)	1
C3	6638(4)	6467(3)	3584(1)	21(1)	1
C4	8070(4)	6451(3)	3613(1)	23(1)	1
C5	8957(5)	6031(3)	3326(2)	26(1)	1
C6	10264(5)	6044(3)	3476(2)	30(1)	1
C7	10774(4)	6480(3)	3902(2)	26(1)	1
C8	9948(4)	6897(3)	4177(2)	23(1)	1
C9	8573(4)	6876(3)	4045(1)	19(1)	1
C10	7444(4)	7464(3)	4785(1)	20(1)	1
C11	7293(4)	8305(3)	4905(1)	21(1)	1
C12	7130(4)	9014(3)	4555(1)	22(1)	1
C13	4830(4)	6900(3)	4161(2)	28(1)	1
C14	7662(4)	6849(3)	5152(1)	22(1)	1
C15	7792(5)	5975(3)	5055(2)	31(1)	1
C16	8007(5)	5408(3)	5409(2)	40(1)	1
C17	8096(5)	5696(3)	5884(2)	42(1)	1
C18	7960(5)	6530(3)	5993(2)	32(1)	1
C19	7720(4)	7128(3)	5634(2)	27(1)	1
C20	7521(4)	7986(3)	5740(2)	27(1)	1
C21	7295(4)	8560(3)	5391(2)	26(1)	1
C22	8032(4)	10177(3)	3884(1)	22(1)	1
C23	6727(5)	10446(3)	3816(1)	27(1)	1
C24	6532(5)	11296(3)	3741(2)	34(1)	1
C25	7632(5)	11902(3)	3718(2)	35(1)	1
C26	8907(5)	11645(3)	3777(2)	34(1)	1
C27	9104(5)	10791(3)	3866(2)	28(1)	1
C28	9943(4)	9082(3)	4276(1)	20(1)	1
C29	10956(4)	9115(3)	3949(2)	22(1)	1
C30	12286(4)	9063(3)	4087(2)	27(1)	1
C31	12629(4)	8955(3)	4561(2)	31(1)	1
C32	11653(4)	8937(3)	4893(2)	28(1)	1
C33	10321(4)	9008(3)	4751(2)	24(1)	1
C34	7259(4)	8991(3)	2520(2)	27(1)	1
C35	6342(4)	8848(4)	2141(2)	35(1)	1
C36	5773(5)	9539(4)	1933(2)	44(1)	1
C37	6090(5)	10357(4)	2091(2)	49(2)	1
C38	7032(5)	10510(4)	2473(2)	44(1)	1
C39	7594(5)	9831(3)	2682(2)	33(1)	1
C40	7658(4)	7169(3)	2450(1)	21(1)	1
C41	8624(4)	6772(3)	2208(1)	25(1)	1
C42	8307(5)	5997(3)	1977(2)	31(1)	1
C43	7021(5)	5606(3)	1967(2)	31(1)	1
C44	6019(5)	6008(3)	2191(2)	31(1)	1
C45	6358(4)	6772(3)	2433(2)	28(1)	1
C46	9823(4)	8395(3)	2697(1)	20(1)	1
C47	10220(4)	8879(3)	2310(2)	29(1)	1
C48	11576(5)	9019(3)	2211(2)	35(1)	1
C49	12524(4)	8670(3)	2504(2)	32(1)	1
C50	12150(4)	8182(3)	2881(2)	27(1)	1
C51	10801(4)	8051(3)	2979(2)	20(1)	1
C101	2297(4)	2350(3)	732(2)	22(1)	1
C102	3372(5)	2113(3)	1028(2)	27(1)	1
C103	2857(4)	1717(3)	1447(2)	27(1)	1
C104	1435(5)	1639(3)	1393(2)	27(1)	1
C105	412(5)	1198(3)	1660(2)	34(1)	1
C106	−872(5)	1154(3)	1484(2)	35(1)	1
C107	−1245(5)	1552(3)	1057(2)	35(1)	1
C108	−305(4)	1993(3)	795(2)	26(1)	1
C109	1064(5)	2037(3)	957(2)	24(1)	1
C110	2390(4)	2657(3)	236(2)	26(1)	1
C111	2700(4)	3515(3)	126(2)	29(1)	1

C112	2881(5)	4237(3)	483(2)	29(1)	1
C113	4815(4)	2204(3)	905(2)	36(1)	1
C114	2158(5)	2020(3)	−136(2)	27(1)	1
C115	1853(5)	1144(3)	−44(2)	39(1)	1
C116	1633(6)	556(3)	−405(2)	56(2)	1
C117	1703(7)	820(4)	−878(2)	67(2)	1
C118	2015(6)	1655(4)	−979(2)	53(2)	1
C119	2252(5)	2277(3)	−614(2)	35(1)	1
C120	2605(5)	3152(3)	−712(2)	36(1)	1
C121	2820(5)	3739(3)	−356(2)	32(1)	1
C122	2006(5)	5377(3)	1138(1)	25(1)	1
C123	3310(5)	5736(3)	1241(2)	35(1)	1
C124	3560(5)	6607(3)	1337(2)	38(1)	1
C125	2518(5)	7133(3)	1337(2)	39(1)	1
C126	1225(5)	6786(3)	1240(2)	36(1)	1
C127	972(5)	5921(3)	1136(2)	31(1)	1
C128	15(4)	4138(3)	715(2)	24(1)	1
C129	−1030(4)	4124(3)	1024(2)	26(1)	1
C130	−2360(5)	3987(3)	872(2)	29(1)	1
C131	−2667(5)	3846(3)	395(2)	33(1)	1
C132	−1656(5)	3858(3)	82(2)	32(1)	1
C133	−326(5)	4008(3)	234(2)	28(1)	1
C134	2417(4)	4321(3)	2486(1)	22(1)	1
C135	3271(4)	4342(3)	2883(2)	28(1)	1
C136	3716(4)	5115(3)	3104(2)	31(1)	1
C137	3327(5)	5881(3)	2927(2)	34(1)	1
C138	2474(4)	5868(3)	2527(2)	30(1)	1
C139	2024(4)	5097(3)	2312(2)	28(1)	1
C140	2208(4)	2464(3)	2556(1)	24(1)	1
C141	1306(4)	1886(3)	2771(1)	27(1)	1
C142	1739(5)	1156(3)	2992(2)	35(1)	1
C143	3100(5)	1018(3)	3007(2)	38(1)	1
C144	4007(5)	1610(3)	2809(2)	35(1)	1
C145	3572(5)	2311(3)	2575(2)	31(1)	1
C146	−71(4)	3385(3)	2331(1)	22(1)	1
C147	−412(4)	3718(3)	2762(2)	27(1)	1
C148	−1743(5)	3744(3)	2870(2)	33(1)	1
C149	−2749(5)	3428(3)	2549(2)	32(1)	1
C150	−2427(4)	3082(3)	2126(2)	32(1)	1
C151	−1094(4)	3061(3)	2017(2)	24(1)	1
C301	2042(8)	9299(4)	769(2)	65(2)	1
C302	3298(8)	9703(4)	863(2)	61(2)	1
C303	4420(8)	9478(4)	646(2)	70(2)	1
C304	4243(8)	8781(5)	325(2)	76(2)	1
C305	3016(8)	8386(4)	226(2)	67(2)	1
C306	1904(8)	8626(4)	443(2)	69(2)	1
C401	6037(6)	3258(4)	4580(2)	49(2)	1
C402	7300(6)	3166(3)	4743(2)	45(1)	1
C403	8395(6)	3653(3)	4562(2)	46(1)	1
C404	8139(6)	4243(3)	4210(2)	44(1)	1
C405	6868(6)	4322(3)	4042(2)	46(1)	1
C406	5796(6)	3841(4)	4226(2)	56(2)	1
P1	8214(1)	9044(1)	4036(1)	20(1)	1
P2	8062(1)	8128(1)	2832(1)	20(1)	1
P101	1729(1)	4222(1)	978(1)	24(1)	1
P102	1688(1)	3336(1)	2178(1)	22(1)	1
Cl1	5394(1)	8461(1)	3406(1)	26(1)	1
Cl2	4418(1)	3817(1)	1631(1)	27(1)	1
Ru1	7457(1)	7829(1)	3603(1)	18(1)	1
Ru2	2277(1)	3054(1)	1413(1)	22(1)	1

Table 3. Bond lengths [Å] and angles [°].

C1–C2	1.426(5)
C1–C9	1.456(5)
C1–C10	1.487(5)
C1–Ru1	2.212(4)
C2–C3	1.426(5)
C2–C13	1.499(6)
C2–Ru1	2.221(4)
C3–C4	1.433(6)
C3–Ru1	2.210(4)
C4–C5	1.421(6)
C4–C9	1.434(6)
C4–Ru1	2.283(4)
C5–C6	1.354(6)
C6–C7	1.429(6)
C7–C8	1.358(6)
C8–C9	1.406(6)
C9–Ru1	2.282(4)
C10–C11	1.372(6)
C10–C14	1.440(6)
C11–C21	1.427(6)
C11–C12	1.505(6)
C12–P1	1.859(4)
C14–C15	1.405(6)
C14–C19	1.424(6)
C15–C16	1.364(6)
C16–C17	1.410(7)
C17–C18	1.353(6)
C18–C19	1.412(6)
C19–C20	1.400(6)
C20–C21	1.365(6)
C22–C27	1.377(6)
C22–C23	1.409(6)
C22–P1	1.843(4)
C23–C24	1.373(6)
C24–C25	1.390(6)
C25–C26	1.372(6)
C26–C27	1.387(6)
C28–C33	1.387(6)
C28–C29	1.397(6)
C28–P1	1.824(4)
C29–C30	1.378(6)
C30–C31	1.384(6)
C31–C32	1.380(6)
C32–C33	1.387(6)
C34–C35	1.383(6)
C34–C39	1.392(6)
C34–P2	1.840(5)
C35–C36	1.384(7)
C36–C37	1.354(7)
C37–C38	1.409(7)
C38–C39	1.368(6)
C40–C45	1.389(6)
C40–C41	1.390(6)
C40–P2	1.843(4)
C41–C42	1.374(6)
C42–C43	1.373(6)
C43–C44	1.396(6)
C44–C45	1.378(6)
C46–C51	1.382(6)
C46–C47	1.387(6)
C46–P2	1.831(4)

C47–C48	1.394(6)
C48–C49	1.381(6)
C49–C50	1.362(6)
C50–C51	1.386(6)
C101–C102	1.409(6)
C101–C109	1.461(6)
C101–C110	1.491(6)
C101–Ru2	2.206(4)
C102–C103	1.436(6)
C102–C113	1.493(6)
C102–Ru2	2.208(4)
C103–C104	1.418(6)
C103–Ru2	2.212(4)
C104–C105	1.429(6)
C104–C109	1.432(6)
C104–Ru2	2.293(4)
C105–C106	1.352(6)
C106–C107	1.412(7)
C107–C108	1.366(6)
C108–C109	1.420(6)
C109–Ru2	2.268(4)
C110–C111	1.388(6)
C110–C114	1.436(6)
C111–C121	1.419(6)
C111–C112	1.499(6)
C112–P101	1.846(4)
C114–C115	1.403(6)
C114–C119	1.418(6)
C115–C116	1.364(7)
C116–C117	1.405(7)
C117–C118	1.350(7)
C118–C119	1.406(7)
C119–C120	1.414(6)
C120–C121	1.351(6)
C122–C123	1.391(6)
C122–C127	1.391(6)
C122–P101	1.848(5)
C123–C124	1.382(6)
C124–C125	1.378(7)
C125–C126	1.373(7)
C126–C127	1.378(6)
C128–C129	1.389(6)
C128–C133	1.395(6)
C128–P101	1.832(4)
C129–C130	1.378(6)
C130–C131	1.380(6)
C131–C132	1.371(6)
C132–C133	1.380(6)
C134–C135	1.378(6)
C134–C139	1.391(6)
C134–P102	1.837(4)
C135–C136	1.382(6)
C136–C137	1.379(6)
C137–C138	1.386(6)
C138–C139	1.373(6)
C140–C141	1.382(6)
C140–C145	1.401(6)
C140–P102	1.834(4)
C141–C142	1.394(6)
C142–C143	1.394(7)
C143–C144	1.378(7)
C144–C145	1.375(6)
C146–C151	1.385(6)

C146–C147	1.386(6)
C146–P102	1.835(4)
C147–C148	1.380(6)
C148–C149	1.380(6)
C149–C150	1.370(6)
C150–C151	1.383(6)
C301–C302	1.370(8)
C301–C306	1.385(8)
C302–C303	1.370(8)
C303–C304	1.404(9)
C304–C305	1.342(8)
C305–C306	1.368(9)
C401–C402	1.345(7)
C401–C406	1.385(7)
C402–C403	1.397(7)
C403–C404	1.390(7)
C404–C405	1.353(7)
C405–C406	1.377(7)
P1–Ru1	2.2999(12)
P2–Ru1	2.3272(11)
P101–Ru2	2.2977(12)
P102–Ru2	2.3153(11)
Cl1–Ru1	2.4054(11)
Cl2–Ru2	2.4113(11)

C2–C1–C9	107.5(3)
C2–C1–C10	125.4(3)
C9–C1–C10	125.3(4)
C2–C1–Ru1	71.6(2)
C9–C1–Ru1	73.7(2)
C10–C1–Ru1	132.3(3)
C3–C2–C1	108.7(3)
C3–C2–C13	126.3(4)
C1–C2–C13	124.9(4)
C3–C2–Ru1	70.8(2)
C1–C2–Ru1	70.9(2)
C13–C2–Ru1	127.3(3)
C2–C3–C4	107.9(4)
C2–C3–Ru1	71.7(2)
C4–C3–Ru1	74.2(2)
C5–C4–C3	131.4(4)
C5–C4–C9	119.9(4)
C3–C4–C9	108.3(4)
C5–C4–Ru1	131.0(3)
C3–C4–Ru1	68.6(2)
C9–C4–Ru1	71.6(2)
C6–C5–C4	118.0(4)
C5–C6–C7	122.3(4)
C8–C7–C6	120.6(4)
C7–C8–C9	119.2(4)
C8–C9–C4	120.0(4)
C8–C9–C1	132.5(4)
C4–C9–C1	107.3(4)
C8–C9–Ru1	129.3(3)
C4–C9–Ru1	71.7(2)
C1–C9–Ru1	68.5(2)
C11–C10–C14	119.8(4)
C11–C10–C1	122.9(4)
C14–C10–C1	117.3(4)
C10–C11–C21	120.1(4)
C10–C11–C12	124.7(4)
C21–C11–C12	115.2(4)
C11–C12–P1	117.2(3)

C15–C14–C19	118.1(4)
C15–C14–C10	122.8(4)
C19–C14–C10	119.1(4)
C16–C15–C14	121.5(4)
C15–C16–C17	119.9(5)
C18–C17–C16	120.4(4)
C17–C18–C19	120.9(4)
C20–C19–C18	121.6(4)
C20–C19–C14	119.2(4)
C18–C19–C14	119.2(4)
C21–C20–C19	121.2(4)
C20–C21–C11	120.5(4)
C27–C22–C23	118.0(4)
C27–C22–P1	123.3(3)
C23–C22–P1	118.6(3)
C24–C23–C22	120.9(4)
C23–C24–C25	120.0(5)
C26–C25–C24	119.5(5)
C25–C26–C27	120.5(5)
C22–C27–C26	121.0(4)
C33–C28–C29	117.6(4)
C33–C28–P1	125.3(3)
C29–C28–P1	116.9(3)
C30–C29–C28	121.9(4)
C29–C30–C31	119.3(4)
C32–C31–C30	120.1(4)
C31–C32–C33	120.0(4)
C28–C33–C32	121.0(4)
C35–C34–C39	119.1(4)
C35–C34–P2	123.7(4)
C39–C34–P2	117.2(3)
C34–C35–C36	119.5(5)
C37–C36–C35	121.7(5)
C36–C37–C38	119.1(5)
C39–C38–C37	119.5(5)
C38–C39–C34	121.0(5)
C45–C40–C41	117.7(4)
C45–C40–P2	119.1(3)
C41–C40–P2	122.9(3)
C42–C41–C40	120.7(4)
C43–C42–C41	121.1(4)
C42–C43–C44	119.4(4)
C45–C44–C43	119.0(4)
C44–C45–C40	122.1(4)
C51–C46–C47	118.5(4)
C51–C46–P2	118.0(3)
C47–C46–P2	123.4(3)
C46–C47–C48	120.6(4)
C49–C48–C47	119.2(4)
C50–C49–C48	120.9(4)
C49–C50–C51	119.5(4)
C46–C51–C50	121.3(4)
C102–C101–C109	106.5(4)
C102–C101–C110	126.1(4)
C109–C101–C110	125.8(4)
C102–C101–Ru2	71.4(2)
C109–C101–Ru2	73.2(2)
C110–C101–Ru2	131.7(3)
C101–C102–C103	109.7(4)
C101–C102–C113	124.8(4)
C103–C102–C113	125.4(4)
C101–C102–Ru2	71.3(2)
C103–C102–Ru2	71.2(2)

C113–C102–Ru2	127.1(3)
C104–C103–C102	107.5(4)
C104–C103–Ru2	74.8(3)
C102–C103–Ru2	70.9(3)
C103–C104–C105	132.3(4)
C103–C104–C109	108.2(4)
C105–C104–C109	119.2(4)
C103–C104–Ru2	68.6(2)
C105–C104–Ru2	130.6(3)
C109–C104–Ru2	70.7(2)
C106–C105–C104	118.4(4)
C105–C106–C107	122.7(4)
C108–C107–C106	121.0(5)
C107–C108–C109	118.5(4)
C108–C109–C104	120.2(4)
C108–C109–C101	131.5(4)
C104–C109–C101	107.9(4)
C108–C109–Ru2	129.8(3)
C104–C109–Ru2	72.6(2)
C101–C109–Ru2	68.7(2)
C111–C110–C114	120.1(4)
C111–C110–C101	122.8(4)
C114–C110–C101	117.2(4)
C110–C111–C121	118.6(4)
C110–C111–C112	124.5(4)
C121–C111–C112	116.9(4)
C111–C112–P101	118.2(3)
C115–C114–C119	118.3(4)
C115–C114–C110	122.3(4)
C119–C114–C110	119.4(4)
C116–C115–C114	120.9(5)
C115–C116–C117	120.4(5)
C118–C117–C116	120.3(5)
C117–C118–C119	120.7(5)
C118–C119–C120	121.5(5)
C118–C119–C114	119.5(5)
C120–C119–C114	118.9(4)
C121–C120–C119	120.6(4)
C120–C121–C111	122.3(5)
C123–C122–C127	118.0(4)
C123–C122–P101	119.1(4)
C127–C122–P101	122.8(4)
C124–C123–C122	120.6(5)
C125–C124–C123	120.4(5)
C126–C125–C124	119.6(5)
C125–C126–C127	120.3(5)
C126–C127–C122	121.1(5)
C129–C128–C133	117.4(4)
C129–C128–P101	117.1(3)
C133–C128–P101	125.2(3)
C130–C129–C128	122.5(4)
C129–C130–C131	118.9(4)
C132–C131–C130	119.9(5)
C131–C132–C133	121.1(4)
C132–C133–C128	120.2(4)
C135–C134–C139	118.3(4)
C135–C134–P102	125.0(4)
C139–C134–P102	116.6(3)
C134–C135–C136	120.8(4)
C137–C136–C135	120.4(5)
C136–C137–C138	119.4(5)
C139–C138–C137	119.9(5)
C138–C139–C134	121.3(4)

C141–C140–C145	118.5(4)
C141–C140–P102	123.1(3)
C145–C140–P102	117.8(3)
C140–C141–C142	120.7(4)
C143–C142–C141	119.7(5)
C144–C143–C142	119.6(5)
C145–C144–C143	120.4(4)
C144–C145–C140	120.8(5)
C151–C146–C147	118.5(4)
C151–C146–P102	119.7(3)
C147–C146–P102	121.7(3)
C148–C147–C146	120.7(4)
C147–C148–C149	120.0(4)
C150–C149–C148	120.0(4)
C149–C150–C151	120.0(4)
C150–C151–C146	120.8(4)
C302–C301–C306	118.4(7)
C303–C302–C301	123.1(6)
C302–C303–C304	116.8(7)
C305–C304–C303	120.7(7)
C304–C305–C306	121.6(6)
C305–C306–C301	119.4(7)
C402–C401–C406	120.4(5)
C401–C402–C403	121.0(5)
C404–C403–C402	118.0(5)
C405–C404–C403	120.7(5)
C404–C405–C406	120.8(5)
C405–C406–C401	119.1(6)
C28–P1–C22	102.61(19)
C28–P1–C12	106.16(19)
C22–P1–C12	96.53(19)
C28–P1–Ru1	116.04(14)
C22–P1–Ru1	127.94(14)
C12–P1–Ru1	104.14(14)
C46–P2–C34	100.7(2)
C46–P2–C40	100.36(19)
C34–P2–C40	104.3(2)
C46–P2–Ru1	120.88(14)
C34–P2–Ru1	118.02(14)
C40–P2–Ru1	110.11(13)
C128–P101–C112	106.9(2)
C128–P101–C122	102.4(2)
C112–P101–C122	97.24(19)
C128–P101–Ru2	114.96(14)
C112–P101–Ru2	103.77(15)
C122–P101–Ru2	128.57(15)
C140–P102–C146	101.77(19)
C140–P102–C134	104.1(2)
C146–P102–C134	98.88(19)
C140–P102–Ru2	108.17(14)
C146–P102–Ru2	121.83(14)
C134–P102–Ru2	119.57(13)
C3–Ru1–C1	63.23(15)
C3–Ru1–C2	37.54(14)
C1–Ru1–C2	37.53(14)
C3–Ru1–C9	62.29(15)
C1–Ru1–C9	37.77(14)
C2–Ru1–C9	62.12(15)
C3–Ru1–C4	37.14(15)
C1–Ru1–C4	62.35(14)
C2–Ru1–C4	61.73(15)
C9–Ru1–C4	36.62(14)
C3–Ru1–P1	149.29(11)

C1–Ru1–P1	86.40(11)
C2–Ru1–P1	113.96(11)
C9–Ru1–P1	96.91(11)
C4–Ru1–P1	132.38(11)
C3–Ru1–P2	105.14(11)
C1–Ru1–P2	157.39(11)
C2–Ru1–P2	140.60(11)
C9–Ru1–P2	120.17(10)
C4–Ru1–P2	96.37(10)
P1–Ru1–P2	104.96(4)
C3–Ru1–Cl1	97.69(11)
C1–Ru1–Cl1	113.09(11)
C2–Ru1–Cl1	87.29(11)
C9–Ru1–Cl1	148.82(10)
C4–Ru1–Cl1	133.98(12)
P1–Ru1–Cl1	89.88(4)
P2–Ru1–Cl1	86.85(4)
C101–Ru2–C102	37.22(15)
C101–Ru2–C103	63.51(15)
C102–Ru2–C103	37.91(15)
C101–Ru2–C109	38.08(15)
C102–Ru2–C109	61.81(16)
C103–Ru2–C109	62.04(16)
C101–Ru2–C104	62.62(15)
C102–Ru2–C104	61.48(16)
C103–Ru2–C104	36.65(16)
C109–Ru2–C104	36.61(15)
C101–Ru2–P101	86.82(11)
C102–Ru2–P101	114.89(12)
C103–Ru2–P101	150.20(11)
C109–Ru2–P101	96.78(11)
C104–Ru2–P101	132.04(12)
C101–Ru2–P102	157.87(11)
C102–Ru2–P102	138.87(12)
C103–Ru2–P102	103.32(11)
C109–Ru2–P102	120.76(11)
C104–Ru2–P102	95.98(11)
P101–Ru2–P102	105.72(4)
C101–Ru2–Cl2	112.65(11)
C102–Ru2–Cl2	88.17(12)
C103–Ru2–Cl2	99.40(12)
C109–Ru2–Cl2	149.09(11)
C104–Ru2–Cl2	135.35(12)
P101–Ru2–Cl2	89.08(4)
P102–Ru2–Cl2	86.19(4)

Symmetry transformations used to generate equivalent atoms:

Table 4. Anisotropic displacement parameters [$Å^2 \times 10^3$]. The anisotropic displacement factor exponent takes the form: $-2\pi^2[h^2a^{*2}U^{11} + \cdots + 2\,h\,k\,a^*\,b^*\,U^{12}]$.

Atom	U^{11}	U^{22}	U^{33}	U^{23}	U^{13}	U^{12}
C1	21(2)	18(2)	15(2)	−4(2)	5(2)	−2(2)
C2	21(2)	20(2)	14(2)	3(2)	−1(2)	−6(2)
C3	21(2)	25(3)	16(2)	−4(2)	−2(2)	−7(2)
C4	31(3)	22(3)	14(2)	1(2)	5(2)	−1(2)
C5	37(3)	21(3)	21(3)	1(2)	3(2)	0(2)
C6	35(3)	29(3)	27(3)	7(2)	8(2)	5(2)
C7	20(2)	26(3)	32(3)	4(2)	−1(2)	5(2)
C8	23(3)	20(3)	27(3)	2(2)	−1(2)	2(2)
C9	19(2)	15(2)	21(2)	2(2)	1(2)	4(2)
C10	17(2)	24(3)	18(2)	−2(2)	1(2)	−5(2)
C11	19(2)	25(3)	17(2)	1(2)	3(2)	−3(2)
C12	22(2)	27(3)	18(2)	−3(2)	5(2)	1(2)
C13	20(2)	38(3)	26(3)	0(2)	1(2)	−4(2)
C14	22(2)	25(3)	18(2)	2(2)	2(2)	−1(2)
C15	39(3)	31(3)	25(3)	−3(2)	3(2)	9(2)
C16	61(4)	30(3)	31(3)	4(2)	13(3)	9(3)
C17	58(4)	45(4)	26(3)	13(2)	6(3)	10(3)
C18	37(3)	37(3)	22(3)	2(2)	4(2)	2(2)
C19	28(3)	33(3)	18(3)	5(2)	2(2)	0(2)
C20	30(3)	35(3)	16(2)	−7(2)	2(2)	−3(2)
C21	28(3)	29(3)	21(3)	−6(2)	6(2)	−2(2)
C22	27(3)	23(3)	16(2)	−1(2)	1(2)	0(2)
C23	29(3)	27(3)	23(3)	−1(2)	−3(2)	−3(2)
C24	37(3)	35(3)	30(3)	−1(2)	−8(2)	13(3)
C25	51(3)	26(3)	30(3)	7(2)	3(2)	7(3)
C26	38(3)	29(3)	34(3)	−1(2)	3(2)	−2(2)
C27	30(3)	26(3)	26(3)	−2(2)	2(2)	4(2)
C28	22(2)	15(2)	22(2)	−4(2)	−2(2)	0(2)
C29	21(2)	21(3)	23(2)	−2(2)	−3(2)	−1(2)
C30	24(3)	25(3)	31(3)	−9(2)	3(2)	−4(2)
C31	17(2)	30(3)	44(3)	−9(2)	−6(2)	3(2)
C32	32(3)	27(3)	25(3)	−5(2)	−8(2)	0(2)
C33	26(3)	23(3)	23(3)	−1(2)	−3(2)	−2(2)
C34	21(2)	42(3)	19(2)	5(2)	7(2)	11(2)
C35	19(3)	59(4)	27(3)	10(2)	2(2)	9(2)
C36	32(3)	68(4)	33(3)	21(3)	3(2)	12(3)
C37	46(4)	61(4)	47(4)	28(3)	21(3)	33(3)
C38	55(4)	49(4)	32(3)	5(3)	12(3)	24(3)
C39	41(3)	39(3)	22(3)	6(2)	5(2)	14(3)
C40	22(2)	29(3)	12(2)	1(2)	−2(2)	0(2)
C41	23(3)	33(3)	19(2)	−4(2)	5(2)	−4(2)
C42	36(3)	35(3)	23(3)	−8(2)	7(2)	4(2)
C43	32(3)	34(3)	25(3)	−6(2)	0(2)	−10(2)
C44	25(3)	45(3)	21(3)	−6(2)	2(2)	−11(2)
C45	23(3)	41(3)	19(2)	−5(2)	3(2)	0(2)
C46	18(2)	23(3)	19(2)	−3(2)	3(2)	−3(2)
C47	28(3)	32(3)	26(3)	2(2)	3(2)	1(2)
C48	27(3)	44(3)	34(3)	5(2)	15(2)	−1(2)
C49	14(2)	38(3)	45(3)	−8(2)	6(2)	0(2)
C50	21(3)	25(3)	33(3)	−6(2)	−6(2)	3(2)
C51	17(2)	23(3)	20(2)	−2(2)	2(2)	−5(2)
C101	27(3)	17(2)	23(2)	−3(2)	0(2)	6(2)
C102	30(3)	24(3)	28(3)	−6(2)	1(2)	4(2)
C103	32(3)	33(3)	17(2)	−1(2)	−4(2)	9(2)
C104	43(3)	20(3)	19(2)	−7(2)	2(2)	−4(2)
C105	52(3)	26(3)	22(3)	−4(2)	10(2)	−8(2)
C106	38(3)	30(3)	36(3)	−13(2)	9(2)	−10(2)
C107	32(3)	33(3)	38(3)	−12(2)	2(2)	−5(2)
C108	28(3)	29(3)	21(3)	−6(2)	4(2)	0(2)

C109	35(3)	15(2)	21(2)	−7(2)	1(2)	−2(2)
C110	28(3)	29(3)	22(3)	−2(2)	5(2)	4(2)
C111	28(3)	36(3)	24(3)	−1(2)	9(2)	8(2)
C112	38(3)	25(3)	26(3)	4(2)	11(2)	2(2)
C113	35(3)	38(3)	33(3)	−11(2)	4(2)	5(2)
C114	38(3)	28(3)	17(2)	−5(2)	1(2)	3(2)
C115	62(4)	33(3)	23(3)	−3(2)	3(3)	3(3)
C116	106(5)	27(3)	32(3)	−7(2)	1(3)	−3(3)
C117	126(6)	45(4)	29(3)	−18(3)	6(4)	−2(4)
C118	98(5)	43(4)	19(3)	−6(2)	7(3)	5(3)
C119	53(3)	28(3)	27(3)	−3(2)	6(2)	11(3)
C120	51(3)	37(3)	22(3)	0(2)	12(2)	12(3)
C121	42(3)	29(3)	24(3)	2(2)	9(2)	3(2)
C122	34(3)	25(3)	15(2)	0(2)	6(2)	−1(2)
C123	42(3)	33(3)	30(3)	−2(2)	5(2)	7(3)
C124	42(3)	30(3)	39(3)	−3(2)	0(2)	−5(3)
C125	56(4)	22(3)	37(3)	−4(2)	0(3)	−2(3)
C126	50(3)	26(3)	32(3)	−2(2)	13(2)	6(3)
C127	36(3)	33(3)	23(3)	1(2)	11(2)	0(2)
C128	29(3)	17(2)	25(3)	0(2)	1(2)	−1(2)
C129	33(3)	20(3)	27(3)	1(2)	−2(2)	3(2)
C130	34(3)	27(3)	28(3)	−2(2)	5(2)	5(2)
C131	32(3)	33(3)	32(3)	6(2)	0(2)	0(2)
C132	40(3)	33(3)	22(3)	3(2)	−7(2)	4(2)
C133	34(3)	30(3)	22(3)	0(2)	2(2)	6(2)
C134	15(2)	32(3)	19(2)	−4(2)	4(2)	−4(2)
C135	29(3)	28(3)	26(3)	0(2)	3(2)	−2(2)
C136	23(3)	39(3)	28(3)	−3(2)	0(2)	−8(2)
C137	29(3)	39(3)	32(3)	−10(2)	11(2)	−7(2)
C138	31(3)	31(3)	28(3)	−4(2)	9(2)	1(2)
C139	26(3)	38(3)	19(2)	−2(2)	4(2)	0(2)
C140	23(2)	31(3)	17(2)	−2(2)	−4(2)	4(2)
C141	24(3)	36(3)	20(2)	−3(2)	−1(2)	0(2)
C142	49(3)	31(3)	27(3)	0(2)	0(2)	2(3)
C143	55(4)	39(3)	23(3)	−2(2)	−4(3)	25(3)
C144	25(3)	57(4)	24(3)	−5(2)	−2(2)	18(3)
C145	27(3)	45(3)	22(3)	−4(2)	0(2)	7(2)
C146	18(2)	27(3)	21(2)	6(2)	2(2)	3(2)
C147	28(3)	33(3)	20(3)	1(2)	3(2)	1(2)
C148	36(3)	31(3)	31(3)	−6(2)	8(2)	0(2)
C149	21(3)	37(3)	38(3)	5(2)	4(2)	−1(2)
C150	19(3)	42(3)	35(3)	4(2)	−5(2)	−4(2)
C151	25(3)	27(3)	19(2)	2(2)	4(2)	−3(2)
C301	93(6)	66(5)	39(4)	15(3)	−6(4)	25(4)
C302	100(6)	41(4)	41(4)	−11(3)	−21(4)	14(4)
C303	89(5)	73(5)	46(4)	−13(4)	−17(4)	3(4)
C304	76(5)	104(6)	50(4)	−18(4)	−4(4)	30(5)
C305	97(6)	51(4)	52(4)	−13(3)	−4(4)	4(4)
C306	88(5)	67(5)	49(4)	5(4)	−12(4)	−13(4)
C401	54(4)	55(4)	38(3)	13(3)	13(3)	0(3)
C402	57(4)	39(4)	39(3)	3(3)	5(3)	7(3)
C403	51(4)	45(4)	43(3)	−10(3)	3(3)	0(3)
C404	54(4)	35(3)	42(3)	−1(3)	15(3)	−4(3)
C405	60(4)	38(3)	41(3)	8(3)	4(3)	10(3)
C406	53(4)	59(4)	58(4)	5(3)	11(3)	8(3)
P1	19(1)	22(1)	18(1)	−1(1)	0(1)	0(1)
P2	16(1)	28(1)	16(1)	−1(1)	−1(1)	2(1)
P101	28(1)	26(1)	19(1)	−1(1)	4(1)	1(1)
P102	19(1)	29(1)	18(1)	−2(1)	0(1)	0(1)
Cl1	16(1)	37(1)	24(1)	0(1)	−1(1)	4(1)
Cl2	20(1)	33(1)	27(1)	−5(1)	1(1)	−3(1)
Ru1	16(1)	23(1)	15(1)	−2(1)	0(1)	−1(1)
Ru2	22(1)	25(1)	17(1)	−2(1)	1(1)	0(1)

University of Southampton · Department of Chemistry

Crystallography Service

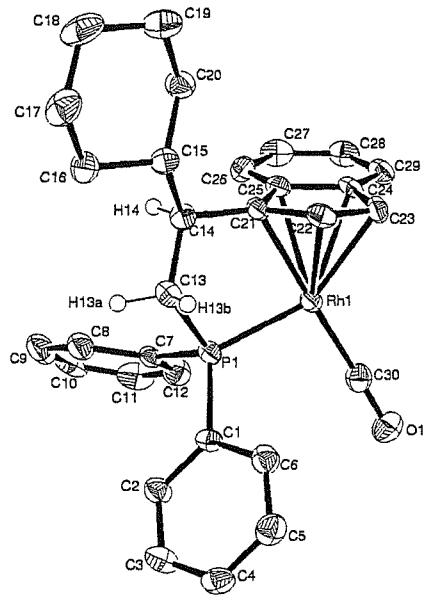

Table 1. Crystal data and structure refinement.

Compound name	***rac*-(η^5:η^1-indenyl-CH(Cy)CH_2PPh_2)Rh^1CO**	
Empirical formula	$C_{30}H_{30}OPRh$	
Formula weight	540.42	
Temperature	150(2) K	
Wavelength	0.71073 Å	
Crystal system	Orthorhombic	
Space group	*Pbca*	
Unit cell dimensions	a = 17.055(3) Å	α = 90°
	b = 16.304(3) Å	β = 90°
	c = 17.645(4) Å	γ = 90°
Volume	4906.5(17) $Å^3$	
Z	8	
Density (calculated)	1.463 Mg / m^3	
Absorption coefficient	0.782 mm^{-1}	
F(000)	2224	
Crystal	Block; orange	
Crystal size	0.10 × 0.05 × 0.05 mm^3	
θ range for data collection	2.08 – 27.49°	
Index ranges	$-22 \le h \le 22$, $-18 \le k \le 21$, $-22 \le l \le 22$	
Reflections collected	31323	
Independent reflections	5617 [R_{int} = 0.1083]	
Completeness to θ = 27.49°	99.9 %	
Absorption correction	Semi–empirical from equivalents	
Max. and min. transmission	0.9619 and 0.9259	
Refinement method	Full-matrix least-squares on F^2	
Data / restraints / parameters	5617 / 0 / 298	
Goodness-of-fit on F^2	0.945	
Final R indices [$F^2 > 2\sigma(F^2)$]	$R1$ = 0.0432, $wR2$ = 0.0764	
R indices (all data)	$R1$ = 0.0972, $wR2$ = 0.0896	
Largest diff. peak and hole	0.750 and –0.620 e $Å^{-3}$	

Diffractometer: *Enraf Nonius KappaCCD* area detector (ϕ scans and ω scans to fill *Ewald* sphere). **Data collection and cell refinement**: *Denzo* (Z. Otwinowski & W. Minor, *Methods in Enzymology* (1997) Vol. **276**: *Macromolecular Crystallography*, part A, pp. 307–326; C. W. Carter, Jr. & R. M. Sweet, Eds., Academic Press). **Absorption correction**: *SORTAV* (R. H. Blessing, Acta Cryst. A**51** (1995) 33–37; R. H. Blessing, J. Appl. Cryst. **30** (1997) 421–426). **Program used to solve structure**: *SHELXS97* (G. M. Sheldrick, Acta Cryst. (1990) A**46** 467–473). **Program used to refine structure**: *SHELXL97* (G. M. Sheldrick (1997), University of Göttingen, Germany).
Further information: http://www.soton.ac.uk/~xservice/strat.htm

Table 2. Atomic coordinates [$\times 10^4$], equivalent isotropic displacement parameters [$Å^2 \times 10^3$] and site occupancy factors. U_{eq} is defined as one third of the trace of the orthogonalized U^{ij} tensor.

Atom	*x*	*y*	*z*	U_{eq}	*S.o.f.*
C1	3400(2)	7626(2)	1641(2)	22(1)	1
C2	3772(2)	8324(2)	1910(2)	27(1)	1
C3	4557(2)	8467(2)	1747(2)	34(1)	1
C4	4975(2)	7920(2)	1307(2)	32(1)	1
C5	4614(2)	7214(2)	1046(2)	34(1)	1
C6	3836(2)	7072(2)	1215(2)	30(1)	1
C7	1920(2)	8352(2)	2128(2)	20(1)	1
C8	1917(2)	8603(2)	2874(2)	32(1)	1
C9	1556(2)	9330(2)	3086(2)	42(1)	1
C10	1214(2)	9826(2)	2545(3)	39(1)	1
C11	1227(2)	9588(2)	1799(2)	40(1)	1
C12	1576(2)	8843(2)	1593(2)	33(1)	1
C13	2377(2)	6710(2)	2637(2)	27(1)	1
C14	1583(2)	6282(2)	2722(2)	23(1)	1
C15	1597(2)	5562(2)	3287(2)	25(1)	1
C16	1902(2)	5799(2)	4070(2)	30(1)	1
C17	1896(2)	5082(2)	4618(2)	43(1)	1
C18	1098(2)	4681(2)	4665(2)	45(1)	1
C19	811(2)	4422(2)	3899(2)	40(1)	1
C20	806(2)	5145(2)	3349(2)	31(1)	1
C21	1292(2)	6004(2)	1948(2)	21(1)	1
C22	1640(2)	5390(2)	1475(2)	25(1)	1
C23	1223(2)	5366(2)	789(2)	25(1)	1
C24	525(2)	5869(2)	864(2)	22(1)	1
C25	562(2)	6259(2)	1588(2)	22(1)	1
C26	−40(2)	6801(2)	1803(2)	28(1)	1
C27	−659(2)	6927(2)	1320(2)	32(1)	1
C28	−694(2)	6545(2)	617(2)	33(1)	1
C29	−105(2)	6033(2)	377(2)	29(1)	1
C30	2218(2)	7047(2)	96(2)	28(1)	1
O1	2557(2)	7301(2)	−420(2)	44(1)	1
P1	2368(1)	7390(1)	1805(1)	22(1)	1
Rh1	1750(1)	6626(1)	949(1)	21(1)	1

Table 3. Bond lengths† [Å] and angles [°].

C1–C2	1.385(4)
C1–C6	1.391(4)
C1–P1	1.826(3)
C2–C3	1.390(4)
C3–C4	1.380(5)
C4–C5	1.384(5)
C5–C6	1.380(5)
C7–C12	1.371(5)
C7–C8	1.379(5)
C7–P1	1.834(3)
C8–C9	1.386(5)
C9–C10	1.382(5)
C10–C11	1.373(5)
C11–C12	1.400(5)
C13–C14	1.532(4)
C13–P1	1.841(3)
C14–C21	1.521(4)
C14–C15	1.541(4)
C15–C20	1.513(4)
C15–C16	1.526(4)
C16–C17	1.517(5)
C17–C18	1.512(5)
C18–C19	1.499(5)
C19–C20	1.526(5)
C21–C22	1.433(4)
C21–C25	1.458(4)
C21–Rh1	2.179(3)
C22–C23	1.404(4)
C22–Rh1	2.227(3)
C23–C24	1.452(4)
C23–Rh1	2.261(3)
C24–C29	1.402(4)
C24–C25	1.428(4)
C24–Rh1	2.433(3)
C25–C26	1.407(4)
C25–Rh1	2.395(3)
C26–C27	1.373(5)
C27–C28	1.390(5)
C28–C29	1.373(5)
C30–O1	1.155(4)
C30–Rh1	1.836(4)
P1–Rh1	2.2226(9)
C2–C1–C6	118.3(3)
C2–C1–P1	124.1(2)
C6–C1–P1	117.6(2)
C1–C2–C3	120.5(3)
C4–C3–C2	120.3(3)
C3–C4–C5	119.7(3)
C6–C5–C4	119.7(3)
C5–C6–C1	121.4(3)
C12–C7–C8	118.8(3)
C12–C7–P1	117.7(3)
C8–C7–P1	123.5(3)
C7–C8–C9	121.0(4)
C10–C9–C8	120.1(4)
C11–C10–C9	119.4(4)
C10–C11–C12	120.1(4)
C7–C12–C11	120.7(4)
C14–C13–P1	110.1(2)
C21–C14–C13	109.7(3)

C21–C14–C15	111.0(3)
C13–C14–C15	113.3(3)
C20–C15–C16	110.6(3)
C20–C15–C14	112.0(3)
C16–C15–C14	113.5(3)
C17–C16–C15	112.3(3)
C18–C17–C16	111.9(3)
C19–C18–C17	111.5(3)
C18–C19–C20	110.9(3)
C15–C20–C19	112.9(3)
C22–C21–C25	107.4(3)
C22–C21–C14	126.6(3)
C25–C21–C14	125.7(3)
C22–C21–Rh1	72.83(18)
C25–C21–Rh1	79.66(18)
C14–C21–Rh1	118.0(2)
C23–C22–C21	108.2(3)
C23–C22–Rh1	73.10(18)
C21–C22–Rh1	69.23(17)
C22–C23–C24	108.7(3)
C22–C23–Rh1	70.44(17)
C24–C23–Rh1	78.55(17)
C29–C24–C25	119.9(3)
C29–C24–C23	132.9(3)
C25–C24–C23	107.2(3)
C29–C24–Rh1	126.8(2)
C25–C24–Rh1	71.33(17)
C23–C24–Rh1	65.64(16)
C26–C25–C24	119.2(3)
C26–C25–C21	133.2(3)
C24–C25–C21	107.5(3)
C26–C25–Rh1	126.0(2)
C24–C25–Rh1	74.26(18)
C21–C25–Rh1	63.55(16)
C27–C26–C25	119.3(3)
C26–C27–C28	121.3(3)
C29–C28–C27	121.1(3)
C28–C29–C24	119.2(3)
O1–C30–Rh1	175.8(3)
C1–P1–C7	105.69(14)
C1–P1–C13	104.18(14)
C7–P1–C13	105.71(15)
C1–P1–Rh1	117.87(11)
C7–P1–Rh1	119.51(11)
C13–P1–Rh1	102.04(11)
C30–Rh1–C21	173.12(13)
C30–Rh1–P1	98.13(11)
C21–Rh1–P1	83.20(9)
C30–Rh1–C22	135.71(13)
C21–Rh1–C22	37.94(11)
P1–Rh1–C22	105.34(9)
C30–Rh1–C23	114.18(13)
C21–Rh1–C23	62.30(12)
P1–Rh1–C23	141.52(9)
C22–Rh1–C23	36.46(11)
C30–Rh1–C25	147.88(13)
C21–Rh1–C25	36.79(11)
P1–Rh1–C25	102.78(8)
C22–Rh1–C25	60.42(11)
C23–Rh1–C25	59.68(11)
C30–Rh1–C24	120.84(13)
C21–Rh1–C24	60.33(11)
P1–Rh1–C24	137.19(8)

C22–Rh1–C24	59.57(11)
C23–Rh1–C24	35.81(11)
C25–Rh1–C24	34.41(10)

Symmetry transformations used to generate equivalent atoms:

†H atoms refined at calculated positions, full details available in '.cif' file.

Table 4. Anisotropic displacement parameters [$Å^2 \times 10^3$]. The anisotropic displacement factor exponent takes the form: $-2\pi^2[h^2a^{*2}U^{11} + \cdots + 2\,h\,k\,a^*\,b^*\,U^{12}]$.

Atom	U^{11}	U^{22}	U^{33}	U^{23}	U^{13}	U^{12}
C1	19(2)	21(2)	25(2)	5(2)	−3(2)	−2(2)
C2	24(2)	23(2)	34(2)	−3(2)	1(2)	−1(2)
C3	24(2)	28(2)	49(3)	−3(2)	−4(2)	−5(2)
C4	16(2)	43(2)	37(2)	9(2)	−4(2)	−1(2)
C5	25(2)	44(2)	32(2)	−3(2)	0(2)	6(2)
C6	30(2)	26(2)	33(2)	−4(2)	−1(2)	−2(2)
C7	23(2)	15(2)	23(2)	0(2)	−1(1)	−5(2)
C8	26(2)	34(2)	36(2)	−10(2)	4(2)	−6(2)
C9	29(2)	45(3)	51(3)	−25(2)	6(2)	−8(2)
C10	19(2)	28(2)	71(3)	−15(2)	2(2)	−7(2)
C11	28(2)	29(2)	62(3)	7(2)	0(2)	2(2)
C12	32(2)	30(2)	38(2)	−1(2)	0(2)	0(2)
C13	28(2)	25(2)	27(2)	−1(2)	−4(2)	−4(2)
C14	27(2)	20(2)	23(2)	3(2)	−3(2)	1(2)
C15	25(2)	24(2)	25(2)	4(2)	−1(2)	1(2)
C16	32(2)	35(2)	23(2)	3(2)	−4(2)	0(2)
C17	46(3)	57(3)	25(2)	11(2)	−5(2)	4(2)
C18	41(3)	59(3)	36(3)	25(2)	1(2)	0(2)
C19	38(2)	37(2)	46(3)	15(2)	1(2)	−5(2)
C20	32(2)	32(2)	29(2)	5(2)	−4(2)	−6(2)
C21	23(2)	19(2)	21(2)	1(2)	−1(2)	−5(2)
C22	25(2)	18(2)	33(2)	2(2)	−2(2)	−2(2)
C23	26(2)	23(2)	27(2)	−7(2)	1(2)	−3(2)
C24	20(2)	19(2)	27(2)	1(2)	−5(2)	−7(2)
C25	21(2)	21(2)	24(2)	2(2)	0(2)	−5(2)
C26	32(2)	29(2)	24(2)	−2(2)	5(2)	−3(2)
C27	22(2)	31(2)	43(3)	9(2)	0(2)	5(2)
C28	24(2)	36(2)	38(2)	8(2)	−9(2)	−2(2)
C29	30(2)	28(2)	29(2)	2(2)	−7(2)	−8(2)
C30	30(2)	29(2)	26(2)	−2(2)	−4(2)	4(2)
O1	50(2)	55(2)	29(2)	5(1)	5(1)	−9(2)
P1	23(1)	21(1)	24(1)	0(1)	−2(1)	−3(1)
Rh1	22(1)	20(1)	21(1)	−1(1)	−1(1)	−3(1)